PART I.

THE EFFECT OF TEMPERATURE AND PARTIAL MELTING ON VELOCITY AND ATTENUATION IN A SIMPLE BINARY SYSTEM

PART II.

EFFECT OF TEMPERATURE AND PRESSURE ON ELASTIC PROPERTIES OF POLYCRYSTALLINE AND SINGLE CRYSTAL MgO

Thesis by

Hartmut A. W. Spetzler

In Partial Fulfillment of the Requirements

For the Degree of

Doctor of Philosophy

California Institute of Technology

Pasadena, California

1969

(Submitted May 20, 1969)

ACKNOWLEDGEMENTS

The author gratefully acknowledges the advise and encouragement during this study from Professor D. L. Anderson. Mr. D. Newbigging's assistance in all phases of the experiments was invaluable. Frequent discussion with staff members and fellow students of the Seismological Laboratory at the California Institute of Technology were very useful. Particularly, the help of Mr. B. Julian in writing the computer program and stimulating discussions with Professors C. Archambeau and T. Ahrens are appreciated. Dr. F. Horz advised the author and helped with all X-ray data and microscopic work.

Only the courteous cooperation and assistance from the following personnel at the California Institute of Technology made it possible to proceed rapidly in building the laboratory and executing the experiments; Messrs: B. Barber, W. Gile, E. Fantine, F. Lehner, N. Motta, A. Papetti, E. Steffenson, and J. Van Der Woode.

Dr. O. L. Anderson while visiting the California Institute of Technology first introduced the author to this field of study. His continued interest and cooperation are appreciated. Dr. E. Schreiber has collaborated with the author and was actively involved in the development of some of the techniques which made the measurements reported in this thesis possible.

The samples studied in this thesis were provided by Dr. T. Vasilos from Avco Corporation and from Drs. O. L. Anderson and P. Andreatch of Bell Telephone Laboratories.

The author has benefited greatly from discussions with individuals in most of the high pressure laboratories in this country. In particular, he would like to acknowledge the advice, encouragement and courtesy as well as some well intended warnings of the following institutions and individuals who have allowed him to inspect their facilities: Bell Laboratories (H. McSkimin, D. McWhan, A. Jayaraman); Brigham Young University (T. Hall and staff); Columbia University (O. Anderson, E. Schreiber, N. Soga); General Electric Company, Schenectady, New York (F. Bundy H. Strong); Geophysical Laboratory (F. Boyd, B. Brace); Harvard University (F. Birch, C. Wang, J. Hays); Iowa State University (C. Swenson); Massachusetts Institute of Technology (D. G. Simmons, W. Brace, D. Chung); National Bureau of Standards (P. Heydemann); Princeton (R. Phinney, W. Daniels); Rensselaer Polytechnic Institution, Troy, New York (S. Katz and students); Shell Research Company (H. Heard); South West Institute of Advanced Study (MacGregor); University of California, Berkeley (G. Jura); University of California, Los Angeles (G. Kennedy); University of Chicago (N. Nachtrieb, J. Jamieson); University of Illinois (H. Drickamer); University of Pennsylvania (W. Buessem, G. Barsch); University of Texas (D. Hughes, R. Brandt); and Yale University (S. Clark, R. Gordon, R. Vaisnys).

Special thanks are due to Dr. N. Nachtrieb of the University of Chicago and C. Swenson of Iowa State University for permitting the author to spend several profitable weeks gathering experience in their respective laboratories.

Mrs. Barbara Sloan typed the manuscript and Mr. Laszlo Lenches drafted most of the figures.

The inexhaustible patience and encouragement of my wife, and my children and the understanding of parents as well as parents-in-law provided the moral support for these many years.

The author held a National Science Foundation Graduate Fellowship during most of the time when the work presented here was carried out. The research was supported by the National Science Foundation under Grant GA 1003. The author gratefully acknowledges this financial support.

ABSTRACT

A possible explanation of the low-velocity, low-Q zone in the upper mantle is partial melting, but laboratory data has not been available to test this conjecture. As a first step in obtaining an idea of the role that partial melting plays in affecting seismic variables, the longitudinal and shear velocites and attenuations were measured in a simple binary system that is completely solid at low temperatures and involves 17% melt at the highest experimental temperature. The system investigated was $NaCl \cdot H_2O$. At temperatures below the eutectic the material is a solid mixture of H_2O (ice) and $NaCl \cdot 2\ H_2O$. At higher temperatures the system is a mixture of ice and NaCl brine. In the completely solid regime the velocities and Q change slowly with temperature. There is a marked drop in the velocities and Q at the onset of melting. For ice containing 1% NaCl, the longitudinal and shear velocities change discontinuously at this temperature by 9.5 and 13.5%, respectively. The corresponding Q's drop by 48 and 37%. The melt content of the mixture at temperatures on the warm side of the eutectic for this composition is about 3.3%. The abrupt drop in velocities at the onset of partial melting is about three times as much for the ice containing 2% NaCl; for this composition, the longitudinal and shear Q's drop at the eutectic temperature by 71 and 73%, respectively. If these results can be used as a guide in understanding the effect of melting on

seismic properties in the mantle, we should expect sharp discontinuities in velocity and Q where the geotherm crosses the solidus. The phenomena associated with the onset of melting are more dramatic than those associated with further melting.

The theory for randomly oriented fluid-filled penny-shaped cracks satisfactorily explains the velocity data. The anomalous behavior on the warm side of the eutectic temperature is attributed to thermochemical effects associated with interaction of the sound wave with the phase equilibria. This phenomenon is not observed when supercooling is possible.

A laboraory has been constructed to measure the elastic properties of solids to 12 kbar and 1200°K by ultrasonic interferometry techniques. The elastic constants and their temperature and pressure derivatives have been measured to high temperature and pressure for both single crystal and polycrystalline MgO. A pseudoresonance technique involving pulse superposition and a lapped buffer rod without bond were used in order to obtain the necessary precision. The results for the single crystal are tabulated below.

Prop.	Units	P = 0 kb T = 300°K	P = 0kb T = 800°K	P = 8kb T = 300°K	P = 8kb T = 800°K
C_{11}	kb	2974	2663	3042	2732
C_{12}	kb	955.7	973.2	965.3	983.8
C_{44}	kb	1562	1487	1571	1496
K_S	kb	1628	1536	1657	1566
K_T	kb	1605	1459	1634	1490
$\left(\frac{\partial C_{11}}{\partial P}\right)_T$		8.70	8.55	8.80	8.66
$\left(\frac{\partial C_{12}}{\partial P}\right)_T$		1.42	1.34	1.42	1.32
$\left(\frac{\partial C_{44}}{\partial P}\right)_T$		1.09	1.18	1.09	1.18
$\left(\frac{\partial K_S}{\partial P}\right)_T$		3.85	3.74	3.88	3.77
$\left(\frac{\partial K_T}{\partial P}\right)_T$		3.89	3.89	3.92	3.91
$\left(\frac{\partial C_{11}}{\partial T}\right)_P$	kb $°K^{-1}$	-.606	-.621	-.602	-.622
$\left(\frac{\partial C_{12}}{\partial T}\right)_P$	kb $°K^{-1}$	.074	.011	.076	.014
$\left(\frac{\partial C_{44}}{\partial T}\right)_P$	kb $°K^{-1}$	-.103	-.130	-.102	-.130
$\left(\frac{\partial K_S}{\partial T}\right)_P$	kb $°K^{-1}$	-.153	-.200	-.150	-.198
$\left(\frac{\partial K_T}{\partial T}\right)_P$	kb $°K^{-1}$	-.272	-.301	-.268	-.298

Polycrystalline data is shown to be not reproducible after the sample has been cycled to high temperature and pressure. Additional sintering, deformation and recrystallization takes place which change the properties of the sample. These problems, and the problem of sintering isotropic aggregates of theoretical density limit the usefulness of this widely used procedure.

TABLE OF CONTENTS

Page

Page

APPENDICES

Page

INTRODUCTION

Geophysics is traditionally an observational science with the earth as its laboratory. No other laboratory is so stubborn or so erratic in yielding data which can be interpreted uniquely. Much of the excitement and frustration in geophysics stems from attempts to obtain a coherent earth model from seemingly unrelated observations.

Individual seismic observations yield only the travel times for various modes of propagation. Many observations are required in order to determine the velocity structure of the Earth. Information on the attenuation of seismic waves is now becoming available from observations of free oscillations and studies of body wave amplitude. Heat flow and seismic measurements on continents and in the oceans suggest that there are fundamental differences in the histories of the oceans and continents. Low velocity zones and ocean floor spreading together with the theory of plate tectonics have given new insights into the evolution and constitution of the earth.

Any interpretation of the above mentioned observations in terms of a real earth model involves a knowledge of the physical and chemical properties of the proposed constituents. Meaningful laboratory measurements of these properties are complicated because of the high temperatures and pressures which are involved. Much progress has been made in the field of high pressure,high temperature petrology and geochemistry. Phase changes and melting have been studied by exposing samples to high temperature and high pressure

for a period of time, then quenching them and examining the new phases. Phases which cannot be quenched may be missed entirely. Shock wave experiments yield equations of state data but have the disadvantage that phase changes which are very sluggish may not be observed due to the short duration of the high pressure pulse.

Dynamic measurements under high temperature and high pressure have so far not been available. Seismic observations had to be interpreted by using velocity data from laboratories where the measurements had been performed either as a function of pressure at room temperature or as a function of temperature at atmospheric pressure.

The object of this thesis was to select some problems in geophysics which are amenable to laboratory experiments and which would give new insights into some pertinent physical phenomena. The first of the experiments was performed to better understand a possible mechanism which may cause the low velocity zone. Toward this end, the velocities of stress waves and their attenuation were measured as a function of temperature and melt concentration in a simple binary system. This experiment and the results are described in Part I of this thesis. The second problem which is described in Part II was selected to provide some experimental basis for high temperature, high pressure equations of state. To accomplish this task it was necessary to advance the state of the art in acoustic measurements and design and build laboratory facilities which could provide the high temperatures and the high

pressures simultaneously. The experiments were performed on MgO because of its possible importance in the lower mantle and because of its availability as single crystal as well as polycrystalline samples.

PART I

THE EFFECT OF TEMPERATURE AND PARTIAL MELTING ON VELOCITY AND ATTENUATION IN A SIMPLE BINARY SYSTEM

Introduction

Knowledge of the mechanical properties of multicomponent systems in the vicinity of their melting points is required in various geophysical problems. In particular, the behavior of seismic velocity and attenuation near the melting point is pertinent to discussions of the upper mantle low-velocity zone. In this study the velocity and attenuation of longitudinal and shear waves have been measured in the vicinity of the eutectic temperature in a simple dilute binary system. By varying the composition, the effects of temperature and partial melting have been isolated. Dilute solutions were chosen to investigate the region involving partial melting. In the system studied, $NaCl \cdot H_2O$, the amount of melt could be changed simply by varying either the temperature or the initial concentration of NaCl.

Previous studies of this sort have used pure materials or eutectic mixtures, both of which have sharply defined melting temperatures rather than a melting interval. Mizutani and Kanamori (1964) measured the compressional and shear velocities and the Q in compression for an alloy consisting of Pb, Bi, Sn, and Cd. The variation of the velocities was approximately linear with temperature until T/T_m was about 0.97, at which point they decreased rapidly. The P velocity dropped 20% upon melting, and the quality factor Q dropped by about an order of magnitude. The Q decreased very rapidly as the melting point was approached. Similar results were obtained by Porkorny (1965) who

obtained a velocity drop of about 15% and a Q drop of an order of magnitude as melting progressed. Again the mechanical properties started to anticipate the melting point at a T/T_m of about 0.97.

Both of the above studies used the ultrasonic pulse method and frequencies in the high kilocycle or megacycle range, i.e., very short wavelengths. The actual amount of melt as a function of temperature and the configuration of the melted zones with respect to the solid zones is not known.

In the NaCl-ice system both the phase diagram and the geometry of the components are well known. The melt phase (brine) occurs at the grain boundaries in cylindrical channels or thin films, depending on the temperature. In polycrystalline specimens the melt occurs in irregularly shaped pockets between crystal and sub-crystal boundaries. A resonance technique and large samples were used to insure that the wavelengths were always large compared to crystal or melt zone dimensions.

Water and NaCl form a simple binary system which can easily be studied in the vicinity of its eutectic temperature. Ice rods were frozen from dilute NaCl solutions and the resonant frequencies were measured to obtain longitudinal and shear velocities. The quality factors (Q's) were obtained by measuring the width, and in some cases the decay, of the resonance peaks. These measurements were performed on pure H_2O ice and on NaCl-ice mixtures as a function of NaCl concentration and temperature for the fundamental mode and several overtones.

Experimental Procedure

The experiments were performed in a "So-Low Environmental Equipment Company" refrigerator. To assure temperature stability the refigerator was packed with ice, and the experiment was placed inside a styrofoam insulating box.

A carefully measured amount of distilled water was heated close to its boiling point and the appropriate quantity of NaCl added. In order to remove entrapped air, the solution was placed in an airtight container and a vacuum (10 torr) was pumped until the solution was boiling slowly. The solution was pumped under vacuum into a teflon tube, one inch inside diameter and twelve inches in length. The shear or longitudinal transducers were supported from teflon plugs at both ends of the tube. To avoid separation of the ice crystals from the brine during the freezing process, the teflon tubes were rotated at one revolution per minute while in a horizontal position. The solution was frozen at approximately -30°C. After the resonance experiments were performed the ice rods were melted and the salinity of the solution was remeasured.

The measurements gave values of $\approx$ 0.1% lower than the salt concentration according to the measured values of salt and water prior to freezing. Salinity was also measured on one ice rod as a function of position within the rod. There was a slight concentration of salt toward the center of the rod and away from the ends. The total variation, however, was less than $\pm$0.15% of salt concentration.

Photomicrographs of thin sections cut from the ice rods were taken to give the size and orientation of the ice platelets as well as the distribution of the brine.

Figure 1 shows a radial cut close to one end of a 2% NaCl ice rod. The view is parallel to the c-axis of the platelets. The temperature was -5.3°C. The hexagonal platelets have an average diameter of 0.5 mm. Their diameter to thickness ratio is on the order of 8 to 1. Photographs of 1% ice reveals a platelet diameter of approximately 1 mm.

A solenoid arrangement was used to excite longitudinal modes in the ice. A small bar magnet was frozen into each end of the ice rod and the external transducer coils were enclosed in small aluminum boxes which were covered with μ-metal to avoid electromagnetic coupling between driving and receiving transducers. The transducers at each end of the ice-rod were idential and arranged symmetrically.

The shear transducers consisted of small flat coils which were frozen into the ice at both ends. To reduce electromagnetic coupling between the coils, they were oriented 90° to each other. Permanent magnets were used at the driver and receiver end to complete the motor and dynamo action, respectively.

The ice rods were supported by two narrow copper-band slings at the nodal points of the second harmonic. Various other supports were tried, including three slings and foam rubber pads, but the best reproducibility and the highest Q values were obtained with the two sling arrangement.

To monitor the temperature of the specimen, a separate ice rod was prepared under identical conditions to the one used for velocity measurements. This control rod contained one thermocouple in the center and one on the outside. By connecting the constantan of the two iron-constantan couples, it was possible to record the absolute temperature and the difference temperature between the outside and the inside of the rod.

The resistance between the top and the center and the center and the bottom of the rod was also measured. This measurement was performed to check for a possible brine drainage in the region warmer than the eutectic. No settling of brine was recorded on the time scale of the experiment.

The absolute temperature was measured with the aid of a Leeds and Northrup potentiometer. Small temperature increments were read with a digital voltmeter. Periodic cross calibration between the voltmeter, the potentiometer, and various thermocouples suggest an absolute accuracy in temperature of ±0.15°C and a relative accuracy between measurements of ±0.05°C.

The reference ice bath was aerated and carefully maintained using distilled water and shaved ice.

Instrumentation

Figure 2 shows the circuitry which was used to measure and record the resonant frequencies and the Q's of the various modes of the ice rods. A Schomandle ND30M frequency synthesizer was

driven by a synchronous motor to sweep through the appropriate frequency range. To excite the longitudinal modes the output of the synthesizer was amplified and applied directly to the driving solenoid.

The shear transducer arrangement, shown in Figure 2, is somewhat more complicated. An arrangement of resistors between synthesizer and amplifier served to select amplitudes for various frequency ranges. This enabled the operator to perform all measurements without disturbing the output level of the synthesizer. The output of the receiving transducer was amplified in two stages and then detected. The detected signal was recorded on a strip chart recorder and displayed on a digital voltmeter. The driving signal and the undetected output signal were displayed on an oscilloscope.

A typical record of a frequency sweep is shown in Figure 3. The frequency at the peak of the resonance was read from the synthesizer. The width of the resonance peak was measured by changing the frequency to the values where the digital voltmeter was 0.707 of the peak value, thus giving the half-energy points. In cases of high noise levels the resonance widths were measured from the graph. Many data points for Q were checked by measuring Q from the decay of the rod oscillations after power was turned off. The results were compatible.

The perpendicular orientation of the shear-transducer coils was not sufficient to reduce the electromagnetic coupling between driver and receiver. To cancel the coupling, a second driver and receiver coil were placed outside the refrigerator and adjusted

such that the electromagnetic coupling was the same as that for the coils embedded in the ice. The two receiver coils were connected to a center tapped transformer. By tuning off resonance and adjusting the coupling of the compensating coils, the output of the two receiver coils could be made to be 180° out of phase and cancel. The transformer served also to match the low impedance of the coils to the high input impedance of the amplifier. On the driver side, a transformer was used to match the impedance between amplifier and transducer coil.

Experimental Results

Measurements of resonant frequency and peak width were made for the fundamental and several harmonics as a function of temperature. The temperature was varied slowly so that the difference temperature between the center of the rod and the outside never exceeded 0.1°C. This required a cooling or heating rate between one to two degrees per hour, slower in the eutectic region. A typical data run from -35°C to -8°C and reverse through the eutectic would take approximately 100 hours. The velocities were calculated from the fundamental resonance frequencies of the longitudinal and shear modes of the ice rods

$$V = \frac{2\ell f}{n}$$

where f is the fundamental frequency of the appropriate mode, n the mode number, ℓ is the length of the ice rod. No correction was

applied for the temperature dependence of ℓ. According to the estimates of Weeks (1961) the maximum length change in the temperature from -30°C to -10°C for the 2% NaCl ice would be approximately 0.3%.

Velocity data from the fundamental mode of the 1% and 2% salt-ice-rods are presented in Figure 4 as a function of temperature. The eutectic temperature for the $NaCl \cdot H_2O$ system is -21.3°C. Figure 5 gives the same data as a function of brine content. At temperatures colder than the eutectic, the velocity decreases approximately linearly with temperature and at a faster rate than pure ice. In these experiments the absolute temperature was always greater than 0.94 of the eutectic temperature.

The normalized temperature derivatives of the velocities, $-(1/V)\ dV/dT$, are 0.6×10^{-4}, 0.9×10^{-3}, and $1.4 \times 10^{-3}\ °C^{-1}$ for longitudinal waves in pure ice and 1% NaCl and 2% NaCl ice, respectively, for temperatures colder than the eutectic. The corresponding shear velocity derivatives are 0.8×10^{-3}, 1.4×10^{-3}, and $2.8 \times 10^{-3}\ °C^{-1}$, significantly larger than the longitudinal derivatives. The drops in longitudinal velocities across the eutectic. for the ice containing 1% and 2% NaCl are 9.5% and 28%, respectively. The corresponding drops for the shear velocities are 13.5% and 40%. These velocity decreases occur within 0.1°C but over a time span of several hours when warming up the ice. When cooling the ice through the eutectic point, the system is able to supercool by 1.5 to 2.5°C. In this case the eutectic region is spread over a larger temperature range but occurs in a shorter time interval.

While warming up the ice, the velocities increase for several degrees immediately after the eutectic has been passed. When the temperature is reversed the velocities do not show this dip.

Figure 6 gives the brine content as a function of temperature and salinity. To achieve a given brine content the ice containing 1% NaCl must be much warmer than the ice containing 2% NaCl. For example, 7% brine content occurs at -8.4°C for the ice containing 1% NaCl and at -19°C for the ice containing 2% NaCl. Contrary to initial expectations the velocity is not a unique function of the melt fraction. In the 1% NaCl system the velocities decrease by about 1.2 to 1.4% for each 1% increment in brine content. In the 2% NaCl system the corresponding decrease in velocity is about 2%.

The Q measurements (Figures 7 through 12) were taken simultaneously with the velocity measurements. The Q decreases slowly with temperature to about - 30°C then begins to rise gradually. A small maximum in Q appears just below the eutectic temperature. There is an abrupt decrease in Q at the eutectic temperature which in all cases recovers slightly as the temperature is further raised. A peak in anelasticity is often observed at critical points in gas or fluid mixtures. In the present case, this phenomenon is complicated by the large change in mechanical properties which occurs when the system goes from a solid-solid to a solid-fluid mixture. It is this mechanical effect which is of primary interest here. The elastic wave upsets the local thermodynamic equilibrium in a mixed phase region, in this case a salt-water-ice system. This effect is superimposed on the grain boundary loosening associated with the onset of partial melting.

When the temperature is reversed, i.e. when the sample is cooled, the ability to supercool (which is related to the difficulty of nucleation) permits nonequilibrium conditions to be maintained during the passage of a stress wave, and there is no loss associated with thermodynamic relaxation effects. In this case the losses are associated with mechanical, presumably grain-boundary effects alone. On the warming cycle the drop in Q at the eutectic point amounted to 48% and 71% for the fundamental frequency of the longitudinal Q's for the 1 and 2% NaCl ice. The corresponding values for the shear Q's were 57% and 73%.

A further increase in temperature leads to a small increase in Q for the longitudinal modes. For the shear modes, especially for the 1% NaCl mixture,the increase was very pronounced. At warmer temperatures as the brine content further increases, the Q's begin to decrease. For comparison, the longitudinal and shear Q's for pure ice are shown in Figures 11 and 12. For pure ice, and for salt ice below 35°C, Q increases with frequency for the first few harmonics. For higher temperatures in the salt ice, Q decreases as the frequency increases. Above the eutectic temperature this generalization does not hold.

The shear Q data of pure ice show minima for the first three haromonics at -28°C, -16°C, and -12°C, respectively. Figure 12 shows the relation of these minima to temperature and relaxation time. The activation energy corresponding to this frequency response is approximately 7.5 kcal/mole.

Size of Ice Platelets and Velocity

The spacing between centers of adjacent ice platelets is a linear function of salt concentration and directly proportional to the square root of the freezing time (Rohatgi and Adams, 1967). The freezing time for the 1 and 2% ice-rods in this experiment are on the order of 100 to several hundred seconds. This freezing time corresponds approximately to that used in Figure 14 of the above mentioned reference. The spacing between the centers of the platelets of the 1 and 2% ice is therefore quite similar, and this is confirmed by the photographs described earlier. The crystal size of the 1% ice is approximately twice that of the 2% ice.

The crystal platelets in the ice rod radiate out from the axis of the rod as a consequence of the freezing process. The c-axis is perpendicular to the plane of the individual platelets, and is approximately normal to the surface of the rods. This preferred orientation of the platelets introduces anisotropy.

Comparing the velocities of the two samples as given in Figure 5, it is clear that the mechanical properties are not simple functions of the brine or melt content. Most of the brine is contained both in layers between sub-crystal platelets and as irregular pockets between crystals. The function of the liquid (brine) at the grain boundaries seems to be one of decoupling. The number of grain boundaries per unit volume can be expected to be an important parameter. The number of grain boundaries per unit volume is inversely proportional to the surface area of a grain.

The velocity is roughly a single valued function of the brine content times the surface area of the crystals.

Velocity and Q Averages

Several methods for finding the average velocity of a solid-liquid mixture have been proposed. Sato (1952) has extended a theory by MacKenzie (1950) which concerns a solid containing spherical empty holes, to a theory where the holes are filled with a liquid. The equations for the shear and compressional velocities, V_S and V_P, are given below:

$$V_S = V_{SO} \left\{ 1 - (1-\rho) \frac{1}{2} \left[15 \frac{1-\sigma_o}{7-5\sigma_o} - (1-D) \right] \right\}$$

$$V_P = V_{PO} \left\{ 1 - (1-\rho) \frac{1}{2} \left[\frac{(1-K)(1+\sigma_o)}{2(1-2\sigma_o) + K(1+\sigma_o)} + 10 \frac{(1-2\sigma_o)}{(7-5\sigma_o)} - (1-D) \right] \right\}$$

where

V_{SO} = shear velocity of solid without holes

V_{PO} = compressional velocity of solid without holes

ρ = relative density of actual material with holes empty vs solid material

σ_o = Poisson's ratio of solid without holes

K = ratio of the bulk modulus of the liquid to that of the solid

D = ratio of the density of the liquid to that of the solid

Using these equations and the data given in Table 1, V_S and V_P were calculated. Sato's theory has no provisions for any geometrical effect and therefore gives a single valued function for brine content versus velocity. As mentioned earlier, this is not the case when the 1% NaCl ice data are compared with the 2% NaCl data. The values obtained from the above equations are included in Figure 13.

Walsh (1969) has treated a more realistic model for the present experiment. He has considered the liquid inclusions to be in the form of randomly distributed thin films. In addition to the melt concentration, the aspect ratio of the penny-like liquid inclusion is considered. The equations as they are given in his paper (Walsh, 1969) are reproduced here:

$$\frac{K_1}{K} - 1 = c\left(\frac{K_1-K_2}{K_1}\right) \frac{3K_1+4\mu_2}{3K_2+4\mu_2+3\pi\alpha\mu_1(3K_1+\mu_1)/(3K_1+4\mu_1)}$$

$$\frac{\mu_1}{\mu} - 1 = \frac{c}{5}\left[1 + \frac{8\mu_1}{4\mu_2+3\pi\alpha\mu_1(3K_1+2\mu_1)/(3K_1+4\mu_1)} + \frac{2(3K_2+2\mu_2+2\mu_1)}{3K_2+4\mu_2+3\pi\alpha\mu_1(3K_1+\mu_1)/(3K_1+4\mu_1)}\right]$$

where

K_1 = bulk modulus of solid material

K = bulk modulus of solid with liquid inclusion

μ_1 = shear modulus of solid material

μ_2 = complex shear modulus of liquid inclusion

C = volume fraction of liquid inclusions

α = aspect ratio of liquid inclusions

Several calculations have been made using Walsh's equation.

Most velocity measurements on ice have been made by the resonance technique which gives the shear and the Young's modulus. An error in length measurement which may result in a discrepancy of 1.5% for the shear and the longitudinal velocities leads to bulk moduli which differ by a factor of two. A shear velocity of 1.88 km/sec and a longitudinal velocity of 3.18 km/sec yield a bulk modulus of 223 kb, while 1.92 km/sec and 3.15 km/sec for shear and longitudinal velocities give a bulk modulus of 102 kb. Fortunately, some data exist on the single crystal elastic constants of ice (Bass et al, 1957). The Voigt-Reuss-Hill average for the bulk modulus from these data gives K_l = 75.3 kb. Two sets of calculations have been performed; in the first a bulk modulus of 223 kb was used, in the second K_l was 75.3 kb.

The aspect ratios have also been varied as shown in Figures 13 and 14. If the film surrounds individual grains, their aspect ratio will increase with increasing melt content and be a function of the relative volume of the liquid. The aspect ratios can, at most, be proportional to the volume of the brine. Marked curves in Figures 13 and 14 show the effects of the aspect ratio being proportional to volume. The solid lines are for experimentally determined ratios. The aspect ratio for the 1% NaCl ice is approximately twice that of the 2% NaCl ice which is consistent with their relative platelet sizes. In all cases, the slope of the experimental

velocities are bracked by the slope of the velocities predicted from constant aspect ratio calculations and those for which the aspect ratio is proportional to the relative brine volume. Slightly different aspect ratios are needed to fit the longitudinal and shear velocities. This is believed to be due to the anisotropy mentioned earlier.

Considering the large anisotropy in the ice rods which were used in this experiment, the agreement of these data with the theory of Walsh can be considered as a confirmation of the latter.

The treatment of attenuation due to penny-shaped liquid inclusions (Walsh, 1968) considers the matrix material to have an infinite Q. The Q of the composite material is assumed to be due only to the inclusion of the viscous liquid. Only the shear component of the elastic wave shows appreciable attenutaion. According to Walsh's equations (Walsh, 1969), Q is inversely proportional to frequency as is observed for the longitudinal case. In the case of shear waves the data are not as complete but suggest that the inverse may hold.

For ease of computation, Walsh's (1969) equations #2 have been rewritten and are given below:

$$Q_{\beta}^{-1} = \frac{c\omega\eta}{30D}\left[\frac{4LS}{\alpha^2} + \frac{N}{P+\alpha R}\right]$$

where

$$D = 1 + \frac{C}{7.5}\left[\frac{L}{\alpha} + M\right]$$

$$L = \frac{4}{3\pi}\left(\frac{3K_1 + 4\mu_1}{3K_1 + 2\mu_1}\right), \quad M = 3 + \frac{2\mu_1}{K_2}, \quad N = \frac{8\mu_1}{K_2} + \frac{9K_2}{\mu_1} + 12$$

$$S = \frac{2}{3\pi\mu_1}\left(\frac{3K_1 + 4\mu_1}{3K_1 + 2\mu_1}\right), \quad P = \left(\frac{2\,K_2}{3}\right), \quad R = \frac{2\pi\mu_1}{3}\left(\frac{3K_1 + \mu_1}{3K_1 + 4\mu_1}\right)$$

Since $\omega_c >> \omega$ and $\omega_d >> \omega$ terms like $1 + \left(\frac{\omega}{\omega_c}\right)^2$ have been neglected. The parameters $\frac{d^3}{V}$ in Walsh's equation (1969) are related to the concentration and the size of the liquid inclusions. In the present case, where the thin films of liquid are separating individual grains, this parameter becomes $\frac{4c}{\pi\alpha}$. The viscosity of the fluid is η; all other parameters are those used in the velocity calculations.

Using the above equations, values for Q have been calculated for several aspect ratios for the 1% and 2% shear data. The absolute Q values were much too high when the viscosity of water was used; therefore, the calculated values were normalized to correspond roughly to the observed values. These are shown in Figures 15 and 16 for constant aspect ratio and for an aspect ratio which is proportional to the volume. It should be noted that according to these calculations, Q increases for the varying aspect ratio while the velocities decrease slightly (see Figures 13 and 14).

Vaisnys (1968) treats the problem of propagation of acoustic waves through a system which undergoes phase transitions. He treats only the part of the sound absorption which is due to disturbing a system which otherwise is in thermodynamic equilibrium. Due to the large mechanical effects of grain boundary loosening, all of the present experimental data are not amenable to his treatment.

The minima in both Q and velocity at the eutectic point suggest that the absorption there is largely due to the perturbation of the thermodynamical equilibrium. The relative energy loss according to equation 12 (Vaisnys, 1968) is given by:

$$Q^{-1} = \frac{C_\infty^2 - C_0^2}{C_0^2} \frac{v}{C_0} \frac{\omega/\kappa}{1 + \left(\frac{\omega}{\kappa}\right)^2}$$

where ω is the frequency of the acoustic wave and v its phase velocity. C_0 and C_∞ are the velocities at thermodynamic equilibrium and at constant extent of reaction, respectively. That is, C_0 corresponds to the equilibrium velocity and C_∞ to the frozen velocity. κ is the characteristic rate of the phase transformation.

The velocities obtained at the eutectic temperature while increasing and decreasing the temperature give approximate values of C_0 and C_∞, respectively. To a first approximation $\frac{v}{C_0}$ is one. The corresponding values of Q have been estimated from Figures 8 and 10. Since inverse Q's are additive, the appropriate values for Q^{-1} are given by $Q^{-1} = \Delta Q Q_1^{-1} Q_2^{-1}$; where ΔQ is the depth of the dip and Q_1 and Q_2 are the values at the top and the bottom of the dip. The necessary data are therefore available to calculate the characteristic reaction rate for the freezing of the brine at the eutectic temperature. Table 2 gives the appropriate values. The reaction rate is on the order of 200 cycles/sec, thus lower than the experimental frequencies, which implies an increasing Q with increasing frequency as observed.

Conclusions

There are a number of generalizations which can be made from the data of this investigation. A small volume fraction of liquid has a large effect on the velocity and attenuation of shear and longitudinal waves. As expected, the effect on the shear velocity is considerably more than the effect on the longitudinal velocity.

Due to the anisotropy of the ice rods, no direct comparison can be made between the velocities and Q's of the shear and the longitudinal modes. The sharp dip in Q at the eutectic point, however, is of more than passing interest. This dip was observed on all ice rods but was most pronounced in the shear data for ice containing 1% NaCl. This dip may be explained as follows:

Any multicomponent, multiphase system which is in equilibrium will be disturbed by an acoustical signal. The degree to which the equilibrium is disturbed is a function of the frequency and amplitude of the signal. The chemical kinetics, that is, the rate at which the chemical equilibrium can follow temperature and pressure fluctuations, controls the frequency dependence of the ultrasonic absorption. At a given frequency, the absorption is a function of the concentration gradients associated with the temperature and pressure fluctuations caused by the stress wave.

Energy is absorbed from the acoustic signal and converted into chemical energy. This chemical energy is released in the form of heat as the system returns to its predisturbance equilibrium. The slope of the curves in Figure 6 gives a measure of the extent to which

the equilibrium may be disturbed by a small change in temperature. At the eutectic where the slope is discontinuous, the absorption should be a maximum, as is observed.

The above described absorption mechanism is well known and has been used to study reaction kinetics in liquids (Tabuchi, 1957, 1958; Yasunaga et al, 1965; Tatsumoto, 1967) in the megacycles-per-second range.

The above arguments suggest that a sharp dip in Q will be associated with the onset of partial melting in the mantle. Solid-solid phase changes may show similar dips.

The low-velocity zone of the upper mantle has been interpreted in terms of (a) proximity to the melting point (Press, 1959), (b) high temperature gradients (Gutenberg, 1959; Birch, 1952; Valle, 1956), and (c) chemical inhomogeneity in the mantle (Ringwood, 1962).

As Clark and Ringwood (1964) point out, data on KCl and NaCl (Hunter and Siegel, 1942; Enck, 1960) indicate that melting is a discontinuous phenomenon which occurs over a very small temperature range. The data of the present investigation confirms this conclusion. It furthermore indicates that in a multicomponent system the physical properties drop abruptly at the solidus.

REFERENCES

Bass, Rossberg, and Ziegler, Zeitz. Phys., 149, 199, 1957.

Birch, F., Elasticity and constitution of the earth's interior, J. Geophys. Res., 57, 227-286, 1952.

Clark, S. P., Jr., and A. E. Ringwood, Density distribution and construction of the mantle, Rev. Geophys., 2, 1, 35-88, 1964.

Enck, F. D. Behavior of the principal elastic moduli and specific heat at constant volume of KCl at elevated temperatures, Phys. Rev., 119, 1873-1877, 1960.

Gutenberg, B., The asthenosphere low-velocity layer, Annali di Geofisica, 12, 439-460, 1959.

Hunter, L., and S. Siegel, The variation with temperature of the principal elastic moduli of chlorides near the melting point, Phys. Rev., 61, 84-90, 1942.

MacKenzie, J. K., The elastic constants of a solid containing spherical holes, Proc. Phys. Soc., 63, 1950.

Mizutani, H., and H. Kanamori, Variation of elastic wave velocity and attenuative property near the melting temperature, J. Physics of the Earth, 12, 2, 43-49, 1964.

Porkorny, M., Variation of velocity and attenuation of longitudinal waves during the solid-liquid transition on Wood's alloy, Studia Geoph. et Geod., 9, 1965.

Press, F., Some implications on mantle and crustal structure from G waves and Love waves, J. Geophys. Res., 64, 565-568, 1959.

Ringwood, A. E., A model for the upper mantle, J. Geophys. Res., 67, 857-867, 1962b.

Ringwood, A. E., A model for the upper mantle, 2, J. Geophys. Res., 67, 4473-4477, 1962c.

Rohatgi, P. K., C. M. Adams, Jr., Ice-brine dendritic aggregate form on freezing of aqueous solutions, J. of Glaciology, 6, 47, 1967.

Sato, Yasuo, Velocity of elastic waves propagated in media with small holes, Bull. Earthq. Res. Inst., 7, 102-119, 1952.

Tabuchi, D., Dispersion and absorption of sound in liquids in general chemical equlibrium and its application to chemical kinetics, J. Chem. Phys., 26, 5, 993-1001, 1957.

Tabuchi, D., Dispersion and absorption of sound in ethyl formate and study of the rotational isomers, J. Chem. Phys., 28, 6, 1014-1021, 1958.

Tatsumoto, N., Ultrasonic absorption in propionic acid, J. Chem. Phys., 47, 11, 4561-4570, 1967.

Vaisnys, J. R., Propagation of acoustic waves through a system undergoing phase transformations, J. Geophys. Res., 73, 24, 1968.

Valle, P. E., On the temperature gradient necessary for the formation of a low velocity layer, Ann. Geofis. Rome, 9, 371-377, 1956.

Walsh, J. B., A new analysis of attenuation in partially melted rock, in press, 1969.

Walsh, J. B., Attenuation in partially melted material, J. Geophys. Res., 73, 6, 2209-2216, 1968.

Weeks, W. F., Studies of salt ice, 1: The tensile strength of NaCl ice, Research Report 80, U. S. Army Cold Regions Research and

Engineering Laboratory, Corps of Engineers, New Hampshire.

Yasunaga, T., N. Tatsumoto, and M. Miura, Ultrasonic absorption in sodium metaborate solution, J. Chem. Phys., 43, 8, 2735-2738, 1965.

Table 1

Values used in calculating the velocities in a solid with isolated spherical brine-filled holes by the method of Sato.

T°C	Salinity	ρ_{liquid}	ρ_{ice}	(1-D)	(1-ρ)	V_P	V_S	V_L
-20°C	1%	1.190	.9198	-.294	.035	3.467	1.808	2.930
	2%	1.215	.9198	-.321	.065	3.370	1.744	2.830
-13°C	1%	1.133	.9185	-.234	.049	3.432	1.782	2.890
	2%	1.135	.9185	-.236	.096	3.280	1.687	2.741
-10°C	1%	1.113	.9180	-.212	.059	3.402	1.763	2.861
	2%	1.114	.9180	-.214	.119	3.210	1.644	2.673
-8°C	1%	1.098	.9178	-.196	.070	3.369	1.742	2.828
	2%	1.102	.9178	-.201	.140	3.146	1.604	2.611

$\sigma_o = .311$, $V_{PO} = 3.59$ km/sec $V_{SO} = 1.88$ km/sec $V_{LO} = 3.04$ km/sec

$K = .266$

Table 2

Values used in the calculation of the characteristic reaction rate κ for the melting-freezing reaction of the brine at the eutectic temperature

Meas.	Frequency	C_∞ km/sec	Co km/sec	Q^{-1}_{min}	Q^{-1}_{max}	ΔQ	Q^{-1}	κ sec^{-1}
1% Long	5×10^3	2.92	2.85	.0091	.0068	37	.0022	220
1% Long	10×10^3	2.92	2.85	.0123	.0111	9	.0012	240
1% Shear	3×10^3	1.92	1.58	.0109	.0077	48	.0037	130

FIGURE CAPTIONS

Figure 1. A view parallel to the c-axis orientation of the ice platelets in ice containing 2% NaCl.

Figure 2. Schematic illustration of the shear resonance experiment.

Figure 3. Tracing of strip chart recording of a typical frequency sweep.

Figure 4. Longitudinal (V_L) and shear (V_S) velocities in pure ice, ice containing 1% NaCl and ice containing 2% NaCl. Note the large drop in velocity at the eutectic temperature and the hysteresis between the warming and cooling cycles.

Figure 5. V_L and V_S as a function of brine volume. The ice crystals in the 1% NaCl-ice system have linear dimensions approximately twice as large as in the 2% NaCl-ice system.

Figure 6. Volume per cent brine vs. temperature and composition in the system studied. Insert shows the phase diagram of the NaCl system (Weeks, 1961). Dashed lines are the compositions studied.

Figure 7. Q for first three harmonics, longitudinal modes, heating cycle.

Figure 8. Q for first three harmonics, shear or torsional modes, heating cycle.

Figure 9. Q for first two harmonics, shear or torsional modes. Arrows indicate whether the data were taken on the warming or cooling cycle.

Figure 10. Q in shear for first three harmonics. Arrows pointing to the left indicate that the data were taken on the warming cycle. Arrows pointing to the right indicate that the data were taken on the cooling cycle -- note the supercooling in this latter case.

Figure 11. Q as a function of temperature and frequency for pure ice, longitudinal modes.

Figure 12. Q as a function of temperature and harmonic for shear modes in pure ice. Also shown are the results in flexure obtained by Kuroiwa (1965).

Figure 13. Observed and calculated values of velocity versus temperature. The data used in the calculations by Sato's method are given in Table 1. Data used in Walsh's are $V_{S_{ice}} = 1.88$ km sec^{-1}, $V_{P_{ice}} = 3.04$ km sec^{-1}, $K_{ice} = 75.3$ kb, $K_{liquid} = 20$ kb, and $\mu_{ice} = 32.4$ kb.

Figure 14. Observed and calculated values of velocity versus temperature according to Walsh. Data: $V_{S_{ice}} = 1.88$ km sec^{-1}, $V_{P_{ice}} = 3.18$ km sec^{-1}, $K_{ice} = 223$ kb, $K_{liquid} = 20$ kb and $\mu_{ice} = 32.4$ kb.

Figure 15. Calculated and observed Q as a function of temperature for shear waves in salt ice containing 1% NaCl. The calculated curves are for constant and varying aspect ratios as described in the text.

Figure 16. Calculated and observed Q as a function of temperature for shear waves in salt ice containing 2% NaCl. The calculated curves are for two constant aspect ratios and one varying aspect ratio.

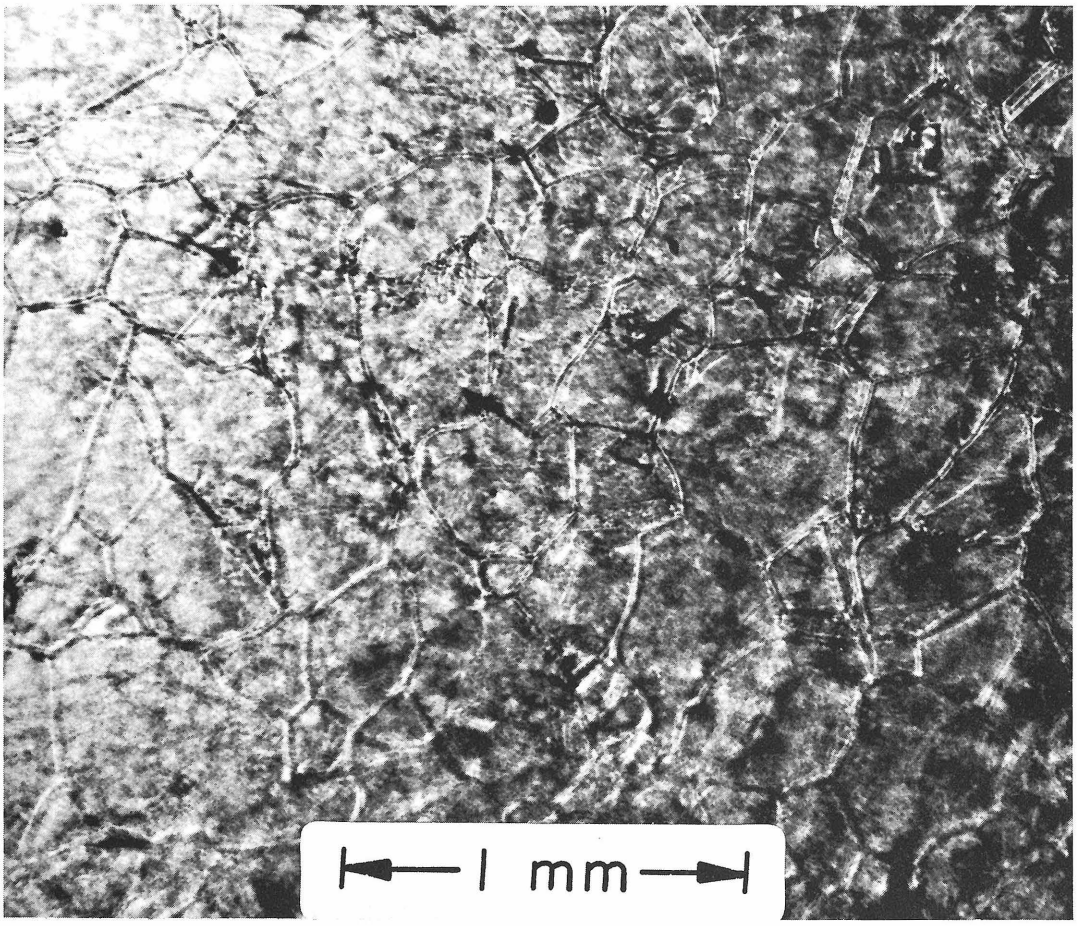

Figure 1

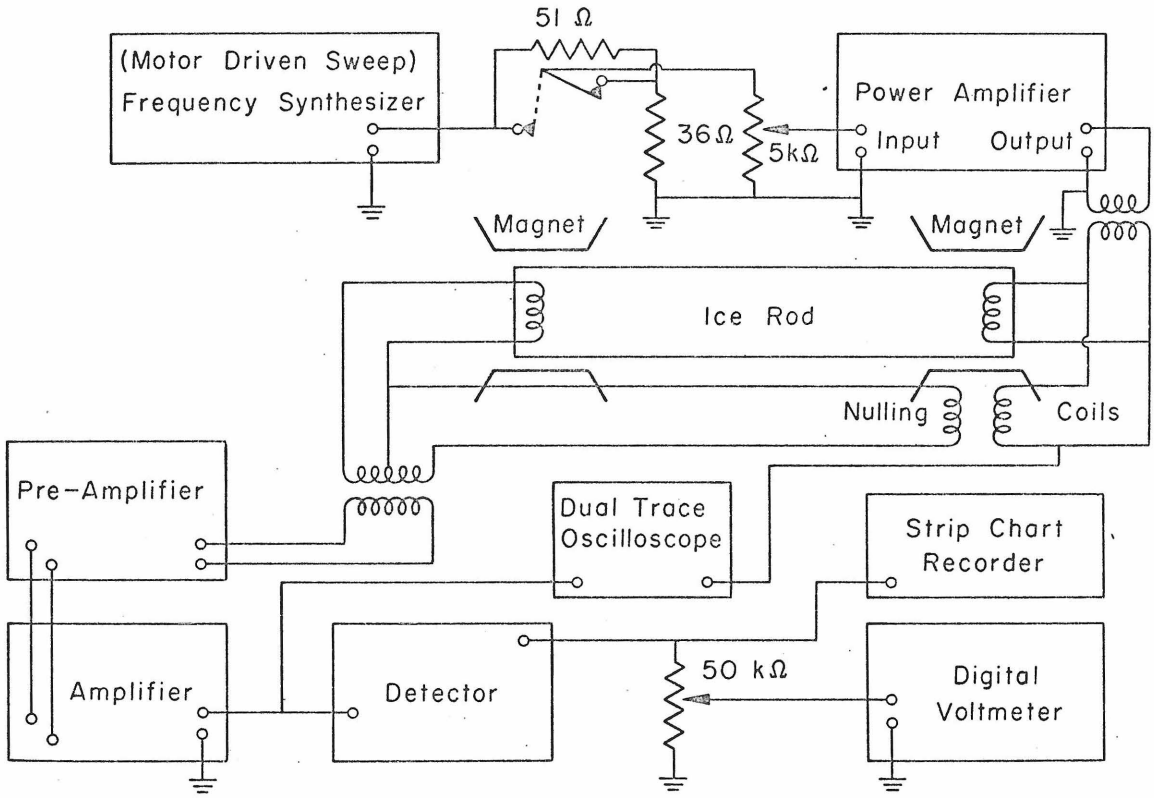
51 Ω
(Motor Driven Sweep)
Frequency Synthesizer
36Ω
5kΩ
Power Amplifier
Input
Output
Magnet
Magnet
Ice Rod
Nulling
Coils
Pre-Amplifier
Dual Trace
Oscilloscope
Strip Chart
Recorder
Amplifier
Detector
50 kΩ
Digital
Voltmeter

Figure 2

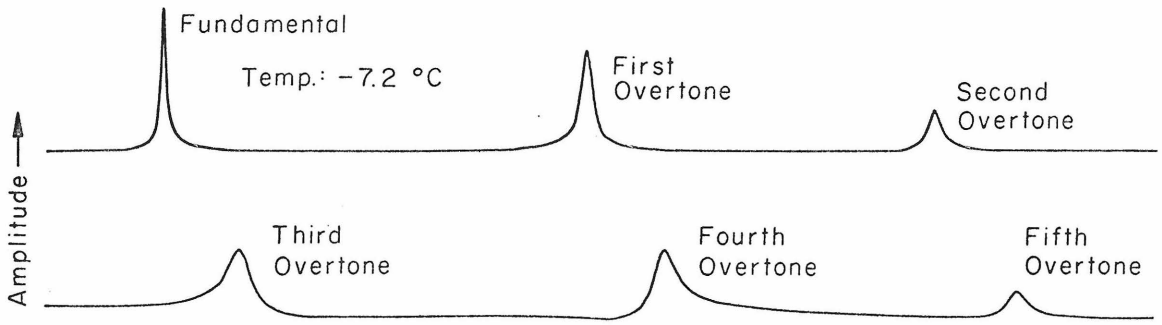

LONGITUDINAL MODES, PURE ICE

Figure 3

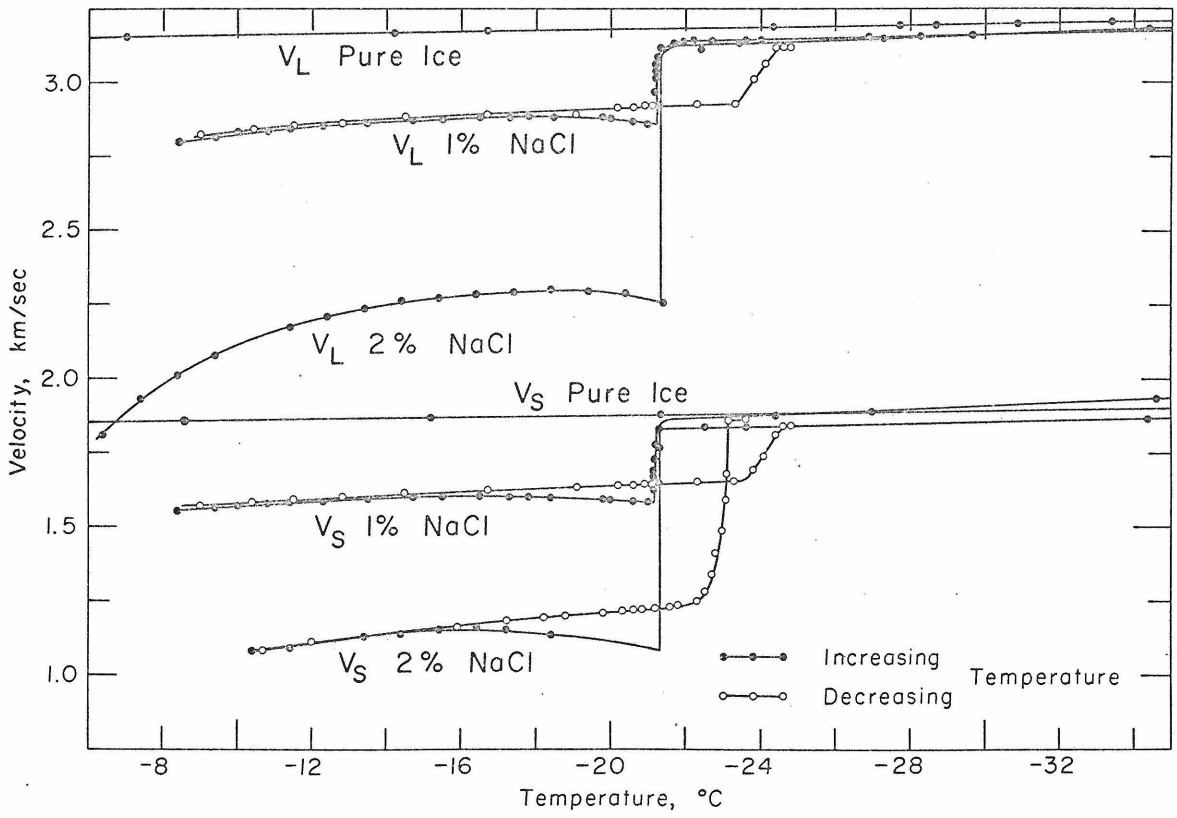
V_L Pure Ice
V_L 1% NaCl
V_L 2% NaCl
V_S Pure Ice
V_S 1% NaCl
V_S 2% NaCl
Increasing
Decreasing
Temperature
Velocity, km/sec
3.0
2.5
2.0
1.5
1.0
-8
-12
-16
-20
-24
-28
-32
Temperature, °C

Figure 4

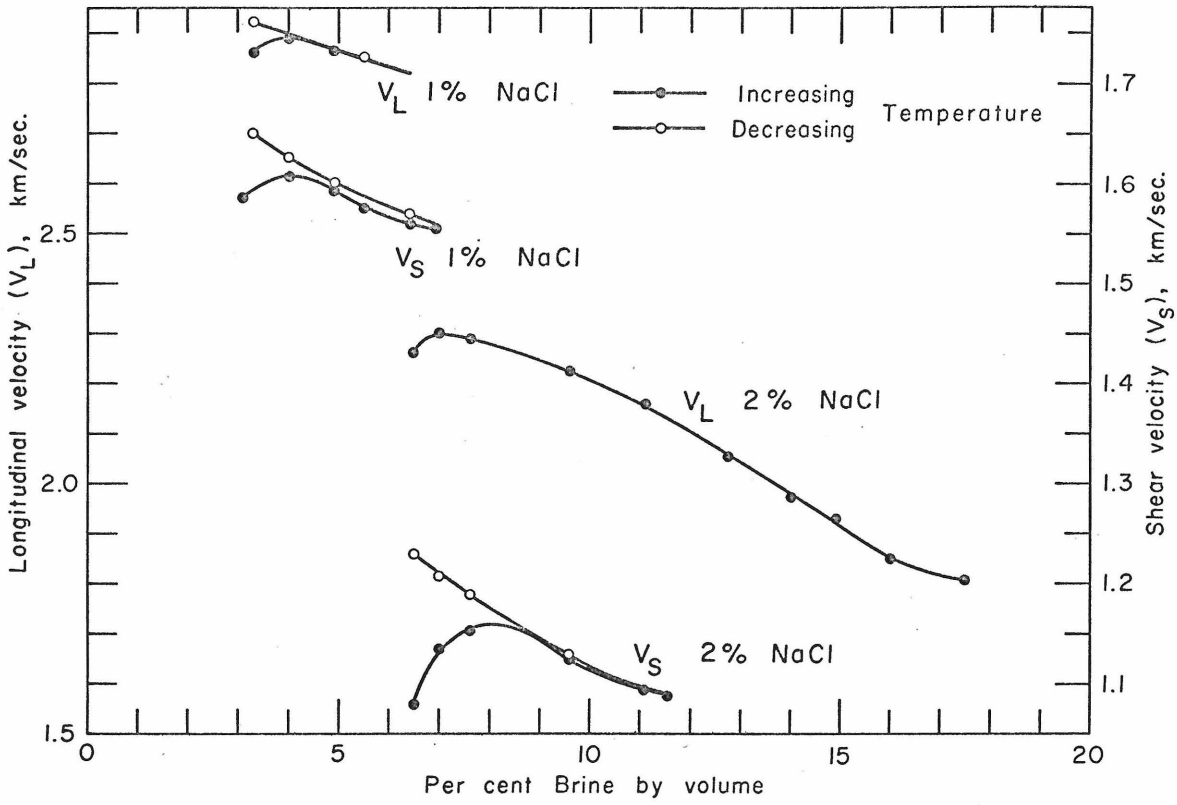
V_L 1% NaCl
Increasing
Decreasing
Temperature
V_S 1% NaCl
V_L 2% NaCl
V_S 2% NaCl
Longitudinal velocity (V_L), km/sec.
Shear velocity (V_S), km/sec.
Per cent Brine by volume
2.5
2.0
1.5
1.7
1.6
1.5
1.4
1.3
1.2
1.1
0
5
10
15
20

Figure 5

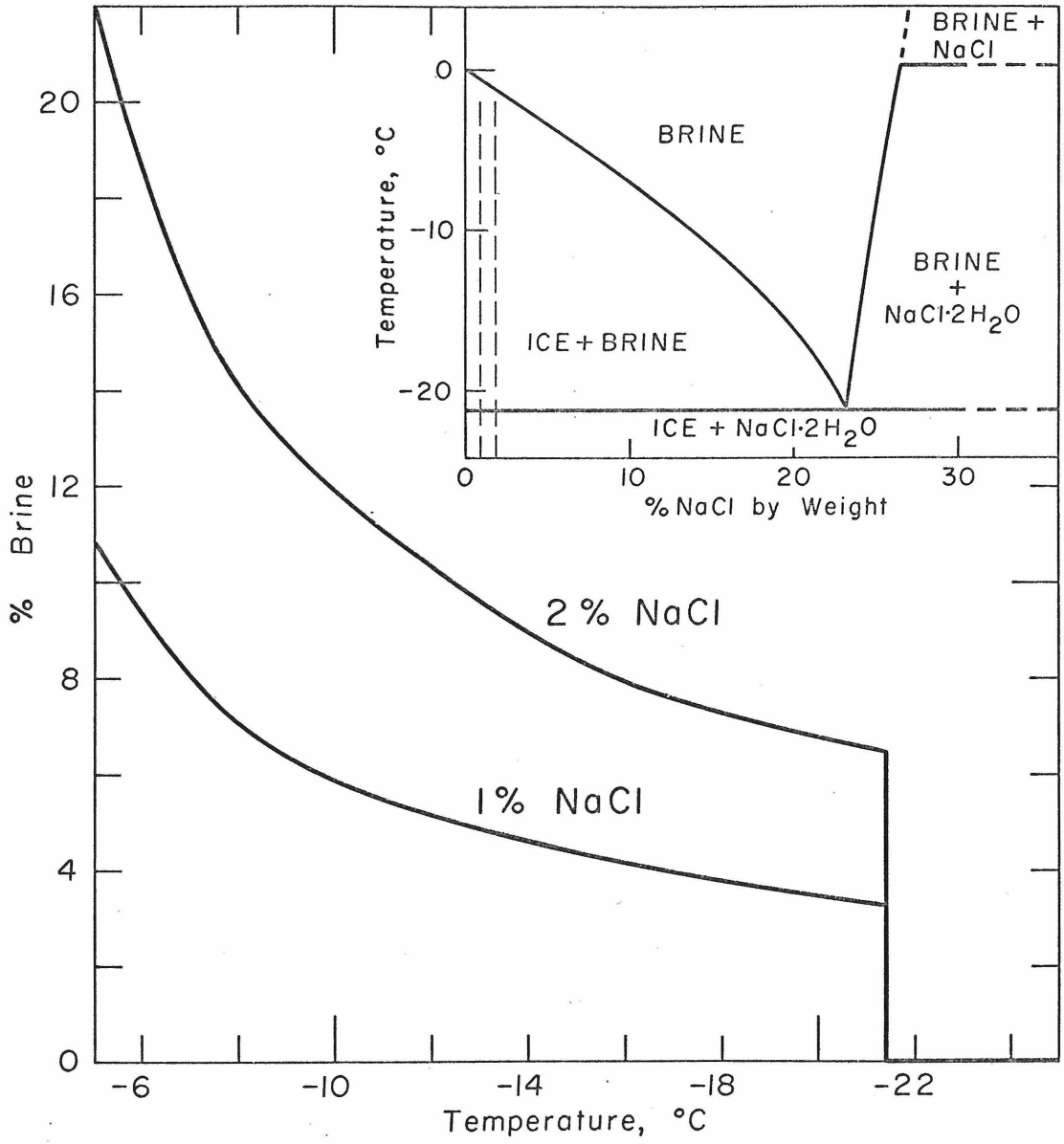
% Brine
20
16
12
8
4
0
-6
-10
-14
-18
-22
Temperature, °C
2 % NaCl
1 % NaCl
Temperature, °C
0
-10
-20
BRINE
ICE + BRINE
BRINE + NaCl
BRINE + NaCl·2H2O
ICE + NaCl·2H2O
0
10
20
30
% NaCl by Weight

Figure 6

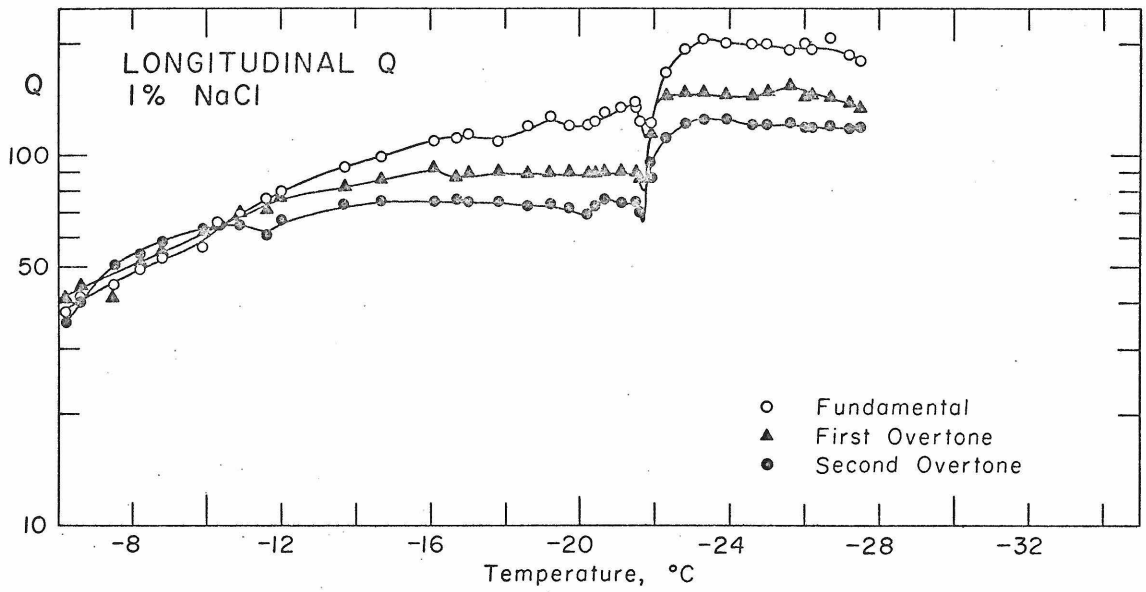
LONGITUDINAL Q
1% NaCl
Q
100
50
10
-8
-12
-16
-20
-24
-28
-32
Temperature, °C
Fundamental
First Overtone
Second Overtone

Figure 7

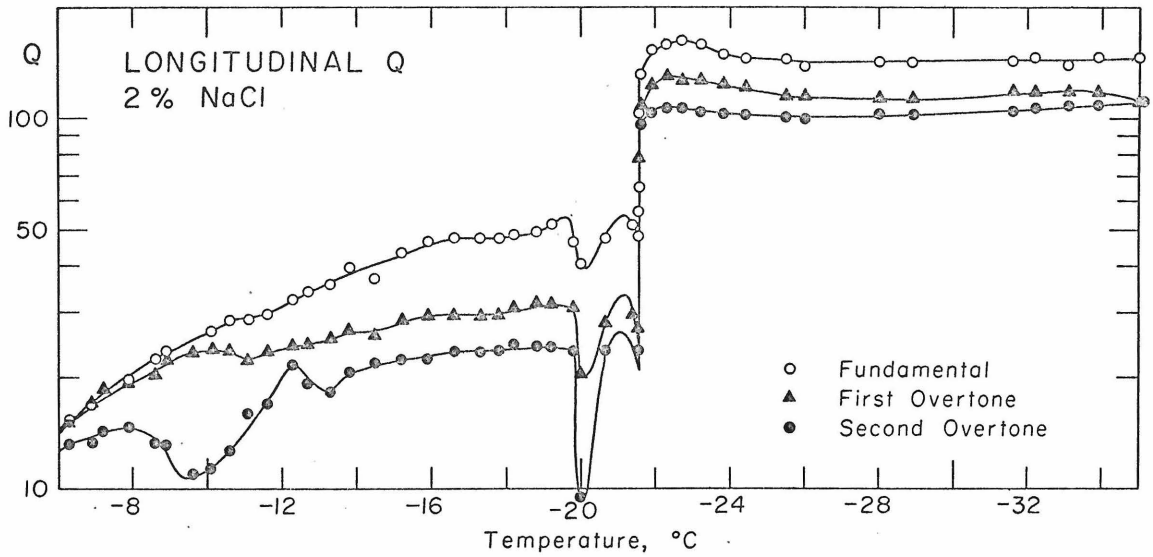
Q
LONGITUDINAL Q
2 % NaCl
100
50
10
-8
-12
-16
-20
-24
-28
-32
Temperature, °C
Fundamental
First Overtone
Second Overtone

Figure 8

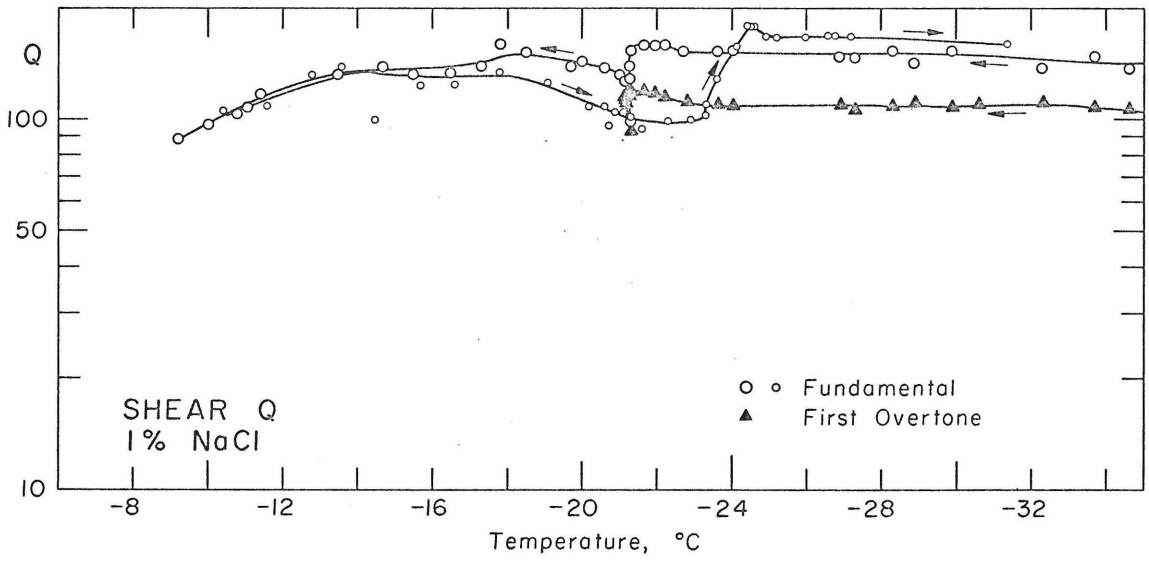
Q
100
50
10
SHEAR Q
1% NaCl
Fundamental
First Overtone
-8
-12
-16
-20
-24
-28
-32
Temperature, °C

Figure 9

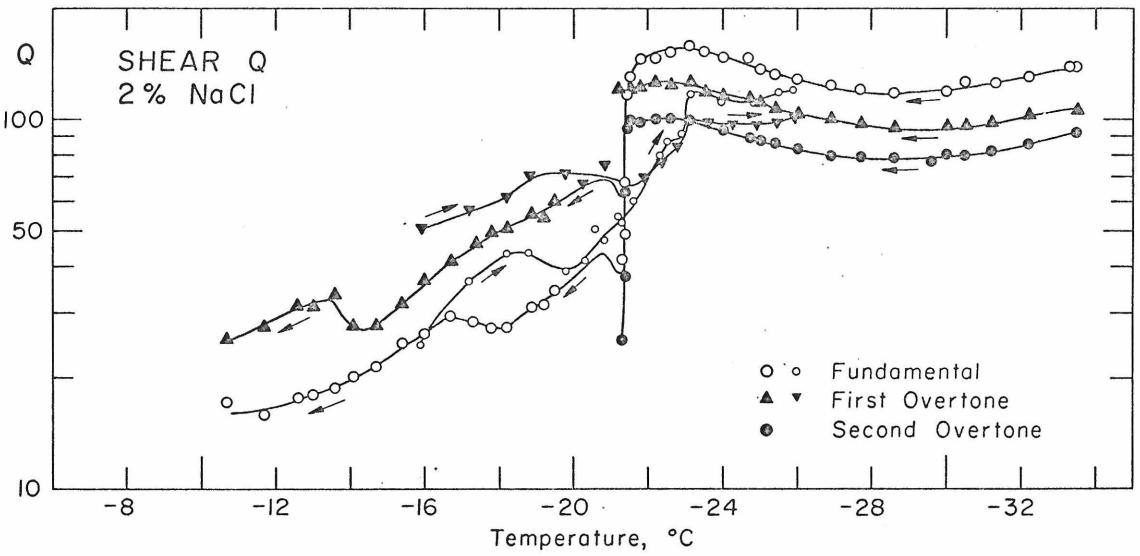
Q
SHEAR Q
2% NaCl
100
50
10
-8
-12
-16
-20
-24
-28
-32
Temperature, °C
Fundamental
First Overtone
Second Overtone

Figure 10

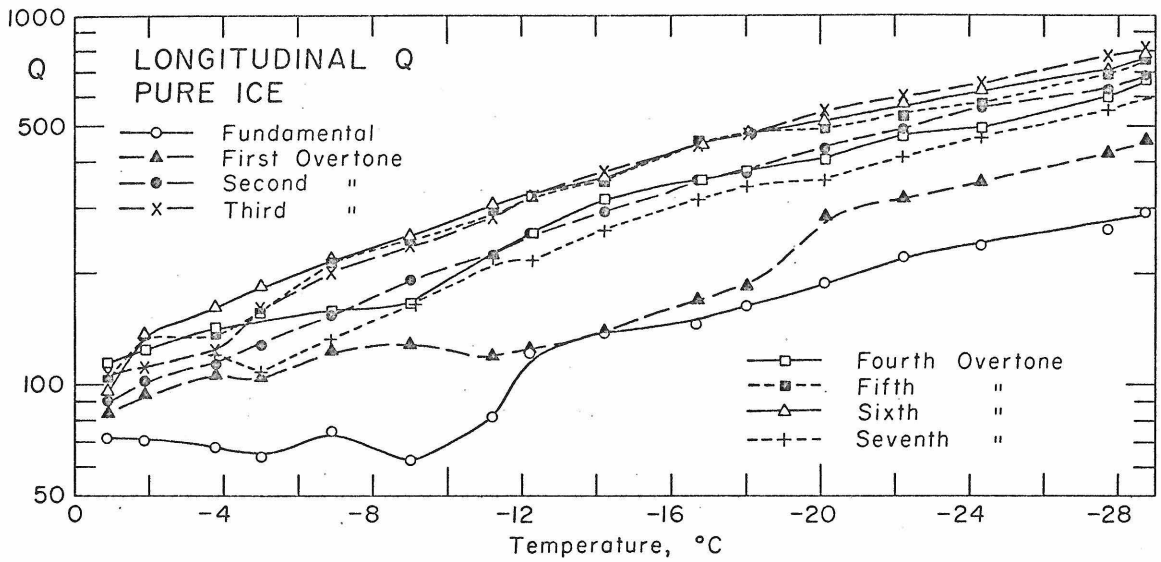
1000
Q
500
100
50
LONGITUDINAL Q
PURE ICE
Fundamental
First Overtone
Second "
Third "
Fourth Overtone
Fifth "
Sixth "
Seventh "
0
-4
-8
-12
-16
-20
-24
-28
Temperature, °C

Figure 11

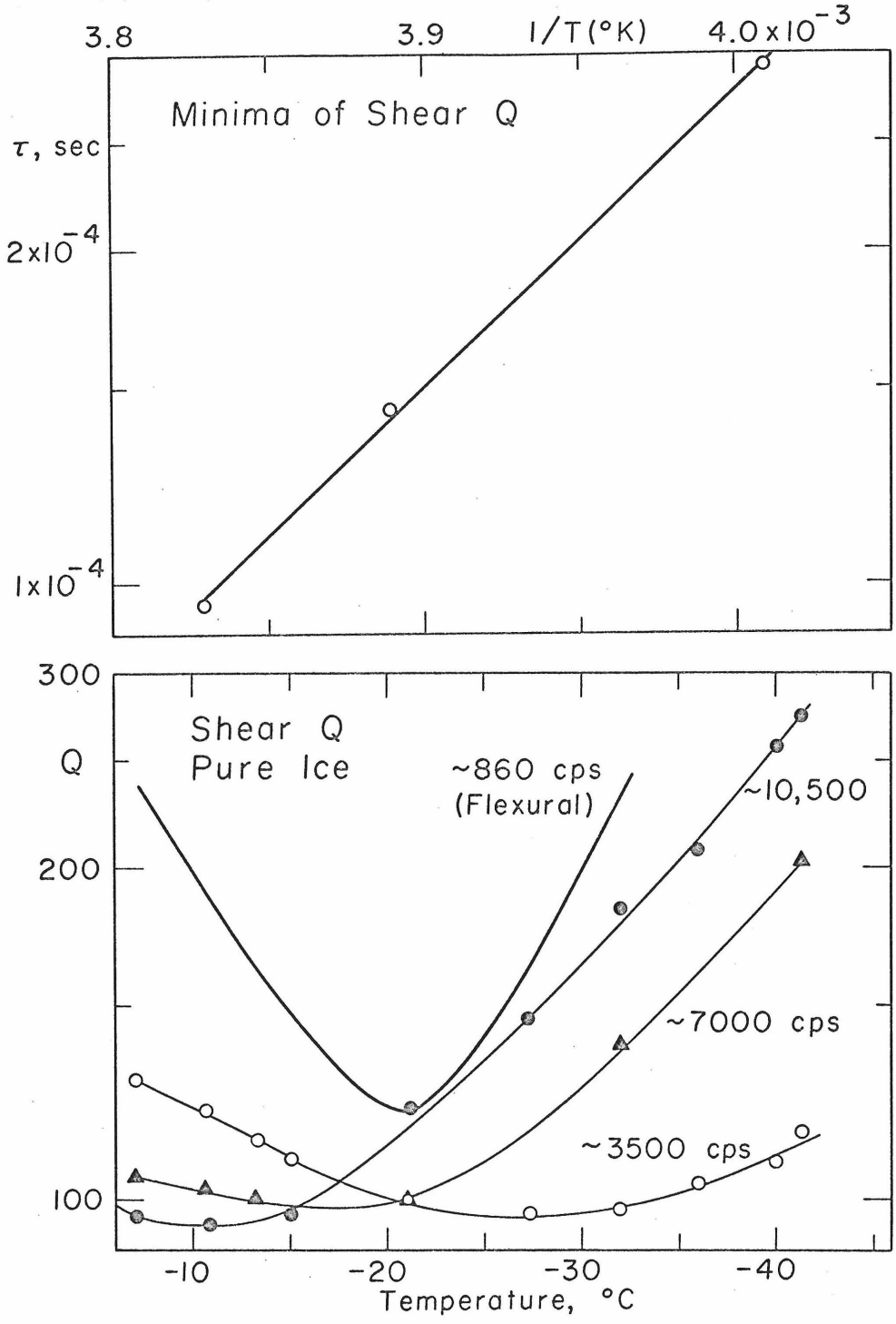
3.8
3.9
1/T(°K)
4.0x10^-3
Minima of Shear Q
τ, sec
2x10^-4
1x10^-4
300
Q
200
100
Shear Q
Pure Ice
~860 cps
(Flexural)
~10,500
~7000 cps
~3500 cps
-10
-20
-30
-40
Temperature, °C

Figure 12

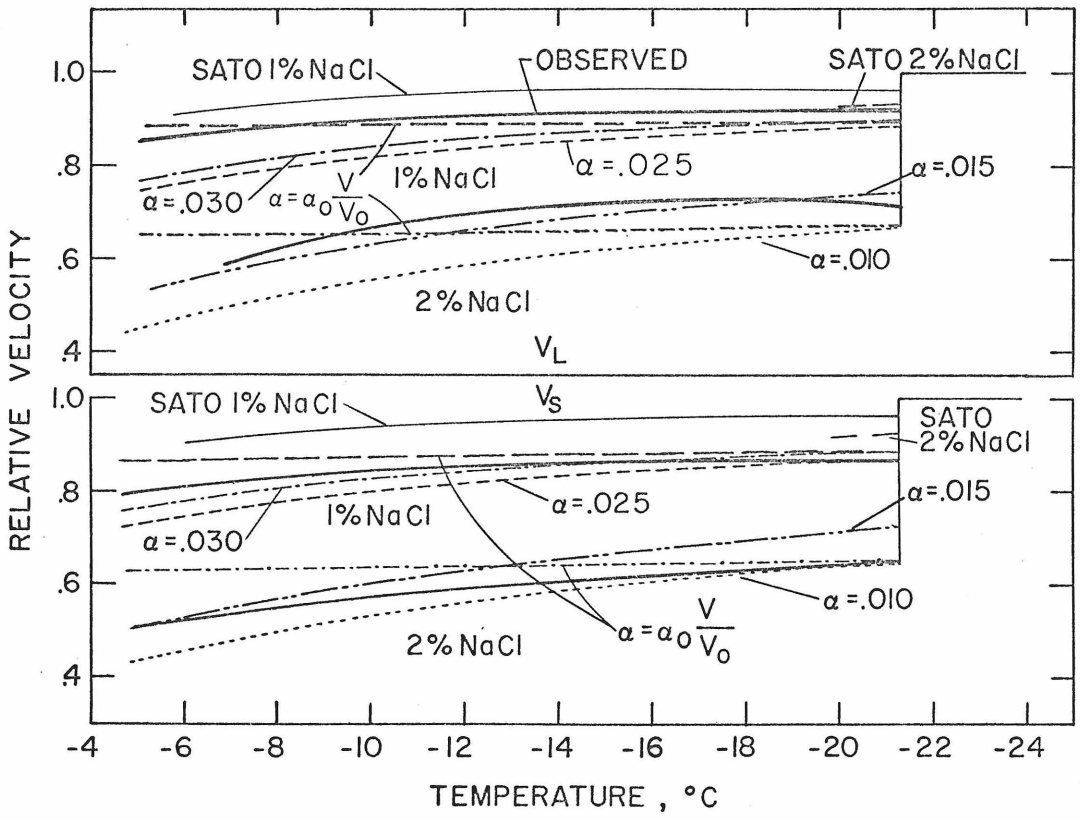
RELATIVE VELOCITY
1.0
.8
.6
.4
SATO 1% NaCl
OBSERVED
SATO 2% NaCl
α = .025
α = .015
α = .030
α = α₀ V/V₀
1% NaCl
α = .010
2% NaCl
V_L
V_S
SATO 1% NaCl
SATO 2% NaCl
α = .025
α = .015
1% NaCl
α = .030
α = .010
α = α₀ V/V₀
2% NaCl
-4
-6
-8
-10
-12
-14
-16
-18
-20
-22
-24
TEMPERATURE , °C

Figure 13

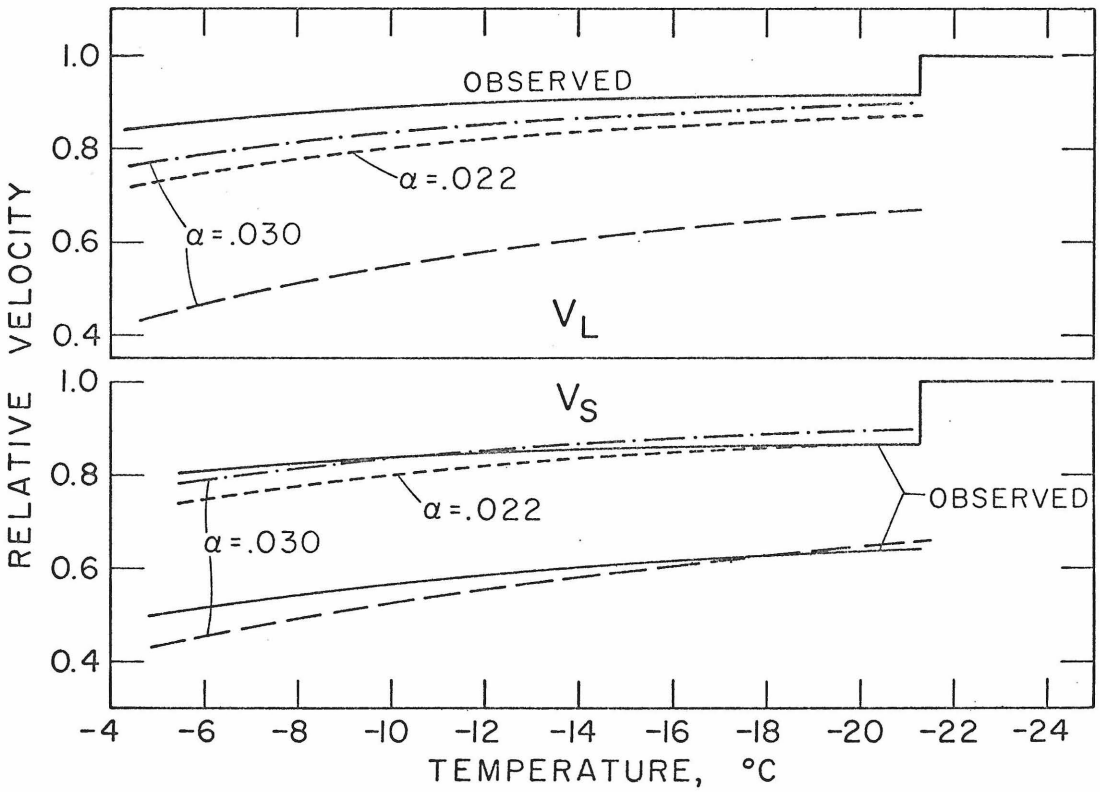
RELATIVE VELOCITY
1.0
0.8
0.6
0.4
OBSERVED
α = .022
α = .030
V_L
V_S
OBSERVED
-4
-6
-8
-10
-12
-14
-16
-18
-20
-22
-24
TEMPERATURE, °C

Figure 14

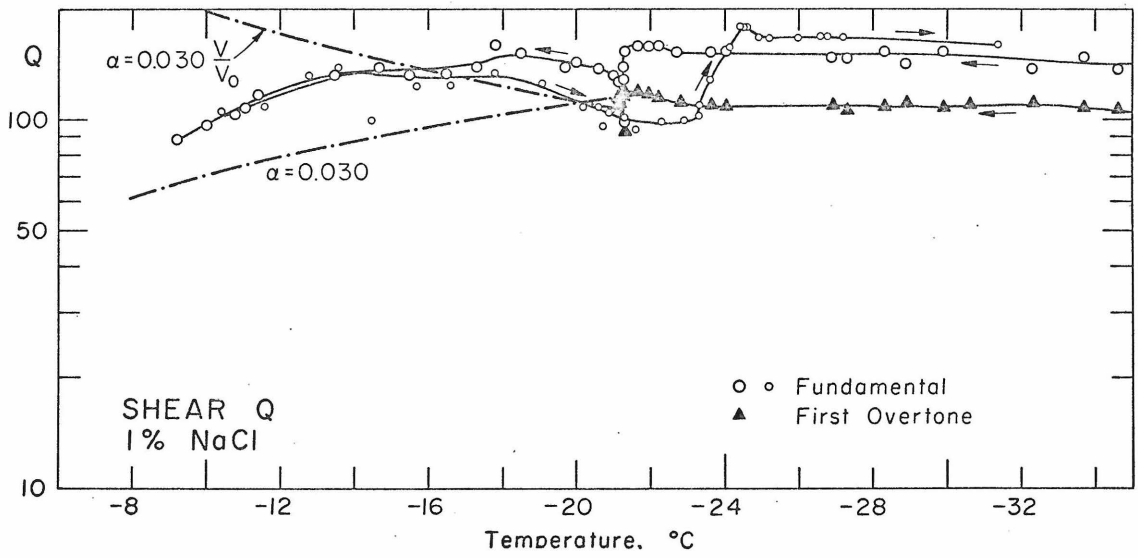
Q
100
50
10
α=0.030 V/V0
α=0.030
SHEAR Q
1% NaCl
Fundamental
First Overtone
-8
-12
-16
-20
-24
-28
-32
Temperature, °C

Figure 15

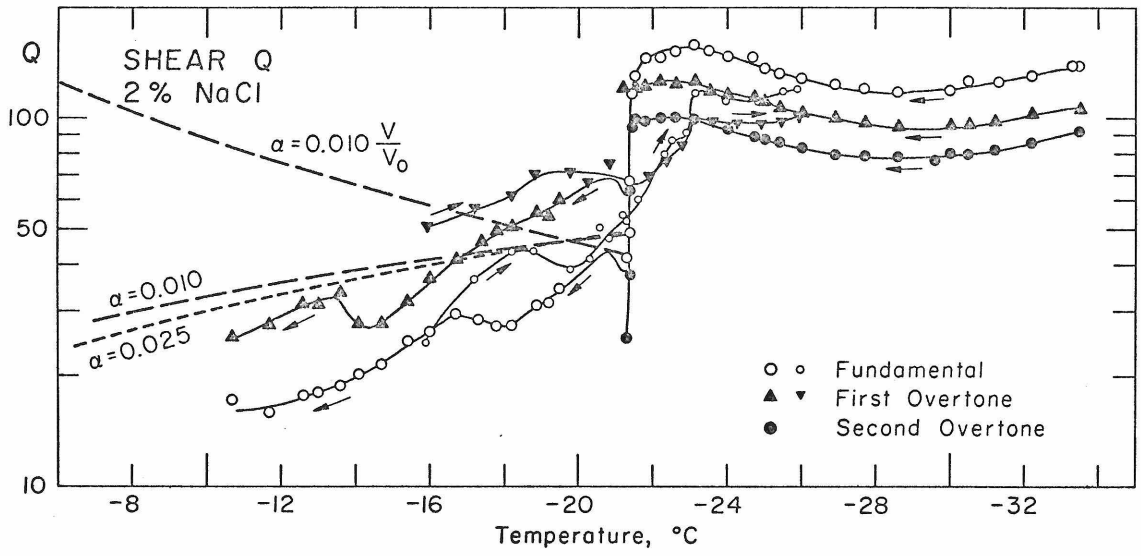
Q
SHEAR Q
2% NaCl
α = 0.010 V/Vo
α = 0.010
α = 0.025
100
50
10
-8
-12
-16
-20
-24
-28
-32
Temperature, °C
Fundamental
First Overtone
Second Overtone

Figure 16

PART II

Chapter 1

EQUATION OF STATE OF POLYCRYSTALLINE MgO TO 9 KB AND 1000°K

Introduction

The study of the elastic constants and their temperature and pressure dependence are of great interest to geophysics. In seismology, a detailed knowledge of the temperature and pressure derivatives of the elastic constants is necessary to determine the internal structure and composition of the earth. This required information is basically obtainable in three ways. The first and oldest technique uses uniaxial presses with appropriate furnaces to obtain length changes in the specimens as a function of temperature and pressure. Maximum pressures and temperatures for this technique are approximately 50 kb and 800°K. The second method involves shock loading the specimen and determining the volume and pressure in the short time during which the sample experiences the high shock pressures. With this technique pressures on the order of several megabars have been reached. The temperatures which exist during shock loading are difficult to measure and have so far been estimated by theoretical means. Specimens which absorb large amounts of energy while being shocked have reached temperatures of several thousand degrees. In the third technique the sound velocity is measured in the sample while the latter is under pressure and temperature. The elastic velocities, being directly related to the elastic constants can be measured very accurately. The data yield not only the elastic constants and their pressure and

temperature derivatives, but also the cross derivatives between temperature and pressure. This method is the most accurate of the three mentioned, but has only been extended to 10 kb and 1100°K.

To date most measurements on geophysically interesting materials have been made as a function of temperature at atmospheric pressure and as a function of pressure at room temperature. The pressure dependence of the temperature derivatives and the temperature dependence of the pressure derivatives of the elastic constants have not been measured.

Until recently (Appendix A) most high temperature data have been obtained by resonance techniques which are not applicable at high pressure. Ultrasonic interferometric methods are, in principle at least, adaptable to high temperature while the specimen is at high pressure. The major difficulty is the bonding of the transducer to the specimen or the specimen to a buffer rod. This difficulty has been overcome with a lapped bond described in Appendices A and B.

Experimental Technique

The ultrasonic technique is illustrated in Figure 1. A Schomandl frequency synthesizer is used as an accurate frequency source, to provide a carrier frequency of about 20 MHz. The output of the synthesizer is brought into an Arenberg Model PG-650C pulsed oscillator which is operated as a gated amplifier. Gate pulses for external operation of the PG-650C must be -80 volts. These are obtained from a General Radio Type 1395A modular pulse generator.

The 1395A is rated at a maximum pulse height of ±20 volts when operated as a modular unit using the internal adder or mixer. In single pulse operation this pulse generator with its P-4 plug-in is capable of supplying a ±100 volt pulse. Three time delay modules operating in series are needed in addition to the P-4 to achieve dual pulse operation. The first and third module control amplitude and width of the first and second pulse independently. The second module provides variable spacing between the pulses. Sufficient isolation between the modules is obtained if the first module is connected directly to the P-4 power amplifier module, while the third module is connected through a 500 Ω resistor. Pulses of ±100 volts are now available from the 1395A. These pulses, when applied to the PG-650C, control the on-time of the 20 MHz RF bursts. An isolation network consisting of four diodes and a 93 Ω attenuator is used to protect the PG-650C from back reflections. The impedance between the isolation network and the quartz transducer, is matched when necessary with an air coupled transformer where both the primary and the secondary are variable (Mattaboni and Schreiber, 1966). The return signals from the transducer are applied without amplification to the top trace of the oscilloscope. They are also displayed after amplification and detection with an Arenberg PG-620 tunable preamplifier and an Arenberg W-600E wide band amplifier. The input of the tunable amplifier is protected by another isolation network as shown. The main sweep of the Hewlett-Packard (HP) 180A

oscilloscope is triggered from the GR 1395A. Each pulse from the GR 1395A also triggers a fast rise time HP 222 pulse generator, which provides the input signal to an HP 5257A time interval counter. The time between the two RF pulses is thus read on the time interval counter and is equal to twice the travel time through the sample.

The delayed sweep is adjusted such that the first echo from the buffer rod-sample interfaceof the first pulse appears at the start of the sweep. The duration of the sweep is adjusted to cover the time for a round trip in the buffer rod. This is sufficient to observe several reverberations in the sample. The delay between the first and second applied pulse is adjusted such that the first echo of the second pulse from the buffer rod-sample interface overlaps the first echo of the first pulse from the free end of the sample. Thus, all further echoes of both pulses overlap.

Since the two applied pulses originate from a common continuous RF source, they are phase coherent. Their respective echoes are only phase coherent when the RF is adjusted such that the number of wavelenths in twice the sample-length corresponds to an integral or half integral number. Whether a half integral or integral number is required for phase coherence depends upon the relative acoustic impedance between the buffer rod and the sample.

In order to determine the phase shift at the buffer rod sample interface and at the free end of the sample, one must recall several facts. A piezoelectric transducer responds to stress and not to particle displacement. The acoustic impedance

of a substance is defined as the product of velocity times density. Consider plane waves normally incident to a plane boundary which separates two media, 1 and 2, having acoustic impedances R_1 and R_2, respectively. Let R_1 be smaller than R_2; a sound wave traveling from medium 1 into medium 2 will be reflected without any change in phase of stress. On the other hand, if the wave is incident from medium 2, the stress wave reflected into medium 2 will show a phase shift of π radians.

The buffer rod-sample system is illustrated in Figure 2. Let the impedance of the buffer rod and the sample be R_1 and R_2, respectively. Consider the two cases illustrated. When the buffer rod impedance is less than the impedance of the sample, every reflection within the sample causes a phase shift of π. In the case where the buffer rod impedance is higher, a phase shift of π within the sample is only realized at the free end.

For the case $R_1 < R_2$ the total phase shift within the sample may be written for the nth echo which is received from the free end

$$\phi_n = \left[1 + 2n\left(\frac{2\ell - m\lambda}{\lambda}\right)\right] \pi$$

where ℓ is the sample length, λ the acoustic wavelength in the sample, and m an integer denoting the number of whole wavelengths within 2ℓ. Maximum or minimum interference between the echo trains of the two applied pulses occurs only if $\frac{(2\ell - m\lambda)}{\lambda}$ is zero or half integer. Let $\frac{(2\ell - m\lambda)}{\lambda}$ equal zero, which implies that there is an integral (m) multiple of the wavelength in 2ℓ. All echoes are phase

shifted by an equal amount and this addition results in a maximum amplitude; i.e., the velocity may be written as:

$$V = \frac{2\ell f}{m}$$

where f is a carrier frequency at which a maximum occurs.

When $\frac{(2\ell - m\lambda)}{\lambda} = 1/2$, $\phi_n = (n + 1)\pi$, i.e., the phase shift between consecutive echoes alternates by π and a minimum in amplitude is realized for an applied pulse spacing equal to one round trip time in the sample.

For the second case, where $R_1 > R_2$, the phase shift in the sample may be written as:

$$\phi_n = n\pi \left[1 + 2 \left(\frac{2\ell - m\lambda}{\lambda} \right) \right]$$

In this case, for $\frac{2\ell - m\lambda}{\lambda} = 0$,

$$\phi_n = n\pi$$

Therefore, a minimum will be realized for the same condition where a maximum is obtained when $R_1 < R_2$. Similarly, for $\frac{2\ell - m\lambda}{\lambda} = 1/2$. It is interesting to note that when a minimum condition exists with two pulses, a maximum condition is reached upon changing the pulse separation by one round trip time of the sample.

The basic components of the high pressure system were designed and built by Harwood Engineering Company of Walpole, Massachusetts, according to our specifications.

Figure 3 shows the pressure generating equipment; the physical construction and operating instructions are described in Appendix D. Argon, from a conventional gas cylinder, is forced into the high pressure vessel, the intensifier (I), and the liquid piston one-to-one converter (LP). The pressure from the bottled gas is sufficient to prime the liquid piston vessel. A 150 psi air tank supplies the air pressure necessary for the hydraulic pumps, DP1 and DP2. The gas is compressed in two stages. The pump DP1 is used to advance the liquid piston vessel (LP), which primes the intensifier (I), and compresses the gas into the vessel to approximately 25,000 psi. The intensifier (I) being charged, is then supplied with up to 15,000 psi from pump DP2. The gas is being compressed to a maximum of 200,000 psi (~14.7 kb). The pressure is read on G-2 to 30,000 psi, on G-9 to 60,000 psi, and with a bridge consisting of manganin coils (Appendix F) above 60,000 psi. Cross checks are being made over the appropriate ranges. A small amount of radioactive Kr^{85} is added to the argon to aid in the detection of small leaks. Kr^{85} is a β emitter and can easily be detected upon escape from the pressure system into the atmosphere (Appendix C).

The furnace assembly, which is shown in Figure 4, is described in Appendix B. The temperature at the sample is measured with two chromel-alumel thermocouples. A Pace Wiancko, Model LRT 47-8TT-1508, thermocouple reference junction is used to provide a stable 150°F reference temperature. The power which is applied to the heating element is controlled by a proportional temperature controller;

Thermac Controller Model MPRY. The high pressure vessel is equipped with a water cooling jacket which maintains the steel body at a low temperature. A flow switch is inserted in the cooling system which disconnects the power from the heater in case the water is shut off.

The proportional temperature controller generates an internal reference potential, the size of which is determined by a ten-turn potentiometer which is calibrated against temperature. The output from the temperature controller is a 60 cycle sine wave which has part of every cycle missing. The most sensitive temperature control is achieved when the firing angle is a minimum, i.e., when the sine wave is almost complete. The disadvantage of a large firing angle is a considerable R. F. Component in the power spectrum. The disadvantages of a silicon controlled rectifier as a power control are overcome by having an adjustable inductive load as a buffer between the power source and the noninductively wound furnace windings. This load is in form of a powerstat which acts as a voltage divider, and a 1:2 transformer acting as a voltage doubler and heavy inductive load. The powerstat is adjusted such that the output from the temperature controller is almost a complete sine wave.

The temperature indicated by the thermocouple which is used to furnish a potential for the temperature controller, is not exact. The reference potential within the controller introduces an error voltage. The effect of this error voltage is eliminated by

isolating the thermocouple from the controller with an impedance matching amplifier. An integrated Fairchild operational amplifier, No. 66E 7741393, is used in a unity gain configuration, the input impedance being in excess of 1 megohm and the output impedance as low as 10 ohms.

Both thermocouple potentials are read on a K-5 Leeds and Northrup potentiometer. The absolute error in temperature due to the pressure effect on the thermocouples is less than ±1°C (Bell et al).

The temperature gradient across the sample is in general less than 1°C, but depends very much on the convection of the gas in the pressure vessel. At a given temperature the convection problems are usually less at high pressure where the viscosity of the gas is high. If the temperature difference between the center and the end of the sample exceeds 1°C the data points are rejected and the pressure is increased. For the highest experimental temperatures of about 1100°K the lowest unstable pressure is on the order of 2.5 kb.

Sample Description

A polycrystalline sample of MgO was obtained through the courtesy of Dr. Vasilos of Avco Corporation, and used in the experiments to be described. The sample was hot-pressed for two hours at 1400°C, at a nominal pressure of 4000 psi (.27 kb); it was cooled slowly in its mold after the pressure was released. No

additives were used in the sintering process. It should be noted that the sample described and measured by Schreiber and Anderson (1968) was obtained from the same source. The density reported in this reference is 3.5797 gr/cm^3 and agrees with the density (3.5798 gr/cm^3) measured in this laboratory to better than one part in 10,000. The grain size was measured on a thin section prepared from a chip from the polycrystalline sample and found to be on the order of 10 to 15 μ. While studying the thin section it was noted that some of the grains did not extinguish under crossed polarizers; i.e., the sample was optically anisotropic. Figure 5 shows the thin section under transmitted light. Figures 6 and 7 show the same thin section under crossed polarizers at two different magnifications. The optical anisotropy implies internal strain.

Debye-Scherrer X-ray patterns were taken of the polycrystalline specimen, using NaCl as an internal standard. The results are given in Table 1 and are compared with an MgO powder (MgO powder analytical agent 6015 from Mallinckrodt Chemical Works). The errors indicated are maximum errors. These data give only the separation between the 100 planes and would correspond to the unit cell dimension in an undistorted cubic lattice. According to the data in Table 1, the average distance between the 100 planes in the polycrystalline sample is smaller than in the powder.

Additional information about possible preferred orientation and distortion of the grains was obtained by standard X-ray

diffractometer techniques using Co radiation. Two cylinders of approximately 1.2 cm length and 1.2 cm diameter were cored from the polycrystalline specimen. The specimen denoted by Avco X-1 was cored along the axis of compression during hot-pressing. The elastic constants of this sample were measured under high pressure and high temperature. The specimen Avco Z1 was cored perpendicular to the compression axis. Several X-ray scans were made of each cylinder by rotating the specimens about their cylinder axis; thus, always exposing the same surface with various azimuth angles to the X-ray beam. Both flat ends of the two samples were scanned. The X-ray intensities are given in Table 2. There is only a slight difference between relative intensities of Avco X-1 and Avco Z-1. There is a slight suggestion of a preferred orientation of the 111 planes along the axis of compression. When the relative intensities of the two polycrystalline specimens are compared with the ASTM values or with the standard MgO powder, however, there is a definite increase in the 111 and 222 intensities and a slight increase in the 220 intensities.

The above data suggest a preferred distortion of 100 planes over the 111 and possibly over the 110 planes. There is little indication of preferred orientation of the individual crystals in the aggregate. Under hydrostatic compression and changes of temperature, a single crystal of cubic symmetry does not alter its shape. Under uniaxial compression, however, the length changes along different directions are different. Uniaxial

compression is controlled by the Youngs-modulus in that direction; measurements of Youngs modulus along the three symmetry axis by resonance techniques have been made by Chung and Lawrence (1964). The three Youngs-moduli are $E_{[100]}$ = 2608 kb, $E_{[110]}$ = 3246 kb, and $E_{[111]}$ = 3534 kb. When a powder of random crystallites is compressed, those crystals making initial contact on 100 planes will be compressed relatively easier than those resting on their 110 or 111 planes. It should also be noted, that the shear-moduli order inversely to the Youngs-moduli, namely, $\mu_{[100]}$ = 1568, $\mu_{[110]}$ = 1269, and $\mu_{[111]}$ = 1191. This implies that shear stresses in the 111 planes are effective in deforming lattice-planes which are perpendicular to 111.

Data

All measurements were made along isotherms over a pressure range over which a good signal could be maintained. The frequency at which the data were taken was also determined by the quality of the signal. This frequency was always between 18 and 22 MHz. Again, depending on the signal quality, several maxima and minima were taken to define an average slope. This is illustrated in the frequency versus pressure plot for the 1073°K data run in Figure 8. A good signal is shown in Figure 9. The compressional frequency versus pressure data is shown in Figure 10, where the dashed line at the 773°K isotherm is considered the minimum possible slope and will be referred to later. Figure 11 depicts all data normalized

to one at 300°K and zero pressure. The difference between the effect of temperature on the compressional and the shear frequencies is illustrated in Figure 12. For comparison of the pressure effect on the temperature derivatives, Figure 13 is included. The values for the 10 kb isotherms are taken from the plot in Figure 11.

Data Reduction and Results

As can be seen from the raw data, i.e., frequency versus pressure, straight lines fit frequency versus pressure and temperature very well. The data at this time do not justify a higher order fit. It should be realized, however, that when extrapolating to very high pressures the frequency versus pressure lines for different isotherms will cross, which is physically unrealistic. For lack of more accurate data, equations of the form

$$f = a + bT + (c + dT)P$$

have been fitted to the raw frequency data. The values of the coefficients for the compressional and shear data are given in Table 3.

Various approaches have been used to reduce the frequency data as it is obtained in the laboratory. The methods of Cook (1957) and Thurston (1965) have been utilized most extensively in the literature (Ahrens and Katz, 1962; Anderson and Schreiber, 1965). These methods are applicable over a limited range of temperature and pressure. The conversion of the frequency data to the elastic

constants has therefore been accomplished by writing a set of partial differential equations and solving them simultaneously on a computer. This set is shown in Table 4. The equations are rigorous except for $\left.\frac{\partial \alpha}{\partial T}\right)_P$. In this case it is assumed that the thermodynamic Gruneisen parameter γ is independent of temperature at constant pressure and that the Einstein model gives a good approximation to the vibrational energy of a solid in the range of interest. The Einstein temperature is also assumed to be independent of temperature. Figure 14 gives an indication of the validity of these assumptions by comparing the calculated coefficient of thermal expansion to experimentally determined points. The derivation of the expressions in Table 4 and a description of the computer program will be given in another chapter.

The computed values of the compressional and shear velocities, V_P and V_S, are given in Figures 15 and 16, the adiabatic and isothermal bulk moduli in Figures 17 and 18, and the Poisson's ratio and the shear modulus in Figures 19 and 20. Table 5 shows some values of the data and their pressure and temperature derivatives at selected values of temperature and pressure. Some values of other investigators are included. The values in parentheses correspond to the lowest estimate of the slope of the 773°K isotherm for the compressional frequency as indicated in Figure 10. Due to the limitation of the data, as is evident in the straight line approximations to the variation of the frequency with respect to both temperature and pressure, no information about the change of

the temperature derivatives with temperature is contained in Table 5. This also holds for the change of the pressure derivatives as a function of pressure.

REFERENCES

Ahrens, T. J., and S. Katz, An ultrasonic interferometer for high-pressure research, J. Geophys. Res., 67, 7, 2935-2944, 1962.

Anderson, O. L., and E. Schreiber, The pressure derivatives of the sound velocities of polycrystalline magnesia, J. Geophys. Res., 70, 20, 5241-5248, 1965.

Austin, J. B., Thermal expansion of some refractory oxides, J. Am. Ceram. Soc., 14, 11, 795-810, 1931.

Bell, P. M., F. R. Boyd and T. L. England, The effects of pressure on rhodium and chromel/alumel thermocouples, in press.

Chung, D. H., and W. G. Lawrence, Relation of single-crystal elastic constants to polycrystalline isotropic elastic moduli of MgO: II, Temperature dependence, J. Amer. Ceram. Soc., 47, 9, 448-455, 1964.

Chung, D. H., and G. Simmons, Elastic properties of polycrystalline periclase, J. Geophys. Res., submitted for publication, 1968b.

Cook, R. K., Variation of elastic constants and static strains with hydrostatic pressure: A method for calculation from ultrasonic measurements, J. Acoust. Soc. Am., 29, 4, 445-449, 1957.

Durand, M. A., Coefficient of thermal expansion of magnesium oxide, Physics, 7, 297-99, 1936.

Ganesan, S., Temperature variation of Gruneisen parameter in magnesium oxide, Phil. Mag., 7, 74, 197-205, 1962.

Mattaboni, P., and E. Schreiber, Variable air transformer for impedance matching, Rev. Scientific Inst., 37, 11, 1625-1626, 1966.

Schreiber, E., and O. L. Anderson, Temperature dependence of the velocity derivatives of periclase, J. Geophys. Res., 71, 12, 3007-3012, 1966.

Schreiber, E., and O. L. Anderson, Revised data on polycrystalline magnesium oxide, J. Geophys. Res., 73, 8, 2837-2838, 1968.

Sharma, S. C., Thermal expansion of crystals: IV, Proc. Ind. Acad. Sci., 32A, 4, 268-74, 1950.

Skinner, B. J. Thermal expansions of thoria, periclase, and diamond, Am. Mineralogist, 42, 1-2, 39-55, 1957.

Thurston, R. N., Ultrasonic data and thermodynamics of solids, Proc. IEEE, 53, 10, 1320-1336, 1965.

White, G. K., and O. L. Anderson, Gruneisen parameter of magnesium oxide, J. Appl. Phys., 37, 1, 430-432, 1966.

Table 1

X-ray data for polycrystalline MgO specimen and MgO powder taken with $Cu_{k\alpha}$ radiation.

	a_o in Å
ASTM	4.212
Polycrystalline	4.2198 ± .0010
Powder	4.2241 ± .0010

Table 2

X-ray intensities from diffractometer scans of polycrystalline samples Avco X-1 and Avco Z-1. The cylindrical samples were scanned on both flat ends. One end of Avco Z-1 was also scanned at 3 azimuth angles (60° intervals).

2θ	42.9	50.2	73.8	94.6
hkℓ	111	200	220	222
Sample	Relative Intensities			
Theoretical (ASTM)	10	100	52	12
Powder (Analy. Gr.)	8	100	44	12
Avco X-1 Top	25	100	67	30
Bottom	24	100	79	40
Avco Z-1 Top	19	100	54	27
Bottom I	16	100	51	20
Bottom II	20	100	80	20
Bottom III	16	100	57	22

Table 3

Values used in fitting frequency data to the form

$$f = a + bT + (c + dT)P$$

	a	b	c	d
compressional	1.0213	-7.114×10^{-5}	7.688×10^{-4}	8.940×10^{-7}
shear	1.0303	-10.10×10^{-5}	7.235×10^{-4}	3.452×10^{-7}

Table 4

Relations used in data reduction

Temperature Derivatives

$$\left(\frac{\partial L}{\partial T}\right)_P = \frac{L\alpha}{3} \; ; \; \left(\frac{\partial \rho}{\partial T}\right)_P = -\rho\alpha$$

$$\left(\frac{\partial K_S}{\partial T}\right)_P = -\alpha K_S + 2\rho\left[V_P\left(\frac{\partial V_P}{\partial T}\right)_P - \frac{4}{3}V_S\left(\frac{\partial V_S}{\partial T}\right)_P\right]$$

$$\left(\frac{\partial V_P}{\partial T}\right)_P = V_{PO}\left[\left(\frac{\partial L}{\partial T}\right)_P F_P + L\left(\frac{\partial F_P}{\partial T}\right)_P\right]$$

$$\left(\frac{\partial V_S}{\partial T}\right)_P = V_{SO}\left[\left(\frac{\partial L}{\partial T}\right)_P F_S + L\left(\frac{\partial F_S}{\partial T}\right)_P\right]$$

$$\left(\frac{\partial K_T}{\partial T}\right)_P = \left(\frac{\partial K_S}{\partial T}\right)_P (1+\alpha\gamma T)^{-1} - \frac{K_S\gamma}{(1+\alpha\gamma T)^2}\left[T\left(\frac{\partial \alpha}{\partial T}\right)_P + \alpha\right]$$

$$\left(\frac{\partial \alpha}{\partial T}\right)_P = \frac{\gamma\rho}{K_T}\left(\frac{\partial C_V}{\partial T}\right)_P - \frac{\alpha}{K_T}\left(\frac{\partial K_T}{\partial T}\right)_P - \alpha^2$$

$$\left(\frac{\partial \gamma}{\partial T}\right)_P = 0 \text{ (Assumption)}$$

$$\left(\frac{\partial C_V}{\partial T}\right)_P = \frac{0.2497 \times n}{M}\,\frac{\Theta^2 e^{\Theta/T}}{T^4\left(e^{\frac{\Theta}{T}}-1\right)^2}\left[\frac{\Theta\left(e^{\frac{\Theta}{T}}+1\right)}{T\left(e^{\frac{\Theta}{T}}-1\right)} - 2T\right]$$

$$\left(\frac{\partial \Theta}{\partial T}\right)_P = 0 \text{ (Assumption)}$$

n = No. of atoms per molecular formula

M = Molecular weight

Θ = Einstein temperature

Pressure Derivatives

$$\left(\frac{\partial L}{\partial P}\right)_T = -\frac{L}{3KT}\left(\frac{\partial \rho}{\partial P}\right)_T = \frac{\rho}{K_T}$$

$$\left(\frac{\partial K_S}{\partial P}\right) = \frac{K_S}{K_T} + 2\rho\left[V_P\left(\frac{\partial V_P}{\partial P}\right)_T - \frac{4}{3}V_S\left(\frac{\partial V_S}{\partial P}\right)_T\right]$$

$$\left(\frac{\partial V_P}{\partial P}\right)_T = V_{PO}\left[\left(\frac{\partial L}{\partial P}\right)_T F_P + L\left(\frac{\partial F_P}{\partial P}\right)_T\right]$$

$$\left(\frac{\partial V_S}{\partial P}\right)_T = V_{SO}\left[\left(\frac{\partial L}{\partial P}\right)_T F_S + L\left(\frac{\partial F_S}{\partial P}\right)_T\right]$$

$$\left(\frac{\partial K_T}{\partial P}\right)_T = \left(\frac{\partial K_S}{\partial P}\right)_T (1+\alpha\gamma T)^{-1} - \frac{K_S T}{(1+\alpha\gamma T)^2}\left(\gamma\left(\frac{\partial \alpha}{\partial P}\right)_T + \alpha\left(\frac{\partial \gamma}{\partial P}\right)_T\right)$$

$$\left(\frac{\partial \alpha}{\partial P}\right)_T = +\frac{1}{K_T^2}\left(\frac{\partial K_T}{\partial T}\right)_P$$

$$\left(\frac{\partial \gamma}{\partial P}\right)_T = \gamma\left[\left(\frac{\partial \ell n\, K_S}{\partial P}\right)_T + \left(\frac{\partial \ell n\, \alpha}{\partial P}\right)_T - \left(\frac{\partial \ell n\, \rho}{\partial P}\right)_T + \frac{\gamma T}{\alpha K_S}\left(\alpha^2 + \left(\frac{\partial \alpha}{\partial T}\right)_P\right)\right]$$

$$\left(\frac{\partial \Theta}{\partial P}\right)_T = \Theta\,\frac{\left[\frac{1}{V_P^4}\frac{\partial V_P}{\partial P} + \frac{2}{V_S^4}\frac{\partial V_S}{\partial P}\right]}{\left[\frac{1}{V_P^3} + \frac{2}{V_S^3}\right]}$$

$V_P = V_{PO}\, L\, F_P$;

$V_S = V_{SO}\, L\, F_S$ $\qquad L = \frac{\ell}{\ell_o}$ $\quad F_{P,S} = 1$ at $P = 0$ $\quad T = 300°K$

$K_S = \rho\left(V_P^2 - \frac{4}{3}V_S^2\right)$ $\qquad F = \frac{f}{f_o}$

$K_T = K_S\,(1+\alpha\gamma T)^{-1}$

$\gamma = \frac{\alpha K_S}{C_P \rho}$

Table 5

Selected values of pressure and temperature derivatives at different pressures and temperatures

	$\frac{\partial V_P}{\partial T}$	$\frac{\partial V_S}{\partial T}$	$\frac{\partial V_P}{\partial P}$	$\frac{\partial V_S}{\partial P}$	$\frac{\partial K_S}{\partial T}$	$\frac{\partial K_T}{\partial T}$	$\frac{\partial K_S}{\partial P}$	$\frac{\partial K_T}{\partial P}$	$\frac{\partial \sigma}{\partial T}$	$\frac{\partial \sigma}{\partial P}$
Multiply by	10^{-4}	10^{-4}	10^{-3}	10^{-3}	10^{-1}	10^{-1}	10^{-0}	10^{-0}	10^{-5}	10^{-4}
Units	km sec^{-1}	$°K^{-1}$	km sec^{-1}	kb^{-1}	kb $°K^{-1}$				$°K^{-1}$	kb^{-1}
300°K		-								
0 kb	-5.0[1]	-4.8[1]	8.66[2]	4.23[2]	-1.2[1]	-2.0[1]	4.58[2]		2.9[1]	1.95[2]
			7.80[3]	3.75[3]			4.28[3]	4.35[3]		1.85[3]
This work.	-5.89	-5.47	8.04	3.73	1.45	-2.64	4.44	4.46	3.64	2.59
800°K	-5.64	-5.32	11.84	4.48	1.51	-2.52	6.45	6.26	3.88	5.79
0 kb			(10.53)				(5.51)			
300°K	-5.11	-5.31	8.05	3.75	-1.01	-2.20	4.50	4.50	4.29	2.53
10 kb										
800°K	-4.90	-5.18	11.87	4.51	-1.13	-2.18	6.57	6.31	4.49	5.62
10 kb										

Table 5 (continued)

Numbers in parenthesis refer to dashed line in Figure 7.

Superscripts 1, 2, 3, indicate data from Schreiber and Anderson (1966), Schreiber and Anderson (1968) and Chung and Simmons (in press), respectively.

FIGURE CAPTIONS

Figure 1. Block diagram for ultrasonic interferometric and time of flight measurements.

Figure 2. Schematic representation of phase shifts of stress waves in buffer rod-sample system. The phase shifts indicated are for an integral number of wave length in twice the sample length.

Figure 3. Schematic of pressure generating equipment. Maximum system capability is 15 kb in a two inch diameter by 6 inch length sample space.

Figure 4. Cross-section through furnace with sample and buffer-rod in place. A second thermocouple (not shown) is rotated 90° with respect to the one shown and is at the end of the sample.

Figure 5. Microphotograph of polycrystalline MgO; transmitted light.

Figure 6. Microphotograph of polycrystalline MgO; transmitted light, crossed polarizers.

Figure 7. Microphotograph of polycrystalline MgO; transmitted light, crossed polarizers.

Figure 8. Frequency versus pressure data at 1073°K for shear waves.

Figure 9. Oscilloscope echo pattern for shear waves taken at 800°K and 7 kb. Top trace is the unamplified RF signal; bottom trace is the detected and amplified signal.

Figure 20. Shear modulus as function of temperature and pressure. Data reduction according to equations in Table 4.

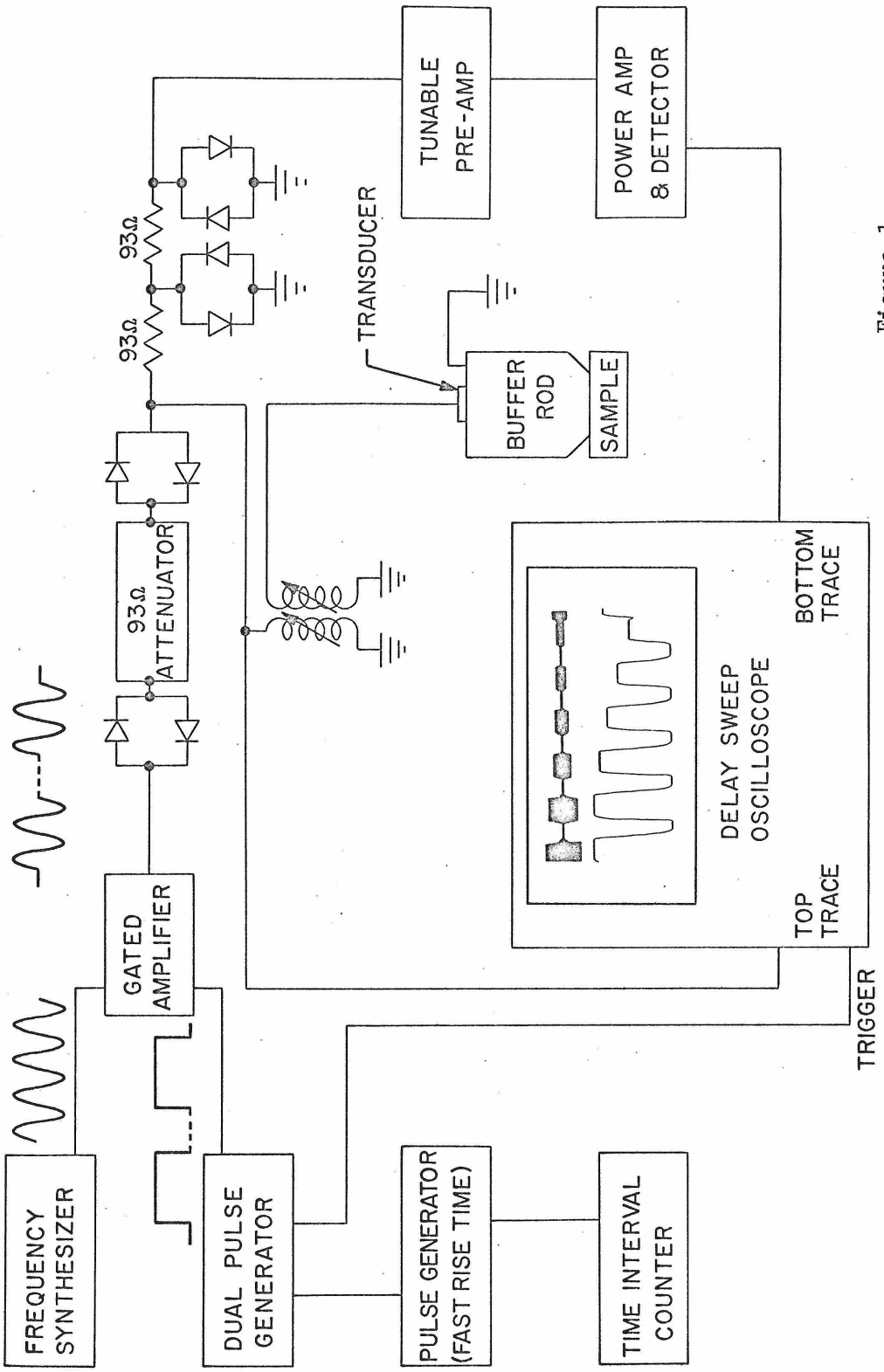
FREQUENCY SYNTHESIZER
DUAL PULSE GENERATOR
PULSE GENERATOR (FAST RISE TIME)
TIME INTERVAL COUNTER
GATED AMPLIFIER
93Ω ATTENUATOR
93Ω
93Ω
TRANSDUCER
TUNABLE PRE-AMP
POWER AMP & DETECTOR
BUFFER ROD
SAMPLE
DELAY SWEEP OSCILLOSCOPE
TOP TRACE
BOTTOM TRACE
TRIGGER

Figure 1

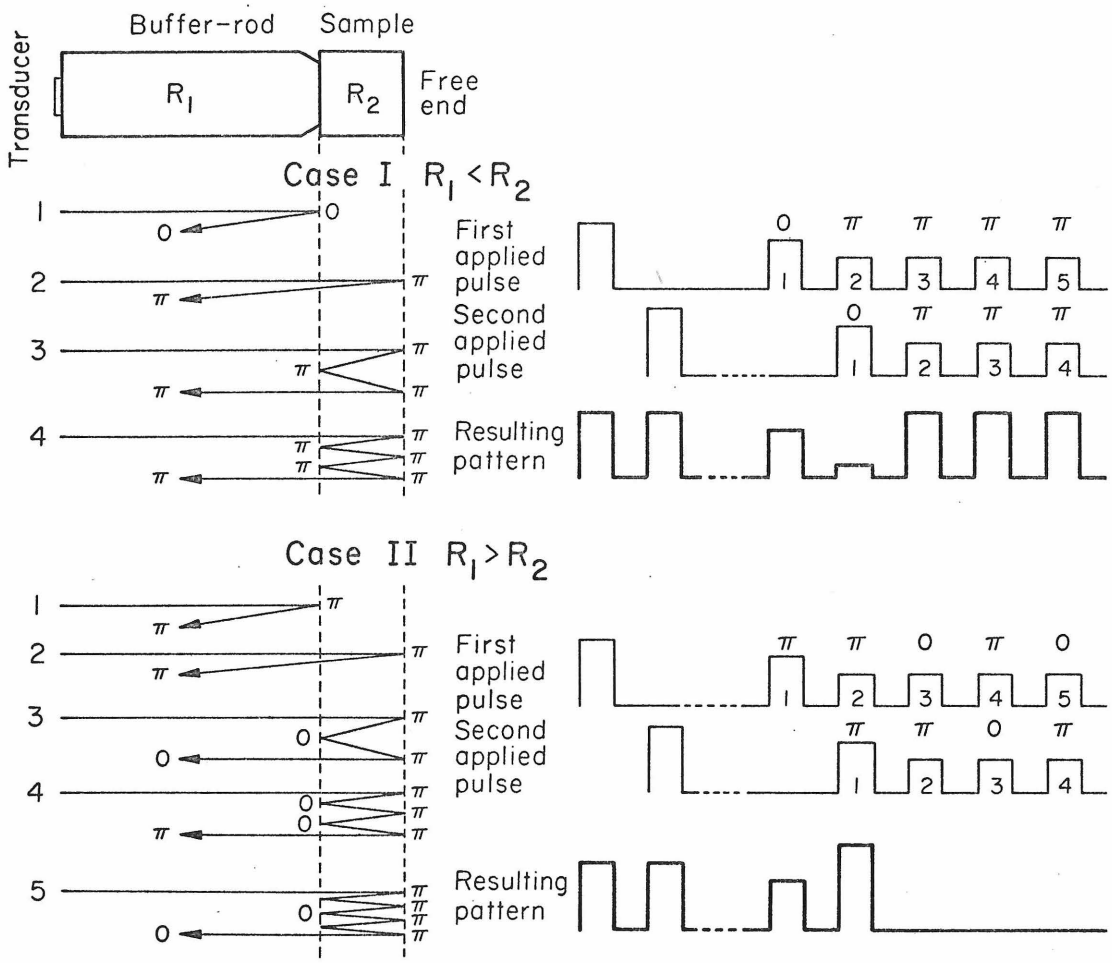
Buffer-rod
Sample
Transducer
R_1
R_2
Free end
Case I $R_1 < R_2$
First applied pulse
Second applied pulse
Resulting pattern
Case II $R_1 > R_2$
First applied pulse
Second applied pulse
Resulting pattern

Figure 2

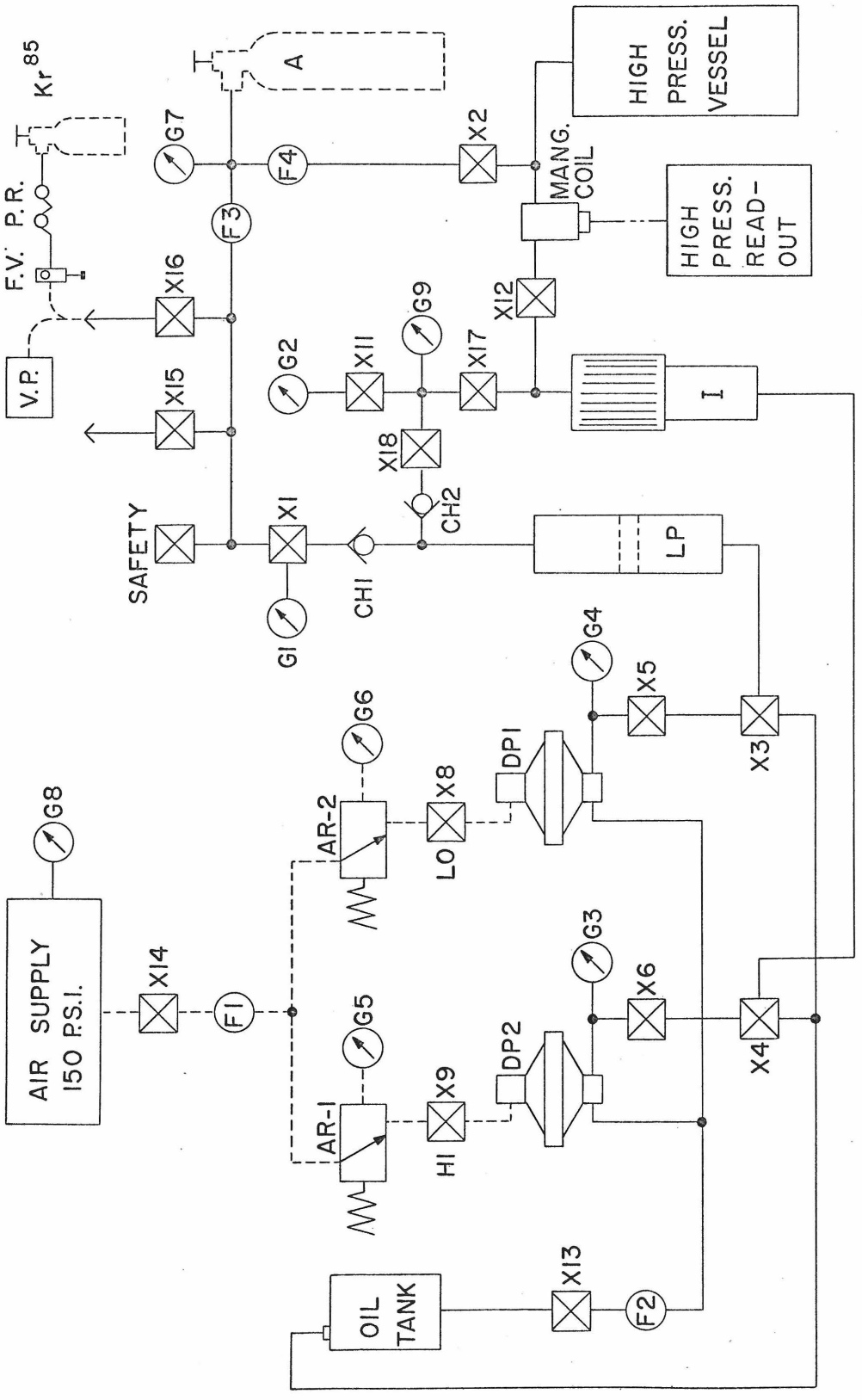
HIGH PRESS. VESSEL
HIGH PRESS. READ-OUT
MANG. COIL
A
Kr 85
P.R.
F.V.
V.P.
G7
F4
F3
X2
X16
X15
X12
G9
G2
X11
X17
X18
I
CH2
SAFETY
X1
CH1
LP
G1
G4
X5
X3
G6
AR-2
X8
LO
DP1
G8
AIR SUPPLY 150 P.S.I.
X14
F1
G3
X6
X4
G5
AR-1
X9
HI
DP2
OIL TANK
X13
F2

Figure 3

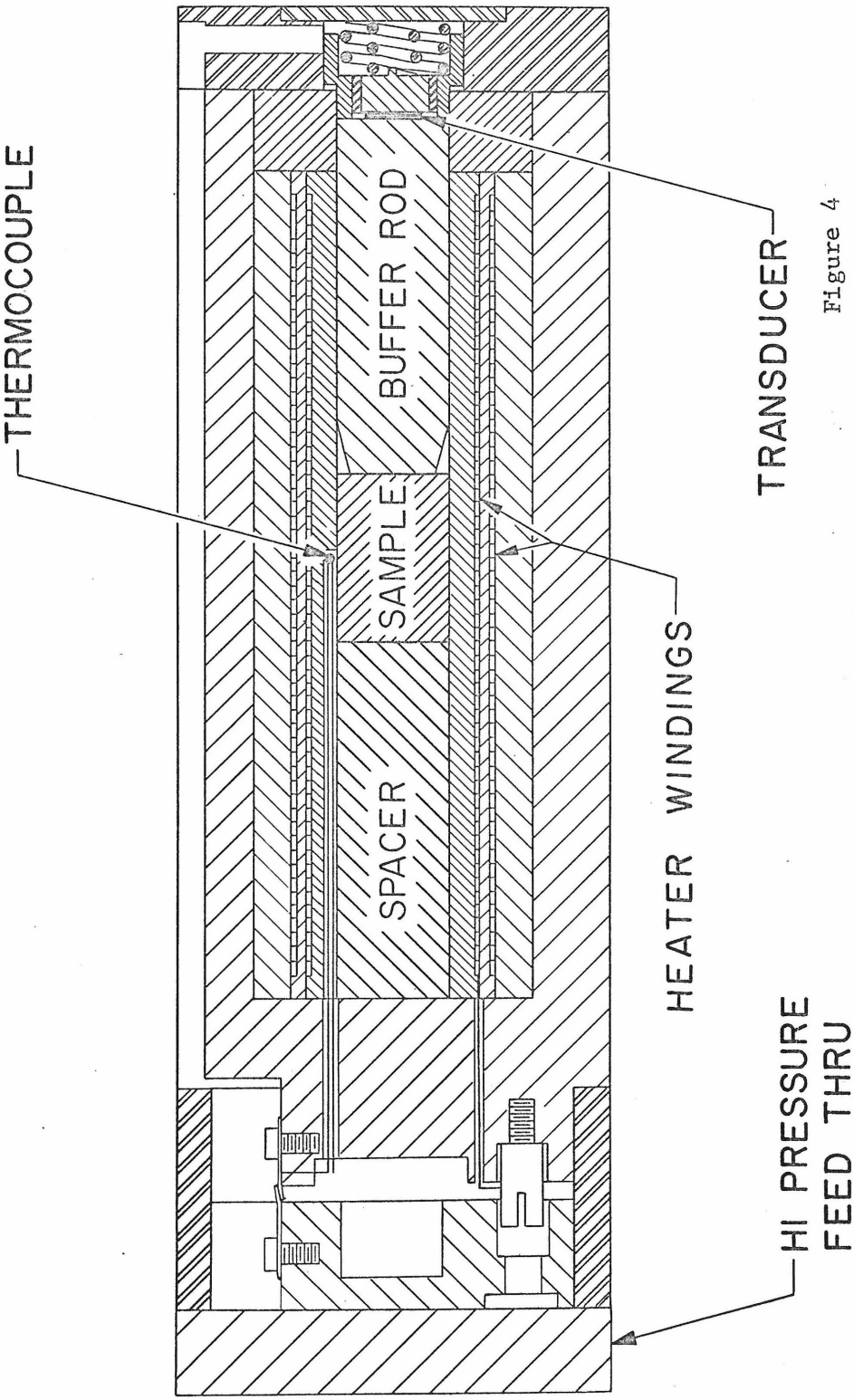
THERMOCOUPLE
BUFFER ROD
SAMPLE
SPACER
TRANSDUCER
HEATER WINDINGS
HI PRESSURE
FEED THRU

Figure 4

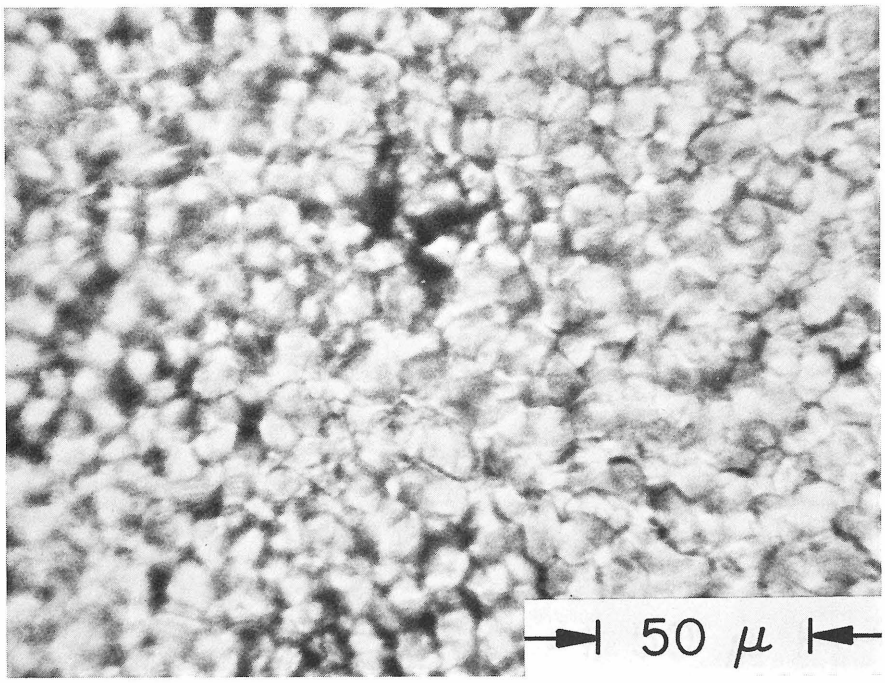

Figure 5

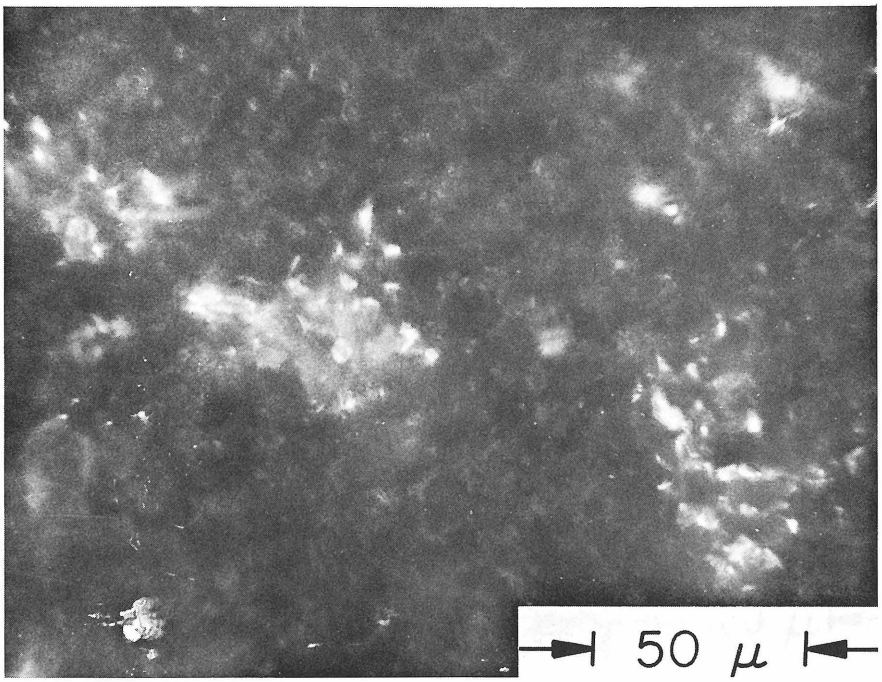

Figure 6

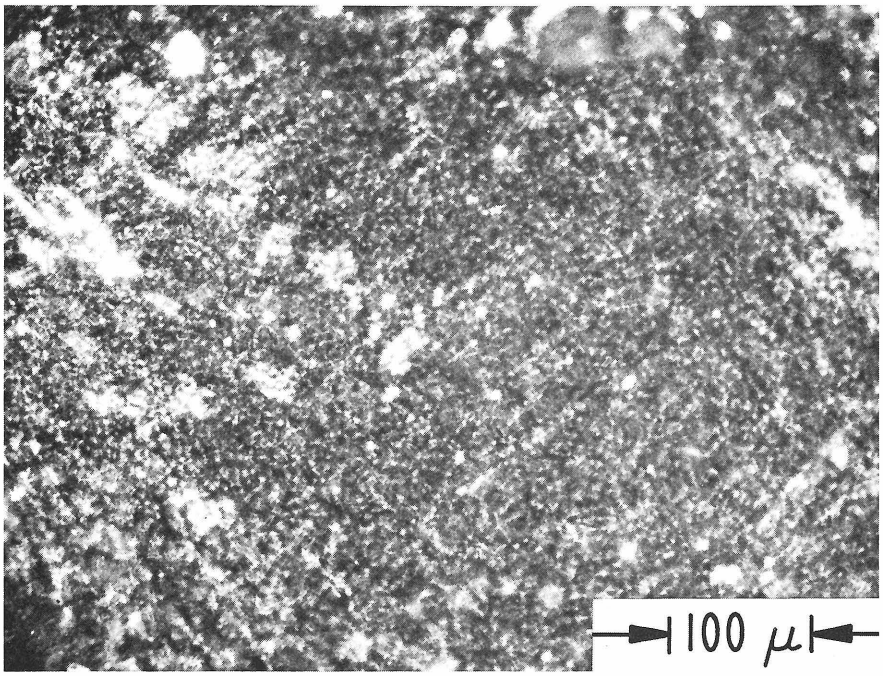

Figure 7

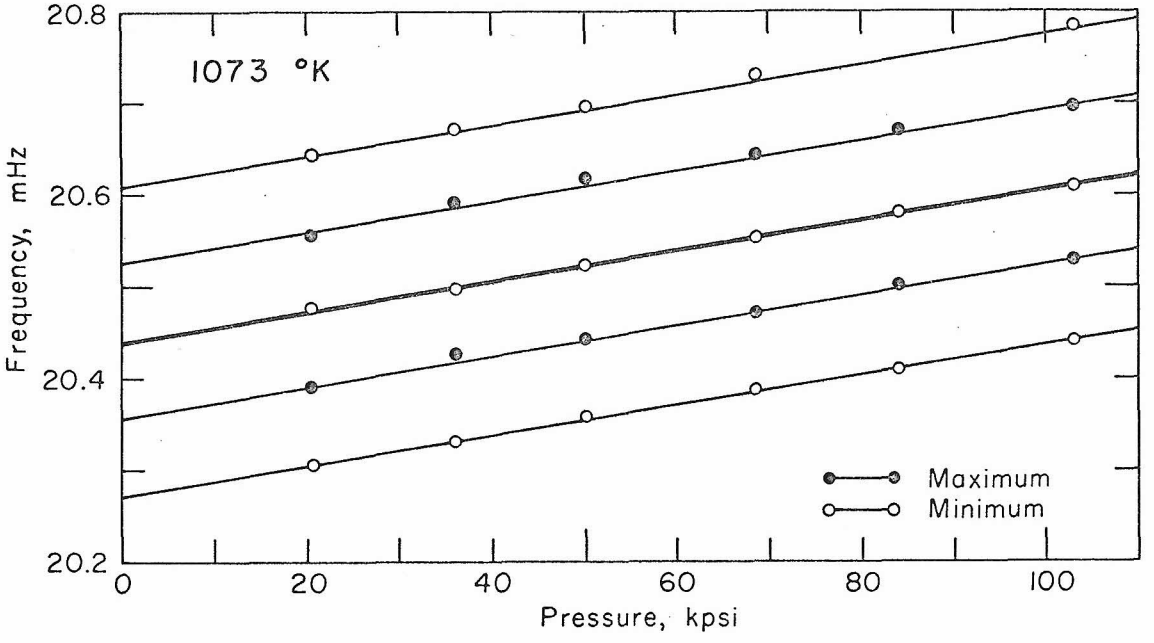
1073 °K
Frequency, mHz
20.8
20.6
20.4
20.2
0
20
40
60
80
100
Pressure, kpsi
Maximum
Minimum

Figure 8

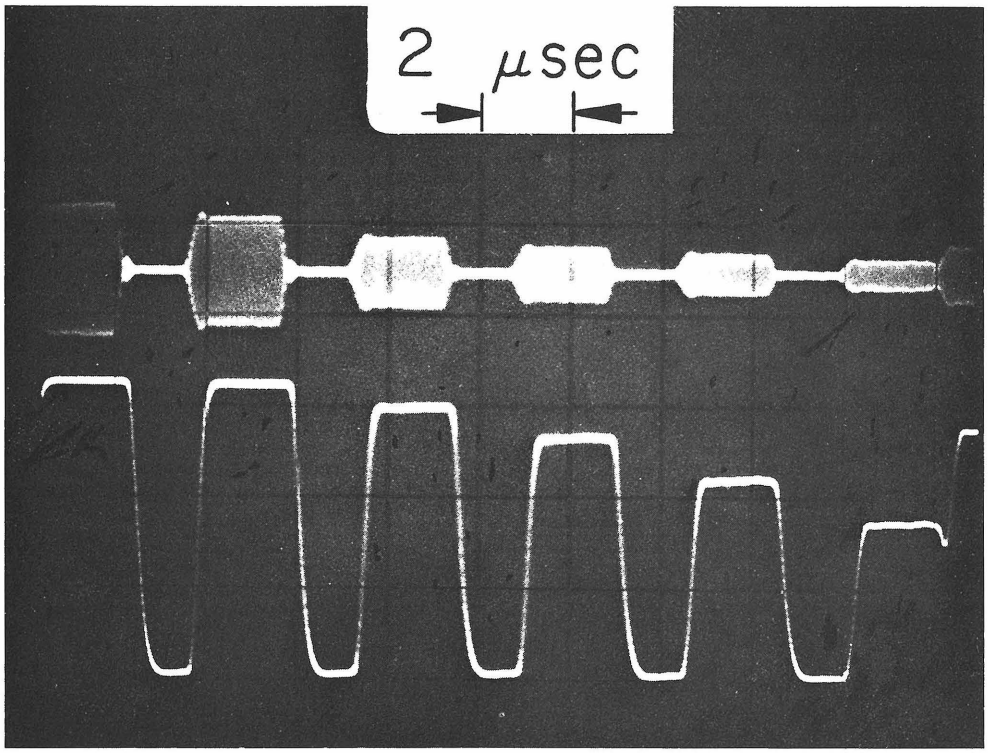

Figure 9

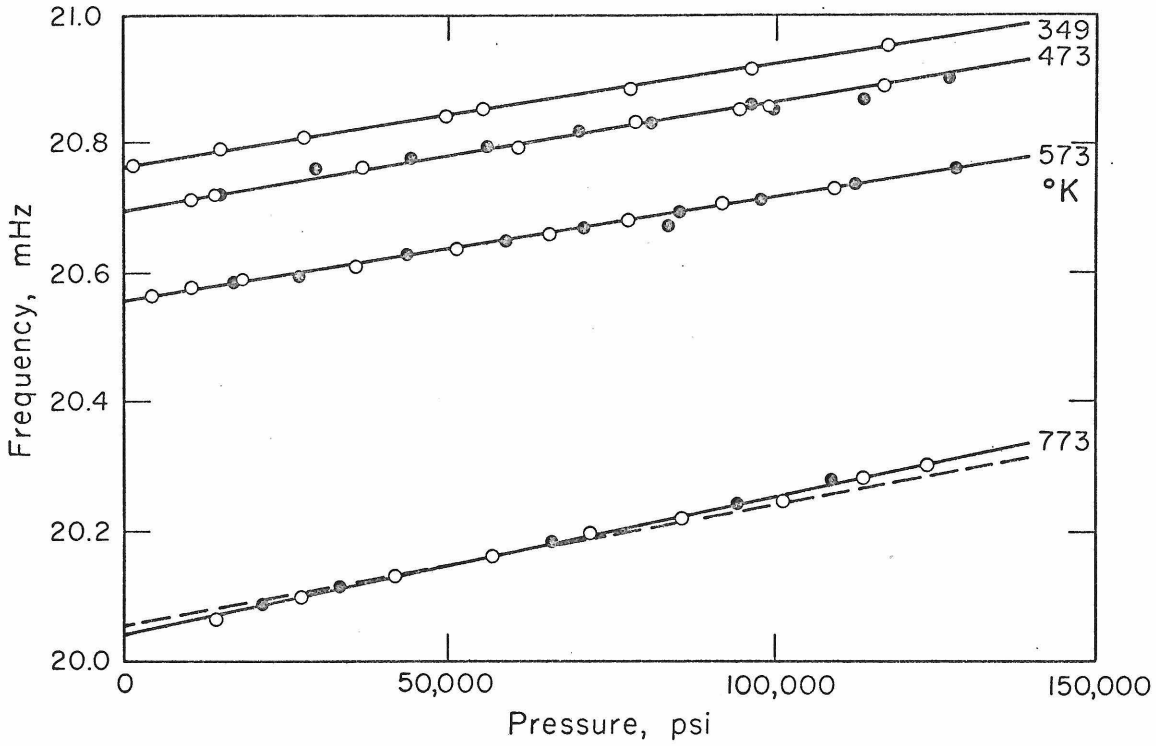
21.0
20.8
20.6
20.4
20.2
20.0
Frequency, mHz
0
50,000
100,000
150,000
Pressure, psi
349
473
573
°K
773

Figure 10

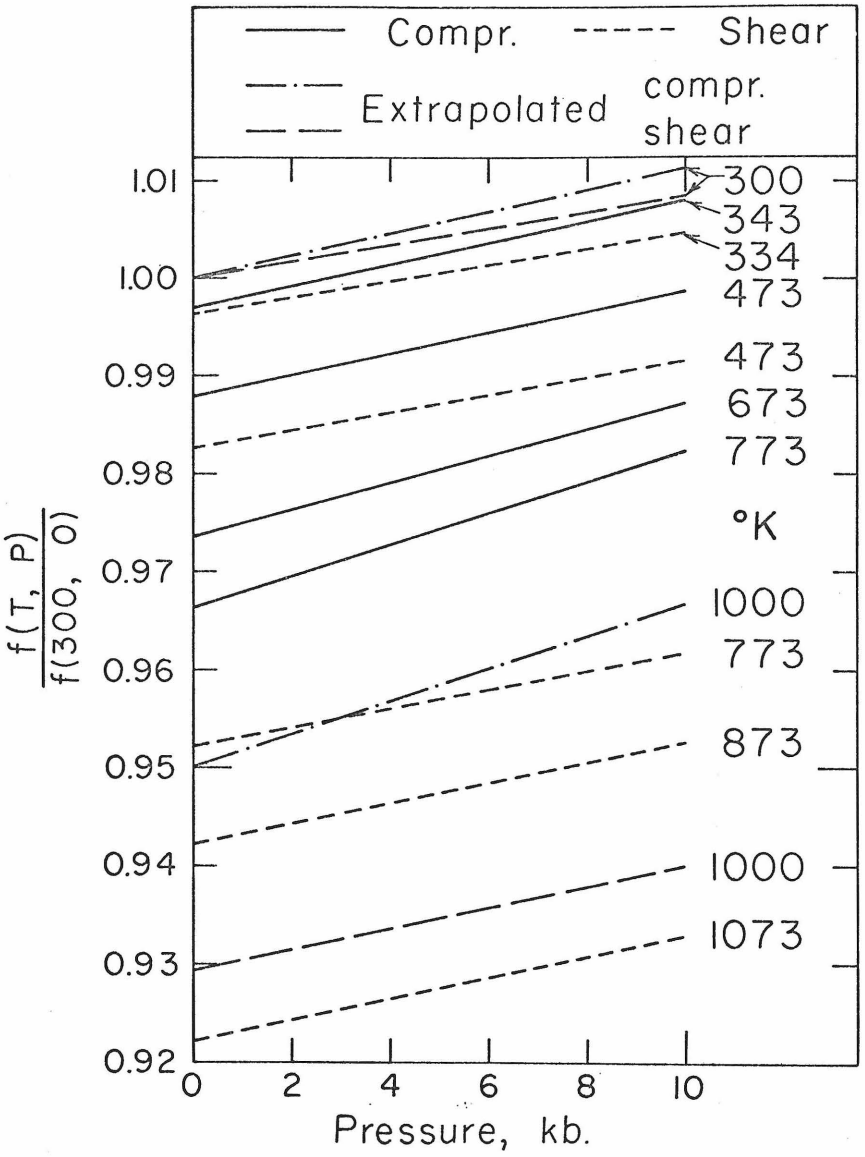
Compr.
Shear
Extrapolated compr.
shear
300
343
334
473
473
673
773
°K
1000
773
873
1000
1073
1.01
1.00
0.99
0.98
0.97
0.96
0.95
0.94
0.93
0.92
f(T, P) / f(300, 0)
0
2
4
6
8
10
Pressure, kb.

Figure 11

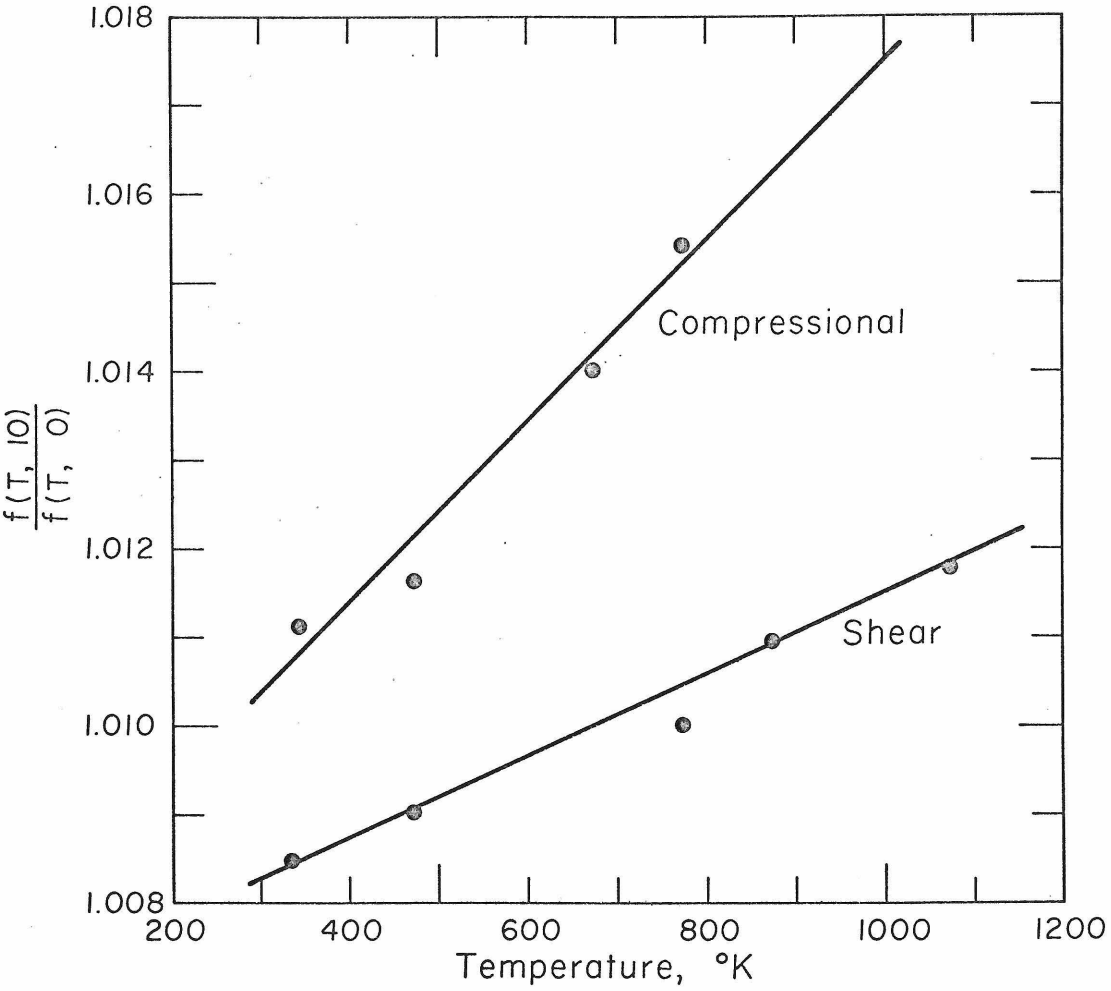
1.018
1.016
1.014
1.012
1.010
1.008
f(T, 10)/f(T, 0)
Compressional
Shear
200
400
600
800
1000
1200
Temperature, °K

Figure 12

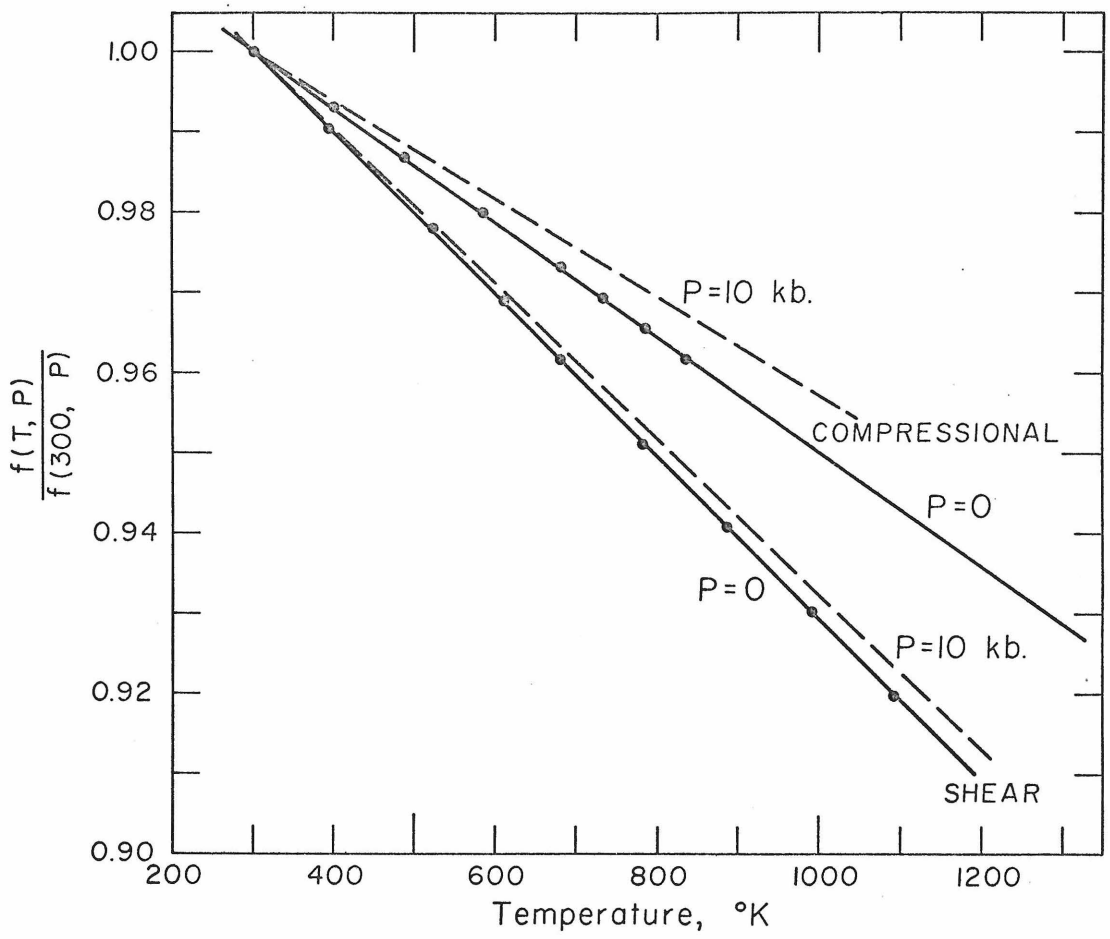
1.00
0.98
0.96
0.94
0.92
0.90
f(T, P) / f(300, P)
200
400
600
800
1000
1200
Temperature, °K
P=10 kb.
COMPRESSIONAL
P=0
P=0
P=10 kb.
SHEAR

Figure 13

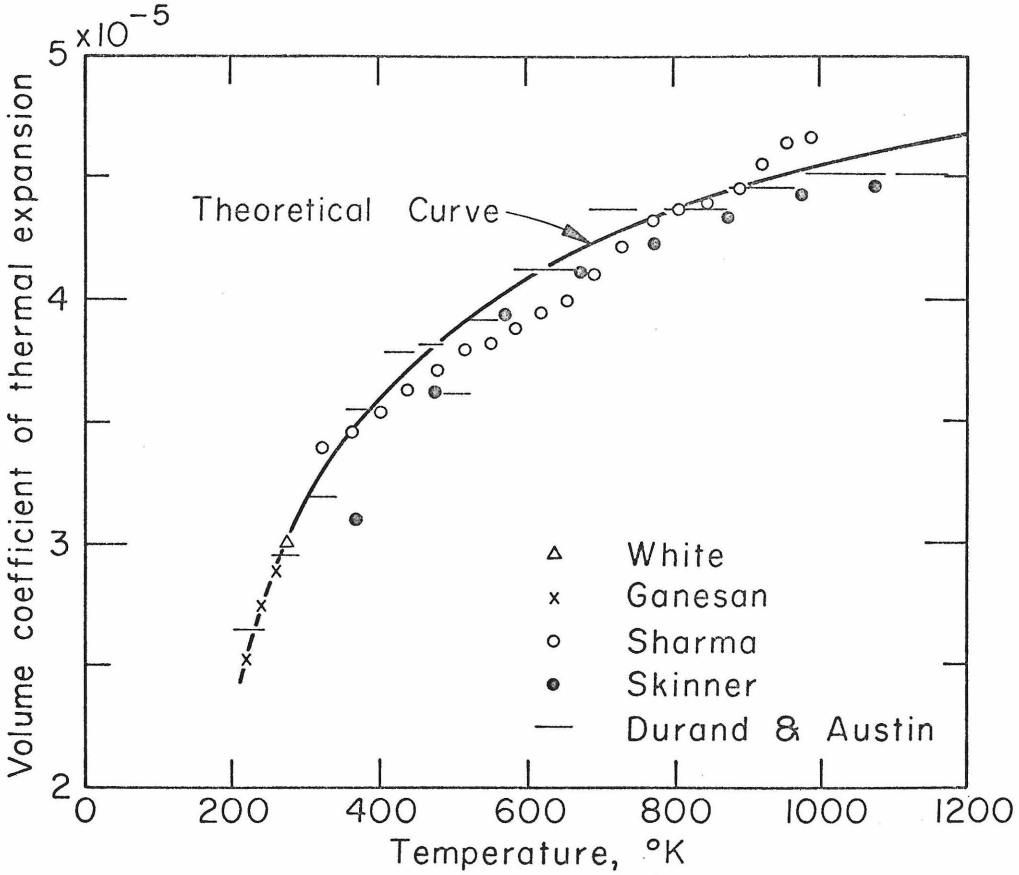
Volume coefficient of thermal expansion
5 x10⁻⁵
4
3
2
0
200
400
600
800
1000
1200
Temperature, °K
Theoretical Curve
White
Ganesan
Sharma
Skinner
Durand & Austin

Figure 14

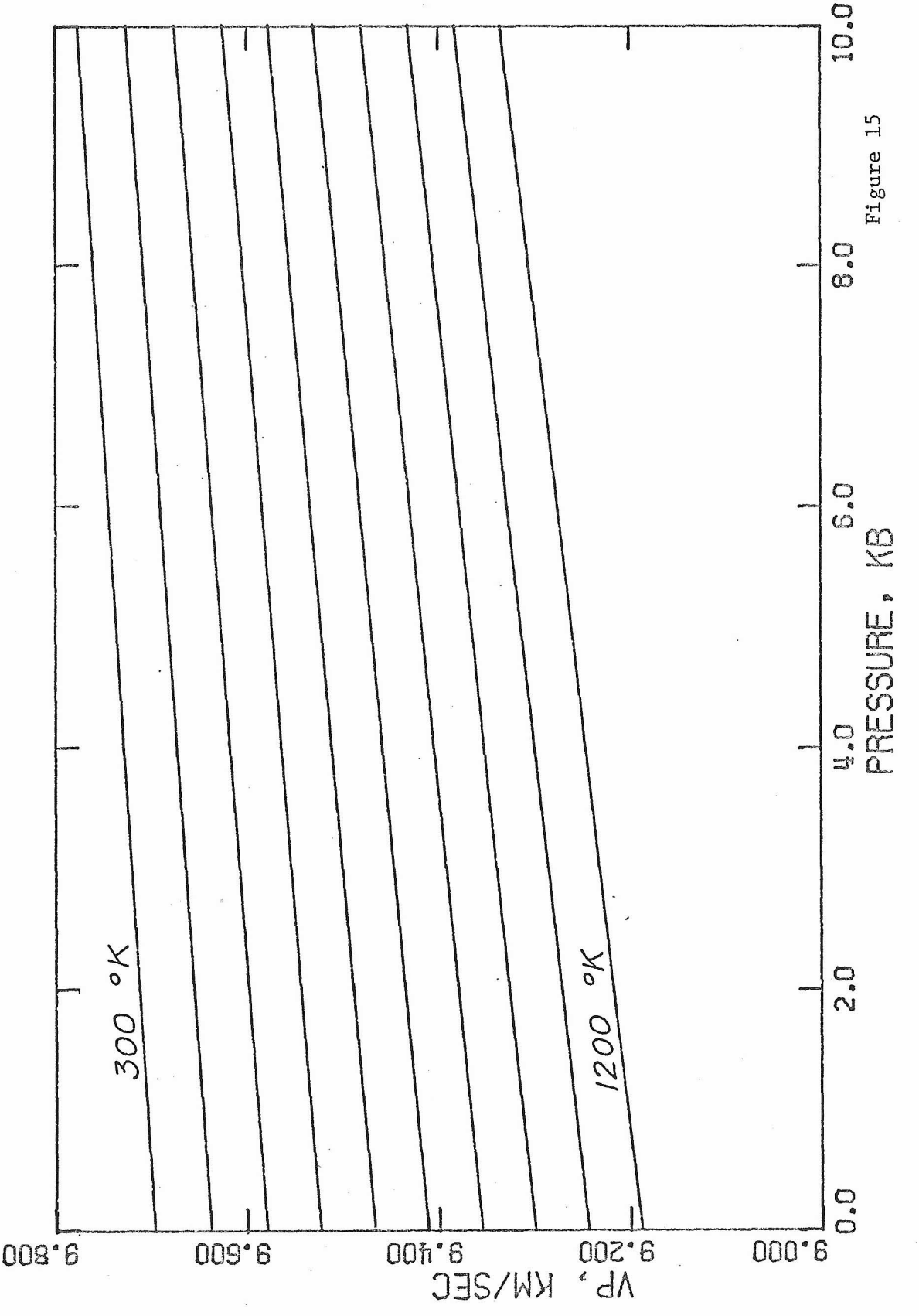
9.000
9.200
9.400
9.600
9.800
VP, KM/SEC
0.0
2.0
4.0
6.0
8.0
10.0
PRESSURE, KB
300 °K
1200 °K

Figure 15

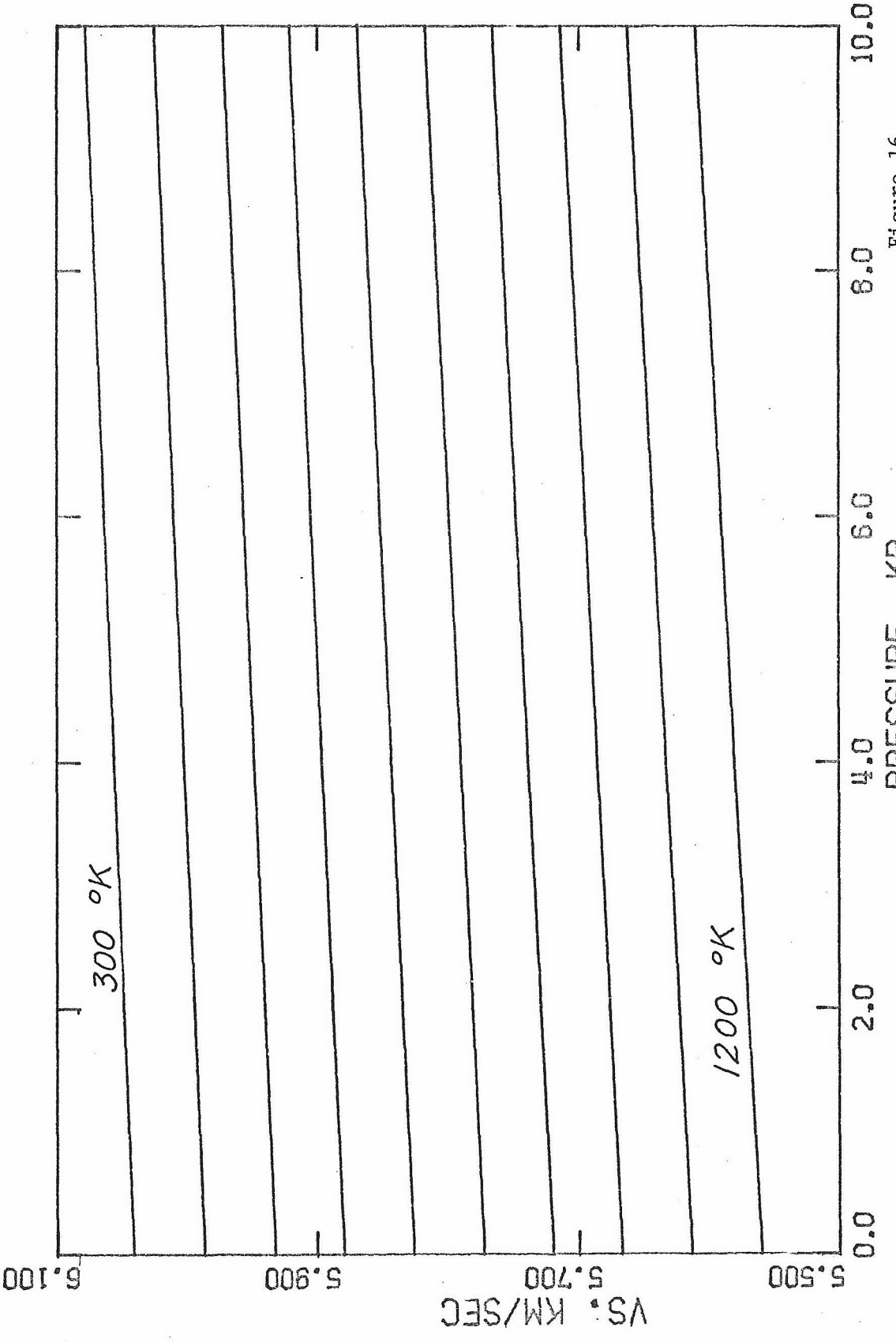
VS, KM/SEC
5.500
5.700
5.900
6.100
PRESSURE, KB
0.0
2.0
4.0
6.0
8.0
10.0
300 °K
1200 °K

Figure 16

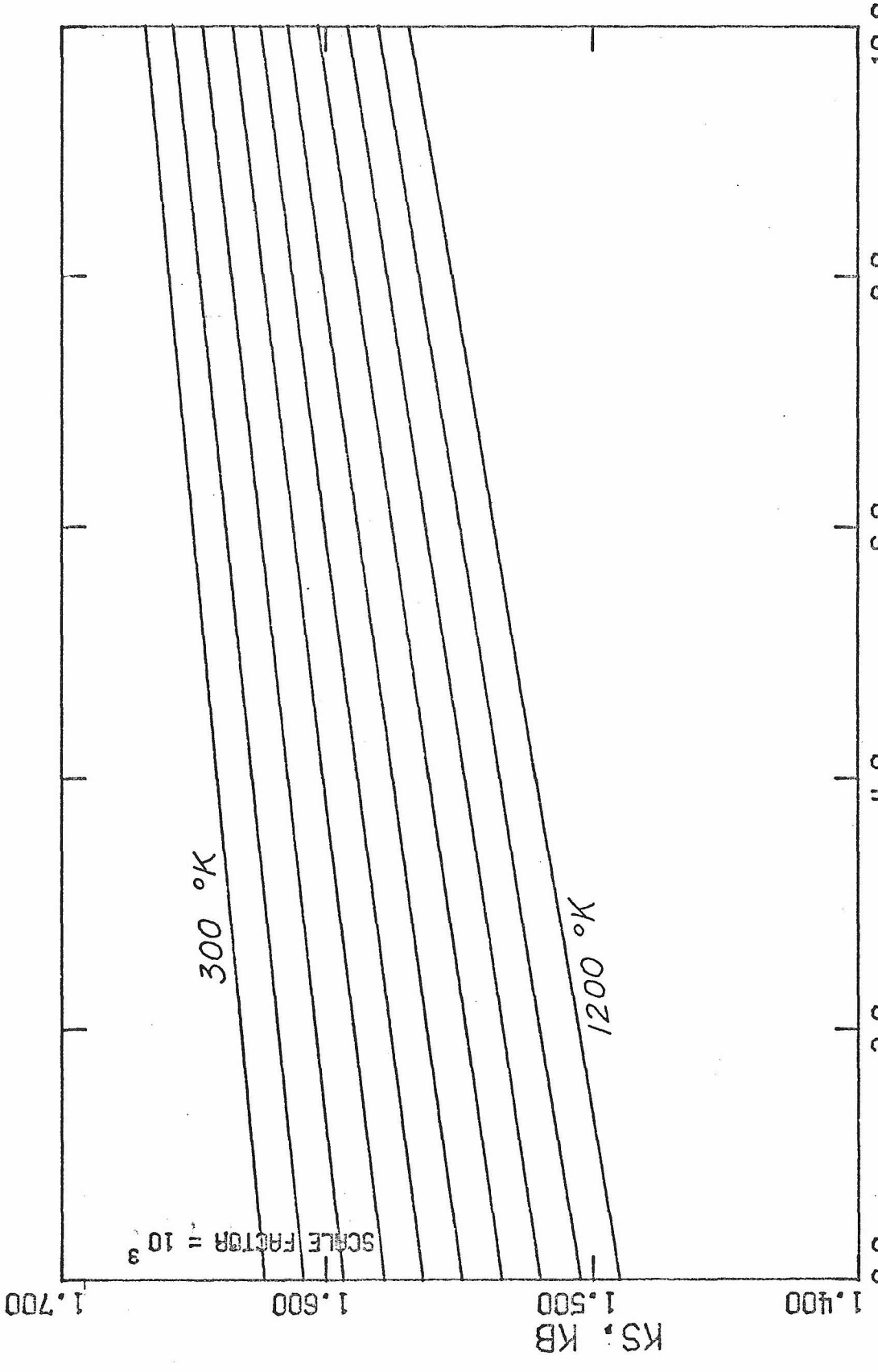
KS, KB
1.400
1.500
1.600
1.700
SCALE FACTOR = 10 3
300 °K
1200 °K
0.0
2.0
4.0
6.0
8.0
10.0
PRESSURE, KB

Figure 17

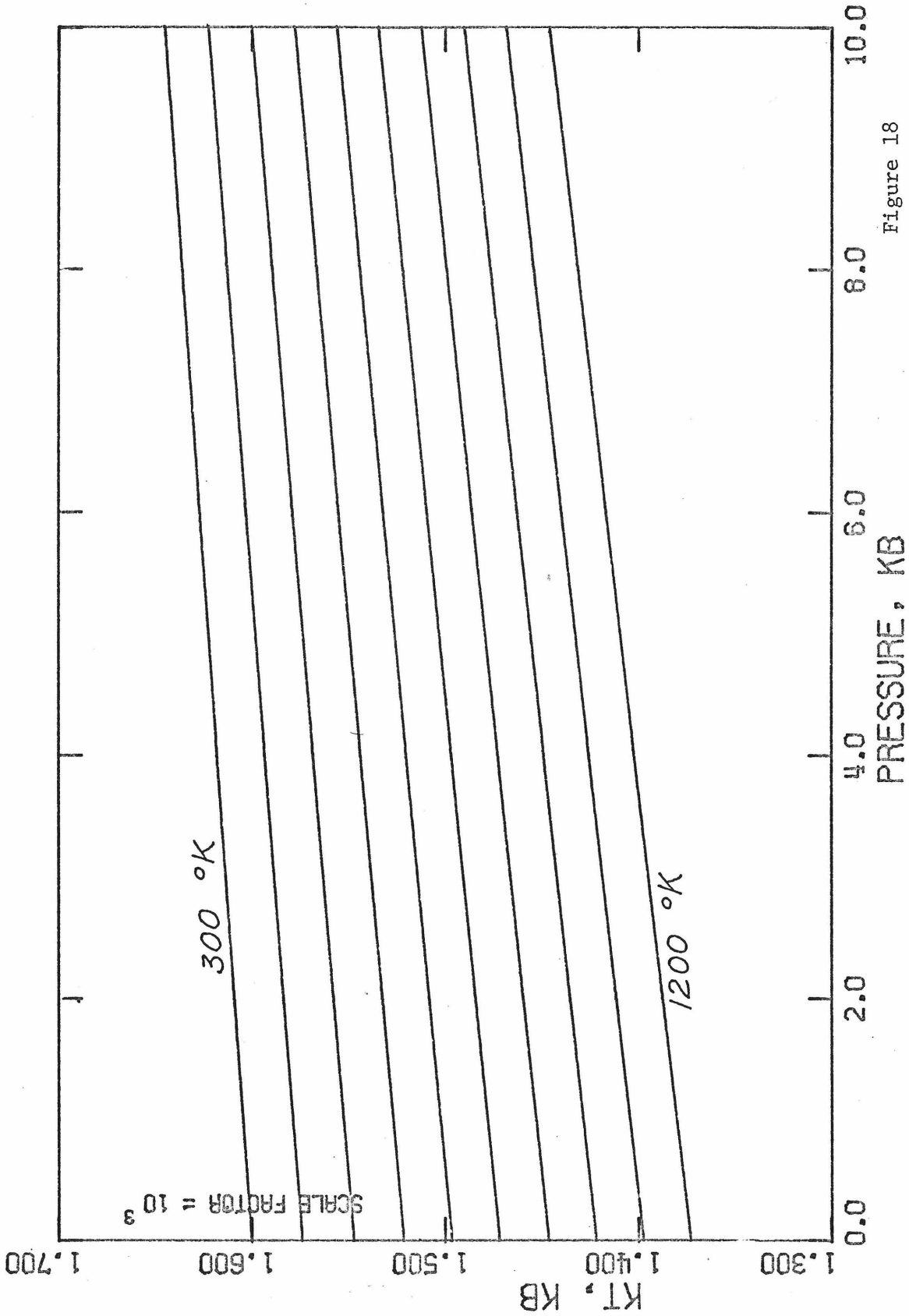
KT, KB
1.300
1.400
1.500
1.600
1.700
SCALE FACTOR = 10^3
300 °K
1200 °K
PRESSURE, KB
0.0
2.0
4.0
6.0
8.0
10.0

Figure 18

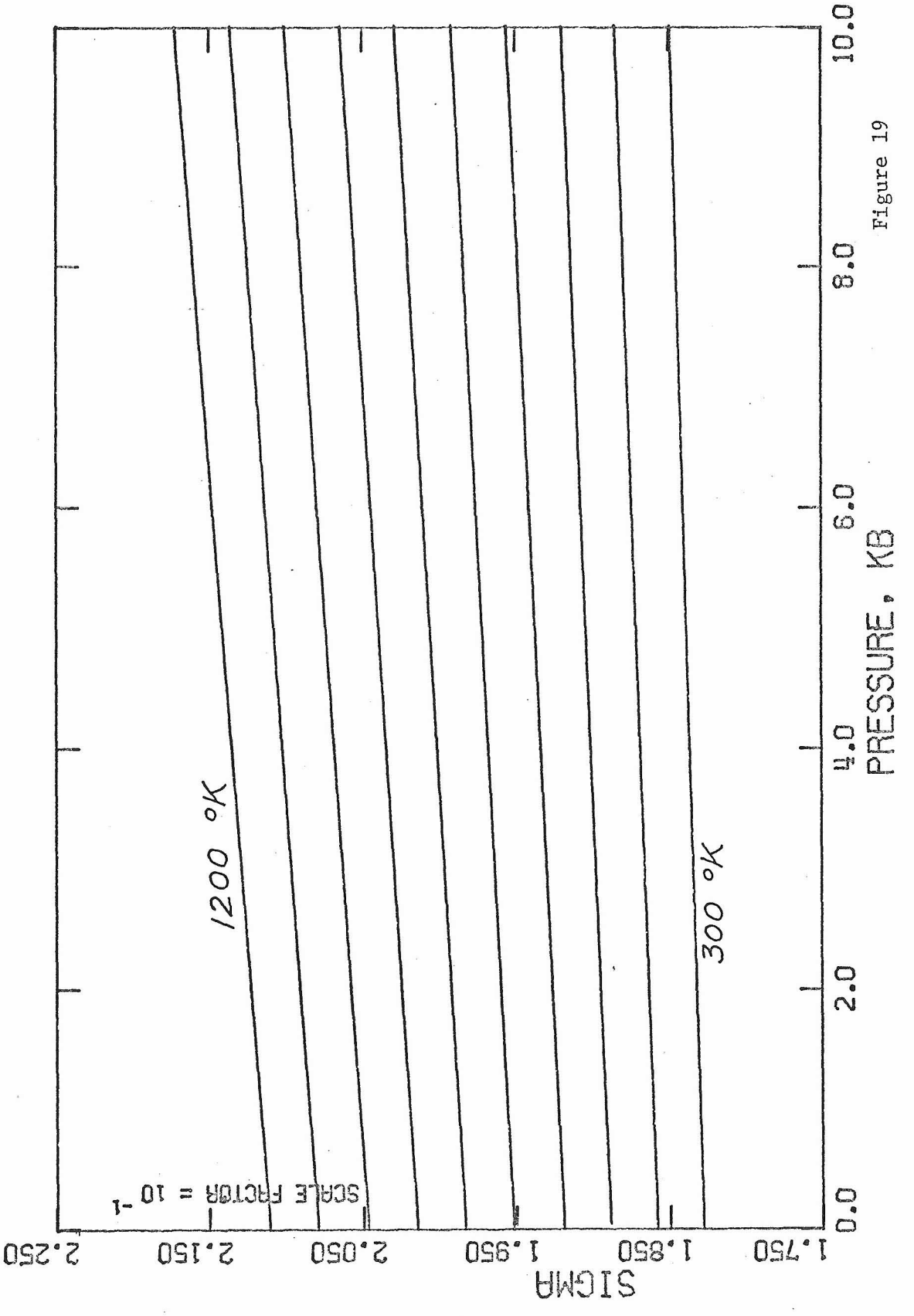
SIGMA
1.750
1.850
1.950
2.050
2.150
2.250
PRESSURE, KB
0.0
2.0
4.0
6.0
8.0
10.0
1200 °K
300 °K
SCALE FACTOR = 10 -1

Figure 19

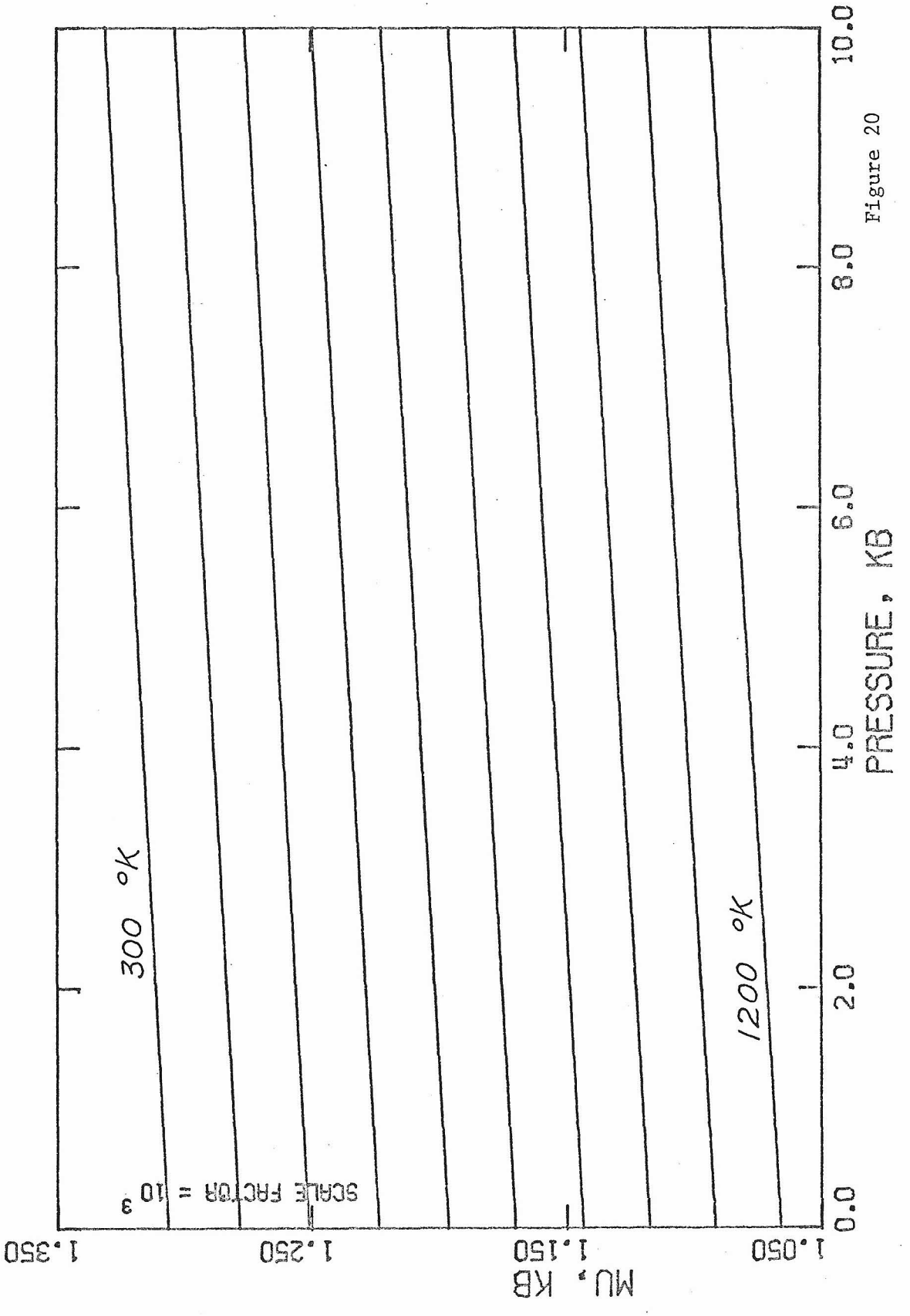
MU, KB
1.050
1.150
1.250
1.350
PRESSURE, KB
0.0
2.0
4.0
6.0
8.0
10.0
300 °K
1200 °K
SCALE FACTOR = 10 3

Figure 20

PART II

Chapter 2

REDUCTION OF ULTRASONIC DATA OVER LARGE RANGES OF TEMPERATURE AND PRESSURE

Introduction

Ultrasonic measurements have been used for some time to determine the elastic constants of materials. The direct data which are obtained in these experiments are always in terms of frequency or travel time, where the frequencies are proportional to some pseudoresonant frequencies and the travel times correspond to the time which is required to transmit an ultrasonic signal through a specimen. The velocity in the direction in which the signal is propagated is proportional to the frequency and inversely proportional to the travel time; i.e.,

$$v = \frac{\ell f}{n} = \frac{\ell}{\tau}$$

where ℓ is the length over which the velocity is being measured, f, the measured frequency, n, is some integral multiple of a pseudo-resonance frequency and τ is the travel time required by the ultrasonic signal to travel the distance ℓ. The elastic constants are simply related to the velocity by

$$M = v_M^2 \rho$$

where M is an elastic constant or modulus, v_M is the appropriate velocity and ρ is the density. Thus if the length ℓ and the density ρ are known, the elastic constants may be determined directly from the measured frequencies or travel times. This is the case when

the elastic constants are desired at room temperature and room pressure. If, however, the information is required as a function of temperature and pressure, the density and the length have to be determined under the appropriate conditions. In the absence of phase changes within the region of pressure and temperature over which the experiments are performed, it is possible to calculate the density and, therefore, obtain all elastic constants.

Methods for reducing ultrasonic data have been given by Cook (1957) and Thurston (1965). These methods are applicable to small temperature ranges over a reasonable pressure range and have been used extensively in the literature (Ahrens and Katz, 1962; Anderson and Schreiber, 1965; Chung and Simmons, 1968). The present study describes a system of equations which can be used to reduce ultrasonic data which has been taken over a large range of temperature and pressure.

Derivation of Equations

In the high precision methods of ultrasonic interferometry, or pulse superposition, the data obtained from experiments consists of frequencies as a function of temperature and pressure. Initial values of the needed parameters are obtainable at atmospheric pressure and room temperature. Table 1 gives a complete list of the equations as they are used to reduce the ultrasonic data of an isotropic material.

The compressional and shear velocities may be expressed as:

$$v_P = v_{P_o} \; L \; F_P$$

and (1)

$$v_S = v_{S_o} \; L \; F_S$$

where L, F_P, and F_S are the normalized length, compressional and shear frequencies, respectively. The normalizaton is with respect to atmospheric pressure and room temperature or some other convenient condition. The adiabatic bulk modulus is defined as

$$K_S = - V \left(\frac{\partial P}{\partial V}\right)_S$$

and in terms of the velocities as

$$K_S = \rho \left(v_P^2 - \frac{4}{3} v_S^2\right) \qquad (2)$$

The relationship between the adiabatic and the isothermal bulk moduli is given by:

$$K_T = K_S \left(1 + \alpha\gamma T\right)^{-1} \qquad (3)$$

where γ is the thermodynamic Gruneisen parameter

$$\gamma = \frac{\alpha \; K_S}{C_P \; \rho} = \frac{\alpha K_T}{C_V \; \rho}$$

The pressure and temperature derivatives of the velocities may be written as:

$$\left.\frac{\partial v_P}{\partial P}\right)_T = v_{P_o}\left[F_P \left.\frac{\partial L}{\partial P}\right)_T + L \left.\frac{\partial F_P}{\partial P}\right)_T\right] \tag{4}$$

$$\left.\frac{\partial v_P}{\partial T}\right)_P = v_{P_o}\left[F_P \left.\frac{\partial L}{\partial T}\right)_P + L \left.\frac{\partial F_P}{\partial T}\right)_P\right] \tag{5}$$

similarly, for $\left.\frac{\partial v_S}{\partial P}\right)_T$ and $\left.\frac{\partial v_S}{\partial T}\right)_P$.

All initial velocities are known, the frequencies and their temperature and pressure derivaties are obtained from the experiment. The unknowns are the length and its derivatives. The conditions of the sample under which the ultrasonic data are taken are isothermal while the data itself is adiabatic. The length derivatives may be expressed in terms of the isothermal bulk modulus and the volume coefficient of thermal expansion $\alpha = \frac{1}{V}\left(\frac{\partial V}{\partial T}\right)_P$. Thus,

$$\left.\frac{\partial L}{\partial T}\right)_P = \frac{L\alpha}{3} \quad ; \quad \left.\frac{\partial \rho}{\partial T}\right)_P = -\rho\alpha \tag{6}$$

$$\left.\frac{\partial L}{\partial P}\right)_T = -\frac{L}{3K_T} \quad ; \quad \left.\frac{\partial \rho}{\partial P}\right)_T = \frac{\rho}{K_T} \tag{7}$$

The variation of α and K_T are needed as a function of temperature and pressure. At this point it is convenient to treat the pressure and temperature derivatives separately. Starting with the pressure derivatives; from equation (3) the pressure derivatives of K_T may be written as:

$$\frac{\partial K_T}{\partial P}\Big)_T = \frac{\partial K_S}{\partial P}\Big)_T \left(1 + \alpha\gamma T\right)^{-1} - \frac{K_S T}{(1+\alpha\gamma T)^2}\left[\gamma \frac{\partial \alpha}{\partial P}\Big)_T + \alpha \frac{\partial \gamma}{\partial P}\Big)_T\right] \quad (8)$$

Taking the undetermined terms in order, one obtains from equation (2)

$$\frac{\partial K_S}{\partial P}\Big)_T = \frac{\partial \rho}{\partial P}\Big)_T \left(v_P^2 - \frac{4}{3} v_S^2\right) + 2\rho \left[v_P \frac{\partial v_P}{\partial P}\Big)_T - \frac{4}{3} v_S \frac{\partial v_S}{\partial P}\Big)_T\right] \quad (9)$$

using equation (7) and the definition of K_S reduces equation (9) to

$$\frac{\partial K_S}{\partial P}\Big)_T = \frac{K_S}{K_T} + 2\rho \left[v_P \frac{\partial v}{\partial P}\Big)_T - \frac{4}{3} v_S \frac{\partial v_S}{\partial P}\Big)_T\right] \quad (10)$$

The expression for $\frac{\partial \alpha}{\partial P}\Big)_T$ may be derived from the definition of α.

$$\alpha = \frac{1}{V}\frac{\partial V}{\partial T}\Big)_P \quad (11)$$

$$\left.\frac{\partial\alpha}{\partial P}\right)_T = -\frac{1}{V^2}\left.\frac{\partial V}{\partial P}\right)_T \left.\frac{\partial V}{\partial T}\right)_P + \frac{1}{V}\left.\frac{\partial\left.\frac{\partial V}{\partial T}\right)_P}{\partial P}\right)_T \tag{12}$$

Noting the symmetry between α and $\frac{1}{K_T}$

$$\frac{1}{K_T} = -\frac{1}{V}\left.\frac{\partial V}{\partial P}\right)_T \qquad \text{and} \qquad \alpha = \frac{1}{V}\left.\frac{\partial V}{\partial T}\right)_P$$

one observes

$$\left.\frac{\partial\alpha}{\partial P}\right)_T = -\left.\frac{\partial\frac{1}{K_T}}{\partial T}\right)_P = \frac{1}{K_T^2}\left.\frac{\partial K_T}{\partial T}\right)_P \tag{13}$$

which is a well known thermodynamic identity. $\left.\frac{\partial K_T}{\partial T}\right)_P$ will be found later. $\left.\frac{\partial\gamma}{\partial P}\right)_T$ may be obtained from the definition of γ.

$$\left.\frac{\partial\gamma}{\partial P}\right)_T = \gamma\left[\left.\frac{\partial\ \ell n\ \alpha}{\partial P}\right)_T + \left.\frac{\partial\ \ell n\ K_S}{\partial P}\right)_T - \left.\frac{\partial\ \ell n\ \rho}{\partial P}\right)_T - \left.\frac{\partial\ \ell n\ C_P}{\partial P}\right)_T\right] \tag{14}$$

The definition of C_P and the thermodynamic identity $\left.\frac{\partial S}{\partial P}\right)_T = -\left.\frac{\partial V}{\partial T}\right)_P$ lead to

$$C_P = T\left.\frac{\partial S}{\partial T}\right)_P \qquad \text{(definition)}$$

$$\left.\frac{\partial C_P}{\partial P}\right)_T = T\,\frac{\partial^2 S}{\partial P)_T \partial T)_P}$$

$$= \left.\frac{\partial^2 V}{\partial T^2}\right)_P$$

$$\left.\frac{\partial C_P}{\partial P}\right)_T = -TV\left[\left.\frac{\partial \alpha}{\partial T}\right)_P + \alpha^2\right] \tag{15}$$

Substituting (15) into (14) and collecting terms yields

$$\left.\frac{\partial \gamma}{\partial P}\right)_T = \gamma\left[\left.\frac{\partial\, \ell n\, \alpha}{\partial P}\right)_T + \left.\frac{\partial\, \ell n\, K_S}{\partial P}\right)_T - \left.\frac{\partial\, \ell n\, \rho}{\partial P}\right)_T + \frac{\gamma T}{\alpha K_S}\left[\left.\frac{\partial \alpha}{\partial T}\right)_P + \alpha^2\right] \tag{16}$$

The important pressure derivatives have now been found. Only some temperature derivatives remain to be determined. $\left(\frac{\partial K_T}{\partial T}\right)_P$ is needed to determine $\left(\frac{\partial \alpha}{\partial P}\right)_T$; it is obtained directly by differentiating equation (3) with respect to temperature which yields

$$\left(\frac{\partial K_T}{\partial T}\right)_P = \left(\frac{\partial K_S}{\partial T}\right)_P (1 + \alpha\gamma T)^{-1} - \frac{K_S\gamma}{(1+\alpha\gamma T)^2}\left(\gamma T \left(\frac{\partial \alpha}{\partial T}\right)_P + \alpha\right) \tag{17}$$

Proceeding similarly as before:

$$\left(\frac{\partial K_S}{\partial T}\right)_P = -\alpha K_S + 2\rho\left[v_P\left(\frac{\partial v_P}{\partial T}\right)_P - \frac{4}{3} v_S \left(\frac{\partial v_S}{\partial T}\right)_P\right] \tag{18}$$

$\left(\frac{\partial \gamma}{\partial T}\right)_P$ is taken to be zero. Experimental evidence (Soga and Anderson, 1966; White and Anderson, 1966) suggests that this is indeed a valid assumption in the range of interest. From the definition of γ and the above assumption one may write $\alpha = \frac{C_V\rho\gamma}{K_T}$ and

$$\left(\frac{\partial \alpha}{\partial T}\right)_P = \frac{\gamma\rho}{K_T}\left(\frac{\partial C_V}{\partial T}\right)_P - \frac{\alpha}{K_T}\left(\frac{\partial K_T}{\partial T}\right)_P - \alpha^2 \tag{19}$$

$\left(\frac{\partial C_V}{\partial T}\right)_P$ may be obtained from the internal energy as given by the Einstein model. The Einstein heat capacity is

$$C_V = 3NK\left(\frac{\Theta}{T}\right)^2 \frac{e^{\frac{\Theta}{T}}}{\left(e^{\frac{\Theta}{T}} - 1\right)^2} \tag{20}$$

Hence,

$$\left(\frac{\partial C_V}{\partial T}\right)_P = \frac{3NK\ \Theta^2\ e^{\frac{\Theta}{T}}}{T^4\ \left(e^{\frac{\Theta}{T}} - 1\right)^2}\left[\frac{\Theta\left(e^{\frac{\Theta}{T}} + 1\right)}{\left(e^{\frac{\Theta}{T}} - 1\right)} - 2T\right] \tag{21}$$

Converting units to make the numerical value for equation 21 compatible with ρ in gr/cm and K_T in kb yields

$$\left(\frac{\partial C_V}{\partial T}\right)_P = \frac{0.2497 \times n}{M} \frac{\Theta^2\ e^{\frac{\Theta}{T}}}{T^4\ \left(e^{\frac{\Theta}{T}} - 1\right)^2}\left[\frac{\Theta\left(e^{\frac{\Theta}{T}} + 1\right)}{\left(e^{\frac{\Theta}{T}} - 1\right)} - 2T\right] \tag{22}$$

where n is the number of atoms per molecule, M the molecular weight and Θ the Einstein temperature.

The Einstein model gives a good representation of the heat capacity for temperatures above about $\Theta/4$. Below this value the more complicated Debye model has to be used. Both the Debye and the Einstein model were developed for monoatomic substances, where the vibrational energy is largely confined to the acoustic phonon spectrum. In the case of compounds, where the vibration of the molecules contribute mainly to the acoustic branch and the vibrations within the molecules contribute mostly to the optical branch, a combination of Debye and Einstein distributions may be needed to obtain a good fit for the measured heat capacities. For simple structures like that of NaCl a single Debye or Einstein distribution is sufficient (Slater, 1939).

The pressure dependence of the Einstein temperature can be estimated from the relation

$$k\Theta = h\,\nu_E,$$

where ν_E is the characteristic frequency. The characteristic frequency may be obtained by proper averaging of the possible models of vibration within a solid. For isotropic solids it is given as (Debye, 1912; Gruneisen, 1926; Schrodinger, 1928; Barron, 1957)

$$\nu_E = \frac{9\rho N}{4\pi \bar{M}} \left(\frac{1}{v_P^3} + \frac{2}{v_S^3} \right)^{-1} \tag{23}$$

The pressure derivative of Θ becomes upon differentiation of (23)

$$\left.\frac{\partial \Theta}{\partial P}\right)_T = \Theta \left[\frac{1}{v_P^4} \left.\frac{\partial v_P}{\partial P}\right)_T + \frac{2}{v_S^4} \left.\frac{\partial v_S}{\partial P}\right)_T \right] \left[\frac{1}{v_P^3} + \frac{2}{v_S^3} \right]^{-1}$$

The pertinent equations which have been derived above are tabulated in Table 1. This set of partial differential equations correspond to a complete equation of state which enables one to calculate the thermodynamic variables as a function of temperature and pressure.

A computer program has been written to integrate the above equations simultaneously: first along a zero-pressure isobar to a desired temperature, then along an isotherm to the desired pressure. Table 2 briefly describes the programs operation and gives the formats for the input data.

REFERENCES

Ahrens, T. J., and S. Katz, An ultrasonic interferometer for high-pressure research, J. Geophys. Res., 67, 7, 2935-2944, 1962.

Anderson, O. L., and E. Schreiber, The pressure derivatives of the sound velocities of polycrystalline magnesia, J. Geophys. Res., 70, 20, 5241-5248, 1965.

Barron, T. H. K., Gruneisen parameters for the equation of state of solids, Ann. Phys. N. Y., 1, 77-90, 1957.

Chung, D. H., and G. Simmons, The pressure and temperature dependences of the isotropic elastic moduli of polycrystalline alumina, J. Appl. Phys., submitted for publication, 1968.

Cook, R. K., Variation of elastic constants and static strains with hydrostatic pressure: A method for calculation from ultrasonic measurements, J. Acoust. Soc. Am., 29, 4, 445-449, 1957.

Debye, P., Zur Theorie der spezifischen Warmen, Ann. Phys. Berlin, 39, 789-839, 1912.

Gruneisen, E., Die Zustandsanderungen des fester Korpers (in German), in Handbuch der Physics, 10, 1-52, 1926. (English translation: The State of a Solid Body, 76 pp., NASA Re-publication RF 2-18-59 W, Feb. 1959).

Schrodinger, F., Spezifische Warme (theoretischer Teil), in Handbuch der Physik, 10, 30-318, 1928.

Slater, J. C., Introduction to Chemical Physics, McGraw-Hill Book Company, New York and London, 1939.

Soga, N., and O. L. Anderson, High-temperature elastic properties of polycrystalline MgO and Al_2O_3, J. Am. Ceram. Soc., 49, 7, 335-359, 1966.

Thurston, R. N., Ultrasonic data and thermodynamics of solids, Proc. IEEE, 53, 10, 1320-1336, 1965.

White, G. K., and O. L. Anderson, Gruneisen parameter of magnesium oxide, J. Appl. Phys., 37, 430-432, 1966.

Table 1

Relations used in data reduction.

Temperature Derivatives	Pressure Derivatives
$\left(\frac{\partial L}{\partial T}\right)_P = \frac{L\alpha}{3}$; $\left(\frac{\partial \rho}{\partial T}\right)_P = -\rho\alpha$	$\left(\frac{\partial L}{\partial P}\right)_T = -\frac{L}{3KT}\left(\frac{\partial \rho}{\partial P}\right)_T = \frac{\rho}{K_T}$
$\left(\frac{\partial K_S}{\partial T}\right)_P = -\alpha K_S + 2\rho\left[V_P\left(\frac{\partial V_P}{\partial T}\right)_P - \frac{4}{3}V_S\left(\frac{\partial V_S}{\partial T}\right)_P\right]$	$\left(\frac{\partial K_S}{\partial P}\right) = \frac{K_S}{K_T} + 2\rho\left[V_P\left(\frac{\partial V_P}{\partial P}\right)_T - \frac{4}{3}V_S\left(\frac{\partial V_S}{\partial P}\right)_T\right]$
$\left(\frac{\partial V_P}{\partial T}\right)_P = V_{PO}\left[\left(\frac{\partial L}{\partial T}\right)_P F_P + L\left(\frac{\partial F_P}{\partial T}\right)_P\right]$	$\left(\frac{\partial V_P}{\partial P}\right)_T = V_{PO}\left[\left(\frac{\partial L}{\partial P}\right)_T F_P + L\left(\frac{\partial F_P}{\partial P}\right)_T\right]$
$\left(\frac{\partial V_S}{\partial T}\right)_P = V_{SO}\left[\left(\frac{\partial L}{\partial T}\right)_P F_S + L\left(\frac{\partial F_S}{\partial T}\right)_P\right]$	$\left(\frac{\partial V_S}{\partial P}\right)_T = V_{SO}\left[\left(\frac{\partial L}{\partial P}\right)_T F_S + L\left(\frac{\partial F_S}{\partial P}\right)_T\right]$
$\left(\frac{\partial K_T}{\partial T}\right)_P = \left(\frac{\partial K_S}{\partial T}\right)_P (1+\alpha\gamma T)^{-1} - \frac{K_S\gamma}{(1+\alpha\gamma T)^2}\left[T\left(\frac{\partial \alpha}{\partial T}\right)_P + \alpha\right]$	$\left(\frac{\partial K_T}{\partial P}\right)_T = \left(\frac{\partial K_S}{\partial P}\right)_T (1+\alpha\gamma T)^{-1} - \frac{K_S T}{(1+\alpha\gamma T)^2}\left(\gamma\left(\frac{\partial \alpha}{\partial P}\right)_T + \alpha\left(\frac{\partial \gamma}{\partial P}\right)_T\right)$
$\left(\frac{\partial \alpha}{\partial T}\right)_P = \frac{\gamma\rho}{K_T}\left(\frac{\partial C_V}{\partial T}\right)_P - \frac{\alpha}{K_T}\left(\frac{\partial K_T}{\partial T}\right)_P - \alpha^2$	$\left(\frac{\partial \alpha}{\partial P}\right)_T = +\frac{1}{K_T^2}\left(\frac{\partial K_T}{\partial T}\right)_P$
$\left(\frac{\partial \gamma}{\partial T}\right)_P = 0$ (Assumption)	$\left(\frac{\partial \gamma}{\partial P}\right)_T = \gamma\left[\left(\frac{\partial \ell n\ K_S}{\partial P}\right)_T + \left(\frac{\partial \ell n\ \alpha}{\partial P}\right)_T - \left(\frac{\partial \ell n\ \rho}{\partial P}\right)_T + \frac{\gamma T}{\alpha K_S}\left(\alpha^2 + \left(\frac{\partial \alpha}{\partial T}\right)_P\right)\right]$
$\left(\frac{\partial C_V}{\partial T}\right)_P = \frac{0.2497 \times n}{M}\frac{\Theta^2 e^{\Theta/T}}{T^4\left(e^{\frac{\Theta}{T}}-1\right)^2}\left[\frac{\Theta\left(e^{\frac{\Theta}{T}}+1\right)}{\left(e^{\frac{\Theta}{T}}-1\right)} - 2T\right]$	$\left(\frac{\partial \Theta}{\partial P}\right)_T = \Theta\frac{\left[\frac{1}{V_P^4}\frac{\partial V_P}{\partial P} + \frac{2}{V_S^4}\frac{\partial V_S}{\partial P}\right]}{\left[\frac{1}{V_P^3} + \frac{2}{V_S^3}\right]}$
$\left(\frac{\partial \Theta}{\partial T}\right)_P = 0$ (Assumption)	

n = No. of atoms per molecular formula

M = Molecular weight

Θ = Einstein temperature

$V_P = V_{PO}\ L\ F_P$;

$V_S = V_{SO}\ L\ F_S$ $\qquad L = \frac{\ell}{\ell_o}$ $F_{P,S} = 1$ at $P = 0$ $T = 300°K$

$K_S = \rho\left(V_P^2 - \frac{4}{3}V_S^2\right)$ $\qquad F = \frac{f}{f_o}$

$K_T = K_S\ (1+\alpha\gamma T)^{-1}$

$\gamma = \frac{\alpha K_S}{C_p\rho}$

Table 2

```
C  PTR - REDUCTION OF HIGH PRESSURE,HIGH TEMPERATURE ULTRASONIC DATA
C
C     THIS PROGRAM PERFORMS THE LENGTH CORRECTION TO ULTRASONIC DATA AT HIGH
C    TEMPERATURE AND PRESSURE FOR A CUBIC CRYSTAL.
C
C  DATA FORMAT
C
C    CARD:
C      1-80   IDENT (20A4) - 80 COLUMNS OF IDENTIFICATION
C
C    CARD:
C      1-10   AN (F10.5) - NUMBER OF ATOMS PER MOLECULAR FORMULA
C      11-20  AM (F10.5) - MOLECULAR WEIGHT
C      21-30  THO (F10.5) - INITIAL VALUE OF EINSTEIN TEMPERATURE (DEG. K)
C      31-40  RO (F10.5) - INITIAL DENSITY (GM/CC)
C      41-50  VPO (F10.5) - INITIAL VALUE OF COMPRESSIONAL VELOCITY (KM/SEC)
C      51-60  VSO (F10.5) - INITIAL VALUE OF SHEAR VELOCITY (KM/SEC)
C      61-70  AO (F10.5) - INITIAL VALUE OF COEFFICIENT OF VOLUME THERMAL
C                    EXPANSION (DEG.K**-1)
C      71-80  GO (F10.5) - INITIAL VALUE OF GRUNHEISEN PARAMETER
C
C  SPECIFIC HEAT DATA AS A FUNCTION OF TEMPERATURE AT ATMOSPHERIC PRESSURE
C
C    CARD
C      1-5    NTCP (I5) - NO. OF DATA POINTS
C
C    CARD: (REPEATED NTCP TIMES)
C      1-10   TCP (F10.5) TEMPERATURE(DEG.K)
C      11-20  CP (F10.5) SPECIFIC HEAT AT CONSTANT PRESSURE (KCAL/MOLE)
C
C  OBSERVED ULTRASONIC DATA-RESULTS OF EACH PRESSURE RUN ARE EXPRESSED IN FORM
C                          F=FO+A*P AND THE FO AND A ARE READ IN AS DATA.
C                          F IS NORMALIZED TO 1.0 AT STANDARD CONDITIONS
C                          (300 DEG. K AND ZERO PRESSURE).
C
C    CARD :
C      1-8    NF (I8)
C      9-16   NPF(1) (I8) NO. OF TEMPERATURES FOR WHICH FO IS GIVEN FOR V1
C      17-24  NPF(2) (I8) NO. OF TEMPERATURES FOR WHICH FO IS GIVEN FOR V2
C      25-32  NPF(3) (I8) NO. OF TEMPERATURES FOR WHICH FO IS GIVEN FOR V3
C      33-40  NPF(4) (I8) NO. OF TEMPERATURES FOR WHICH FO IS GIVEN FOR V4
C      41-48  NA (I8)
C      49-56  NPA(1) (I8) - NO. OF TEMPERATURES FOR WHICH A IS GIVEN FOR V1
C      57-64  NPA(2) (I8) - NO. OF TEMPERATURES FOR WHICH A IS GIVEN FOR V2
C      65-72  NPA(3) (I8) - NO. OF TEMPERATURES FOR WHICH A IS GIVEN FOR V3
C      73-80  NPA(4) (I8) - NO. OF TEMPERATURES FOR WHICH A IS GIVEN FOR V4
C
C  REPEAT THE FOLLOWING SECTION 4 TIMES, FOR V1, V2, V3, V4. (I=1,4)
C*************************************************************************
C*
C*   CARD: (REPEAT NPF(I) TIMES)
C*     1-20   TF (E20.6) - TEMPERATURE FOR FO VALUE
C*     21-40  F (E20.6) - FO VALUE
C*     41-60  SF (E20.6) - STANDARD DEVIATION OF FO VALUE.
C*
C*   CARD: (REPEAT NPA(I) TIMES)
C*     1-20   TA (E20.6) - TEMPERATURE FOR A VALUE
C*     21-40  A (E20.6) - A VALUE
C*     41-60  SA (E20.6) - STANDARD DEVIATION FOR A VALUE
C*************************************************************************
C
C    CARD:
C      5-10   IFIT (I5)
C      1-5    NT (I5) - NUMBER OF TEMPERATURES FOR WHICH PRESSURE INTEGRATION
C                       IS TO BE PERFORMED.
C    CARD: (REPEATED NT TIMES)
C      1-10   DT (F10.5) - TEMPERATURE INTEGRATION STEP SIZE (DEG.K)
C      11-20  TF (F10.5) - FINAL TEMPERATURE VALUE (DEG.K)
C      21-30  DP (F10.5) - PRESSURE INTEGRATION STEP SIZE (KB)
C      31-40  PF (F10.5) - FINAL PRESSURE VALUE (KB)
C      41-50  EPS (F10.5) - RELATIVE ACCURACY TO BE PRESERVED DURING INTEGRATION
C
C  PLOTTING PARAMETERS - REPEAT AS MANY TIMES AS DESIRED.
C
C    CARD:
C      1-10   XL (F10.5) X LENGTH ( INCHES )
C      11-20  YL (F10.5) Y LENGTH ( INCHES )
C      21-30  XMIN (F10.5) - MINIMUM X (PRESSURE) VALUE (KB)
C      31-40  XMAX (F10.5) - MAXIMUM X VALUE
C      41-50  YMIN (F10.5) - MINIMUM Y VALUE (DEPENDS ON QUANTITY BEING
C                            PLOTTED - SEE IV, BELOW)
C      51-60  YMAX (F10.5) - MAXIMUM Y VALUE
C      61-62  IV (I2) - FLAG INDICATING QUANTITY TO BE PLOTTED
C                 ( 1:KS,     2:KT,     3:VPH,    4:VSH,    5:SIGMA,  6:MU,
C                   7:DVPDT,  8:DVSDT,  9:C11,    10:C12,   11:C44,   12:DKTDT,
C                  12:DKSDT, 14:RHO,    15:ALPHA)
C      63-64  NX (I2) - NO. OF INTERVALS ALONG X AXIS
C      65-66  NY (I2) - NO. OF INTERVALS ALONG Y AXIS
```

PART II

Chapter 3

EQUATION OF STATE OF SINGLE CRYSTAL MgO UNDER PRESSURE AND TEMPERATURE

Introduction

In the previous chapter and the appendices, experimental details and data have been described for equation of state measurements on polycrystalline MgO. The startling results, especially the large temperature effect upon the pressure derivatives of the isotropic moduli, lead the author to suspect the validity of using polycrystalline data to predict the behavior of single crystals. Various comparisons between single crystal and polycrystalline MgO samples have been reported in the literature (Chung and Buessem, 1967; Chung, 1967). Anderson, Schreiber, and Liebermann (1968) give a summary of the elastic constants measured in their laboratory. The apparent good agreement found in the above mentioned references is in part due to the large body of data to choose from. Extending the measurements to higher pressures and temperatures simultaneously provides not only the important cross derivatives of the elastic constants with respect to temperature and pressure, but also provides a means to check the validity of the above comparisons.

Experimental Procedure and Sample Description

A high quality MgO single crystal was obtained through the courtesy of O. L. Anderson and P. Andreatch, Jr. The crystal is one of the three described in their paper (Anderson and Andreatch, Jr., 1966). The purity is quoted as 99.4 + %. Slight traces of Si, Al, and Fe were reportedly found by spectrochemical analysis. The specimen faces are (100), $(0\bar{1}1)$, and (011). Orientations were held to ±5 min with corresponding faces flat to 0.5 wavelengths of Na light and within 5×10^{-5} in/in. A ground finish of approximately 10μ is quoted for all sides.

The density of the specimen was determined by the Archimedes method and was found to be 3.5833 gm/cm^3, which agrees exactly with the X-ray density reported by Skinner (1957).

The dimensions of the nearly cubic specimen were measured as 0.4388 in. perpendicular to the (100) plane, and 0.4298 and 0.4206 in. for the other two directions. The surface finish was refined in this laboratory by polishing with 0.05μ polishing compound. The flatness over the contact area between the buffer rod and the sample was on the order of .1 wavelengths of Na light. The contact area is a circle of approximately 0.3 inch diameter.

The furnace which was used in the polycrystalline MgO experiment was redesigned to accommodate a cubic specimen instead of the cylindrical polycrystalline specimen. Detailed construction drawings and pictures are included in Appendix B. The electronic arrangement

and the high pressure systems are the same as those used for the polycrystalline measurements.

Two compressional and two shear velocities were measured. For the compressional velocities a 15 MHz transducer was bonded to the buffer rod and operated at a nominal frequency of 45 MHz. The shear velocities were measured at 20 MHz with a 20 MHz transducer. The signal quality was excellent throughout the experiment. Neither an increase in pressure nor temperature seemed to affect the quality or coherence of the signal. The attenuation at 800°K was slightly larger than at lower temperatures.

Data and Data Reduction

The velocities and the directions in which they were measured on the single crystal are given in Table 1.

The velocities at any temperature and pressure are directly related to the length and the frequency by

$$V = V_o \; L \; F$$

where V_o is the velocity at standard conditions, in this case 300°K and zero pressure. L and F are normalized length and frequency, respectively; i.e., they are both one at 300°K and 0 kb. The frequency data were taken along isotherms in the same manner as for the polycrystalline specimen. From 5 to 9 pairs of maxima and minima were taken at approximately 10,000 psi intervals from the lowest

permissible pressure to a maximum pressure of about 110,000 psi. The lowest permissible pressure is a function of the convecting gas and was described in more detail in the previous chapter. In no case was this pressure above 40,000 psi. The pressure derivatives are therefore determined over a range of at least 3 to 4 kb.

The slope of frequency versus pressure is fitted by a least square fit to a straight line. The data points which are used for this straight line fit are selected in the following manner. At each pressure point along an isotherm, the pressure, the end thermocouple, and the center thermocouple readings as well as the average of a set of maxima and minima are recorded. Since there are always slight deviations in temperature from a previously selected temperature for an isotherm, a small temperature correction has to be applied to the raw data. The corrections are small and are approximated with the $\frac{\partial F}{\partial T}\Big)_P$ slope at zero pressure. Chromel-Alumel thermocouples are quite linear and have a temperature response of approximately 40μv/°C. The temperature correction then becomes to first order

$$F = F_o + \frac{\partial F}{\partial T} \Delta T$$

or in terms of millivolts

$$F = F_o + 25 \frac{\partial F}{\partial T} \Delta V$$

where ΔV is in millivolts. The values for $\frac{\partial F}{\partial T}$ are measured under vacuum and crosschecked against the values obtained from the isotherms when extrapolated to zero pressure. The temperature correction is

applied to all data points for the end temperature, the center temperature and the average temperature. The data points for which the corrected frequencies for the center and end thermocouple differ by more than one part in 10,000 are rejected. The reason for the temperature difference is thought to be convection of the gas in the vessel, as mentioned earlier.

As an illustration of the above procedure, the data for the 600°K isotherm of

$$V_3 = \sqrt{\frac{C_{11}-C_{12}}{2\rho}}$$

is given in Table 2. Column 1 gives a running index of the data points taken, column 2 indicates the pressure, column 3 gives the average frequency of 9 maxima and 9 minima. The next three columns give the temperature corrected frequency values corresponding to average, the end and the center temperatures. Column 7 gives the frequency values calculated from a least square fit of all data points without temperature corrections. Finally, column 8 gives the values of those points which were chosen according to the above criteria; the values are calculated from a least square fit of the temperature corrected values for the average temperature. σ_y below column 7 and 8 are the standard deviations. The equation for the straight lines and the appropriate standard deviations are given below the data. A handy reference for the error analysis is Beer's Theory of Error. Figure 1 gives a graphical illustration of the type of fit to the data. The solid line represents the fit to the temperature corrected

data.

The above frequency data analysis has been applied to all data which was taken. Frequencies have been measured for the four velocities along isotherms in the vicinity of 300°K and at 500, 600, 700, and 800°K. The normalized frequency data are a function of temperature is given in Table 3. The errors indicated are standard deviation.

Since there are only three independent elastic constants in a cubic crystal, the measurements of four different velocities provide a redundancy check. This check was accomplished by measuring V_4. The equations involved in the error analysis and the redundancy check are given in Table 4. In Table 5 the values for the frequencies and velocities and their pressure and temperature derivatives are given. Figure 2 is a plot of the velocity derivatives with error bars. The error bars with arrows are calculated rather than measured values. The redundancy check is within one standard deviation for all temperatures except at 800°K. This is due to a bad data point on V_1. Assuming the measured value at 800°K for V_4 to be correct yields the value for V_1 which is indicated on the graph. The measured value is $\frac{\partial F}{\partial P} = (11.21 \pm .06) \times 10^{-3}$ while the calculated value becomes $(11.74 \pm .05) \times 10^{-3}$ which is more consistent with the other data and will be used in the further data reductions.

The final data reduction uses a modified version of the reduction scheme which was described in an earlier chapter. The program which was originally written for the reduction of isotropic materials was modified to include the reduction of single crystals of cubic symmetry.

The adiabatic bulk modulus for crystals of cubic symmetry is given by

$$K_s = \frac{1}{3}\left(C_{11} + C_{12}\right)$$

or in terms of velocities as

$$K_s = \rho\left(V_1^2 - \frac{4}{3} V_3^2\right)$$

which is of the same form as in the isotropic case, V_1 corresponding to V_p and V_3 to V_s. For a cubic crystal the linear coefficients of expansion and incompressibility are the same in all directions such that from the above K_s the volume can be determined in the same manner as in the isotropic case. The elastic constants C_{11}, C_{12}, and C_{44}, and their pressure and temperature derivatives have also been incorporated into the computer program. To allow a direct comparison between the single crystal data and the isotropic data the Voigt-Reuss approximations are also included. These are given in a convenient form by Chung (1967). Rewriting them slightly to conform with the notation used here, they are

$$\mu_V = \frac{\rho}{5}\left(2V_3^2 + 3V_2^2\right)$$

$$= \frac{5\rho\, V_3^2\, V_2^2}{3V_3^2 + 2V_2^2}$$

$$\frac{\partial \mu_V}{\partial X} = \frac{1}{5}\frac{\partial C}{\partial X} + \frac{3}{5}\frac{\partial C_{44}}{\partial X}$$

$$\frac{\partial \mu_R}{\partial X} = \frac{4}{5}\left(\frac{\mu_R}{C}\right)^2\left(\frac{\partial C}{\partial X}\right) + \frac{3}{5}\left(\frac{\mu_R}{C_{44}}\right)^2\left(\frac{\partial C_{44}}{\partial X}\right)$$

where $C = C_{11} - C_{12} = 2\rho V_3^2$, and X may be either temperature or pressure. The values of the elastic constants and their pressure and temperature derivatives will be discussed in the next chapter.

REFERENCES

Anderson, O. L., and P. Andreatch, Jr., Pressure derivatives of elastic constants of single-crystal MgO at 23° and -195.8°C, J. Am. Ceram. Soc., 49, 8, 404-409, 1966.

Anderson, O. L., E. Schreiber, R. C. Liebermann, and N. Soga, Some elastic constant data on minerals relevant to geophysics, Rev. Geophys., 6, 491-524, 1968.

Chung, D. H., First pressure derivatives of polycrystalline elastic moduli: their relation to single-crystal acoustic data and thermodynamic relations, J. Appl. Phys., 38, 5104-5113, 1967.

Chung, D. H., and W. R. Buessem, The voigt-Reuss-Hill approximation and elastic moduli of polycrystalline MgO, CaF_2, β-ZnS, ZnSe, and CdTe, J. Appl. Phys., 38, 2535-2540, 1967.

Skinner, B. J., Thermal expansions of thoria, periclase, and diamond, Am. Mineralogist, 42 (1-2), 39-55, 1957.

Table 1

Velocity designation and formula	Direction of wave propagation	Direction of particle motion	Path length (cm)	Velocity (V_o in km/sec)
$V_1 = \sqrt{\frac{C_{11}}{\rho}}$	100	100	2.2286	9.1068
$V_2 = \sqrt{\frac{C_{44}}{\rho}}$	100	011	2.2286	6.6013
$V_3 = \sqrt{\frac{C_{11} - C_{12}}{2\rho}}$	011	$0\bar{1}1$	2.1834	5.3056
$V_4 = \sqrt{\frac{C_{11} + C_{12} + 2C_{44}}{2\rho}}$	011	011	2.1834	9.9184

Table 2

600°K Isotherm

n	Pressure kpsi	F Mean MHz	Av. F Temp. Corr.	End F Temp. Corr.	Center F Temp. Corr.	No Corr. F Calc.	Temp. Corr. to Av. F Calc.
1	9.0	11.5328	11.5308	11.5310	11.5302	11.5320	11.5313
2	16.7	11.5450	11.5448	11.5458	11.5434	11.5436	
3	27.9	11.5595	11.5599	11.5608	11.5586	11.5604	
4	41.0	11.5784	11.5792	11.5798	11.5783	11.5808	11.5797
5	57.3	11.6062	11.6051	11.6025	11.6073	11.6046	
6	80.0	11.6402	11.6391	11.6384	11.6395	11.6388	11.6387
7	91.85	11.6571	11.6563	11.6557	11.6567	11.6566	11.6567
8	103.8	11.6731	11.6740	11.6730	11.6747	11.6745	11.6738
9	91.65	11.6560	11.6563	11.6554	11.6569	11.6563	11.6556
10	85.0	11.6463	11.6456	11.6448	11.6461	11.6463	
11	75.0	11.6313	11.6318	11.6311	11.6321	11.6312	11.6306
12	65	11.6157	11.6166	11.6160	11.6167	11.6162	11.6160
13	55	11.6031	11.6020	11.6016	11.6020	11.6012	

Table 2 (continued)

n	Pressure kpsi	F Mean	Av. F Temp. Corr.	End F Temp. Corr.	Center F Temp. Corr.	No Corr. F Calc.	Temp. Corr. to Av. F Calc.
14	45	11.5866	11.5863	11.5862	11.5861	11.5862	11.5858
15	35	11.5691	11.5708	11.5715	11.5702	11.5711	
16	24.7	11.5566	11.5580	11.5592	11.5566	11.5556	
17	16.2	11.5413	11.5443	11.5457	11.5429	11.5429	
					σ_Y =	.0013	.0006

$Y = (11.5185 \pm .0007) + (15.03 \pm .11) \times 10^{-4} P$

$F = 1 + (13.05 \pm .09) \times 10^{-5} P$

All data no temperature correction

$Y = (11.5177 \pm .0005) + (15.13 \pm .07) \times 10^{-4} P$

$F = 1 + (13.14 \pm .06) \times 10^{-5} P$

Selected data temperature corrected

Corrected and uncorrected frequency versus pressure data for $V_3 = \sqrt{\frac{C_{11}-C_{12}}{2\rho}}$. Pressure is in kpsi, frequencies are in MHz if multiplied by two. (A frequency doubler was used in conjunction with a frequency synthesizer.)

Table 3

Normalized frequency data as a function of temperature.

T (°K)	F for V_1 σ ±.00005	T(°K)	F for V_2 ±.00005	T (°K)	F for V_3 ±.00005	T (°K)	F for V_4 ±.00005
291	1.00251	288	1.00047	295	1.00119	291	1.00045
300	1.00000	300	1.00000	300	1.00000	300	1.00000
360	.99582	320	.99939	319	.99669	310	.99953
389	.99319	370	.99749	361	.98992	339	.99799
458	.98625	399	.99634	431	.97831	368	.99654
531	.97906	450	.99421	504	.96656	388	.99536
589	.97337	509	.99173	575	.95480	438	.99251
667	.96526	625	.98671	643	.94362	474	.99069
732	.95853	699	.98356	711	.93219	552	.98635
813	.95023	800	.97878	800	.91754	617	.98237
						700	.97718
						800	.97120

Table 3 (continued)

$a = \frac{\partial F}{\partial P}$ as a function of temperature

T°K	$a \times 10^{-4}$ a for V_1	T°K	$a \times 10^{-4}$ a for V_2	T°K	$a \times 10^{-4}$ a for V_3	T°K	a for $V_4 \times 10^{-4}$
290	13.62 ± .10	323	2.39 ± .10	288	16.87 ± .10	287	7.49 ± .07
500	14.05 ± .14	500	2.61 ± .03	500	18.15 ± .11	500	7.64 ± .03
600	14.20 ± .11	600	2.61 ± .04	600	19.06 ± .08	600	7.67 ± .09
700	14.46 ± .25	700	2.77 ± .03	700	19.57 ± .11	700	7.98 ± .12
800	14.93 ± .07	800	2.81 ± .02	800	20.02 ± .13	800	8.15 ± .03

Table 4

Relations between V_1, V_2, V_3 and V_4 and their standard deviations

Error Analysis and Redundancy Check

$$V_1^2 = \frac{C_{11}}{\rho}, \quad V_2^2 = \frac{C_{44}}{\rho}, \quad V_3^2 = \frac{C_{11}-C_{12}}{2\rho}, \quad V_4^2 = \frac{C_{11} + C_{12} + 2C_{44}}{2\rho}$$

$$V_4^2 = V_1^2 + V_2^2 - V_3^2$$

$$\frac{\partial V_4}{\partial P} = \frac{1}{V_4}\left[V_1 \frac{\partial V_1}{\partial P} + V_2 \frac{\partial V_2}{\partial P} - V_3 \frac{\partial V_3}{\partial P} \right] \qquad \left(\frac{\partial V_n}{\partial P}\right)_T = V_{no}\left[\left(1 + \frac{\alpha}{3}\Delta T\right)\frac{\partial F_n}{\partial P} - \frac{F_n}{3\left(K_T - \frac{\partial K_T}{\partial T}\Delta T\right)}\right.$$

$$\frac{\partial V_4}{\partial T} = \frac{1}{V_4}\left[V_1 \frac{\partial V_1}{\partial T} + V_2 \frac{\partial V_2}{\partial T} - V_3 \frac{\partial V_3}{\partial T} \right]$$

$$\sigma\left(\frac{\partial V_4}{\partial P}\right) = \frac{1}{V_4}\left[V_1^2\, \sigma(\partial V_1)^2 + V_2^2\, \sigma(\partial V_2)^2 + V_3^2\, (\partial V_3)^2 \right]^{\frac{1}{2}} \quad \leftarrow \text{ standard error}$$

no error is assumed in F, K_T, and V_n

Table 5

n	T°K K_T ρ	F_n	$\frac{\partial F_n}{\partial P}$ x 10^{-4}	$V_n(P=0)$	$\frac{\partial V_n}{\partial P}$ x 10^{-3}
1	300	1.000	13.63 ± .10	9.1068	10.50 ± .09
2	3.5833	1.000	2.39 ± .10	6.6013	.20 ± .07
3	1598	1.000	16.96 ± .10	5.3056	7.88 ± .05
4 meas.		1.000	7.50 ± .07	9.9184	5.36 ± .07
4 calc.		1.000	7.69 ± .14	-	5.56 ± .10
1	500	.98245	14.05 ± .14	8.9437	10.90 ± .12
2	1557	.99200	2.61 ± .03	6.5586	.33 ± .02
3	3.5583	.96705	18.15 ± .11	5.1434	8.55 ± .06
4 meas.		.98910	7.64 ± .03	9.8258	5.54 ± .03
4 calc.					5.66 ± .11

Cross check for pressure derivatives as a function of temperature.

Table 5 (continued)

n	$T°K$ K_T ρ	F_n	$\frac{\partial F_n}{\partial P}$ x 10^{-4}	$V_n(P=0)$	$\frac{\partial V_n}{\partial P}$ x 10^{-3}
1	600	.97215	14.20 ± .12	8.8616	11.04 ± .11
2	1537	.98775	2.61 ± .04	6.5376	.32 ± .03
3	3.5457	.95075	19.06 ± .08	5.0613	9.05 ± .04
4 meas.		.98320	7.67 ± .09	9.7787	5.51 ± .09
4 calc.					5.53 ± .10
1	700	.96195	14.46 ± .25	8.7805	11.29 ± .22
2	1517	.98315	2.77 ± .03	6.5165	.41 ± .02
3	3.5331	.93445	19.57 ± .11	4.9802	9.34 ± .05
4 meas.		.97710	7.98 ± .12	9.7327	5.82 ± .12
4 calc.					5.68 ± .20

Table 5 (continued)

n	$T°K$ K_T ρ	F_n	$\frac{\partial F_n}{\partial P}$ x 10^{-4}	$V_n(P=0)$	$\frac{\partial V_n}{\partial P}$ x 10^{-3}
1	800	.95155	14.36 ± .07	8.6994	11.21 ± .06
2	1496	.97880	2.81 ± .02	6.4955	.43 ± .01
3	3.5206	.91760	20.02 ± .13	4.9892	9.59 ± .06
4 meas.		.97125	8.15 ± .03	9.6856	5.98 ± .03
4 calc.					5.51 ± .07

Values of velocities and normalized frequencies calculated according to the equations given in Table 4.

FIGURE CAPTIONS

Figure 1. Frequency versus pressure for V_3 and 600°K isotherm.

Figure 2. The length of the bars span the total range of data with temperature corrections (see Table 2 and text). Pressure derivatives of the velocities in single crystal MgO as a function of temperature. V_1, V_2, V_3, and V_4 are defined in the text.

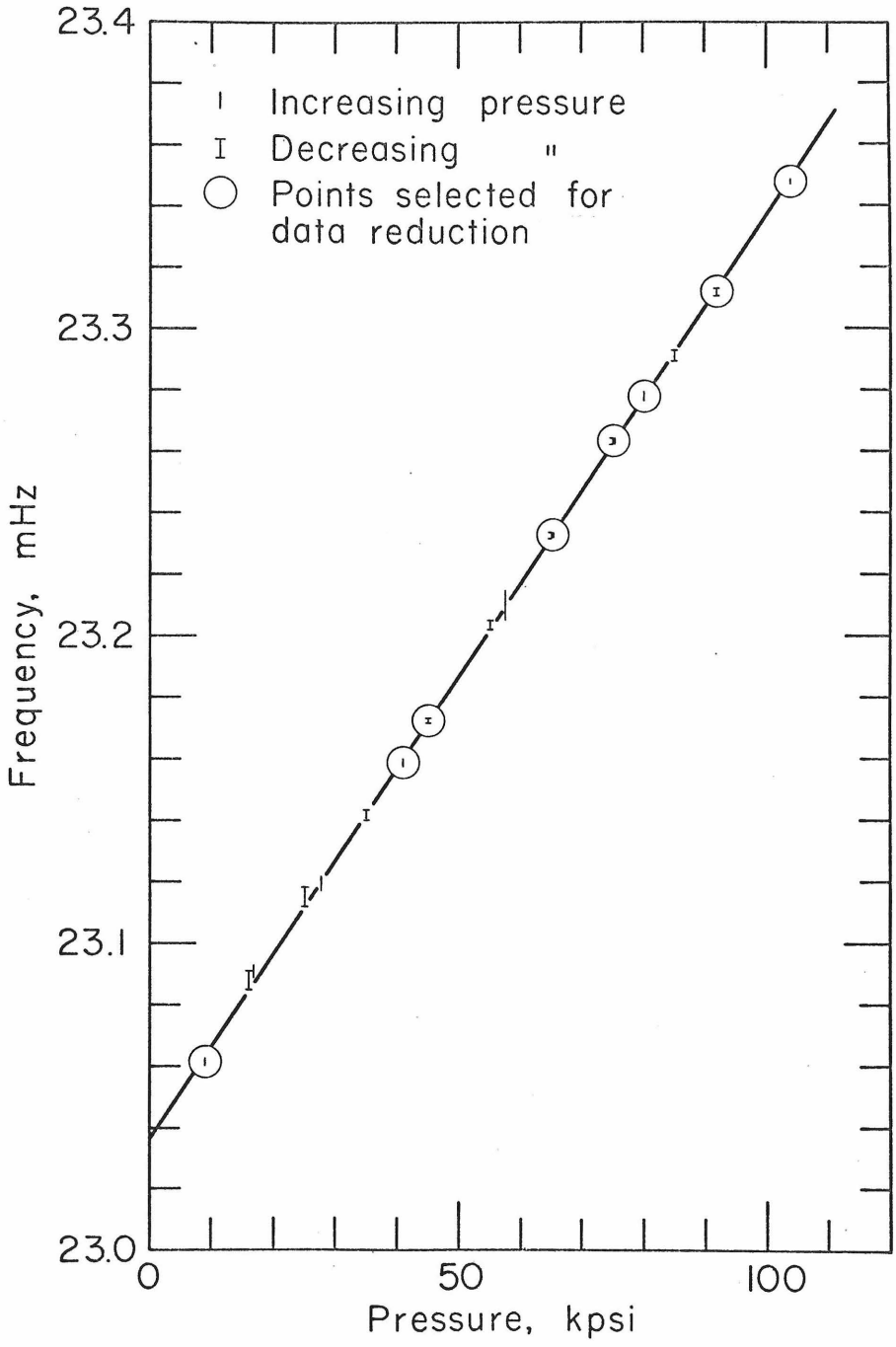
23.4
23.3
23.2
23.1
23.0
Frequency, mHz
Increasing pressure
Decreasing "
Points selected for data reduction
0
50
100
Pressure, kpsi

Figure 1

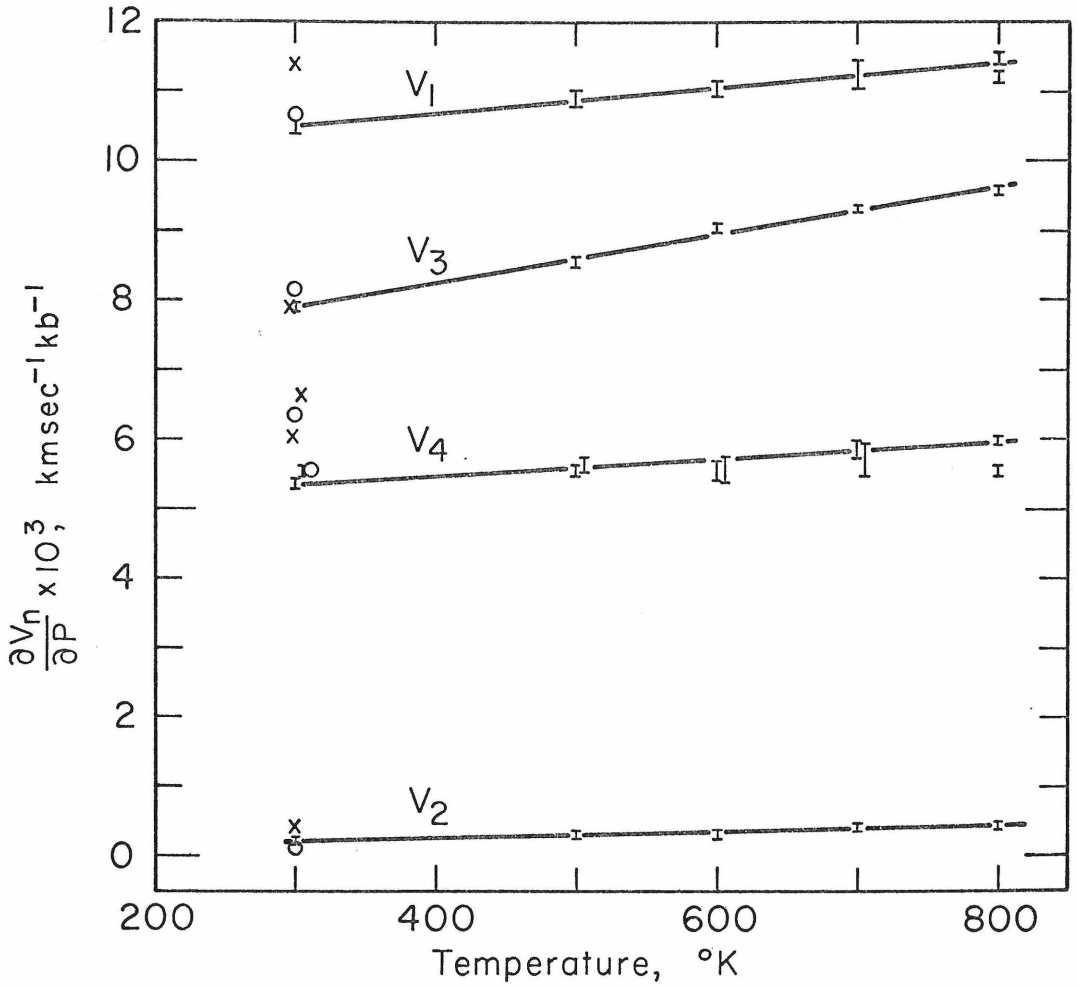
12
10
8
6
4
2
0
200
400
600
800
Temperature, °K
$\frac{\partial V_n}{\partial P} \times 10^3$; kmsec^{-1}kb^{-1}
V_1
V_3
V_4
V_2

Figure 2

PART II

Chapter 4

DATA INTERPRETATION AND COMPARISON WITH PREVIOUS WORK

Introduction

A considerable number of papers have been published on the elastic constants of MgO. These can be divided into two groups, one group of experimenters used a Förster type resonance method; the other, ultrasonic interferometry. Data on single crystal and hot-pressed polycrystalline specimens have been obtained. Several of the reports give direct comparisons between single crystal and polycrystalline data obtained in one laboratory under identical experimental conditions. All high temperature data with the exception of the work reported in this thesis have been obtained under atmospheric pressure by resonance measurements. Data as a function of pressure were obtained by ultrasonic interferometry. Only in one paper (Chung and Simmons, 1969) was a polycrystalline sample checked for anisotropy.

Comparison of Data

A condensed summary of all published data for MgO is presented in Tables 1 and 2. Table 3 gives a short note for each reference in Tables 1 and 2, and provides information about the source of the sample, type of bond, and the frequency range, where applicable.

The data from the resonance experiments are quite consistent

with the exception of the data by Susse. Ignoring her values the C_{ij} obtained by the other investigators agree to within 1% except for Bhagavantam's C_{44} value. Graphical comparisons between the elastic constants as a function of temperature are given in Figures 1, 2, and 3. The data for C_{44} are by far the best and are compatible between the resonance and the interferometer experiments. C_{44} is the only elastic constant which can be determined directly by both methods. Figure 4 gives the adiabatic bulk modulus as a function of temperature. The large discrepancies in the absolute values are probably due to the errors introduced when the shear moduli and the Youngs moduli data, which are obtained by the resonance techniques, are used to compute the bulk modulus. This difficulty is illustrated in Part 1 of this thesis. The temperature dependence is in good agreement except for the data by Susse (1961) and Durand (1936).

To compare the measurements made by interferometry, one has to examine some of the experimental techniques. The pulse superposition method has been used by all previous investigators. This method is due to McSkimin (1961). A transducer is bonded directly to the specimen and the spacing between consecutive echoes from applied R. F. pulses is measured by carefully determining the pulse repetition frequency of the R. F. pulses. Corrections for the effect of the bond and the mass loading of the transducer, when it is operated off resonance, are needed. The bond correction

is reportedly small and is applied to the measurements by the various authors. The bonding materials are usually some type of grease (see Table 3). The velocities in the bond are much lower than in MgO. Therefore, if the bond correction is too small, or ignored entirely, the velocities which are measured appear to be too low and the pressure derivatives too large. A transducer which is operated at its fundamental resonance frequency acts as a quarter wave plate and requires no correction. Under pressure, the resonance frequency of a transducer increases while its Q decreases. The decreasing Q makes it difficult to find the exact resonance frequency of the transducer. Maximum amplitude and minimum stress are obtained at the free end of the transducer. When the pressure is increased and the resonance frequency of the transducer is not followed the point of maximum stress migrates into the sample. This effectively decreases the length of the sample and also leads to larger values for the pressure derivatives of the velocities.

The above mentioned corrections, if applied incorrectly, are not necessarily evident in polycrystalline data. As long as the experiments are performed carefully, the reproducibility may be very good, yet the absolute values may be in error. A case in point is illustrated in Table 4, where the present results of the velocity pressure derivatives of single crystal MgO are compared with the results obtained by Anderson and Andreatch (1966) and Bogardus (1965).

By measuring four velocities and their respective pressure derivatives, a redundancy check is provided. The velocities V_n and their pressure derivatives $\frac{\partial V_n}{\partial P}$ have been defined in the previous chapter. $\frac{\partial V_4}{\partial P}$ measured is compared with $\frac{\partial V_4}{\partial P}$ calculated. K_S in terms of the velocities may be written as $K_S = \rho\left(V_1^2 - \frac{4}{3} V_3^2\right)$. Table 5 gives a condensed summary of the velocities, the adiabatic bulk moduli and $\frac{\partial K_S}{\partial P}$ for three single crystal specimens and three polcrystalline specimens. Two values for $\frac{\partial K_S}{\partial P}$ are given for the single crystal data. These are the results of redundancy checks as illustrated in Table 4. The large discrepancies apparent in the data of Anderson and Andreatch (1966) and Bogardus (1965) confirm the suspicion of inadequate corrections for their measurements. A redundancy can not be made from the data provided by Chang and Barsch (1969). In view of these large discrepancies, it seems that a $\frac{\partial K_S}{\partial P}$ of approximately 3.8 is not inconsistent with all previous data and should be adopted as the correct value.

The low value for $\frac{\partial K_S}{\partial P}$ obtained from the single crystal measurements is in conflict with the considerably higher values measured on high density polycrystalline MgO. In Chapter 1, the elastic constants for a polycrystalline sample were reported. Also the structure of the crystallites was discussed. It was noted that the grains were preferentially compressed in the 100 direction. Macroscopic isotropy was not much affected. This is also confirmed by the studies of Chung and Simmons (1969) quoted earlier. In

Chapter 1 values for $\frac{\partial K}{\partial P}$ and K_S of 4.43 and 1624 kb, respectively, were given, in good agreement with the data obtained on a sample from the same source by Soga and Anderson (1966). The large discrepancy between the polycrystalline results and the single crystal results, and the internal consistency of the latter prompted the author to remeasure the polycrystalline sample. Figure 5 gives a plot of $\frac{\partial F}{\partial P}$ as a function of temperature for both the shear mode and the compressional mode. The first data run as well as the second are shown. The first exposure of the sample to high temperature and pressure occurred during the first measurements of the compressional modes. It is apparent from the data in Figure 5, that the sample underwent further sintering. This exposure to high temperature and high pressure had two pronounced effects upon the sample; further distortion of the grains in the manner discussed in Chapter 1 and vacancy diffusion to the grain boundaries, resulting in purer crystallites. The distortion of the grains leads to a higher proportion of 111 directions, thus, increasing the compressional velocity and decreasing the shear velocity. This is indeed observed when the data for Avco X-1 and Avco Z-1 are compared. The adiabatic bulk modulus is increased in the process to a value of 1657 kb. The vacancy diffusion, in addition to the grain distortion, lowers the $\frac{\partial K_S}{\partial P}$ to 3.78.

The break in the slope which is observed for both compressional velocity runs is as yet unexplained. Several suggestions such as the formation of hydroxide and/or carbonate phases occurring among

the minute impurities and plastic flow of the crystallites have been offered. None of these satisfactorily explain why only the compressional waves are affected.

The data given in Table 5 illustrate the above points. The velocities measured in this laboratory, where neither a bond nor a transducer correction are necessary, are all slightly higher than those measured by the pulse superposition technique. The values in parenthesis are the ratios between the velocities measured in this laboratory and those of other investigators. It should be noted that V_1 and V_4 are compressional velocities, while V_2 and V_3 are shear velocities. Compared to our values the ratio for the compressional velocities are always larger than those for the shear velocities. The consistency of these ratios is a striking result and reflects the ultimate accuracy which may eventually be achieved by ultrasonic interferometry.

Single Crystal MgO Data as a Function of Temperature and Pressure

The unreduced single crystal data given in Chapter 3 have been reduced by the method described in Chapter 2. A complete set of elastic constants is given in Table 7 and a selected portion is illustrated graphically in Figures 6 through 16. The range in pressure is from zero to ten kilobars and the range in temperature from 300°K to 1200°K. Table 6 illustrates the variation of the temperature and pressure derivatives. There is very little effect of pressure upon the temperature derivatives, but a significant effect of

temperature on the pressure derivatives. This is to be expected, since the range of the thermal pressure due to temperature changes is much larger than the range of the hydrostatic pressure which is applied to the sample. A volume change corresponding to 10 kb is achieved by a temperature variation of about 150°C. It is interesting to note that while $\frac{\partial K_S}{\partial P}$ decreases as the temperature is increased, $\frac{\partial K_T}{\partial P}$ remains essentially constant. This gives confidence in long extrapolations over a large pressure range, even at high temperatures.

CONCLUSIONS AND RECOMMENDATIONS

Experimental techniques have been developed to measure the elastic constants of solids and their derivatives at high pressures and high temperatures. These techniques have been applied to measure pseudo-resonance frequencies for MgO over a pressure range from 0 to 10 kb and a range in temperature from room temperature to the Debye temperature. These are the first such measurements which have been made at simultaneous high pressure and temperature. A self-consistent set of linear partial differential equations has been used to reduce the pseudo-resonance frequencies to yield elastic constant data. This set of differential equations is equivalent to a complete equation of state.

Measurements by other authors have been checked for internal consistency and have been compared to the present measurements where

applicable. It has been found that the apparent agreement in the literature, between single crystal and polycrystalline data is fortuitous, and is not borne out by the present measurements or by the reanalysis of published results. The disagreement is explained in terms of preferential deformation of individual crystallites during hot pressing. All previous and present measurements of the pressure derivatives of single crystal and polycrystalline MgO are reviewed and the discrepancies explained.

The difficulties encountered when comparing single crystal and polycrystalline MgO data are believed to be general and should be considered when other single crystal data are compared with data of "high quality" polycrystalline samples.

Hot pressing techniques should be studied very carefully to determine if it is possible to sinter powders into polycrystalline samples which approach not only theoretical density but also maintain the original crystal symmetry of the individual crystallites. When powders of symmetry lower than cubic are sintered at high temperatures and high pressures, the problems of residual strain are expected to be more severe due to the different thermal expansion and compression in different crystal directions.

REFERENCES

Anderson, O. L., and P. Andreatch, Jr., Pressure derivatives of elastic constants of single-crystal MgO at 23° and -195.8°C, J. Am. Ceram. Soc., 49, 8, 404-409, 1966.

Anderson, O. L., and E. Schreiber, The pressure derivatives of the sound velocities of polycrystalline magnesia, J. Geophys. Res., 70, 20, 5241-5248, 1965.

Bogardus, E. H., Third-order elastic constants of Ge, MgO, and fused SiO_2, J. Appl. Phys., 36, 8, 2504-2513, 1965.

Bhagavantam, Symposium on elasticity of crystals: I, Proc. Ind. Acad. of Sci., 41A, 3, 72-90, 1955.

Chang, Z. P., and G. R. Barsch, The pressure dependence of the elastic constants on single crystalline magnesium oxide, in press, 1969.

Chung, D. H., Elastic moduli of single crystal and polycrystalline MgO, Phil. Mag., Ser. 8, 8, 833-841, 1963.

Chung, D. H., J. J. Swica, and W. B. Crandall, Relation of single-crystal elastic constants to polycrystalline isotropic elastic moduli of MgO, J. Am. Ceram. Soc., 46, 9, 452-457, 1963.

Chung, D. H., and W. G. Lawrence, Relation of single-crystal elastic constants to polycrystalline isotropic elastic moduli of MgO: II, Temperature dependence, J. Am. Ceram. Soc., 47, 448-455, 1964.

Chung, D. H., and Gene Simmons, Elastic properties of polycrystalline periclase, J. Geophys. Res., in press, 1969.

Durand, M. A., Temperature variation of elastic moduli of NaCl, KCl, and MgO, Phys. Rev., 50, 5, 449-455, 1936.

McSkimin, H. J., Notes and references for the measurement of elastic moduli by means of ultrasonic waves, J. Acoust. Soc. Am., 33, 606, 1961.

Schreiber, E., and O. L. Anderson, Temperature dependence of the velocity derivatives of periclase, J. Geophys. Res., 71, 12, 3007-3012, 1966.

Schreiber, E., and O. L. Anderson, Revised data on polycrystalline magnesium oxide, J. Geophys. Res., 73, 8, 2837-2838, 1968.

Soga, N., and O. L. Anderson, High-temperature elastic properties of polycrystalline MgO and Al_2O_3, J. Am. Ceram. Soc., 49, 355, 1966.

Susse, C., Measurement of the elastic constants of lithium fluoride and periclase as a function of temperature and pressure, J. Rech. Centr. Natl. Rech. Sci., Lab. Bellevue, Paris, No. 54, 2357, 1961.

Table 1

Consolidated data of elastic constants for MgO

Resonance experiments

Property / Comments	Units	Bhag. Single X'l	Chung Single X'l	Chung et al Single X'l	Chung & Lawrence Single X'l	Durand Single X'l	Soga & Anderson Poly X'l	Susse Single X'l
ρ	gr cm^{-3}		3.581	3.581	3.576	3.5761	3.579	
V_1	km sec^{-1}							
V_2	km sec^{-1}							
V_3	km sec^{-1}							
V_P	km sec^{-1}			9.576				
V_S	km sec^{-1}			6.028				
C_{11}	kb	2860	2891.7	2891.7	2863	2894		3000
C_{12}	kb	870	879.6	879.5	876	877		1010
C_{44}	kb	1480	1546.1	1546.1	1541	1548		1575
K_S	kb	1533	1550	1550	1538	1549	1644	1673

Interferometer experiments

Property / Comments	Units	Temp.°K	Anderson & Andreatch Single X'l	Anderson & Schreiber Poly X'l	Bogardus Single X'l	Chang & Barsch Single X'l	Chung & Simmons Poly X'l	Schreiber & Anderson 1966 Poly X'l	Schreiber & Anderson 1968 Poly X'l	This Work Poly X'l	This Work Single X'l
ρ	gr cm^{-3}	~300	3.5833	3.5800	3.579	3.579	3.582	3.5800	3.5797	3.5797	3.5852
V_1	km sec^{-1}	~300	9.09585		9.09932						9.1068
V_2	km sec^{-1}	~300	6.59539		6.59648						6.6013
V_3	km sec^{-1}	~300	5.30111		5.30189						5.3056
V_P	km sec^{-1}	~300	9.681	9.7662			9.698	9.7662[3]	9.6605	9.6966	9.705
		194.5						9.8179			
V_S	km sec^{-1}	~300	6.041	5.9635			6.009	5.9635[3]	5.9974	6.041	6.047
		194.5						6.0138			
C_{11}	kb	~300	2964.7		2970.77	2966.4					2974
		77.2	3061.7								
C_{12}	kb	~300	950.7		953.65	950.8					955.7
		77.2	937.8								
C_{44}	kb	~300	1588.9		1561.26	1558.1					1562
		77.2	1575.8								
K_S	kb	~300	1622	1717.0	1626.0	1622.6	1644.4	1717.0[3]	1624	1624	1628
		77.2	1646					1729.4[4]			
K_T	kb	~300	1598	1691				1691.0[3]		1601	1605
$\frac{\partial C_{11}}{\partial T}$	kb °K^{-1}	~300						1717.1[4]			-.605
$\frac{\partial C_{12}}{\partial T}$	kb °K^{-1}	~300									.074
$\frac{\partial C_{44}}{\partial T}$	kb °K^{-}	~300									-.103
$\frac{\partial V_P}{\partial T}$	km sec^{-1}	~300						-5.0[3]		-5.89	-5.05
	°K^{-1}x10^4							-4.3[4]			
$\frac{\partial V_S}{\partial T}$	km sec^{-1}	~300						-4.8[3]		-5.47	-4.33
	°K^{-1}x10^4							-3.6[4]			
$\frac{\partial K_S}{\partial T}$	kb °K^{-1}	~300	-.16					-.13[3]		-.15	-.15
		77.2	-.05[2]					-.11[4]			
$\frac{\partial K_T}{\partial T}$	kb °K^{-1}	~300						-.29[3]		-.26	-.27
								-.25[4]			
$\frac{\partial C_{11}}{\partial P}$		~300	9.477			9.16					8.70
		77.2	9.975								
$\frac{\partial C_{12}}{\partial P}$		~300	1.992			1.82					1.42
		77.2	2.166								
$\frac{\partial C_{44}}{\partial P}$		~300	1.160			1.12					1.09
		77.2	1.431								
$\frac{\partial V_P}{\partial P}$	km sec^{-1}	~300		7.71			7.80	7.711[3]	8.66	8.04	7.19
	kb^{-1} x 10^3							7.57[4]			
$\frac{\partial V_S}{\partial P}$	km sec^{-1}	~300		4.35			3.75	4.35[3]	4.23	3.73	3.76
	kb^{-1} x 10^3							4.07[4]			
$\frac{\partial K_S}{\partial P}$		~300	4.497	3.91	4.15[1]	4.27	4.28	3.92[3]	4.58	4.44	3.85
		77.2	4.738					4.00[4]			
$\frac{\partial K_T}{\partial P}$		~300	4.52	3.94				3.94[3]		4.47	3.89
								4.02[4]			

Table 2

Properties of MgO as a function of temperature.

Property	Units	Temp.°K	Chung & Lawrence	Durand	Soga & Anderson	Susse	This Work Polycrystalline 0 kb	This Work Polycrystalline 10 kb	This Work Single X'l 0 kb	This Work Single X'l 10 kb
C_{11}	kb	300	2863	2893		2992			2974	3059
C_{12}	kb		876	877		999			956	968
C_{44}	kb		1541	1547		1574			1562	1573
K_S	kb		1538	1549	1644	1663	1624	1669	1628	1665
K_T	kb						1601	1645	1605	1642
E	kb		3052[5]		3097					
			3052[6]							
μ	kb				1306		1306	1331	1311	1336
σ							.183	.185	.183	.184

Table 2 (continued)

Property	Units	Temp.°K	Chung & Lawrence	Durand	Soga & Anderson	Susse	This Work Polycrystalline 0 kb	This Work Polycrystalline 10 kb	This Work Single X'ℓ 0 kb	This Work Single X'ℓ 10 kb
C_{11}	kb	500	2732	2767		2821			2851	2937
C_{12}	kb		876	893		996			.967	980
C_{44}	kb		1515	1519		1560			1534	1545
K_S	kb		1495	1518	1611	1604	1594	1636	1595	1632
K_T	kb						1548	1590	1549	1587
E	kb		2950[5]		2992					
			2945[6]							
μ	kb				1255		1251	1276	1261	1287
σ							.189	.192	.187	.188

Table 2 (continued)

Property	Units	Temp.°K	Chung & Lawrence	Durand	Soga & Anderson	Susse	This Work Polycrystalline 0 kb	This Work Polycrystalline 10 kb	This Work Single X'ℓ 0 kb	This Work Single X'ℓ 10 kb
C_{11}	kb	700	2598			2655			2725	2811
C_{12}	kb		876			990			972	985
C_{44}	kb		1483			1514			1503	1514
K_S	kb		1450		1574	1545	1564	1626	1556	1594
K_T	kb						1497	1557	1489	1528
E	kb		2845[5]		2862					
			2825[6]							
μ	kb				1202		1197	1223	1211	1236
σ							.195	.199	.191	.192

Table 2 (continued)

Property	Units	Temp.°K	Chung & Lawrence	Durand	Soga & Anderson	Susse	This Work Polycrystalline 0 kb	This Work Polycrystalline 10 kb	This Work Single X'l 0 kb	This Work Single X'l 10 kb
C_{11}	kb	900	2461			2499			2601	2687
C_{12}	kb		876			987			974	988
C_{44}	kb		1450			1480			1471	1438
K_S	kb		1404		1536	1491	1535	1604	1516	1554
K_T	kb						1447	1513	1429	1468
E	kb		2735[5]		2764					
μ	kb		2708[6]		1152		1144	1170	1160	1186
σ							.202	.206	.195	.196

Table 3

Notes on Tables 1 and 2

Bhagavantam (1955)	Single crystal data; resonance experiment in the MHz range.
Chung (1963)	Single crystal and polycrystalline data; Foster type resonance experiment. No specimen dimenions given. Frequency in the kHz range. Polycrystalline sample same source as in Chung and Simmons (1969)
Chung *et al* (1963)	Same experiment as report in Chung (1963)
Chung and Lawrence (1964)	Single crystal and polycrystalline data; resonance experiment; no frequency or specimen size given; sample source same as in Chung and Simmons (1969). 5. Values from polycrystalline specimen 6. VRH approximately from single crystal data.
Durand (1936)	Single crystal data; resonance experiment in the MHz range.

Table 3 (continued)

Soga and Anderson (1966)	Polycrystalline data; resonance experiment; no frequency or specimen size is given; sample from Avco Corp.
Susse (1961)	Single crystal data; resonance experiment (secondary reference).
Anderson and Andreatch (1966)	Single crystal; pulse superposition bonding material was Dow Corning V-9; path length for V_1 = 2.5787 cm, for V_2 = 2.5787 cm, for V_3 = 2.5269 cm shear measurements at 30 MHz; compressional at 40 MHz. 2., measurement at 77.2°K
Anderson and Schreiber (1965)	Polycrystalline; fluoride additive used in hot pressing; phase comparison method; bonding material was Dow Corning resin blend V-9; path length 1.2 cm; measurements at 60 MHz; no anisotropy found by rotating shear transducers. Specimen from Berkley

Table 3 (continued)

Bogardus (1965)	Single crystal; pulse superposition method; bonding material was Nonag stopcock grease; path length for V_1 = 2.43845 cm, for V_2=2.43845 cm, for V_3 = 3.07213 cm; measurements taken at 20 MHz 1., value for $\frac{\partial K_S}{\partial P}$ as reported in paper was in error and has been revised to 4.15.
Chang and Barsch (1969)	Single crystal; same as measured by Bogardus (1965). Refined experimental technique.
Chung and Simmons (1969)	Polycrystalline sample; pulse superposition method; bonding material probably Dow Corning V-9; path length not given; frequency probably 20 MHz; samples prepared and hot pressed at Pennsylvania State University.

Table 3 (continued)

Schreiber and Anderson (1966)	Polycrystalline data; same specimen and technique as in reference Anderson and Schreiber (1965) 3., Values at 307.6°K 4., Values at 194.5°K
Schreiber and Anderson (1968)	Same technique as in Schreiber and Anderson (1966); no additive was used to aid in hot pressing; sample from AVCO Corporation.
This work	Polycrystalline data; measurements described in Chapter 2; no bonding material used between buffer rod and sample path length 3.2858 cm; measurements at 20 MHz; sample from AVCO Corporation.
This work	Single crystal data; technique same as in n., path length V_1 = 2.2286 cm for V_2 = 2.2286 cm for V_3 = 2.1834 cm; shear measurements at 20 MHz; compressional measurements at 45 MHz.

Table 4

Redundancy check of MgO data for various authors

n	Anderson and Andreatch			Bogardus			This Work		
Units	V_n km sec^{-1}	$\frac{\partial F_n}{\partial P}$ x 10^4 Hz kb^{-1}	$\frac{\partial V_n}{\partial P}$ x 10^3 km sec^{-1} kb^{-1}	V_n km sec^{-1}	$\frac{\partial F_n}{\partial P}$ x 10^4 Hz kb^{-1}	$\frac{\partial V_n}{\partial P}$ x 10^3 km sec^{-1} kb^{-1}	V_n km sec^{-1}	$\frac{\partial F_n}{\partial P}$ x 10^4 Hz kb^{-1}	$\frac{\partial V_n}{\partial P}$ x 10^3 km sec^{-1} kb^{-1}
1 meas.	9.09585	14.6370	11.41	9.09932	13.81	10.67	9.1068	13.62	10.51
2 meas.	6.59539	4.0418	.418	6.59648	2.33	.162	6.6013	2.39	.206
3 meas.	5.30111	16.8682	7.84	5.30189	17.51	8.18	5.3056	16.87	7.85
4 meas.	9.90669	8.2166	6.07	9.90973	8.51	6.37	9.9184	7.49	5.37
4 calc.	9.90615		7.14	9.90965		5.53	9.9177		5.56
4m/4 calc.	1.00005		.850	1.000008		1.15	1.00007		.966

Table 5

Sample	V_1	V_2	V_3	V_4	V_P	V_S	K_S	$\frac{\partial K_S}{\partial P}$	ρ(%)
			km/sec				kb	kb/kb	
AVCO X_1					9.7199	6.0110	1657	3.78	99.92
AVCO Z_1					9.6962	6.0411	1624	4.43	99.85
AVCO S. A.					9.6605	5.9974	1624	4.58	99.9
Single Xℓ	9.1068	6.6013	5.3056	9.9184	9.7046	6.0474	1628	3.85	100
This Work								3.74	
Single Xℓ	9.09585	6.59539	5.30111	9.90669	9.681	6.041	1622	4.48	100
A. and A.	(1.00120)	(1.00090)	(1.00085)	(1.00119)				4.14	
Single Xℓ	9.09932	6.59648	5.30189	9.90973			1622	3.82	100
Bog.	(1.00082)	(1.00073)	(1.00070)	(1.00087)				4.42	

Velocity and bulk modulus data for single crystal MgO

The data of several authors is given.

Table 6

	$\frac{\partial V_P}{\partial T}$	$\frac{\partial V_S}{\partial T}$	$\frac{\partial V_P}{\partial P}$	$\frac{\partial V_S}{\partial P}$	$\frac{\partial K_S}{\partial T}$	$\frac{\partial K_T}{\partial T}$	$\frac{\partial K_S}{\partial P}$	$\frac{\partial K_T}{\partial P}$	$\frac{\partial \sigma}{\partial T}$	$\frac{\partial \sigma}{\partial P}$
Multiply by	10^{-4} km/sec°K	10^{-4}	10^{-3} km/sec kb	10^{-3}	10^{-1} kb/°K	10^{-1}	10^{0} kb/kb	10^{0}	10^{-5} °K^{-1}	10^{-4} kb^{-1}
300°K	-5.05	-4.33	7.19	3.76	-1.53	-2.75	3.85	3.90	2.39	1.47
0 kb										
800°K	-5.80	-4.61	7.65	4.37	-2.00	-3.04	3.74	3.89	2.16	.729
300°K	-4.90	-4.21	7.17	3.73	-1.50	-2.70	3.88	3.93	2.34	1.47
10 kb										
800°K	-5.67	-4.52	7.62	4.34	-1.98	-3.00	3.77	3.91	2.12	.735

Temperature and pressure derivatives of single crystal MgO as functions of temperature and pressure

Table 7

Explanation of Table

This table gives data for single crystal MgO; temperature in °K and pressure in kb.

EPS - This gives the change of normalized length such that L = 1 + EPS

ALPHA - Volume coefficient of thermal expansion

THETA - Einstein temperature

CP - Heat capacity at constant pressure (compatible units)

V1, V2, V3, V4, - Velocities defined in text (km/sec)

K_S, C11, C12, C44 - elastic constants (kb)

MU(V) - Voigt average of shear modulus (kb)

MU(R) - Reuss average of shear modulus (kb)

MU(VRH) - Voigt-Reuss-Hill average of shear modulus (kb)

SIGMA(VRH) - Voigt-Reuss-Hill average of Poisson's ratio

VP(VRH) - Voigt-Reuss-Hill average of compressional velocity (km/sec)

VS(VRH) - Voigt-Reuss-Hill average of shear velocity (km/sec)

KT - Isothermal Bulk Modulus (kb)

TEMPERATURE = 300.00 DEG. K. PRESSURE = 0.0 KB.

	EPS	ALPHA	GAMMA	THETA	CP	V1(VP)	V2	V3(VS)	V4	KS
VALUE	0.0	3.1500E-05	1.5400E 00	5.5000E 02	8.9390E 00	9.1074E 00	6.6012E 00	5.3051E 00	9.9185E 00	1.6283E 03
D/DT	1.0500E-05	6.1785E-08	0.0	0.0		-7.8383E-04	-1.4989E-04	-8.0935E-04	-3.8660E-04	-1.5266E-01
D/DP	-2.0769E-04	-1.0573E-07	-1.6186E-03	1.1423E-01	-5.0622E-03	1.0480E-02	2.3908E-04	7.9069E-03	5.2501E-03	3.8482E 00

	C11	C12	C44	MU(V)	MU(R)	MU(VRH)	SIGMA(VRH)	VP(VRH)	VS(VRH)	KT
VALUE	2.9737E 03	9.5566E 02	1.5623E 03	1.3410E 03	1.2813E 03	1.3111E 03	1.8259E-01	9.7046E 00	6.0474E 00	1.6050E 03
D/DT	-6.0554E-01	7.3778E-02	-1.0273E-01	-1.9750E-01	-2.6053E-01	-2.2902E-01	2.3923E-05	-5.0536E-04	-4.3290E-04	-2.7237E-01
D/DP	8.6968E 00	1.4239E 00	1.0866E 00	2.1065E 00	2.7839E 00	2.4452E 00	1.4732E-04	7.1921E-03	3.7551E-03	3.8945E 00

TEMPERATURE = 300.00 DEG. K. PRESSURE = 2.00 KB.

	EPS	ALPHA	GAMMA	THETA	CP	V1(VP)	V2	V3(VS)	V4	KS
VALUE	-4.1434E-04	3.1290E-05	1.5368E 00	5.5023E 02	8.9289E 00	9.1277E 00	6.6017E 00	5.3209E 00	9.9290E 00	1.6356E 03
D/DT	1.0426E-05	6.1441E-08	0.0	0.0		-7.7988E-04	-1.4937E-04	-8.0530E-04	-3.8470E-04	-1.5207E-01
D/DP	-2.0665E-04	-1.0438E-07	-1.5931E-03	1.1375E-01	-5.0271E-03	1.0479E-02	2.4458E-04	7.9050E-03	5.2543E-03	3.8554E 00

	C11	C12	C44	MU(V)	MU(R)	MU(VRH)	SIGMA(VRH)	VP(VRH)	VS(VRH)	KT
VALUE	2.9907E 03	9.5807E 02	1.5645E 03	1.3452E 03	1.2868E 03	1.3160E 03	1.8278E-01	9.7184E 00	6.0549E 00	1.6124E 03
D/DT	-6.0464E-01	7.4223E-02	-1.0260E-01	-1.9733E-01	-2.5932E-01	-2.2833E-01	2.3811E-05	-5.0224E-04	-4.3052E-04	-2.7135E-01
D/DP	8.7221E 00	1.4220E 00	1.0862E 00	2.1118E 00	2.7817E 00	2.4467E 00	1.4724E-04	7.1877E-03	3.7509E-03	3.9008E 00

TEMPERATURE = 300.00 DEG. K. PRESSURE = 4.00 KB.

	EPS	ALPHA	GAMMA	THETA	CP	V1(VP)	V2	V3(VS)	V4	KS
VALUE	-8.2661E-04	3.1082E-05	1.5336E 00	5.5045E 02	8.9189E 00	9.1480E 00	6.6022E 00	5.3367E 00	9.9395E 00	1.6429E 03
D/DT	1.0352E-05	6.1100E-08	0.0	0.0		-7.7594E-04	-1.4885E-04	-8.0126E-04	-3.8280E-04	-1.5147E-01
D/DP	-2.0562E-04	-1.0305E-07	-1.5680E-03	1.1328E-01	-4.9925E-03	1.0479E-02	2.5003E-04	7.9030E-03	5.2584E-03	3.8625E 00

	C11	C12	C44	MU(V)	MU(R)	MU(VRH)	SIGMA(VRH)	VP(VRH)	VS(VRH)	KT
VALUE	3.0077E 03	9.6048E 02	1.5666E 03	1.3494E 03	1.2924E 03	1.3209E 03	1.8296E-01	9.7321E 00	6.0624E 00	1.6197E 03
D/DT	-6.0373E-01	7.4662E-02	-1.0246E-01	-1.9715E-01	-2.5812E-01	-2.2763E-01	2.3699E-05	-4.9913E-04	-4.2815E-04	-2.7035E-01
D/DP	8.7474E 00	1.4201E 00	1.0859E 00	2.1170E 00	2.7795E 00	2.4482E 00	1.4716E-04	7.1833E-03	3.7467E-03	3.9071E 00

TEMPERATURE = 300.00 DEG. K. PRESSURE = 6.00 KB.

	EPS	ALPHA	GAMMA	THETA	CP	V1(VP)	V2	V3(VS)	V4	KS
VALUE	-1.2368E-03	3.0878E-05	1.5305E 00	5.5068E 02	8.9089E 00	9.1683E 00	6.6027E 00	5.3525E 00	9.9500E 00	1.6502E 03
D/DT	1.0280E-05	6.0764E-08	0.0	0.0		-7.7199E-04	-1.4832E-04	-7.9722E-04	-3.8090E-04	-1.5087E-01
D/DP	-2.0461E-04	-1.0173E-07	-1.5430E-03	1.1281E-01	-4.9583E-03	1.0478E-02	2.5543E-04	7.9010E-03	5.2626E-03	3.8697E 00

	C11	C12	C44	MU(V)	MU(R)	MU(VRH)	SIGMA(VRH)	VP(VRH)	VS(VRH)	KT
VALUE	3.0248E 03	9.6287E 02	1.5688E 03	1.3537E 03	1.2980E 03	1.3258E 03	1.8314E-01	9.7458E 00	6.0699E 00	1.6271E 03
D/DT	-6.0279E-01	7.5094E-02	-1.0231E-01	-1.9697E-01	-2.5691E-01	-2.2694E-01	2.3587E-05	-4.9602E-04	-4.2578E-04	-2.6934E-01
D/DP	8.7728E 00	1.4181E 00	1.0855E 00	2.1222E 00	2.7773E 00	2.4497E 00	1.4708E-04	7.1789E-03	3.7425E-03	3.9135E 00

0 C 0 0 0 0 0 0 0 0 0 0 0 C 0 0 0 0 0 0 0 0 0 0 0 0 0 0 0 0 0

MGO SINGLE CRYSTAL

****

TEMPERATURE = 300.00 DEG. K. PRESSURE = 8.CC KB.

	EPS	ALPHA	GAMMA	THETA	CP	V1(VP)	V2	V3(VS)	V4	KS
VALUE	-1.6450E-03	3.0675E-05	1.5274E 00	5.5090E 02	8.8990E 00	9.1885E 00	6.6032E 00	5.3683E 00	9.9605E 00	1.6575E 03
D/DT	1.0208E-05	6.0433E-08	0.0	0.0		-7.68C4E-04	-1.4778E-04	-7.9318E-04	-3.7899E-04	-1.5027E-01
D/DP	-2.0360E-C4	-1.0044E-07	-1.5184E-03	1.1235E-01	-4.9247E-03	1.0477E-02	2.6079E-04	7.8991E-03	5.2666E-03	3.8768E 00

	C11	C12	C44	MU(V)	MU(R)	MU(VRH)	SIGMA(VRH)	VP(VRH)	VS(VRH)	KT
VALUE	3.0419E 03	9.6526E 02	1.5710E 03	1.3579E 03	1.3035E 03	1.3307E 03	1.8332E-01	9.7596E 00	6.0773E 00	1.6345E 03
D/DT	-6.0185E-01	7.5521E-02	-1.0217E-01	-1.9678E-01	-2.5571E-01	-2.2624E-01	2.3475E-05	-4.9292E-04	-4.2341E-04	-2.6834E-01
D/DP	8.7981E 00	1.4162E 00	1.0852E 00	2.1275E CC	2.7750E 00	2.4513E 00	1.4700E-04	7.1745E-C3	3.7383E-03	3.9198E 00

****

TEMPERATURE = 3C0.0C DEG. K. PRESSURE = 10.CO KB.

	EPS	ALPHA	GAMMA	THETA	CP	V1(VP)	V2	V3(VS)	V4	KS
VALUE	-2.0512E-03	3.0476E-05	1.5244E 00	5.5113E 02	8.8892E 00	9.2088E 00	6.6037E 00	5.3842E 00	9.9711E 00	1.6648E 03
D/DT	1.0138E-05	6.0107E-08	0.0	0.0		-7.64C9E-04	-1.4724E-04	-7.8914E-04	-3.7708E-04	-1.4967E-01
D/DP	-2.0260E-04	-9.9172E-08	-1.4939E-03	1.1189E-01	-4.8915E-03	1.0476E-02	2.6610E-04	7.8972E-03	5.2707E-03	3.884CE 00

	C11	C12	C44	MU(V)	MU(R)	MU(VRH)	SIGMA(VRH)	VP(VRH)	VS(VRH)	KT
VALUE	3.0591E 03	9.6764E 02	1.5731E 03	1.3622E 03	1.3091E 03	1.3356E 03	1.8350E-01	9.7733E 00	6.0848E 00	1.6419E 03
D/DT	-6.0088E-01	7.5942E-02	-1.0202E-01	-1.9658E-01	-2.5451E-01	-2.2554E-C1	2.3364E-05	-4.8983E-04	-4.2104E-04	-2.6735E-01
D/DP	8.8234E 00	1.4143E 00	1.C849E 00	2.1328E 00	2.7728E 00	2.4528E CO	1.4693E-04	7.1702E-03	3.7342E-03	3.9261E 00

0 C 0 C 0 0 0 0 0 0 0 0 0 0 0 0 0 0 0 0 0 0 0 0 0 0 0 0 0 0 0 0

MGO SINGLE CRYSTAL

TEMPERATURE = 400.00 DEG. K. PRESSURE = 0.0 KB.

	EPS	ALPHA	GAMMA	THETA	CP	V1(VP)	V2	V3(VS)	V4	KS
VALUE	1.1337E-03	3.6028E-05	1.5400E 00	5.5000E 02	1.0148E 01	9.0273E 00	6.5842E 00	5.2239E 00	9.8770E 00	1.6117E 03
D/DT	1.2023E-05	3.3678E-08	0.0	0.0		-8.1312E-04	-1.9032E-04	-8.1000E-04	-4.4163E-04	-1.7944E-01
D/DP	-2.1165E-04	-1.1791E-07	-1.7844E-03	1.1628E-01	-3.7733E-03	1.0607E-02	2.6353E-04	8.1028E-03	5.3407E-03	3.8314E 00

	C11	C12	C44	MU(V)	MU(R)	MU(VRH)	SIGMA(VRH)	VP(VRH)	VS(VRH)	KT
VALUE	2.9118E 03	9.6165E 02	1.5490E 03	1.3194E 03	1.2538E 03	1.2866E 03	1.8474E-01	9.6498E 00	6.0007E 00	1.5767E 03
D/DT	-6.2944E-01	4.5567E-02	-1.2468E-01	-2.0981E-01	-2.7223E-01	-2.4102E-01	2.2509E-05	-5.5240E-04	-4.5396E-04	-2.9312E-01
D/DP	8.6890E 00	1.4026E 00	1.1064E 00	2.1211E 00	2.8445E 00	2.4828E 00	1.3255E-04	7.2966E-03	3.8870E-03	3.8999E 00

TEMPERATURE = 400.00 DEG. K. PRESSURE = 2.00 KB.

	EPS	ALPHA	GAMMA	THETA	CP	V1(VP)	V2	V3(VS)	V4	KS
VALUE	7.1146E-04	3.5793E-05	1.5365E 00	5.5023E 02	1.0140E 01	9.0480E 00	6.5848E 00	5.2401E 00	9.8877E 00	1.6190E 03
D/DT	1.1940E-05	3.3457E-08	0.0	0.0		-8.0945E-04	-1.8986E-04	-8.0620E-04	-4.3990E-04	-1.7896E-01
D/DP	-2.1057E-04	-1.1644E-07	-1.7595E-03	1.1578E-01	-3.7429E-03	1.0606E-02	2.6928E-04	8.1007E-03	5.3451E-03	3.8385E 00

	C11	C12	C44	MU(V)	MU(R)	MU(VRH)	SIGMA(VRH)	VP(VRH)	VS(VRH)	KT
VALUE	2.9288E 03	9.6410E 02	1.5512E 03	1.3237E 03	1.2595E 03	1.2916E 03	1.8491E-01	9.6639E 00	6.0085E 00	1.5842E 03
D/DT	-6.2887E-01	4.6000E-02	-1.2461E-01	-2.0974E-01	-2.7115E-01	-2.4045E-01	2.2405E-05	-5.4951E-04	-4.5176E-04	-2.9222E-01
D/DP	8.7150E 00	1.4002E 00	1.1061E 00	2.1266E 00	2.8422E 00	2.4844E 00	1.3251E-04	7.2918E-03	3.8824E-03	3.9058E 00

TEMPERATURE = 400.00 DEG. K. PRESSURE = 4.00 KB.

	EPS	ALPHA	GAMMA	THETA	CP	V1(VP)	V2	V3(VS)	V4	KS
VALUE	2.9141E-04	3.5562E-05	1.5330E 00	5.5046E 02	1.0133E 01	9.0686E 00	6.5853E 00	5.2563E 00	9.8984E 00	1.6263E 03
D/DT	1.1857E-05	3.3239E-08	0.0	0.0		-8.0579E-04	-1.8939E-04	-8.0239E-04	-4.3815E-04	-1.7848E-01
D/DP	-2.0949E-04	-1.1500E-07	-1.7349E-03	1.1528E-01	-3.7129E-03	1.0605E-02	2.7497E-04	8.0987E-03	5.3495E-03	3.8456E 00

	C11	C12	C44	MU(V)	MU(R)	MU(VRH)	SIGMA(VRH)	VP(VRH)	VS(VRH)	KT
VALUE	2.9459E 03	9.6655E 02	1.5534E 03	1.3279E 03	1.2652E 03	1.2965E 03	1.8508E-01	9.6779E 00	6.0162E 00	1.5916E 03
D/DT	-6.2828E-01	4.6426E-02	-1.2455E-01	-2.0967E-01	-2.7008E-01	-2.3987E-01	2.2301E-05	-5.4663E-04	-4.4957E-04	-2.9133E-01
D/DP	8.7409E 00	1.3979E 00	1.1057E 00	2.1320E 00	2.8400E 00	2.4860E 00	1.3247E-04	7.2869E-03	3.8779E-03	3.9118E 00

TEMPERATURE = 400.00 DEG. K. PRESSURE = 6.00 KB.

	EPS	ALPHA	GAMMA	THETA	CP	V1(VP)	V2	V3(VS)	V4	KS
VALUE	-1.2651E-04	3.5333E-05	1.5295E 00	5.5069E 02	1.0126E 01	9.0893E 00	6.5859E 00	5.2725E 00	9.9091E 00	1.6337E 03
D/DT	1.1776E-05	3.3023E-08	0.0	0.0		-8.0213E-04	-1.8892E-04	-7.9860E-04	-4.3641E-04	-1.7799E-01
D/DP	-2.0842E-04	-1.1358E-07	-1.7106E-03	1.1479E-01	-3.6834E-03	1.0604E-02	2.8062E-04	8.0966E-03	5.3539E-03	3.8527E 00

	C11	C12	C44	MU(V)	MU(R)	MU(VRH)	SIGMA(VRH)	VP(VRH)	VS(VRH)	KT
VALUE	2.9631E 03	9.6898E 02	1.5556E 03	1.3322E 03	1.2708E 03	1.3015E 03	1.8525E-01	9.6920E 00	6.0240E 00	1.5991E 03
D/DT	-6.2767E-01	4.6847E-02	-1.2448E-01	-2.0959E-01	-2.6901E-01	-2.3930E-01	2.2197E-05	-5.4375E-04	-4.4737E-04	-2.9044E-01
D/DP	8.7669E 00	1.3956E 00	1.1054E 00	2.1375E 00	2.8377E 00	2.4876E 00	1.3244E-04	7.2821E-03	3.8734E-03	3.9178E 00

C 0 0 0 0 0 0 0 0 0 0 0 0 0 0 0 0 0 0 0 0 0 0 0 0 0 0 0 0 0 0 0 0 0

MGO SINGLE CRYSTAL

****

TEMPERATURE = 400.00 DEG. K. PRESSURE = 8.00 KB.

	EPS	ALPHA	GAMMA	THETA	CP	V1(VP)	V2	V3(VS)	V4	KS
VALUE	-5.4229E-04	3.5107E-05	1.5261E 00	5.5092E 02	1.0118E 01	9.1100E 00	6.5864E 00	5.2887E 00	9.9198E 00	1.6410E 03
D/DT	1.1696E-05	3.2811E-08	0.0	0.0		-7.9847E-04	-1.8844E-04	-7.9480E-04	-4.3466E-04	-1.7751E-01
D/DP	-2.0736E-04	-1.1218E-07	-1.6865E-03	1.1430E-01	-3.6543E-03	1.0604E-02	2.8621E-04	8.0945E-03	5.3582E-03	3.8597E 00

	C11	C12	C44	MU(V)	MU(R)	MU(VRH)	SIGMA(VRH)	VP(VRH)	VS(VRH)	KT
VALUE	2.9803E 03	9.7142E 02	1.5578E 03	1.3365E 03	1.2765E 03	1.3065E 03	1.8542E-01	9.7060E 00	6.0317E 00	1.6066E 03
D/DT	-6.2705E-01	4.7262E-02	-1.2440E-01	-2.0950E-01	-2.6794E-01	-2.3872E-01	2.2094E-05	-5.4087E-04	-4.4518E-04	-2.8956E-01
D/DP	8.7928E 00	1.3932E 00	1.1050E 00	2.1429E 00	2.8354E 00	2.4892E 00	1.3240E-04	7.2773E-03	3.8688E-03	3.9237E 00

****

TEMPERATURE = 4C0.00 DEG. K. PRESSURE = 10.00 KB.

	EPS	ALPHA	GAMMA	THETA	CP	V1(VP)	V2	V3(VS)	V4	KS
VALUE	-9.5597E-04	3.4884E-05	1.5228E 00	5.5115E 02	1.0111E 01	9.1306E 00	6.5870E 00	5.3049E 00	9.9305E 00	1.6484E 03
D/DT	1.1617E-05	3.2602E-08	0.0	0.0		-7.9480E-04	-1.8796E-04	-7.9100E-04	-4.3290E-04	-1.7703E-01
D/DP	-2.0632E-04	-1.1081E-07	-1.6627E-03	1.1382E-01	-3.6256E-03	1.0603E-02	2.9175E-04	8.0925E-03	5.3625E-03	3.8668E 00

	C11	C12	C44	MU(V)	MU(R)	MU(VRH)	SIGMA(VRH)	VP(VRH)	VS(VRH)	KT
VALUE	2.9975E 03	9.7383E 02	1.5600E 03	1.3408E 03	1.2822E 03	1.3115E 03	1.8558E-01	9.7200E 00	6.0395E 00	1.6141E 03
D/DT	-6.2642E-01	4.7672E-02	-1.2433E-01	-2.0941E-01	-2.6687E-01	-2.3814E-01	2.1990E-05	-5.3800E-04	-4.4300E-04	-2.8868E-01
D/DP	8.8187E 00	1.3909E 00	1.1047E 00	2.1484E 00	2.8332E 00	2.4908E 00	1.3236E-04	7.2725E-03	3.8643E-03	3.9297E 00

C C 0 C 0 0 0 0 0 0 0 0 0 0 0 0 0 0 0 0 0 0 0 0 0 0 0 0 0 0 0 0 0 0

TEMPERATURE = 500.00 DEG. K. PRESSURE = 0.0 KB.

	EPS	ALPHA	GAMMA	THETA	CP	V1(VP)	V2	V3(VS)	V4	KS
VALUE	2.3839E-03	3.8649E-05	1.5400E 00	5.5000E 02	1.0854E 01	8.9489E 00	6.5646E 00	5.1434E 00	9.8348E 00	1.5951E 03
D/DT	1.2914E-05	2.1132E-08	0.0	0.0		-7.8198E-04	-2.0055E-04	-8.0055E-04	-4.2673E-04	-1.6899E-01
D/DP	-2.1570E-04	-1.1591E-07	-1.5011E-03	1.1836E-01	-3.0625E-03	1.0713E-02	2.8740E-04	8.2898E-03	5.4294E-03	3.8080E 00

	C11	C12	C44	MU(V)	MU(R)	MU(VRH)	SIGMA(VRH)	VP(VRH)	VS(VRH)	KT
VALUE	2.8507E 03	9.6730E 02	1.5340E 03	1.2971E 03	1.2257E 03	1.2614E 03	1.8709E-01	9.5946E 00	5.9527E 00	1.5490E 03
D/DT	-6.0838E-01	5.0701E-02	-1.3012E-01	-2.0989E-01	-2.7313E-01	-2.4151E-01	2.5380E-05	-5.3341E-04	-4.5484E-04	-2.7812E-01
D/DP	8.6660E 00	1.3790E 00	1.1246E 00	2.1322E 00	2.8996E 00	2.5159E 00	1.1656E-04	7.3886E-03	4.0150E-03	3.8758E 00

TEMPERATURE = 500.00 DEG. K. PRESSURE = 2.00 KB.

	EPS	ALPHA	GAMMA	THETA	CP	V1(VP)	V2	V3(VS)	V4	KS
VALUE	1.9536E-03	3.8418E-05	1.5370E 00	5.5024E 02	1.0848E 01	8.9700E 00	6.5652E 00	5.1600E 00	9.8456E 00	1.6025E 03
D/DT	1.2831E-05	2.0981E-08	0.0	0.0		-7.7846E-04	-2.0008E-04	-7.9691E-04	-4.2499E-04	-1.6849E-01
D/DP	-2.1457E-04	-1.1446E-07	-1.4768E-03	1.1783E-01	-3.0358E-03	1.0713E-02	2.9336E-04	8.2876E-03	5.4341E-03	3.8150E 00

	C11	C12	C44	MU(V)	MU(R)	MU(VRH)	SIGMA(VRH)	VP(VRH)	VS(VRH)	KT
VALUE	2.8678E 03	9.6980E 02	1.5363E 03	1.3014E 03	1.2315E 03	1.2664E 03	1.8725E-01	9.6090E 00	5.9608E 00	1.5565E 03
D/DT	-6.0794E-01	5.1231E-02	-1.3010E-01	-2.0989E-01	-2.7214E-01	-2.4102E-01	2.5279E-05	-5.3054E-04	-4.5271E-04	-2.7732E-01
D/DP	8.6925E 00	1.3762E 00	1.1243E 00	2.1378E 00	2.8973E 00	2.5176E 00	1.1657E-04	7.3832E-03	4.0101E-03	3.8815E 00

TEMPERATURE = 500.00 DEG. K. PRESSURE = 4.00 KB.

	EPS	ALPHA	GAMMA	THETA	CP	V1(VP)	V2	V3(VS)	V4	KS
VALUE	1.5256E-03	3.8191E-05	1.5341E 00	5.5047E 02	1.0842E 01	8.9910E 00	6.5658E 00	5.1766E 00	9.8565E 00	1.6099E 03
D/DT	1.2750E-05	2.0832E-08	0.0	0.0		-7.7493E-04	-1.9961E-04	-7.9326E-04	-4.2324E-04	-1.6799E-01
D/DP	-2.1345E-04	-1.1304E-07	-1.4528E-03	1.1732E-01	-3.0095E-03	1.0712E-02	2.9928E-04	8.2854E-03	5.4387E-03	3.822CE 00

	C11	C12	C44	MU(V)	MU(R)	MU(VRH)	SIGMA(VRH)	VP(VRH)	VS(VRH)	KT
VALUE	2.8850E 03	9.7230E 02	1.5385E 03	1.3056E 03	1.2372E 03	1.2714E 03	1.8740E-01	9.6234E 00	5.9688E 00	1.5640E 03
D/DT	-6.0749E-01	5.1756E-02	-1.3007E-01	-2.0989E-01	-2.7115E-01	-2.4052E-01	2.5178E-05	-5.2769E-04	-4.5058E-04	-2.7652E-01
D/DP	8.7190E 00	1.3735E 00	1.1239E 00	2.1435E 00	2.8950E 00	2.5193E 00	1.1657E-04	7.3779E-03	4.0052E-03	3.8871E 00

TEMPERATURE = 500.00 DEG. K. PRESSURE = 6.00 KB.

	EPS	ALPHA	GAMMA	THETA	CP	V1(VP)	V2	V3(VS)	V4	KS
VALUE	1.0998E-03	3.7966E-05	1.5312E 00	5.5070E 02	1.0836E 01	9.0120E 00	6.5664E 00	5.1931E 00	9.8674E 00	1.6173E 03
D/DT	1.2669E-05	2.0686E-08	0.0	0.0		-7.7141E-04	-1.9913E-04	-7.8962E-04	-4.2148E-04	-1.6749E-01
D/DP	-2.1233E-04	-1.1164E-07	-1.4290E-03	1.1680E-01	-2.9837E-03	1.0711E-02	3.0513E-04	8.2831E-03	5.4432E-03	3.8290E 00

	C11	C12	C44	MU(V)	MU(R)	MU(VRH)	SIGMA(VRH)	VP(VRH)	VS(VRH)	KT
VALUE	2.9022E 03	9.7479E 02	1.5408E 03	1.3099E 03	1.2430E 03	1.2765E 03	1.8756E-01	9.6378E 00	5.9768E 00	1.5716E 03
D/DT	-6.0703E-01	5.2275E-02	-1.3004E-01	-2.0988E-01	-2.7016E-01	-2.4002E-01	2.5078E-05	-5.2483E-04	-4.4846E-04	-2.7573E-01
D/DP	8.7456E 00	1.3707E 00	1.1236E 00	2.1491E 00	2.8927E 00	2.5209E 00	1.1658E-04	7.3726E-03	4.0002E-03	3.8928E 00

0 0 0 0 0 0 0 0 0 0 0 0 0 0 0 0 0 0 0 0 0 0 0 0 0 0 0 0 0 0 0 0

MGO SINGLE CRYSTAL

****

TEMPERATURE = 500.00 DEG. K. PRESSURE = 8.00 KB.

	EPS	ALPHA	GAMMA	THETA	CP	V1(VP)	V2	V3(VS)	V4	KS
VALUE	6.7628E-04	3.7744E-05	1.5284E 00	5.5094E 02	1.0830E 01	9.0330E 00	6.5670E 00	5.2097E 00	9.8783E 00	1.6247E 03
D/DT	1.2590E-05	2.0542E-08	0.0	0.0		-7.6788E-04	-1.9865E-04	-7.8598E-04	-4.1972E-04	-1.6699E-01
D/DP	-2.1123E-04	-1.1026E-07	-1.4056E-03	1.1630E-01	-2.9582E-03	1.0711E-02	3.1093E-04	8.2809E-03	5.4477E-03	3.8360E 00

	C11	C12	C44	MU(V)	MU(R)	MU(VRH)	SIGMA(VRH)	VP(VRH)	VS(VRH)	KT
VALUE	2.9195E 03	9.7727E 02	1.5430E 03	1.3142E 03	1.2488E 03	1.2815E 03	1.8771E-01	9.6522E 00	5.9848E 00	1.5791E 03
D/DT	-6.0655E-01	5.2789E-02	-1.3000E-01	-2.0987E-01	-2.6917E-01	-2.3952E-01	2.4977E-05	-5.2199E-04	-4.4634E-04	-2.7494E-01
D/DP	8.7721E 00	1.3679E 00	1.1233E 00	2.1548E 00	2.8904E 00	2.5226E 00	1.1659E-04	7.3672E-03	3.9953E-03	3.8985E 00

****

TEMPERATURE = 500.00 DEG. K. PRESSURE = 10.00 KB.

	EPS	ALPHA	GAMMA	THETA	CP	V1(VP)	V2	V3(VS)	V4	KS
VALUE	2.5491E-04	3.7525E-05	1.5256E 00	5.5117E 02	1.0824E 01	9.0541E 00	6.5677E 00	5.2263E 00	9.8892E 00	1.6321E 03
D/DT	1.2511E-05	2.0401E-08	0.0	0.0		-7.6436E-04	-1.9816E-04	-7.8235E-04	-4.1795E-04	-1.6649E-01
D/DP	-2.1014E-04	-1.0890E-07	-1.3823E-03	1.1579E-01	-2.9332E-03	1.0710E-02	3.1668E-04	8.2787E-03	5.4522E-03	3.8429E 00

	C11	C12	C44	MU(V)	MU(R)	MU(VRH)	SIGMA(VRH)	VP(VRH)	VS(VRH)	KT
VALUE	2.9368E 03	9.7974E 02	1.5453E 03	1.3186E 03	1.2546E 03	1.2866E 03	1.8787E-01	9.6665E 00	5.9928E 00	1.5867E 03
D/DT	-6.0605E-01	5.3298E-02	-1.2997E-01	-2.0985E-01	-2.6819E-01	-2.3902E-01	2.4877E-05	-5.1915E-04	-4.4422E-04	-2.7416E-01
D/DP	8.7986E 00	1.3651E 00	1.1229E 00	2.1605E 00	2.8881E 00	2.5243E 00	1.1659E-04	7.3619E-03	3.9905E-03	3.9041E 00

0 0 0 0 0 0 0 0 0 0 0 0 0 0 0 0 0 0 0 0 0 0 0 0 0 0 0 0 0 0 0 0 0

TEMPERATURE = 600.00 DEG. K. PRESSURE = 0.0 KB.

	EPS	ALPHA	GAMMA	THETA	CP	V1(VP)	V2	V3(VS)	V4	KS
VALUE	3.7080E-03	4.0471E-05	1.5400E 00	5.5000E 02	1.1323E 01	8.8679E 00	6.5444E 00	5.0631E 00	9.7895E 00	1.5764E 03
D/DT	1.3540E-05	1.6035E-08	0.0	0.0		-8.2698E-04	-2.0485E-04	-8.0408E-04	-4.7020E-04	-1.9891E-01
D/DP	-2.2017E-04	-1.3197E-07	-1.9440E-03	1.2065E-01	-2.8821E-03	1.0813E-02	3.0853E-04	8.4653E-03	5.5117E-03	3.7845E 00

	C11	C12	C44	MU(V)	MU(R)	MU(VRH)	SIGMA(VRH)	VP(VRH)	VS(VRH)	KT
VALUE	2.7883E 03	9.7044E 02	1.5185E 03	1.2747E 03	1.1973E 03	1.2360E 03	1.8920E-01	9.5363E 00	5.9042E 00	1.5196E 03
D/DT	-6.3288E-01	1.8077E-02	-1.3185E-01	-2.0930E-01	-2.7510E-01	-2.4220E-01	2.0744E-05	-5.7872E-04	-4.5901E-04	-3.0474E-01
D/DP	8.6345E 00	1.3594E 00	1.1425E 00	2.1405E 00	2.9510E 00	2.5457E 00	1.0139E-04	7.4779E-03	4.1376E-03	3.8958E 00

TEMPERATURE = 600.00 DEG. K. PRESSURE = 2.00 KB.

	EPS	ALPHA	GAMMA	THETA	CP	V1(VP)	V2	V3(VS)	V4	KS
VALUE	3.2688E-03	4.0208E-05	1.5361E 00	5.5024E 02	1.1317E 01	8.8893E 00	6.5450E 00	5.0800E 00	9.8005E 00	1.5838E 03
D/DT	1.3447E-05	1.5891E-08	0.0	0.0		-8.2371E-04	-2.0446E-04	-8.0070E-04	-4.6863E-04	-1.9850E-01
D/DP	-2.1898E-04	-1.3031E-07	-1.9179E-03	1.2010E-01	-2.8513E-03	1.0812E-02	3.1482E-04	8.4630E-03	5.5167E-03	3.7913E 00

	C11	C12	C44	MU(V)	MU(R)	MU(VRH)	SIGMA(VRH)	VP(VRH)	VS(VRH)	KT
VALUE	2.8054E 03	9.7300E 02	1.5208E 03	1.2790E 03	1.2032E 03	1.2411E 03	1.8934E-01	9.5510E 00	5.9125E 00	1.5272E 03
D/DT	-6.3272E-01	1.8602E-02	-1.3186E-01	-2.0938E-01	-2.7418E-01	-2.4178E-01	2.0658E-05	-5.7604E-04	-4.5704E-04	-3.0394E-01
D/DP	8.6615E 00	1.3563E 00	1.1421E 00	2.1463E 00	2.9487E 00	2.5475E 00	1.0145E-04	7.4722E-03	4.1324E-03	3.9009E 00

TEMPERATURE = 600.00 DEG. K. PRESSURE = 4.00 KB.

	EPS	ALPHA	GAMMA	THETA	CP	V1(VP)	V2	V3(VS)	V4	KS
VALUE	2.8321E-03	3.9949E-05	1.5323E 00	5.5048E 02	1.1312E 01	8.9107E 00	6.5456E 00	5.0970E 00	9.8115E 00	1.5912E 03
D/DT	1.3354E-05	1.5749E-08	0.0	0.0		-8.2044E-04	-2.0406E-04	-7.9731E-04	-4.6705E-04	-1.9810E-01
D/DP	-2.1779E-04	-1.2868E-07	-1.8921E-03	1.1955E-01	-2.8211E-03	1.0812E-02	3.2105E-04	8.4607E-03	5.5216E-03	3.7982E 00

	C11	C12	C44	MU(V)	MU(R)	MU(VRH)	SIGMA(VRH)	VP(VRH)	VS(VRH)	KT
VALUE	2.8226E 03	9.7555E 02	1.5231E 03	1.2833E 03	1.2091E 03	1.2462E 03	1.8948E-01	9.5657E 00	5.9208E 00	1.5349E 03
D/DT	-6.3254E-01	1.9121E-02	-1.3186E-01	-2.0945E-01	-2.7326E-01	-2.4135E-01	2.0572E-05	-5.7337E-04	-4.5508E-04	-3.0314E-01
D/DP	8.6885E 00	1.3531E 00	1.1417E 00	2.1521E 00	2.9464E 00	2.5493E 00	1.0150E-04	7.4665E-03	4.1272E-03	3.9060E 00

TEMPERATURE = 600.00 DEG. K. PRESSURE = 6.00 KB.

	EPS	ALPHA	GAMMA	THETA	CP	V1(VP)	V2	V3(VS)	V4	KS
VALUE	2.3977E-03	3.9693E-05	1.5286E 00	5.5072E 02	1.1306E 01	8.9321E 00	6.5463E 00	5.1139E 00	9.8226E 00	1.5987E 03
D/DT	1.3263E-05	1.5609E-08	0.0	0.0		-8.1717E-04	-2.0365E-04	-7.9393E-04	-4.6546E-04	-1.9769E-01
D/DP	-2.1661E-04	-1.2707E-07	-1.8666E-03	1.1901E-01	-2.7914E-03	1.0811E-02	3.2721E-04	8.4584E-03	5.5265E-03	3.8051E 00

	C11	C12	C44	MU(V)	MU(R)	MU(VRH)	SIGMA(VRH)	VP(VRH)	VS(VRH)	KT
VALUE	2.8399E 03	9.7809E 02	1.5254E 03	1.2876E 03	1.2150E 03	1.2513E 03	1.8963E-01	9.5804E 00	5.9290E 00	1.5425E 03
D/DT	-6.3234E-01	1.9636E-02	-1.3186E-01	-2.0951E-01	-2.7234E-01	-2.4092E-01	2.0485E-05	-5.7070E-04	-4.5311E-04	-3.0236E-01
D/DP	8.7156E 00	1.3499E 00	1.1414E 00	2.1580E 00	2.9441E 00	2.5510E 00	1.0155E-04	7.4608E-03	4.1220E-03	3.9111E 00

C 0 0 C 0 0 0 0 0 0 0 0 0 0 0 0 0 0 0 0 0 0 0 0 0 0 0 0 0 0 0 0

MGO SINGLE CRYSTAL

****

TEMPERATURE = 600.00 DEG. K. PRESSURE = 8.00 KB.

	EPS	ALPHA	GAMMA	THETA	CP	V1(VP)	V2	V3(VS)	V4	KS
VALUE	1.9656E-03	3.9441E-05	1.5249E 00	5.5095E 02	1.1300E 01	8.9534E 00	6.5469E 00	5.1308E 00	9.8337E 00	1.6061E 03
D/DT	1.3173E-05	1.5472E-08	0.0	0.0		-8.1389E-04	-2.0324E-04	-7.9055E-04	-4.6387E-04	-1.9728E-01
D/DP	-2.1545E-04	-1.2549E-07	-1.8414E-03	1.1847E-01	-2.7623E-03	1.0811E-02	3.3331E-04	8.4561E-03	5.5313E-03	3.8120E 00

	C11	C12	C44	MU(V)	MU(R)	MU(VRH)	SIGMA(VRH)	VP(VRH)	VS(VRH)	KT
VALUE	2.8571E 03	9.8062E 02	1.5277E 03	1.2919E 03	1.2209E 03	1.2564E 03	1.8977E-01	9.5950E 00	5.9373E 00	1.5502E 03
D/DT	-6.3214E-01	2.0146E-02	-1.3185E-01	-2.0957E-01	-2.7142E-01	-2.4049E-01	2.0400E-05	-5.6804E-04	-4.5115E-04	-3.0157E-01
D/DP	8.7426E 00	1.3467E 00	1.1410E 00	2.1638E 00	2.9418E 00	2.5528E 00	1.0160E-04	7.4551E-03	4.1168E-03	3.9162E 00

****

TEMPERATURE = 600.00 DEG. K. PRESSURE = 10.00 KB.

	EPS	ALPHA	GAMMA	THETA	CP	V1(VP)	V2	V3(VS)	V4	KS
VALUE	1.5358E-03	3.9191E-05	1.5212E 00	5.5119E 02	1.1295E 01	8.9747E 00	6.5476E 00	5.1477E 00	9.8447E 00	1.6136E 03
D/DT	1.3084E-05	1.5337E-08	0.0	0.0		-8.1062E-04	-2.0282E-04	-7.8718E-04	-4.6228E-04	-1.9687E-01
D/DP	-2.1430E-04	-1.2394E-07	-1.8165E-03	1.1794E-01	-2.7337E-03	1.0810E-02	3.3935E-04	8.4538E-03	5.5360E-03	3.8189E 00

	C11	C12	C44	MU(V)	MU(R)	MU(VRH)	SIGMA(VRH)	VP(VRH)	VS(VRH)	KT
VALUE	2.8745E 03	9.8313E 02	1.5300E 03	1.2962E 03	1.2268E 03	1.2615E 03	1.8991E-01	9.6097E 00	5.9455E 00	1.5579E 03
D/DT	-6.3191E-01	2.0652E-02	-1.3185E-01	-2.0962E-01	-2.7050E-01	-2.4006E-01	2.0314E-05	-5.6538E-04	-4.4919E-04	-3.0079E-01
D/DP	8.7697E 00	1.3435E 00	1.1407E 00	2.1696E 00	2.9395E 00	2.5546E 00	1.0165E-04	7.4494E-03	4.1116E-03	3.9214E 00

0 0 0 0 0 0 0 0 0 0 0 0 0 0 0 0 0 0 0 0 0 0 0 0 0 0 0 0 0 0 0 0 0 0

MGO SINGLE CRYSTAL

TEMPERATURE = 7CC.CO DEG. K. PRESSURE = 0.C KB.

	EPS	ALPHA	GAMMA	THETA	CP	V1(VP)	V2	V3(VS)	V4	KS
VALUE	5.0877E-03	4.1901E-05	1.5400E 00	5.5000E 02	1.1656E 01	8.7850E 00	6.5238E 00	4.9826E 00	9.7422E 00	1.5563E 03
D/DT	1.4038E-05	1.3031E-08	0.0	0.0		-8.3050E-04	-2.0565E-04	-8.1099E-04	-4.7185E-04	-1.9997E-01
D/DP	-2.2500E-04	-1.3678E-07	-1.9636E-03	1.2312E-01	-2.8249E-03	1.0903E-02	3.2738E-04	8.6293E-03	5.5886E-03	3.7606E 00

	C11	C12	C44	MU(V)	MU(R)	MU(VRH)	SIGMA(VRH)	VP(VRH)	VS(VRH)	KT
VALUE	2.7251E 03	9.7188E 02	1.5028E 03	1.2523E 03	1.1688E 03	1.2106E 03	1.9115E-01	9.4756E 00	5.8553E 00	1.4890E 03
D/DT	-6.2944E-01	1.4765E-02	-1.3148E-01	-2.0773E-01	-2.7677E-01	-2.4225E-01	2.1327E-05	-5.8299E-04	-4.6318E-04	-3.0327E-01
D/DP	8.5942E 00	1.3439E 00	1.1601E 00	2.1461E 00	2.9990E 00	2.5725E 00	8.6770E-05	7.5638E-03	4.2552E-03	3.8902E 00

TEMPERATURE = 7CC.00 DEG. K. PRESSURE = 2.CC KB.

	EPS	ALPHA	GAMMA	THETA	CP	V1(VP)	V2	V3(VS)	V4	KS
VALUE	4.6389E-03	4.1630E-05	1.5361E 00	5.5025E 02	1.1650E 01	8.8067E 00	6.5244E 00	4.9999E 00	9.7534E 00	1.5638E 03
D/DT	1.3941E-05	1.2899E-08	0.0	0.0		-8.2743E-04	-2.0528E-04	-8.0784E-04	-4.7033E-04	-1.9956E-01
D/DP	-2.2374E-04	-1.3503E-07	-1.9366E-03	1.2254E-01	-2.7915E-03	1.0902E-02	3.3396E-04	8.6268E-03	5.5939E-03	3.7674E 00

	C11	C12	C44	MU(V)	MU(R)	MU(VRH)	SIGMA(VRH)	VP(VRH)	VS(VRH)	KT
VALUE	2.7423E 03	9.7449E 02	1.5051E 03	1.2566E 03	1.1748E 03	1.2157E 03	1.9128E-01	9.4906E 00	5.8638E 00	1.4968E 03
D/DT	-6.2946E-01	1.5384E-02	-1.3151E-01	-2.0787E-01	-2.7592E-01	-2.4190E-01	2.1250E-05	-5.8038E-04	-4.6131E-04	-3.0250E-01
D/DP	8.6217E 00	1.3403E 00	1.1597E 00	2.1521E 00	2.9967E 00	2.5744E 00	8.6865E-05	7.5577E-03	4.2496E-03	3.8949E 00

TEMPERATURE = 700.00 DEG. K. PRESSURE = 4.CO KB.

	EPS	ALPHA	GAMMA	THETA	CP	V1(VP)	V2	V3(VS)	V4	KS
VALUE	4.1927E-03	4.1361E-05	1.5322E 00	5.5049E 02	1.1645E 01	8.8284E 00	6.5251E 00	5.0171E 00	9.7646E 00	1.5712E 03
D/DT	1.3845E-05	1.2768E-08	0.0	0.0		-8.2436E-04	-2.0491E-04	-8.0469E-04	-4.6880E-04	-1.9916E-01
D/DP	-2.2249E-04	-1.3330E-07	-1.9099E-03	1.2197E-01	-2.7587E-03	1.0902E-02	3.4048E-04	8.6244E-03	5.5991E-03	3.7742E 00

	C11	C12	C44	MU(V)	MU(R)	MU(VRH)	SIGMA(VRH)	VP(VRH)	VS(VRH)	KT
VALUE	2.7595E 03	9.7709E 02	1.5074E 03	1.2609E 03	1.1808E 03	1.2209E 03	1.9141E-01	9.5056E 00	5.8723E 00	1.5045E 03
D/DT	-6.2947E-01	1.5998E-02	-1.3154E-01	-2.0802E-01	-2.7507E-01	-2.4154E-01	2.1173E-05	-5.7778E-04	-4.5945E-04	-3.0173E-01
D/DP	8.6493E 00	1.3367E 00	1.1593E 00	2.1581E 00	2.9944E 00	2.5762E 00	8.6959E-05	7.5515E-03	4.2441E-03	3.8995E 00

TEMPERATURE = 7CC.00 DEG. K. PRESSURE = 6.CO KB.

	EPS	ALPHA	GAMMA	THETA	CP	V1(VP)	V2	V3(VS)	V4	KS
VALUE	3.7489E-03	4.1096E-05	1.5285E 00	5.5073E 02	1.1639E 01	8.8501E 00	6.5258E 00	5.0344E 00	9.7758E 00	1.5787E 03
D/DT	1.3750E-05	1.2641E-08	0.0	0.0		-8.2128E-04	-2.0452E-04	-8.0154E-04	-4.6727E-04	-1.9875E-01
D/DP	-2.2125E-04	-1.3161E-07	-1.8836E-03	1.2140E-01	-2.7266E-03	1.0901E-02	3.4693E-04	8.6220E-03	5.6042E-03	3.7810E 00

	C11	C12	C44	MU(V)	MU(R)	MU(VRH)	SIGMA(VRH)	VP(VRH)	VS(VRH)	KT
VALUE	2.7767E 03	9.7969E 02	1.5098E 03	1.2653E 03	1.1868E 03	1.2260E 03	1.9154E-01	9.5206E 00	5.8808E 00	1.5122E 03
D/DT	-6.2947E-01	1.6607E-02	-1.3156E-01	-2.0815E-01	-2.7421E-01	-2.4118E-01	2.1097E-05	-5.7518E-04	-4.5758E-04	-3.0096E-01
D/DP	8.6768E 00	1.3331E 00	1.1589E 00	2.1641E 00	2.9921E 00	2.5781E 00	8.7052E-05	7.5454E-03	4.2386E-03	3.9042E 00

0 0 0 0 0 0 0 0 0 0 0 0 0 0 0 0 0 0 0 0 0 0 0 0 0 0 0 0 0 0 0 0

MGO SINGLE CRYSTAL

****

TEMPERATURE = 700.00 DEG. K. PRESSURE = 8.00 KB.

	EPS	ALPHA	GAMMA	THETA	CP	V1(VP)	V2	V3(VS)	V4	KS
VALUE	3.3077E-03	4.0835E-05	1.5247E 00	5.5097E 02	1.1634E 01	8.8718E 00	6.5265E 00	5.0516E 00	9.7870E 00	1.5862E 03
D/DT	1.3657E-05	1.2515E-08	0.0	0.0		-8.1821E-04	-2.0414E-04	-7.9839E-04	-4.6573E-04	-1.9834E-01
D/DP	-2.2003E-04	-1.2994E-07	-1.8577E-03	1.2083E-01	-2.6950E-03	1.0901E-02	3.5331E-04	8.6196E-03	5.6093E-03	3.7878E 00

	C11	C12	C44	MU(V)	MU(R)	MU(VRH)	SIGMA(VRH)	VP(VRH)	VS(VRH)	KT
VALUE	2.7940E 03	9.8227E 02	1.5121E 03	1.2696E 03	1.1928E 03	1.2312E 03	1.9167E-01	9.5356E 00	5.8892E 00	1.5199E 03
D/DT	-6.2946E-01	1.7213E-02	-1.3158E-01	-2.0828E-01	-2.7336E-01	-2.4082E-01	2.1020E-05	-5.7258E-04	-4.5572E-04	-3.0020E-01
D/DP	8.7043E 00	1.3295E 00	1.1585E 00	2.1701E 00	2.9898E 00	2.5799E 00	8.7144E-05	7.5393E-03	4.2330E-03	3.9089E 00

****

TEMPERATURE = 700.00 DEG. K. PRESSURE = 10.00 KB.

	EPS	ALPHA	GAMMA	THETA	CP	V1(VP)	V2	V3(VS)	V4	KS
VALUE	2.8688E-03	4.0576E-05	1.5210E 00	5.5121E 02	1.1629E 01	8.8934E 00	6.5272E 00	5.0689E 00	9.7982E 00	1.5937E 03
D/DT	1.3564E-05	1.2391E-08	0.0	0.0		-8.1513E-04	-2.0374E-04	-7.9525E-04	-4.6418E-04	-1.9793E-01
D/DP	-2.1882E-04	-1.2830E-07	-1.8320E-03	1.2027E-01	-2.6641E-03	1.0900E-02	3.5963E-04	8.6172E-03	5.6144E-03	3.7946E 00

	C11	C12	C44	MU(V)	MU(R)	MU(VRH)	SIGMA(VRH)	VP(VRH)	VS(VRH)	KT
VALUE	2.8114E 03	9.8484E 02	1.5144E 03	1.2739E 03	1.1988E 03	1.2364E 03	1.9181E-01	9.5505E 00	5.8977E 00	1.5277E 03
D/DT	-6.2943E-01	1.7814E-02	-1.3160E-01	-2.0841E-01	-2.7251E-01	-2.4046E-01	2.0943E-05	-5.6998E-04	-4.5387E-04	-2.9944E-01
D/DP	8.7319E 00	1.3259E 00	1.1582E 00	2.1761E 00	2.9875E 00	2.5818E 00	8.7236E-05	7.5332E-03	4.2275E-03	3.9137E 00

0 0 0 0 0 0 0 0 0 0 0 0 0 0 0 0 0 0 0 0 0 0 0 0 0 0 0 0 0 0 0 0

TEMPERATURE = 800.00 DEG. K. PRESSURE = 0.0 KB.

	EPS	ALPHA	GAMMA	THETA	CP	V1(VP)	V2	V3(VS)	V4	KS
VALUE	6.5130E-03	4.3104E-05	1.5400E 00	5.5000E 02	1.1905E 01	8.7021E 00	6.5033E 00	4.9015E 00	9.6951E 00	1.5363E 03
D/DT	1.4462E-05	1.1359E-08	0.0	0.0		-8.2781E-04	-2.0375E-04	-8.1141E-04	-4.6948E-04	-1.9989E-01
D/DP	-2.2998E-04	-1.4151E-07	-1.9832E-03	1.2567E-01	-2.8980E-03	1.0987E-02	3.4520E-04	8.7818E-03	5.6633E-03	3.7404E 00

	C11	C12	C44	MU(V)	MU(R)	MU(VRH)	SIGMA(VRH)	VP(VRH)	VS(VRH)	KT
VALUE	2.6626E 03	9.7315E 02	1.4871E 03	1.2301E 03	1.1402E 03	1.1852E 03	1.9318E-01	9.4147E 00	5.8058E 00	1.4588E 03
D/DT	-6.2134E-01	1.0834E-02	-1.2959E-01	-2.0419E-01	-2.7609E-01	-2.4014E-01	2.1628E-05	-5.8264E-04	-4.6305E-04	-3.0115E-01
D/DP	8.5484E 00	1.3365E 00	1.1772E 00	2.1487E 00	3.0434E 00	2.5960E 00	7.2870E-05	7.6512E-03	4.3687E-03	3.8881E 00

TEMPERATURE = 800.00 DEG. K. PRESSURE = 2.00 KB.

	EPS	ALPHA	GAMMA	THETA	CP	V1(VP)	V2	V3(VS)	V4	KS
VALUE	6.0544E-03	4.2823E-05	1.5361E 00	5.5025E 02	1.1899E 01	8.7241E 00	6.5040E 00	4.9191E 00	9.7065E 00	1.5438E 03
D/DT	1.4361E-05	1.1232E-08	0.0	0.0		-8.2491E-04	-2.0341E-04	-8.0847E-04	-4.6801E-04	-1.9949E-01
D/DP	-2.2865E-04	-1.3965E-07	-1.9553E-03	1.2506E-01	-2.8608E-03	1.0986E-02	3.5211E-04	8.7792E-03	5.6689E-03	3.7472E 00

	C11	C12	C44	MU(V)	MU(R)	MU(VRH)	SIGMA(VRH)	VP(VRH)	VS(VRH)	KT
VALUE	2.6797E 03	9.7584E 02	1.4894E 03	1.2344E 03	1.1463E 03	1.1904E 03	1.9330E-01	9.4301E 00	5.8146E 00	1.4666E 03
D/DT	-6.2152E-01	1.1532E-02	-1.2964E-01	-2.0440E-01	-2.7530E-01	-2.3985E-01	2.1560E-05	-5.8009E-04	-4.6128E-04	-3.0039E-01
D/DP	8.5764E 00	1.3326E 00	1.1768E 00	2.1548E 00	3.0411E 00	2.5980E 00	7.3008E-05	7.6446E-03	4.3628E-03	3.8923E 00

TEMPERATURE = 800.00 DEG. K. PRESSURE = 4.00 KB.

	EPS	ALPHA	GAMMA	THETA	CP	V1(VP)	V2	V3(VS)	V4	KS
VALUE	5.5984E-03	4.2545E-05	1.5322E 00	5.5050E 02	1.1894E 01	8.7461E 00	6.5047E 00	4.9366E 00	9.7178E 00	1.5513E 03
D/DT	1.4261E-05	1.1107E-08	0.0	0.0		-8.2201E-04	-2.0305E-04	-8.0553E-04	-4.6653E-04	-1.9908E-01
D/DP	-2.2734E-04	-1.3783E-07	-1.9278E-03	1.2446E-01	-2.8244E-03	1.0986E-02	3.5893E-04	8.7767E-03	5.6744E-03	3.7539E 00

	C11	C12	C44	MU(V)	MU(R)	MU(VRH)	SIGMA(VRH)	VP(VRH)	VS(VRH)	KT
VALUE	2.6969E 03	9.7850E 02	1.4918E 03	1.2387E 03	1.1524E 03	1.1956E 03	1.9342E-01	9.4454E 00	5.8233E 00	1.4744E 03
D/DT	-6.2169E-01	1.2226E-02	-1.2969E-01	-2.0460E-01	-2.7451E-01	-2.3955E-01	2.1492E-05	-5.7755E-04	-4.5952E-04	-2.9964E-01
D/DP	8.6044E 00	1.3286E 00	1.1764E 00	2.1610E 00	3.0389E 00	2.5999E 00	7.3144E-05	7.6381E-03	4.3570E-03	3.8965E 00

TEMPERATURE = 800.00 DEG. K. PRESSURE = 6.00 KB.

	EPS	ALPHA	GAMMA	THETA	CP	V1(VP)	V2	V3(VS)	V4	KS
VALUE	5.1450E-03	4.2271E-05	1.5283E 00	5.5075E 02	1.1888E 01	8.7681E 00	6.5054E 00	4.9542E 00	9.7291E 00	1.5588E 03
D/DT	1.4163E-05	1.0984E-08	0.0	0.0		-8.1911E-04	-2.0269E-04	-8.0259E-04	-4.6504E-04	-1.9867E-01
D/DP	-2.2604E-04	-1.3604E-07	-1.9007E-03	1.2386E-01	-2.7887E-03	1.0986E-02	3.6569E-04	8.7741E-03	5.6799E-03	3.7606E 00

	C11	C12	C44	MU(V)	MU(R)	MU(VRH)	SIGMA(VRH)	VP(VRH)	VS(VRH)	KT
VALUE	2.7142E 03	9.8116E 02	1.4941E 03	1.2431E 03	1.1585E 03	1.2008E 03	1.9354E-01	9.4606E 00	5.8320E 00	1.4822E 03
D/DT	-6.2184E-01	1.2916E-02	-1.2973E-01	-2.0479E-01	-2.7372E-01	-2.3925E-01	2.1424E-05	-5.7500E-04	-4.5775E-04	-2.9889E-01
D/DP	8.6324E 00	1.3247E 00	1.1760E 00	2.1671E 00	3.0366E 00	2.6019E 00	7.3279E-05	7.6316E-03	4.3512E-03	3.9008E 00

0 0 0 0 0 0 0 0 0 0 0 0 0 0 0 0 0 0 0 0 0 0 0 0 0 0 0 0 0 0 0 0 0 0

****

TEMPERATURE = 800.00 DEG. K. PRESSURE = 8.00 KB.

	EPS	ALPHA	GAMMA	THETA	CP	V1(VP)	V2	V3(VS)	V4	KS
VALUE	4.6942E-03	4.2001E-05	1.5246E 00	5.5099E 02	1.1882E 01	8.7901E 00	6.5062E 00	4.9717E 00	9.7405E 00	1.5664E 03
D/DT	1.4066E-05	1.0863E-08	0.0	0.0		-8.1620E-04	-2.0232E-04	-7.9965E-04	-4.6355E-04	-1.9826E-01
D/DP	-2.2476E-04	-1.3429E-07	-1.8739E-03	1.2326E-01	-2.7537E-03	1.0985E-02	3.7236E-04	8.7716E-03	5.6853E-03	3.7673E 00

	C11	C12	C44	MU(V)	MU(R)	MU(VRH)	SIGMA(VRH)	VP(VRH)	VS(VRH)	KT
VALUE	2.7315E 03	9.8381E 02	1.4965E 03	1.2474E 03	1.1645E 03	1.2060E 03	1.9366E-01	9.4759E 00	5.8407E 00	1.4900E 03
D/DT	-6.2199E-01	1.3602E-02	-1.2977E-01	-2.0498E-01	-2.7293E-01	-2.3895E-01	2.1357E-05	-5.7247E-04	-4.5598E-04	-2.9814E-01
D/DP	8.6604E 00	1.3207E 00	1.1756E 00	2.1733E 00	3.0343E 00	2.6038E 00	7.3413E-05	7.6251E-03	4.3454E-03	3.9051E 00

****

TEMPERATURE = 800.00 DEG. K. PRESSURE = 10.00 KB.

	EPS	ALPHA	GAMMA	THETA	CP	V1(VP)	V2	V3(VS)	V4	KS
VALUE	4.2459E-03	4.1734E-05	1.5208E 00	5.5124E 02	1.1877E 01	8.8120E 00	6.5069E 00	4.9893E 00	9.7519E 00	1.5739E 03
D/DT	1.3970E-05	1.0745E-08	0.0	0.0		-8.1330E-04	-2.0195E-04	-7.9672E-04	-4.6205E-04	-1.9785E-01
D/DP	-2.2349E-04	-1.3256E-07	-1.8474E-03	1.2267E-01	-2.7194E-03	1.0985E-02	3.7898E-04	8.7691E-03	5.6906E-03	3.7746E 00

	C11	C12	C44	MU(V)	MU(R)	MU(VRH)	SIGMA(VRH)	VP(VRH)	VS(VRH)	KT
VALUE	2.7488E 03	9.8645E 02	1.4988E 03	1.2518E 03	1.1706E 03	1.2112E 03	1.9378E-01	9.4911E 00	5.8494E 00	1.4979E 03
D/DT	-6.2212E-01	1.4285E-02	-1.2981E-01	-2.0517E-01	-2.7214E-01	-2.3865E-01	2.1289E-05	-5.6993E-04	-4.5422E-04	-2.9740E-01
D/DP	8.6884E 00	1.3167E 00	1.1752E 00	2.1795E 00	3.0320E 00	2.6058E 00	7.3546E-05	7.6186E-03	4.3396E-03	3.9094E 00

0 0 0 0 0 0 0 0 0 0 0 0 0 0 0 0 0 0 0 0 0 0 0 0 0 0 0 0 0 0 0 0

MGC SINGLE CRYSTAL

****

TEMPERATURE = 9C0.00 DEG. K.   PRESSURE = 0.C KB.

	EPS	ALPHA	GAMMA	THETA	CP	V1(VP)	V2	V3(VS)	V4	KS
VALUE	7.9785E-03	4.4180E-05	1.5400E 00	5.5000E 02	1.2098E 01	8.6195E C0	6.4830E 00	4.8203E 00	9.6483E 00	1.5163E 03
D/DT	1.4844E-05	1.0415E-08	0.0	0.0		-8.2551E-04	-2.0215E-04	-8.1213E-04	-4.6758E-04	-1.9973E-01
D/DP	-2.3515E-04	-1.4658E-07	-2.0111E-03	1.2831E-01	-3.0638E-03	1.1066E-02	3.6187E-04	8.9236E-03	5.7355E-03	3.7237E 00

	C11	C12	C44	MU(V)	MU(R)	MU(VRH)	SIGMA(VRH)	VP(VRH)	VS(VRH)	KT
VALUE	2.6009E 03	9.7404E 02	1.4713E 03	1.2082E 03	1.1117E 03	1.1599E 03	1.9523E-01	9.3538E 00	5.7562E 00	1.4288E 03
D/DT	-6.1310E-01	6.9569E-03	-1.2770E-01	-2.0063E-01	-2.7536E-01	-2.3800E-01	2.1951E-05	-5.8289E-04	-4.6338E-04	-2.9924E-01
D/DP	8.4984E 00	1.3364E 0C	1.1940E 00	2.1488E 0C	3.C844E 00	2.6166E 00	5.9748E-05	7.7399E-03	4.4782E-03	3.89C1E 00

****

TEMPERATURE = 900.00 DEG. K.   PRESSURE = 2.C0 KB.

	EPS	ALPHA	GAMMA	THETA	CP	V1(VP)	V2	V3(VS)	V4	KS
VALUE	7.5096E-03	4.3889E-05	1.5360E 00	5.5026E 02	1.2092E 01	8.6417E 00	6.4838E 00	4.8382E 00	9.6597E 00	1.5239E 03
D/DT	1.4739E-C5	1.0288E-08	0.0	0.0		-8.2279E-C4	-2.0183E-04	-8.0940E-04	-4.6615E-04	-1.9932E-01
D/DP	-2.3376E-C4	-1.4461E-07	-1.9824E-03	1.2767E-01	-3.0219E-03	1.1066E-02	3.6910E-04	8.9210E-03	5.7415E-03	3.7304E 00

	C11	C12	C44	MU(V)	MU(R)	MU(VRH)	SIGMA(VRH)	VP(VRH)	VS(VRH)	KT
VALUE	2.6180E 03	9.7679E 02	1.4737E 03	1.2125E 03	1.1178E 03	1.1652E 03	1.9534E-01	9.3693E 00	5.7651E 00	1.4367E 03
D/DT	-6.1342E-01	7.7308E-03	-1.2777E-01	-2.0089E-01	-2.7464E-01	-2.3776E-01	2.1893E-05	-5.8041E-04	-4.6171E-04	-2.9850E-01
D/DP	8.5268E 00	1.3322E 00	1.1936E 00	2.1551E C0	3.0822E 00	2.6186E C0	5.9925E-05	7.7330E-03	4.4720E-03	3.8938E 00

****

TEMPERATURE = 900.00 DEG. K.   PRESSURE = 4.C0 KB.

	EPS	ALPHA	GAMMA	THETA	CP	V1(VP)	V2	V3(VS)	V4	KS
VALUE	7.0434E-03	4.3601E-05	1.5321E 00	5.5051E 02	1.2086E 01	8.6640E 00	6.4845E 00	4.8560E 00	9.6712E 00	1.5314E 03
D/DT	1.4636E-05	1.0164E-08	0.0	0.0		-8.2007E-04	-2.0150E-04	-8.0667E-04	-4.6472E-04	-1.9891E-01
D/DP	-2.3238E-04	-1.4269E-07	-1.9540E-03	1.2703E-01	-2.9809E-03	1.1065E-02	3.7626E-04	8.9183E-03	5.7474E-03	3.7370E 00

	C11	C12	C44	MU(V)	MU(R)	MU(VRH)	SIGMA(VRH)	VP(VRH)	VS(VRH)	KT
VALUE	2.6352E 03	9.7954E 02	1.4761E 03	1.2168E 03	1.1240E 03	1.1704E 03	1.9545E-01	9.3849E 00	5.7741E 00	1.4446E 03
D/DT	-6.1374E-01	8.5006E-03	-1.2783E-01	-2.0115E-01	-2.7391E-01	-2.3753E-C1	2.1834E-05	-5.7793E-04	-4.6004E-04	-2.9776E-01
D/DP	8.5553E 00	1.3279E 00	1.1931E 00	2.1614E 00	3.0800E 00	2.6207E 00	6.0103E-05	7.7261E-03	4.4659E-03	3.8977E 00

****

TEMPERATURE = 900.00 DEG. K.   PRESSURE = 6.00 KB.

	EPS	ALPHA	GAMMA	THETA	CP	V1(VP)	V2	V3(VS)	V4	KS
VALUE	6.5800E-03	4.3318E-05	1.5282E 00	5.5076E 02	1.2080E 01	8.6863E 00	6.4853E 00	4.8738E 00	9.6827E 00	1.5390E 03
D/DT	1.4534E-05	1.0043E-08	0.0	0.0		-8.1734E-04	-2.0116E-04	-8.0395E-04	-4.6329E-04	-1.9850E-01
D/DP	-2.3101E-04	-1.4080E-07	-1.9260E-03	1.2640E-01	-2.9406E-03	1.1065E-02	3.8333E-04	8.9157E-03	5.7531E-03	3.7437E 00

	C11	C12	C44	MU(V)	MU(R)	MU(VRH)	SIGMA(VRH)	VP(VRH)	VS(VRH)	KT
VALUE	2.6524E 03	9.8227E 02	1.4785E 03	1.2211E 03	1.1302E 03	1.1756E 03	1.9556E-01	9.4005E 00	5.7830E 00	1.4524E 03
D/DT	-6.1405E-01	9.2672E-03	-1.2789E-01	-2.0140E-01	-2.7318E-01	-2.3729E-01	2.1775E-05	-5.7545E-C4	-4.5836E-04	-2.9702E-01
D/DP	8.5837E 00	1.3236E 00	1.1927E 00	2.1677E 0C	3.0778E 00	2.6227E 00	6.0278E-05	7.7192E-03	4.4598E-03	3.9015E 00

C 0 0 0 0 0 0 0 0 0 0 0 0 0 0 0 0 0 0 0 0 0 0 0 0 0 0 0 0 0 0 0 0

MGO SINGLE CRYSTAL

****

TEMPERATURE = 900.00 DEG. K. PRESSURE = 8.00 KB.

	EPS	ALPHA	GAMMA	THETA	CP	V1(VP)	V2	V3(VS)	V4	KS
VALUE	6.1194E-03	4.3038E-05	1.5244E 00	5.5101E 02	1.2074E 01	8.7085E 00	6.4860E 00	4.8917E 00	9.6942E 00	1.5465E 03
D/DT	1.4434E-05	9.9232E-09	0.0	0.0		-8.1461E-04	-2.0082E-04	-8.0122E-04	-4.6184E-04	-1.9809E-01
D/DP	-2.2966E-04	-1.3894E-07	-1.8983E-03	1.2577E-01	-2.9012E-03	1.1065E-02	3.9033E-04	8.9131E-03	5.7589E-03	3.7503E 00

	C11	C12	C44	MU(V)	MU(R)	MU(VRH)	SIGMA(VRH)	VP(VRH)	VS(VRH)	KT
VALUE	2.6656E 03	9.8499E 02	1.4809E 03	1.2255E 03	1.1363E 03	1.1809E 03	1.9567E-01	9.4160E 00	5.7919E 00	1.4603E 03
D/DT	-6.1434E-01	1.0031E-02	-1.2795E-01	-2.0165E-01	-2.7246E-01	-2.3705E-01	2.1717E-05	-5.7297E-04	-4.5669E-04	-2.9628E-01
D/DP	8.6121E 00	1.3193E 00	1.1923E 00	2.1740E 00	3.0756E 00	2.6248E 00	6.0454E-05	7.7124E-03	4.4537E-03	3.9054E 00

****

TEMPERATURE = 900.00 DEG. K. PRESSURE = 10.00 KB.

	EPS	ALPHA	GAMMA	THETA	CP	V1(VP)	V2	V3(VS)	V4	KS
VALUE	5.6614E-03	4.2762E-05	1.5206E 00	5.5126E 02	1.2068E 01	8.7308E 00	6.4868E 00	4.9095E 00	9.7058E 00	1.5541E 03
D/DT	1.4335E-05	9.8059E-09	0.0	0.0		-8.1188E-04	-2.0046E-04	-7.9850E-04	-4.6039E-04	-1.9768E-01
D/DP	-2.2832E-04	-1.3711E-07	-1.8710E-03	1.2516E-01	-2.8626E-03	1.1065E-02	3.9725E-04	8.9105E-03	5.7645E-03	3.7569E 00

	C11	C12	C44	MU(V)	MU(R)	MU(VRH)	SIGMA(VRH)	VP(VRH)	VS(VRH)	KT
VALUE	2.6870E 03	9.8770E 02	1.4833E 03	1.2298E 03	1.1425E 03	1.1861E 03	1.9578E-01	9.4316E 00	5.8008E 00	1.4682E 03
D/DT	-6.1463E-01	1.0791E-02	-1.2801E-01	-2.0189E-01	-2.7173E-01	-2.3681E-01	2.1658E-05	-5.7050E-04	-4.5502E-04	-2.9556E-01
D/DP	8.6406E 00	1.3150E 00	1.1919E 00	2.1803E 00	3.0733E 00	2.6268E 00	6.0627E-05	7.7055E-03	4.4477E-03	3.9093E 00

0 C 0 0 0 0 0 0 0 0 0 0 0 0 0 C 0 0 0 0 0 0 0 0 0 0 0 0 0 0 0

TEMPERATURE = 1000.00 DEG. K. PRESSURE = 0.0 KB.

	EPS	ALPHA	GAMMA	THETA	CP	V1(VP)	V2	V3(VS)	V4	KS
VALUE	9.4810E-03	4.5185E-05	1.5400E 00	5.5000E 02	1.2251E 01	8.5370E 00	6.4629E 00	4.7391E 00	9.6016E 00	1.4964E 03
D/DT	1.5205E-05	9.8904E-09	0.0	0.0		-8.2345E-04	-2.0073E-04	-8.1305E-04	-4.6596E-04	-1.9951E-01
D/DP	-2.4052E-04	-1.5198E-07	-2.0436E-03	1.3104E-01	-3.2993E-03	1.1140E-02	3.7730E-04	9.0549E-03	5.8053E-03	3.7104E 00

	C11	C12	C44	MU(V)	MU(R)	MU(VRH)	SIGMA(VRH)	VP(VRH)	VS(VRH)	KT
VALUE	2.5400E 03	9.7455E 02	1.4557E 03	1.1865E 03	1.0832E 03	1.1348E 03	1.9732E-01	9.2926E 00	5.7063E 00	1.3990E 03
D/DT	-6.0476E-01	3.1180E-03	-1.2579E-01	-1.9705E-01	-2.7462E-01	-2.3583E-01	2.2295E-05	-5.8354E-04	-4.6400E-04	-2.9747E-01
D/DP	8.4444E 00	1.3433E 00	1.2105E 00	2.1465E 00	3.1219E 00	2.6342E 00	4.7406E-05	7.8298E-03	4.5834E-03	3.8559E 00

TEMPERATURE = 1000.00 DEG. K. PRESSURE = 2.00 KB.

	EPS	ALPHA	GAMMA	THETA	CP	V1(VP)	V2	V3(VS)	V4	KS
VALUE	9.0014E-03	4.4883E-05	1.5359E 00	5.5026E 02	1.2244E 01	8.5595E 00	6.4636E 00	4.7572E 00	9.6132E 00	1.5039E 03
D/DT	1.5096E-05	9.7624E-09	0.0	0.0		-8.2090E-04	-2.0043E-04	-8.1054E-04	-4.6458E-04	-1.9910E-01
D/DP	-2.3905E-04	-1.4990E-07	-2.0139E-03	1.3037E-01	-3.2518E-03	1.1140E-02	3.8489E-04	9.0521E-03	5.8116E-03	3.7170E 00

	C11	C12	C44	MU(V)	MU(R)	MU(VRH)	SIGMA(VRH)	VP(VRH)	VS(VRH)	KT
VALUE	2.5571E 03	9.7738E 02	1.4581E 03	1.1908E 03	1.0894E 03	1.1401E 03	1.9742E-01	9.3085E 00	5.7155E 00	1.4069E 03
D/DT	-6.0524E-01	3.9633E-03	-1.2588E-01	-1.9737E-01	-2.7395E-01	-2.3566E-01	2.2246E-05	-5.8112E-04	-4.6243E-04	-2.9674E-01
D/DP	8.4733E 00	1.3388E 00	1.2100E 00	2.1529E 00	3.1199E 00	2.6364E 00	4.7625E-05	7.8226E-03	4.5771E-03	3.8993E 00

TEMPERATURE = 1000.00 DEG. K. PRESSURE = 4.00 KB.

	EPS	ALPHA	GAMMA	THETA	CP	V1(VP)	V2	V3(VS)	V4	KS
VALUE	8.5247E-03	4.4586E-05	1.5319E 00	5.5052E 02	1.2238E 01	8.5821E 00	6.4644E 00	4.7753E 00	9.6248E 00	1.5115E 03
D/DT	1.4989E-05	9.6368E-09	0.0	0.0		-8.1835E-04	-2.0012E-04	-8.0802E-04	-4.6320E-04	-1.9870E-01
D/DP	-2.3760E-04	-1.4786E-07	-1.9845E-03	1.2970E-01	-3.2052E-03	1.1140E-02	3.9240E-04	9.0494E-03	5.8178E-03	3.7235E 00

	C11	C12	C44	MU(V)	MU(R)	MU(VRH)	SIGMA(VRH)	VP(VRH)	VS(VRH)	KT
VALUE	2.5742E 03	9.8021E 02	1.4605E 03	1.1951E 03	1.0957E 03	1.1454E 03	1.9752E-01	9.3243E 00	5.7246E 00	1.4149E 03
D/DT	-6.0570E-01	4.8050E-03	-1.2596E-01	-1.9768E-01	-2.7329E-01	-2.3548E-01	2.2196E-05	-5.7871E-04	-4.6086E-04	-2.9601E-01
D/DP	8.5021E 00	1.3342E 00	1.2096E 00	2.1593E 00	3.1178E 00	2.6385E 00	4.7841E-05	7.8154E-03	4.5707E-03	3.9027E 00

TEMPERATURE = 1000.00 DEG. K. PRESSURE = 6.00 KB.

	EPS	ALPHA	GAMMA	THETA	CP	V1(VP)	V2	V3(VS)	V4	KS
VALUE	8.0510E-03	4.4292E-05	1.5280E 00	5.5078E 02	1.2232E 01	8.6046E 00	6.4652E 00	4.7934E 00	9.6365E 00	1.5191E 03
D/DT	1.4883E-05	9.5137E-09	0.0	0.0		-8.1580E-04	-1.9981E-04	-8.0551E-04	-4.6182E-04	-1.9829E-01
D/DP	-2.3616E-04	-1.4586E-07	-1.9556E-03	1.2903E-01	-3.1596E-03	1.1140E-02	3.9982E-04	9.0466E-03	5.8240E-03	3.7301E 00

	C11	C12	C44	MU(V)	MU(R)	MU(VRH)	SIGMA(VRH)	VP(VRH)	VS(VRH)	KT
VALUE	2.5914E 03	9.8301E 02	1.4630E 03	1.1994E 03	1.1019E 03	1.1507E 03	1.9762E-01	9.3402E 00	5.7338E 00	1.4228E 03
D/DT	-6.0615E-01	5.6449E-03	-1.2604E-01	-1.9799E-01	-2.7263E-01	-2.3531E-01	2.2147E-05	-5.7630E-04	-4.5929E-04	-2.9528E-01
D/DP	8.5310E 00	1.3297E 00	1.2091E 00	2.1657E 00	3.1156E 00	2.6407E 00	4.8057E-05	7.8082E-03	4.5644E-03	3.9061E 00

C 0 0 0 0 0 0 0 0 0 0 0 0 0 0 0 0 0 0 0 0 0 0 0 0 0 0 0 0 0 0 0 0

MGO SINGLE CRYSTAL

****

TEMPERATURE = 1000.00 DEG. K. PRESSURE = 8.00 KB.

	EPS	ALPHA	GAMMA	THETA	CP	V1(VP)	V2	V3(VS)	V4	KS
VALUE	7.5801E-03	4.4002E-05	1.5241E 00	5.5103E 02	1.2225E 01	8.6271E 00	6.4660E 00	4.8115E 00	9.6481E 00	1.5267E 03
D/DT	1.4779E-05	9.3930E-09	0.0	0.0		-8.1324E-04	-1.9949E-04	-8.0300E-04	-4.6042E-04	-1.9787E-01
D/DP	-2.3474E-04	-1.4389E-07	-1.9271E-03	1.2838E-01	-3.1149E-03	1.1140E-02	4.0716E-04	9.0439E-03	5.8300E-03	3.7367E 00

	C11	C12	C44	MU(V)	MU(R)	MU(VRH)	SIGMA(VRH)	VP(VRH)	VS(VRH)	KT
VALUE	2.6086E 03	9.8582E 02	1.4654E 03	1.2038E 03	1.1081E 03	1.1559E 03	1.9772E-01	9.3560E 00	5.7429E 00	1.4308E 03
D/DT	-6.0659E-01	6.4816E-03	-1.2612E-01	-1.9829E-01	-2.7196E-01	-2.3513E-01	2.2098E-05	-5.7389E-04	-4.5772E-04	-2.9456E-01
D/DP	8.5598E 00	1.3251E 00	1.2087E 00	2.1722E 00	3.1135E 00	2.6428E 00	4.8270E-05	7.8010E-03	4.5580E-03	3.9096E 00

****

TEMPERATURE = 1000.00 DEG. K. PRESSURE = 10.00 KB.

	EPS	ALPHA	GAMMA	THETA	CP	V1(VP)	V2	V3(VS)	V4	KS
VALUE	7.1120E-03	4.3716E-05	1.5203E 00	5.5129E 02	1.2219E 01	8.6496E 00	6.4668E 00	4.8296E 00	9.6598E 00	1.5344E 03
D/DT	1.4676E-05	9.2745E-09	0.0	0.0		-8.1069E-04	-1.9916E-04	-8.0049E-04	-4.5902E-04	-1.9746E-01
D/DP	-2.3333E-04	-1.4195E-07	-1.8989E-03	1.2772E-01	-3.0712E-03	1.1140E-02	4.1441E-04	9.0412E-03	5.8360E-03	3.7433E 00

	C11	C12	C44	MU(V)	MU(R)	MU(VRH)	SIGMA(VRH)	VP(VRH)	VS(VRH)	KT
VALUE	2.6259E 03	9.8861E 02	1.4678E 03	1.2081E 03	1.1143E 03	1.1612E 03	1.9782E-01	9.3718E 00	5.7520E 00	1.4387E 03
D/DT	-6.0702E-01	7.3155E-03	-1.2620E-01	-1.9858E-01	-2.7130E-01	-2.3494E-01	2.2048E-05	-5.7148E-04	-4.5615E-04	-2.9384E-01
D/DP	8.5887E 00	1.3205E 00	1.2083E 00	2.1786E 00	3.1113E 00	2.6449E 00	4.8484E-05	7.7938E-03	4.5517E-03	3.9131E 00

C C 0 0 0 0 0 0 0 0 0 0 0 0 0 0 0 0 0 0 0 0 0 0 0 0 0 0 0 0 0 0

****

TEMPERATURE = 1100.00 DEG. K. PRESSURE = 0.0 KB.

	EPS	ALPHA	GAMMA	THETA	CP	V1(VP)	V2	V3(VS)	V4	KS
VALUE	1.1019E-02	4.6152E-05	1.5400E 00	5.5000E 02	1.2375E 01	8.4548E 00	6.4429E 00	4.6577E 00	9.5551E 00	1.4764E 03
D/DT	1.5554E-05	9.6241E-09	0.0	0.0		-8.2150E-04	-1.9941E-04	-8.1413E-04	-4.6451E-04	-1.9925E-01
D/DP	-2.4610E-04	-1.5774E-07	-2.0784E-03	1.3388E-01	-3.5915E-03	1.1209E-02	3.9143E-04	9.1754E-03	5.8724E-03	3.7002E 00

	C11	C12	C44	MU(V)	MU(R)	MU(VRH)	SIGMA(VRH)	VP(VRH)	VS(VRH)	KT
VALUE	2.4799E 03	9.7467E 02	1.4401E 03	1.1651E 03	1.0547E 03	1.1099E 03	1.9943E-01	9.2312E 00	5.6563E 00	1.3694E 03
D/DT	-5.9638E-01	-6.9237E-04	-1.2388E-01	-1.9346E-01	-2.7384E-01	-2.3365E-01	2.2656E-05	-5.8446E-04	-4.6483E-04	-2.9578E-01
D/DP	8.3867E 00	1.3569E 00	1.2266E 00	2.1419E 00	3.1560E 00	2.6490E 00	3.5856E-05	7.9206E-03	4.6843E-03	3.9053E 00

****

TEMPERATURE = 1100.00 DEG. K. PRESSURE = 2.00 KB.

	EPS	ALPHA	GAMMA	THETA	CP	V1(VP)	V2	V3(VS)	V4	KS
VALUE	1.0528E-02	4.5839E-05	1.5359E 00	5.5027E 02	1.2368E 01	8.4775E 00	6.4437E 00	4.6761E 00	9.5668E 00	1.4840E 03
D/DT	1.5441E-05	9.4928E-09	0.0	0.0		-8.1913E-04	-1.9913E-04	-8.1183E-04	-4.6319E-04	-1.9885E-01
D/DP	-2.4455E-04	-1.5553E-07	-2.0477E-03	1.3317E-01	-3.5374E-03	1.1209E-02	3.9942E-04	9.1725E-03	5.8791E-03	3.7067E 00

	C11	C12	C44	MU(V)	MU(R)	MU(VRH)	SIGMA(VRH)	VP(VRH)	VS(VRH)	KT
VALUE	2.4969E 03	9.7759E 02	1.4426E 03	1.1694E 03	1.0610E 03	1.1152E 03	1.9953E-01	9.2474E 00	5.6656E 00	1.3774E 03
D/DT	-5.9699E-01	2.1958E-04	-1.2398E-01	-1.9383E-01	-2.7325E-01	-2.3354E-01	2.2617E-05	-5.8212E-04	-4.6337E-04	-2.9506E-01
D/DP	8.4159E 00	1.3521E 00	1.2262E 00	2.1485E 00	3.1540E 00	2.6512E 00	3.6111E-05	7.9131E-03	4.6778E-03	3.9082E 00

****

TEMPERATURE = 1100.00 DEG. K. PRESSURE = 4.00 KB.

	EPS	ALPHA	GAMMA	THETA	CP	V1(VP)	V2	V3(VS)	V4	KS
VALUE	1.0041E-02	4.5530E-05	1.5318E 00	5.5053E 02	1.2361E 01	8.5003E 00	6.4445E 00	4.6944E 00	9.5786E 00	1.4917E 03
D/DT	1.5329E-05	9.3641E-09	0.0	0.0		-8.1676E-04	-1.9885E-04	-8.0953E-04	-4.6186E-04	-1.9844E-01
D/DP	-2.4302E-04	-1.5336E-07	-2.0174E-03	1.3246E-01	-3.4845E-03	1.1209E-02	4.0730E-04	9.1697E-03	5.8857E-03	3.7133E 00

	C11	C12	C44	MU(V)	MU(R)	MU(VRH)	SIGMA(VRH)	VP(VRH)	VS(VRH)	KT
VALUE	2.5140E 03	9.8050E 02	1.4450E 03	1.1737E 03	1.0674E 03	1.1205E 03	1.9962E-01	9.2635E 00	5.6750E 00	1.3854E 03
D/DT	-5.9759E-01	1.1301E-03	-1.2409E-01	-1.9419E-01	-2.7265E-01	-2.3342E-01	2.2578E-05	-5.7977E-04	-4.6190E-04	-2.9434E-01
D/DP	8.4451E 00	1.3473E 00	1.2257E 00	2.1550E 00	3.1520E 00	2.6535E 00	3.6366E-05	7.9056E-03	4.6712E-03	3.9112E 00

****

TEMPERATURE = 1100.00 DEG. K. PRESSURE = 6.00 KB.

	EPS	ALPHA	GAMMA	THETA	CP	V1(VP)	V2	V3(VS)	V4	KS
VALUE	9.5561E-03	4.5225E-05	1.5278E 00	5.5079E 02	1.2354E 01	8.5231E 00	6.4453E 00	4.7127E 00	9.5904E 00	1.4993E 03
D/DT	1.5219E-05	9.2380E-09	0.0	0.0		-8.1438E-04	-1.9856E-04	-8.0723E-04	-4.6053E-04	-1.9803E-01
D/DP	-2.4151E-04	-1.5123E-07	-1.9876E-03	1.3176E-01	-3.4327E-03	1.1209E-02	4.1509E-04	9.1669E-03	5.8922E-03	3.7198E 00

	C11	C12	C44	MU(V)	MU(R)	MU(VRH)	SIGMA(VRH)	VP(VRH)	VS(VRH)	KT
VALUE	2.5312E 03	9.8340E 02	1.4475E 03	1.1780E 03	1.0737E 03	1.1258E 03	1.9971E-01	9.2796E 00	5.6843E 00	1.3934E 03
D/DT	-5.9818E-01	2.0375E-03	-1.2418E-01	-1.9455E-01	-2.7205E-01	-2.3330E-01	2.2538E-05	-5.7743E-04	-4.6043E-04	-2.9363E-01
D/DP	8.4744E 00	1.3425E 00	1.2252E 00	2.1615E 00	3.1500E 00	2.6557E 00	3.6618E-05	7.8981E-03	4.6646E-03	3.9142E 00

C 0 0 0 0 0 0 0 0 0 0 0 0 0 0 0 0 0 0 0 0 0 0 0 0 0 0 0 0 0 0 0 0

MGO SINGLE CRYSTAL

****

TEMPERATURE = 1100.00 DEG. K.   PRESSURE = 8.CC KB.

	EPS	ALPHA	GAMMA	THETA	CP	V1(VP)	V2	V3(VS)	V4	KS
VALUE	9.0746E-03	4.4925E-05	1.5238E 00	5.5106E 02	1.2347E 01	8.5459E 00	6.4461E 00	4.7311E 00	9.6022E 00	1.5070E 03
D/DT	1.5111E-05	9.1142E-09	0.0	0.0		-8.1200E-04	-1.9827E-04	-8.0493E-04	-4.5919E-04	-1.9762E-01
D/DP	-2.40C1E-04	-1.4914E-07	-1.9581E-03	1.3107E-01	-3.3820E-03	1.1210E-02	4.2278E-04	9.1640E-03	5.8986E-03	3.7263E 00

	C11	C12	C44	MU(V)	MU(R)	MU(VRH)	SIGMA(VRH)	VP(VRH)	VS(VRH)	KT
VALUE	2.5483E 03	9.8629E 02	1.4499E 03	1.1824E 03	1.0800E 03	1.1312E 03	1.9980E-01	9.2957E 00	5.6936E 00	1.4014E 03
D/DT	-5.9875E-01	2.9438E-03	-1.2428E-01	-1.9491E-01	-2.7146E-01	-2.3318E-01	2.2498E-05	-5.7509E-04	-4.5896E-04	-2.9292E-01
D/DP	8.5036E 00	1.3377E 00	1.2248E 00	2.1681E 00	3.1479E 00	2.6580E 00	3.6871E-05	7.8906E-03	4.6581E-03	3.9173E 00

****

TEMPERATURE = 1100.00 DEG. K.   PRESSURE = 10.00 KB.

	EPS	ALPHA	GAMMA	THETA	CP	V1(VP)	V2	V3(VS)	V4	KS
VALUE	8.5961E-03	4.4629E-05	1.5200E 00	5.5132E 02	1.2340E 01	8.5686E 00	6.4470E 00	4.7494E 00	9.6140E 00	1.5146E 03
D/DT	1.5004E-05	8.9931E-09	0.0	0.0		-8.0962E-04	-1.9797E-04	-8.0264E-04	-4.5784E-04	-1.9721E-01
D/DP	-2.3853E-04	-1.4709E-07	-1.9290E-03	1.3038E-01	-3.3324E-03	1.1210E-02	4.3038E-04	9.1612E-03	5.9050E-03	3.7328E 00

	C11	C12	C44	MU(V)	MU(R)	MU(VRH)	SIGMA(VRH)	VP(VRH)	VS(VRH)	KT
VALUE	2.5656E 03	9.8916E 02	1.4524E 03	1.1867E 03	1.0862E 03	1.1365E 03	1.9989E-01	9.3118E 00	5.7029E 00	1.4095E 03
D/DT	-5.9933E-01	3.8475E-03	-1.2437E-01	-1.9526E-01	-2.7086E-01	-2.3306E-C1	2.2458E-05	-5.7275E-C4	-4.5749E-04	-2.9221E-01
D/DP	8.5328E 00	1.3328E 00	1.2243E 00	2.1746E 00	3.1458E 00	2.66C2E 00	3.7122E-05	7.8831E-03	4.6515E-03	3.9204E 00

C 0 0 0 0 0 0 0 0 0 0 0 0 0 0 0 0 0 0 0 0 0 0 0 0 0 0 0 0 0 0 0

TEMPERATURE = 1200.00 DEG. K. PRESSURE = 0.0 KB.

	EPS	ALPHA	GAMMA	THETA	CP	V1(VP)	V2	V3(VS)	V4	KS
VALUE	1.2591E-02	4.7102E-05	1.5400E 00	5.5000E 02	1.2478E 01	8.3727E 00	6.4230E 00	4.5762E 00	9.5087E 00	1.4565E 03
D/DT	1.5898E-05	9.5263E-09	0.0	0.0		-8.1962E-04	-1.9814E-04	-8.1531E-04	-4.6316E-04	-1.9897E-01
D/DP	-2.5191E-04	-1.6384E-07	-2.1144E-03	1.3683E-01	-3.9332E-03	1.1273E-02	4.0422E-04	9.2851E-03	5.9368E-03	3.693CE 00

	C11	C12	C44	MU(V)	MU(R)	MU(VRH)	SIGMA(VRH)	VP(VRH)	VS(VRH)	KT
VALUE	2.4207E 03	9.7441E 02	1.4246E 03	1.1440E 03	1.0264E 03	1.0852E 03	2.0158E-01	9.1696E 00	5.6059E 00	1.3399E 03
D/DT	-5.8796E-01	-4.4816E-03	-1.2196E-01	-1.8987E-01	-2.7305E-01	-2.3146E-01	2.3035E-05	-5.8558E-04	-4.6582E-04	-2.9415E-01
D/DP	8.3253E 00	1.3768E 00	1.2425E 00	2.1352E 00	3.1864E 00	2.66C8E 00	2.5105E-05	8.0120E-03	4.7807E-03	3.9178E 00

TEMPERATURE = 1200.00 DEG. K. PRESSURE = 2.CO KB.

	EPS	ALPHA	GAMMA	THETA	CP	V1(VP)	V2	V3(VS)	V4	KS
VALUE	1.2089E-02	4.6776E-05	1.5358E 00	5.5027E 02	1.2470E 01	8.3957E 00	6.4238E 00	4.5948E 00	9.5206E 00	1.4642E 03
D/DT	1.5781E-05	9.3903E-09	0.0	0.0		-8.1743E-04	-1.9790E-04	-8.1322E-04	-4.6190E-04	-1.9857E-01
D/DP	-2.5027E-04	-1.6149E-07	-2.0827E-03	1.3607E-01	-3.8717E-03	1.1274E-02	4.1261E-04	9.2822E-03	5.9439E-03	3.6995E 00

	C11	C12	C44	MU(V)	MU(R)	MU(VRH)	SIGMA(VRH)	VP(VRH)	VS(VRH)	KT
VALUE	2.4377E C3	9.7743E 02	1.4271E 03	1.1483E 03	1.0327E 03	1.0905E 03	2.0167E-01	9.1860E 00	5.6155E 00	1.3480E 03
D/DT	-5.8870E-01	-3.5062E-03	-1.2208E-01	-1.9029E-01	-2.7252E-01	-2.3141E-01	2.3006E-05	-5.8331E-04	-4.6446E-04	-2.9344E-01
D/DP	8.3549E 00	1.3718E 00	1.2420E 00	2.1418E 00	3.1845E 00	2.6632E 00	2.5396E-05	8.0042E-03	4.7739E-03	3.9203E 00

TEMPERATURE = 1200.00 CEG. K. PRESSURE = 4.CO KB.

	EPS	ALPHA	GAMMA	THETA	CP	V1(VP)	V2	V3(VS)	V4	KS
VALUE	1.1590E-02	4.6456E-05	1.5317E 00	5.5054E 02	1.2462E 01	8.4187E 00	6.4246E 00	4.6134E 00	9.5325E 00	1.4718E 03
D/DT	1.5665E-05	9.2572E-09	0.0	0.0		-8.1523E-04	-1.9765E-04	-8.1114E-04	-4.6063E-04	-1.9816E-01
D/DP	-2.4866E-04	-1.5919E-07	-2.0514E-03	1.3533E-01	-3.8115E-03	1.1274E-02	4.2089E-04	9.2793E-03	5.9509E-03	3.706CE 00

	C11	C12	C44	MU(V)	MU(R)	MU(VRH)	SIGMA(VRH)	VP(VRH)	VS(VRH)	KT
VALUE	2.4547E 03	9.8043E 02	1.4295E 03	1.1526E 03	1.0391E 03	1.0958E 03	2.0175E-01	9.2024E 00	5.6250E 00	1.3561E 03
D/DT	-5.8943E-01	-2.5316E-03	-1.2220E-01	-1.9070E-01	-2.7200E-01	-2.3135E-01	2.2977E-05	-5.8104E-04	-4.6310E-04	-2.9273E-01
D/DP	8.3844E C0	1.3668E 00	1.2415E 00	2.1484E 00	3.1827E 00	2.6655E 00	2.5687E-05	7.9965E-03	4.7672E-03	3.9229E 00

TEMPERATURE = 1200.00 DEG. K. PRESSURE = 6.CO KB.

	EPS	ALPHA	GAMMA	THETA	CP	V1(VP)	V2	V3(VS)	V4	KS
VALUE	1.1095E-02	4.6140E-05	1.5276E 00	5.5081E 02	1.2455E 01	8.4417E 00	6.4255E 00	4.6319E 00	9.5444E 00	1.4795E 03
D/DT	1.5550E-05	9.1268E-09	0.0	0.0		-8.1303E-04	-1.9738E-04	-8.0906E-04	-4.5935E-04	-1.9776E-01
D/DP	-2.47C6E-04	-1.5693E-07	-2.0206E-03	1.3459E-01	-3.7527E-03	1.1274E-02	4.2907E-04	9.2763E-03	5.9578E-03	3.7125E 00

	C11	C12	C44	MU(V)	MU(R)	MU(VRH)	SIGMA(VRH)	VP(VRH)	VS(VRH)	KT
VALUE	2.4717E 03	9.8342E 02	1.4320E 03	1.1569E 03	1.0455E 03	1.1012E 03	2.0184E-01	9.2188E 00	5.6345E 00	1.3641E 03
D/DT	-5.9015E-01	-1.5593E-03	-1.2232E-01	-1.9111E-01	-2.7147E-01	-2.3129E-01	2.2947E-05	-5.7878E-04	-4.6174E-04	-2.9203E-01
D/DP	8.414CE 00	1.3618E 00	1.2410E 00	2.1551E 00	3.1808E 00	2.6679E 00	2.5976E-05	7.9887E-03	4.7604E-03	3.9255E 00

0 0 0 0 0 0 0 0 0 0 0 0 0 0 0 0 0 0 0 0 0 0 0 0 0 0 0 0 0 0 0 0

MGO SINGLE CRYSTAL

TEMPERATURE = 1200.00 DEG. K. PRESSURE = 8.00 KB.

	EPS	ALPHA	GAMMA	THETA	CP	V1(VP)	V2	V3(VS)	V4	KS
VALUE	1.0602E-02	4.5828E-05	1.5236E 00	5.5108E 02	1.2447E 01	8.4647E 00	6.4264E 00	4.6505E 00	9.5563E 00	1.4872E 03
D/DT	1.5438E-05	8.9991E-09	0.0	0.0		-8.1083E-04	-1.9711E-04	-8.0698E-04	-4.5806E-04	-1.9735E-01
D/DP	-2.4549E-04	-1.5471E-07	-1.9902E-03	1.3386E-01	-3.6951E-03	1.1274E-02	4.3715E-04	9.2734E-03	5.9647E-03	3.719CE 00

	C11	C12	C44	MU(V)	MU(R)	MU(VRH)	SIGMA(VRH)	VP(VRH)	VS(VRH)	KT
VALUE	2.4889E 03	9.8641E 02	1.4345E 03	1.1612E 03	1.0518E 03	1.1065E 03	2.0192E-01	9.2352E 00	5.6441E 00	1.3722E 03
D/DT	-5.9087E-01	-5.8842E-04	-1.2243E-01	-1.9151E-01	-2.7093E-01	-2.3122E-01	2.2917E-05	-5.7651E-04	-4.6038E-04	-2.9133E-01
D/DP	8.4436E 00	1.3567E 00	1.2405E 00	2.1617E 00	3.1788E 00	2.6703E 00	2.6264E-05	7.9810E-03	4.7537E-03	3.9282E 00

TEMPERATURE = 1200.00 DEG. K. PRESSURE = 10.00 KB.

	EPS	ALPHA	GAMMA	THETA	CP	V1(VP)	V2	V3(VS)	V4	KS
VALUE	1.0113E-02	4.5521E-05	1.5196E 00	5.5135E 02	1.2440E 01	8.4877E 00	6.4272E 00	4.6690E 00	9.5682E 00	1.4949E 03
D/DT	1.5327E-05	8.8740E-09	0.0	0.0		-8.0862E-04	-1.9684E-04	-8.0490E-04	-4.5676E-04	-1.9694E-01
D/DP	-2.4393E-04	-1.5253E-07	-1.9602E-03	1.3314E-01	-3.6388E-03	1.1274E-02	4.4513E-04	9.2705E-03	5.9714E-03	3.7255E 00

	C11	C12	C44	MU(V)	MU(R)	MU(VRH)	SIGMA(VRH)	VP(VRH)	VS(VRH)	KT
VALUE	2.5060E 03	9.8938E 02	1.4370E 03	1.1655E 03	1.0582E 03	1.1119E 03	2.0200E-01	9.2516E 00	5.6536E 00	1.3803E 03
D/DT	-5.9157E-01	3.8189E-04	-1.2254E-01	-1.9191E-01	-2.7040E-01	-2.3116E-01	2.2887E-05	-5.7424E-04	-4.5901E-04	-2.9063E-01
D/DP	8.4732E 00	1.3517E 00	1.2401E 00	2.1684E 00	3.1769E 00	2.6726E 00	2.6552E-05	7.9732E-03	4.7470E-03	3.931CE 00

FIGURE CAPTIONS

Figure 1. C_{11} for MgO as a function of temperature.

Figure 2. C_{12} for MgO as a function of temperature.

Figure 3. C_{44} for MgO as a function of temperature.

Figure 4. Adiabatic bulk modulus of MgO as a function of temperature.

Figure 5. Pressure derivatives of compressional and shear frequencies for polycrystalline MgO.

Figure 6. C_{11} for MgO as a function of temperature and pressure.

Figure 7. C_{12} for MgO as a function of temperature and pressure.

Figure 8. C_{44} for MgO as a function of temperature and pressure.

Figure 9. Voigt-Reuss-Hill average for compressional velocity of MgO as a function of temperature and pressure.

Figure 10. Voigt-Reuss-Hill average for shear velocity of MgO as a function of temperature and pressure.

Figure 11. Adiabatic bulk modulus of MgO as a function of temperature and pressure.

Figure 12. Isothermal bulk modulus of MgO as a function of temperature and pressure.

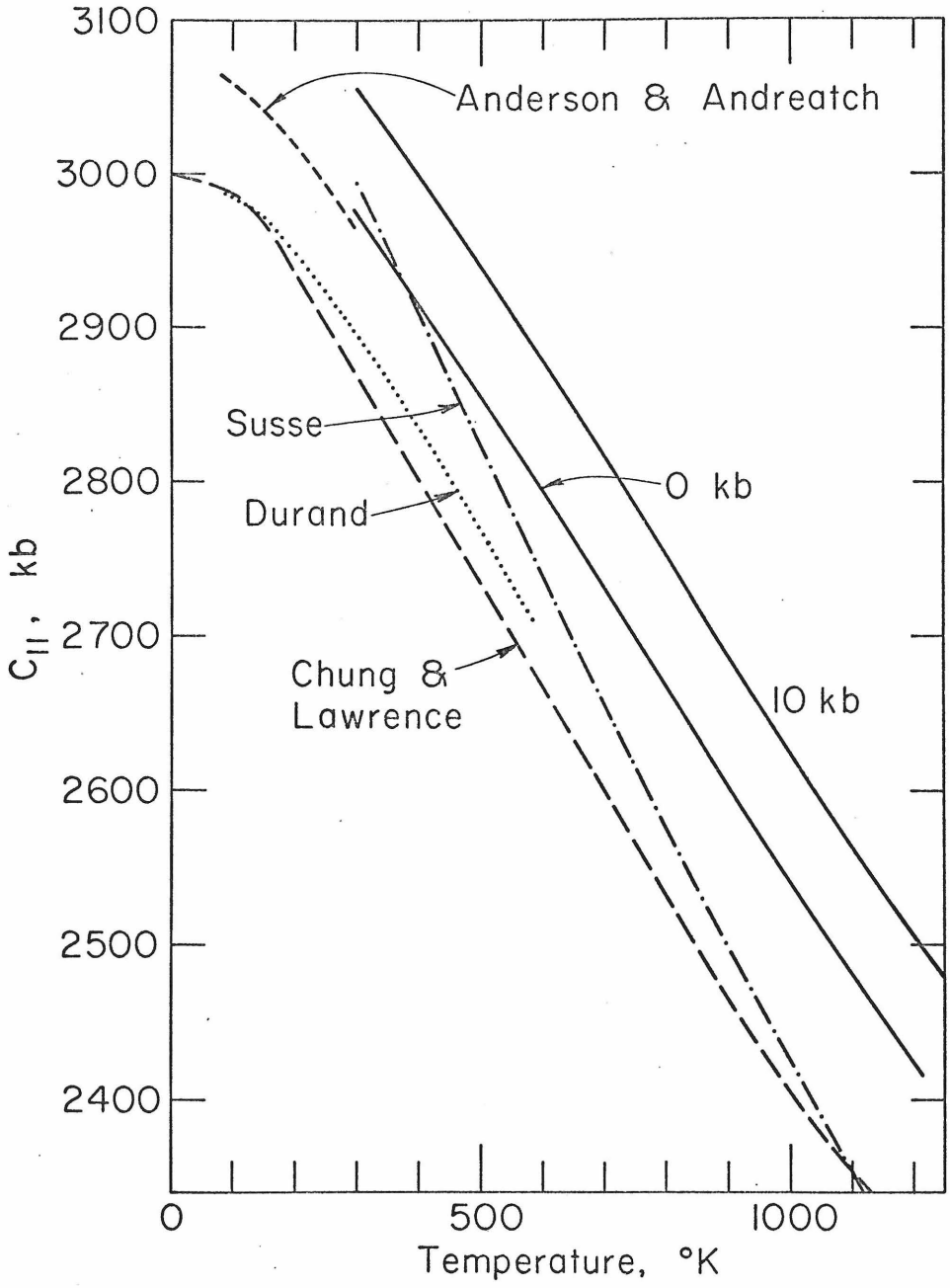
3100
3000
2900
2800
2700
2600
2500
2400
C_{11}, kb
0
500
1000
Temperature, °K
Anderson & Andreatch
Susse
Durand
Chung & Lawrence
0 kb
10 kb

Figure 1

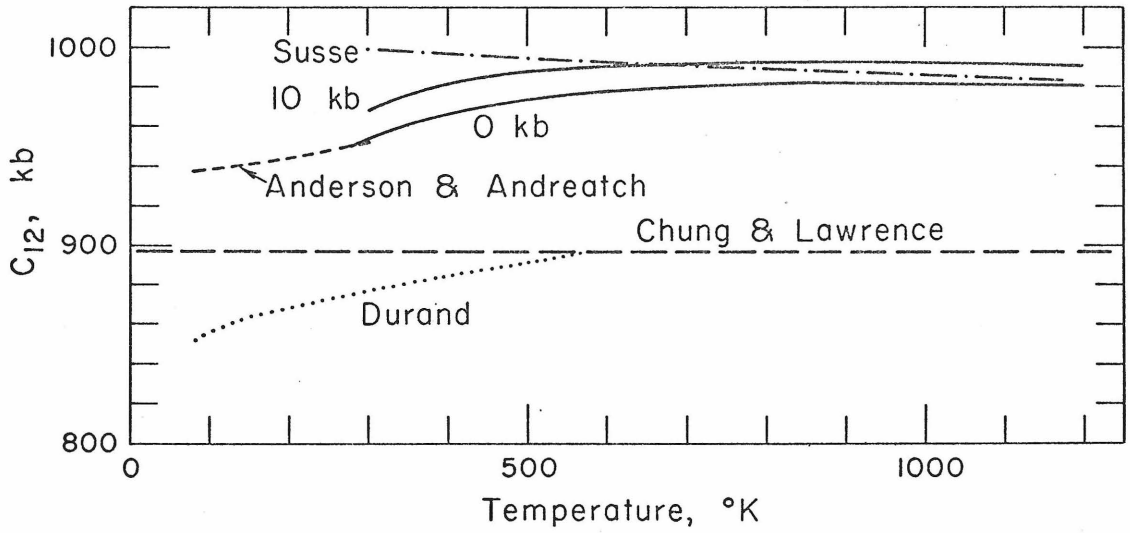
1000
900
800
C_{12}, kb
Susse
10 kb
0 kb
Anderson & Andreatch
Chung & Lawrence
Durand
0
500
1000
Temperature, °K

Figure 2

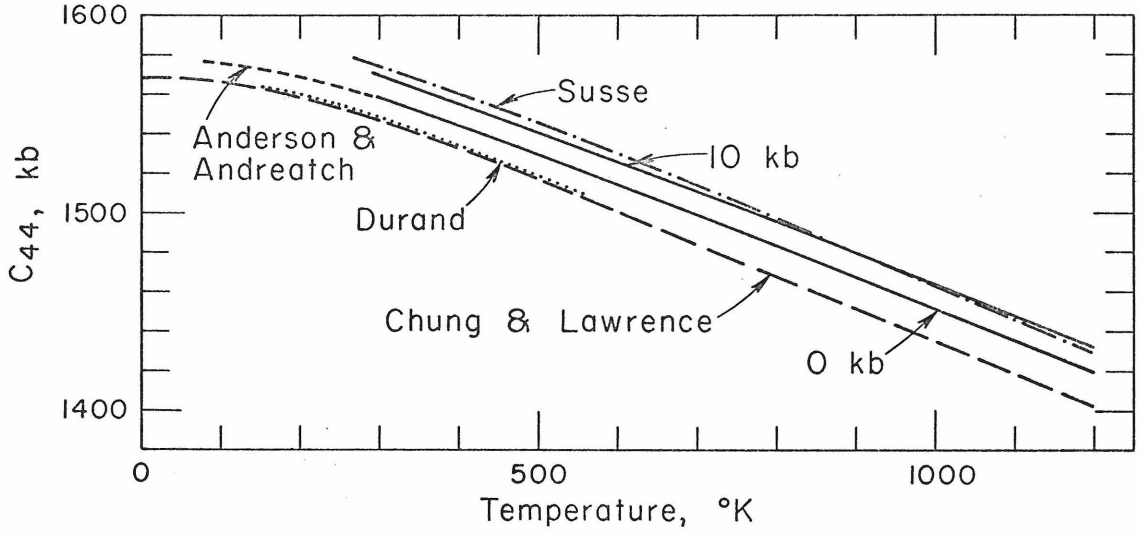
1600
1500
1400
C44, kb
0
500
1000
Temperature, °K
Susse
10 kb
Anderson &
Andreatch
Durand
Chung & Lawrence
0 kb

Figure 3

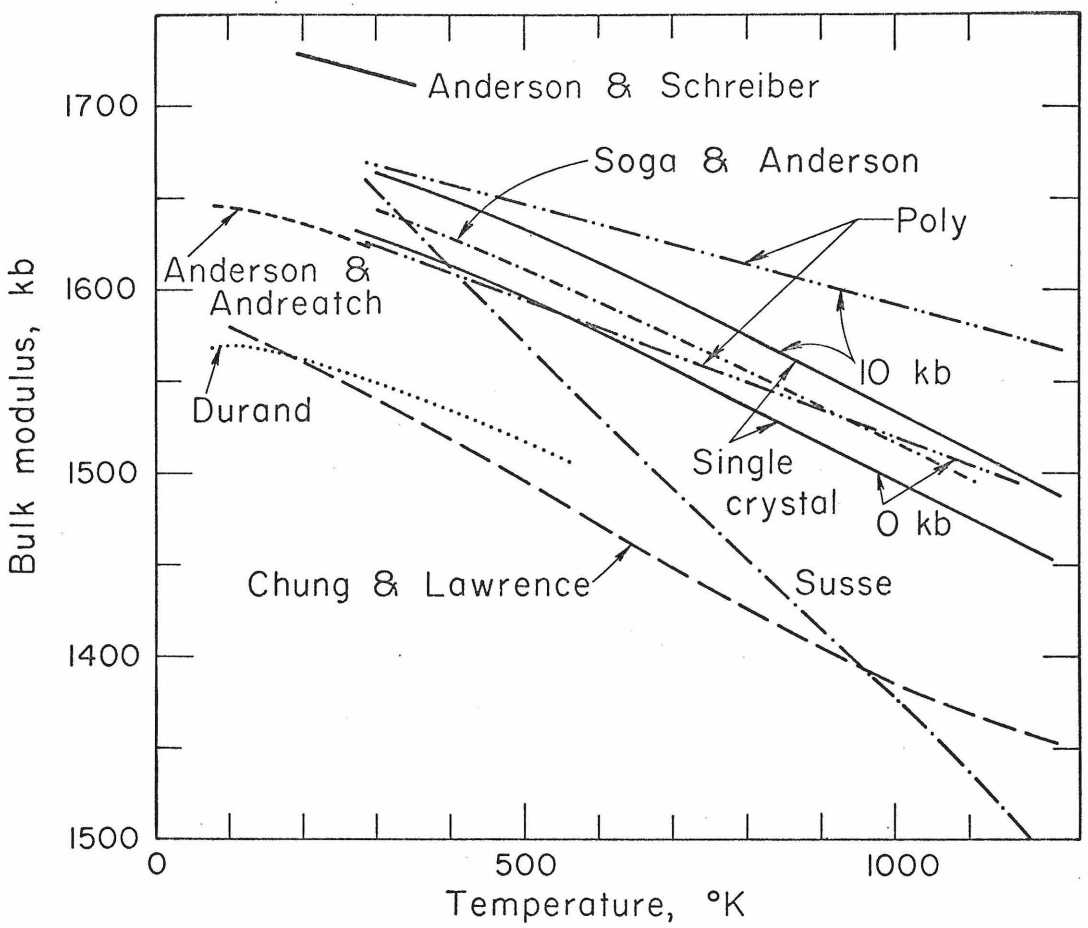
Anderson & Schreiber
Soga & Anderson
Poly
Anderson & Andreatch
10 kb
Durand
Single crystal
0 kb
Chung & Lawrence
Susse
1700
1600
1500
1400
1500
0
500
1000
Bulk modulus, kb
Temperature, °K

Figure 4

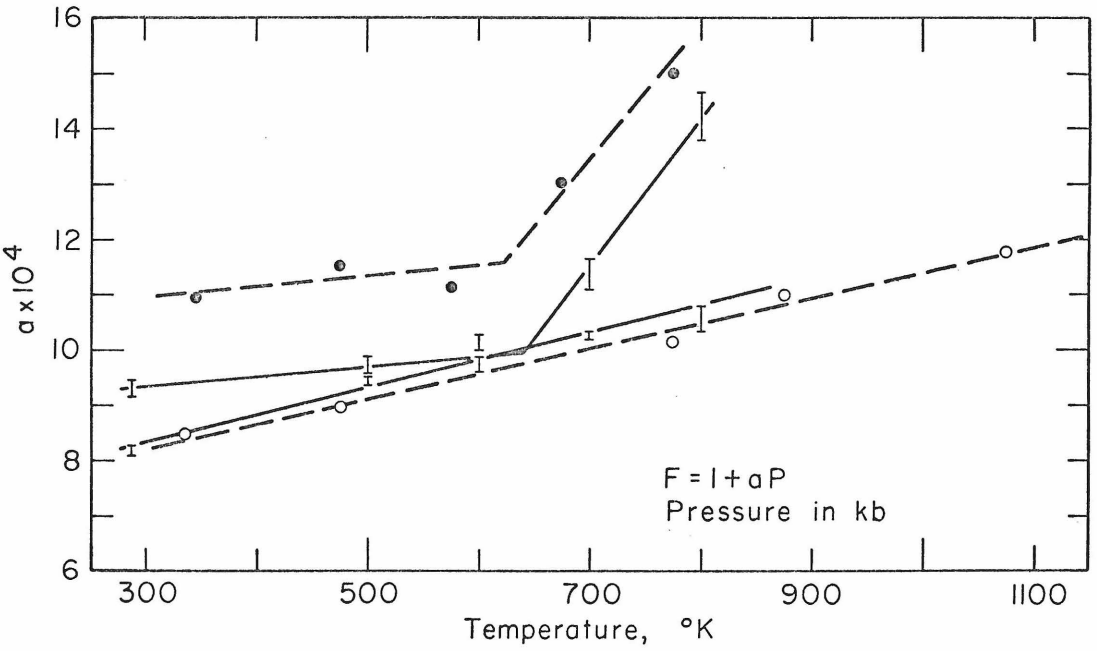
16
14
12
10
8
6
a x 10^4
300
500
700
900
1100
Temperature, °K
F = 1 + aP
Pressure in kb

Figure 5

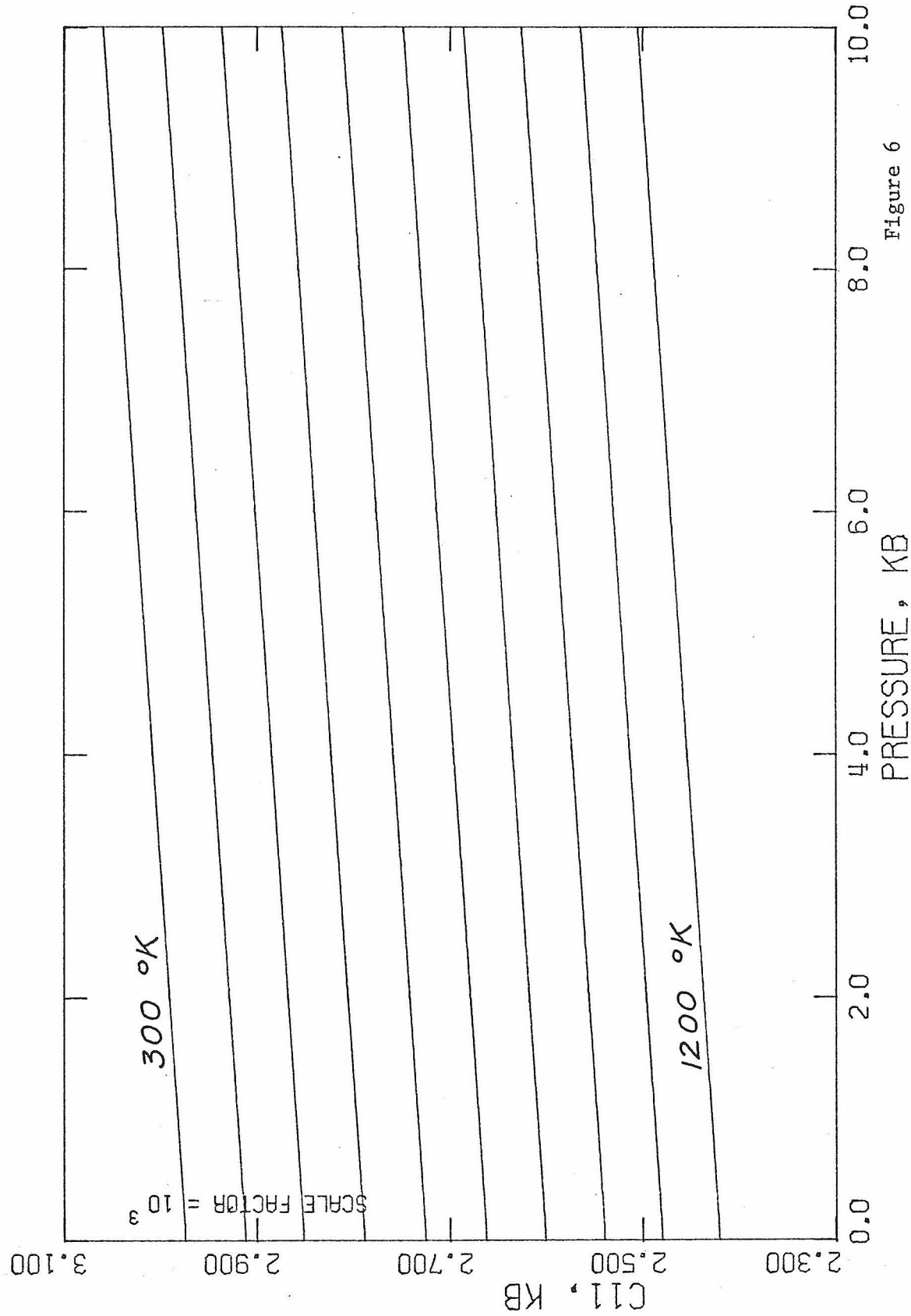
C11, KB
2.300
2.500
2.700
2.900
3.100
PRESSURE, KB
0.0
2.0
4.0
6.0
8.0
10.0
300 °K
1200 °K
SCALE FACTOR = 10 3

Figure 6

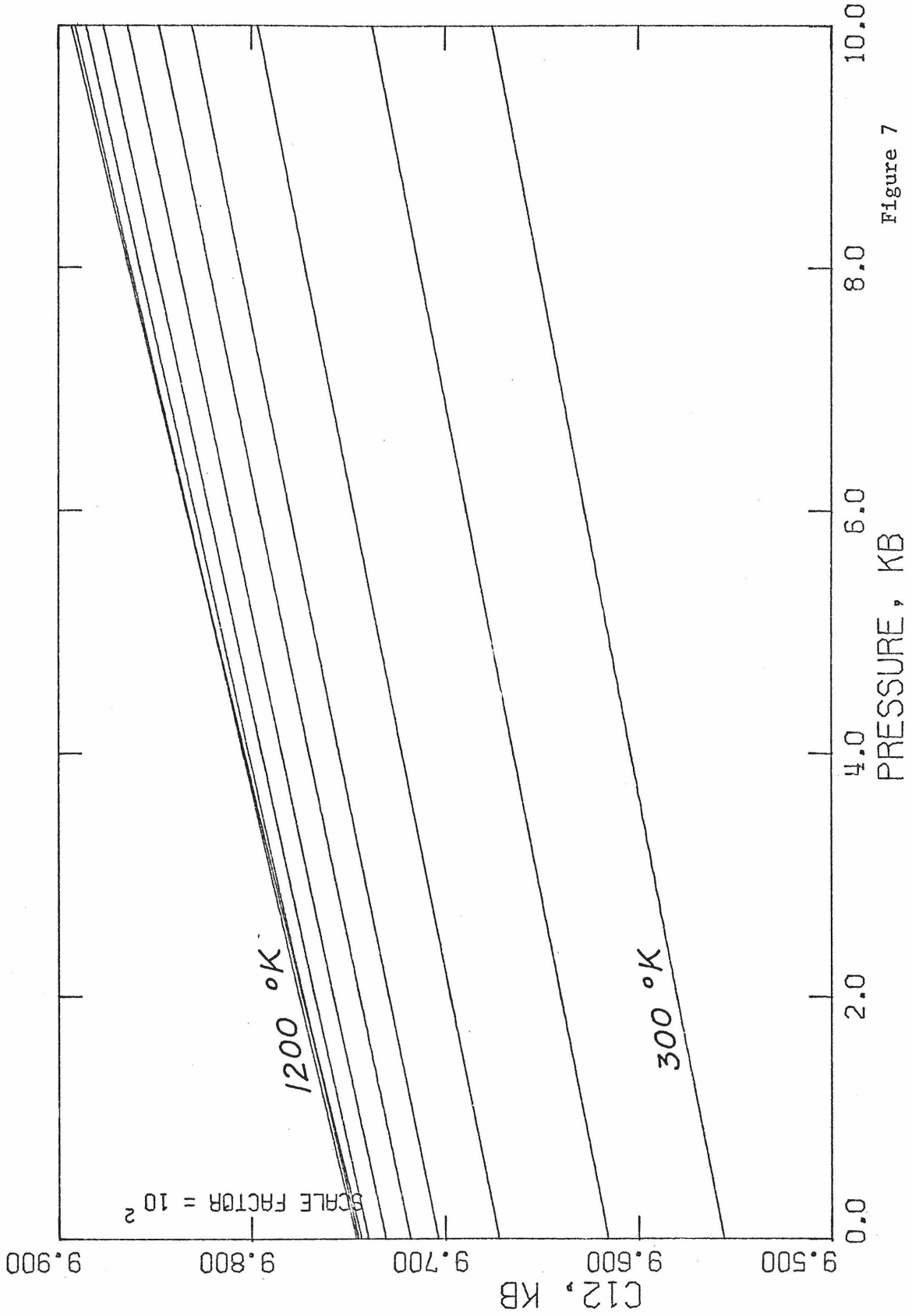
C12, KB
9.500
9.600
9.700
9.800
9.900
PRESSURE, KB
0.0
2.0
4.0
6.0
8.0
10.0
1200 °K
300 °K
SCALE FACTOR = 10 2

Figure 7

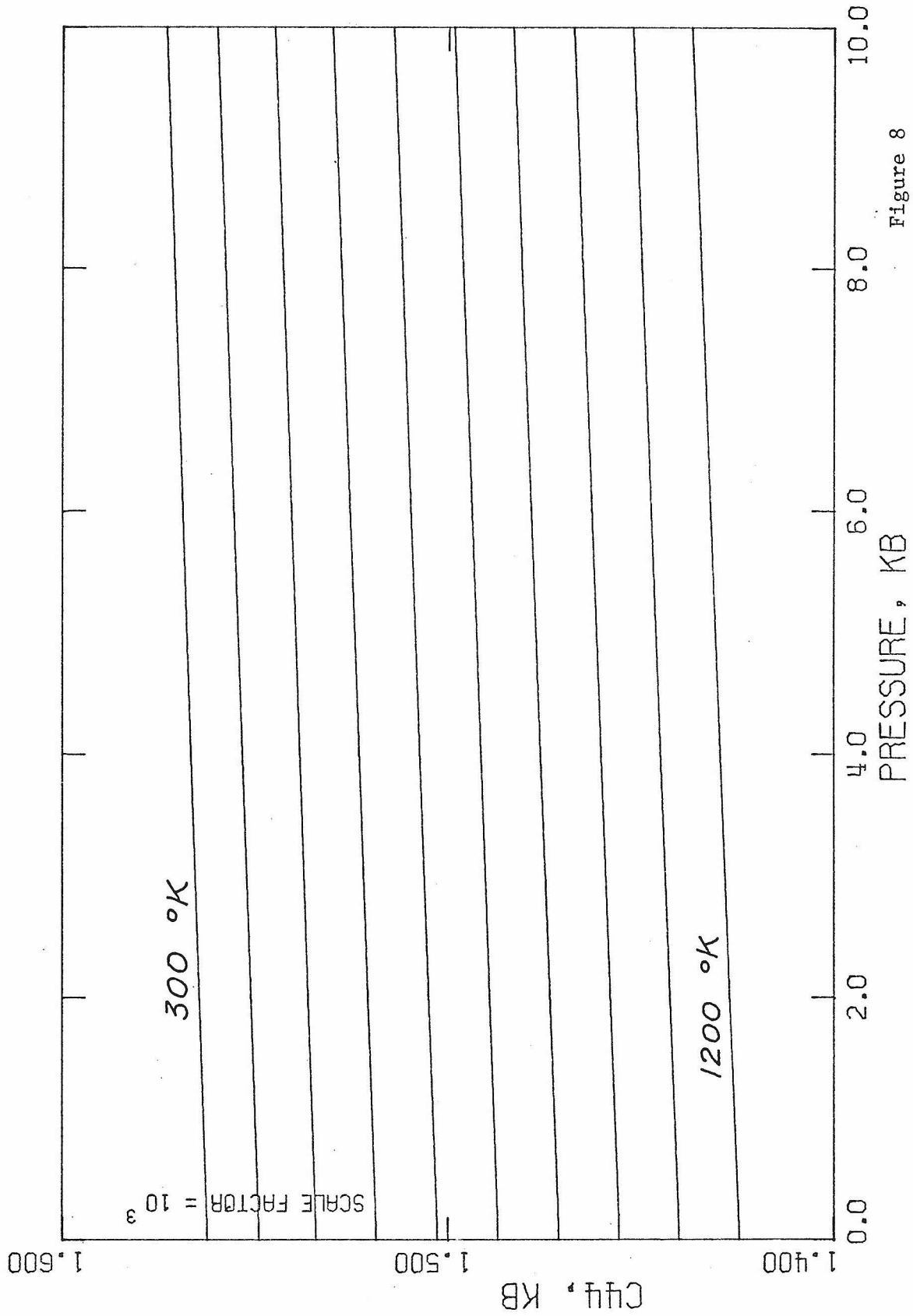
1.600
1.500
1.400
CH4, KB
SCALE FACTOR = 10 3
300 °K
1200 °K
0.0
2.0
4.0
6.0
8.0
10.0
PRESSURE, KB

Figure 8

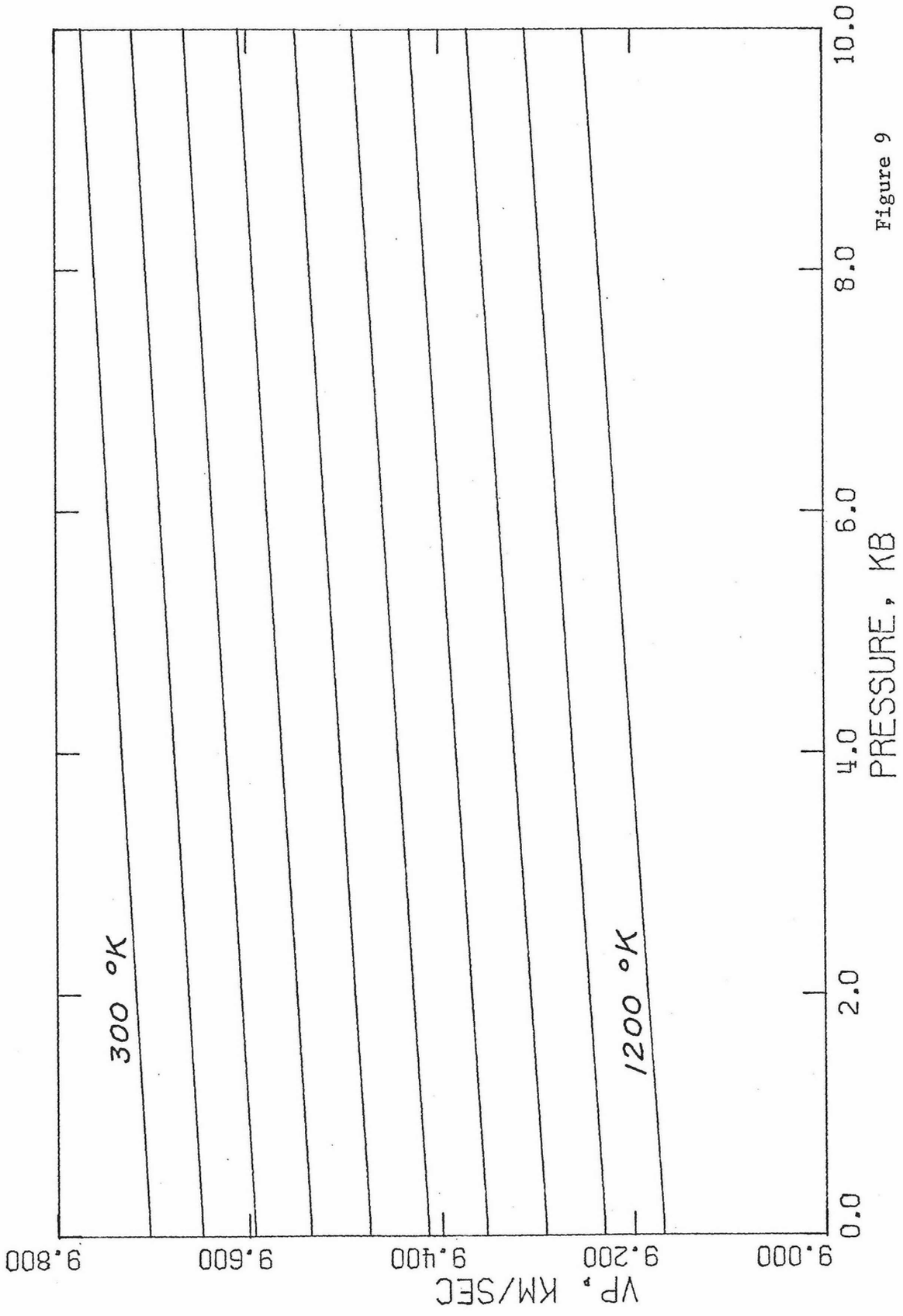
9.000
9.200
9.400
9.600
9.800
VP, KM/SEC
0.0
2.0
4.0
6.0
8.0
10.0
PRESSURE, KB
300 °K
1200 °K

Figure 9

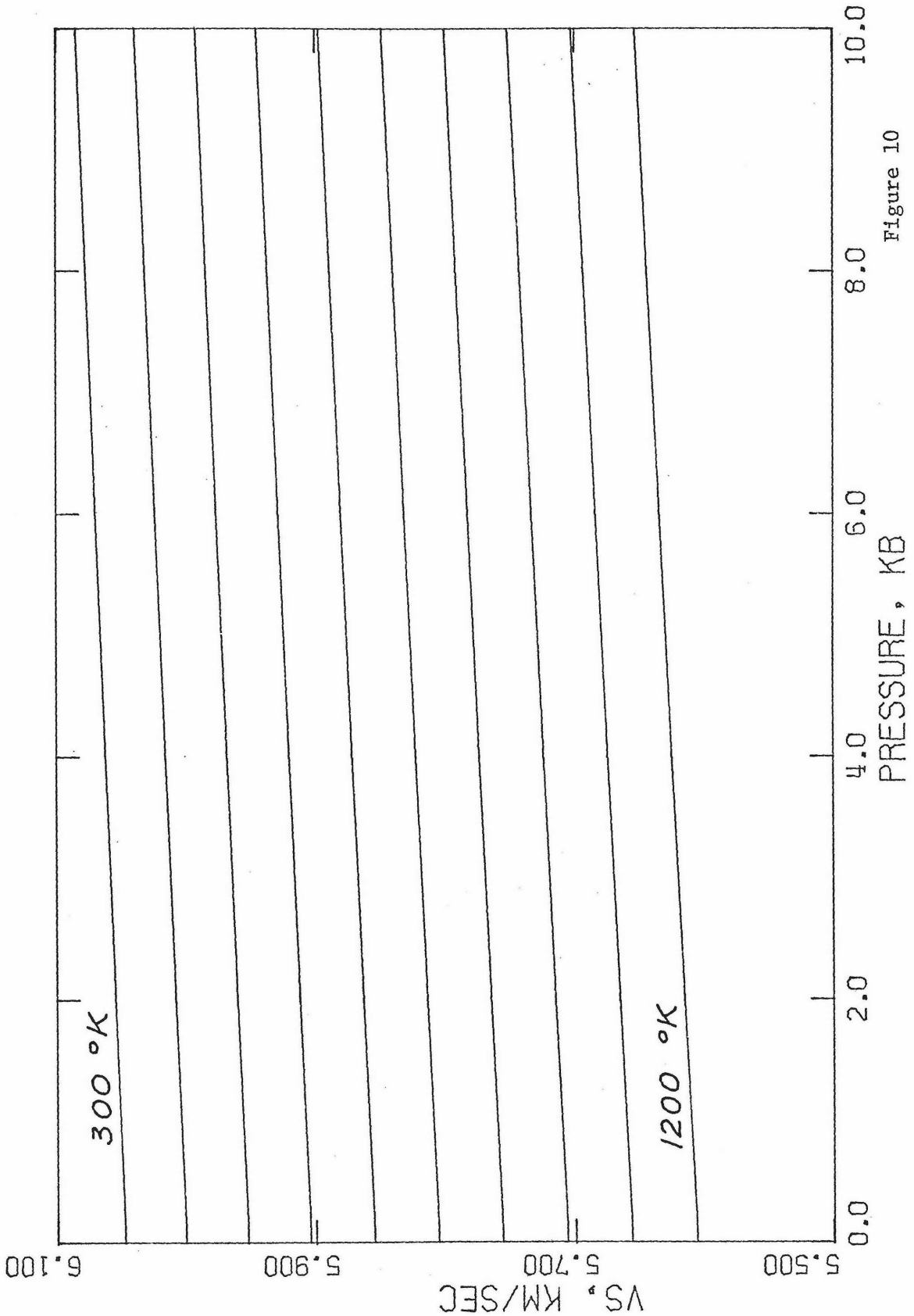
VS, KM/SEC
6.100
5.900
5.700
5.500
PRESSURE, KB
0.0
2.0
4.0
6.0
8.0
10.0
300 °K
1200 °K

Figure 10

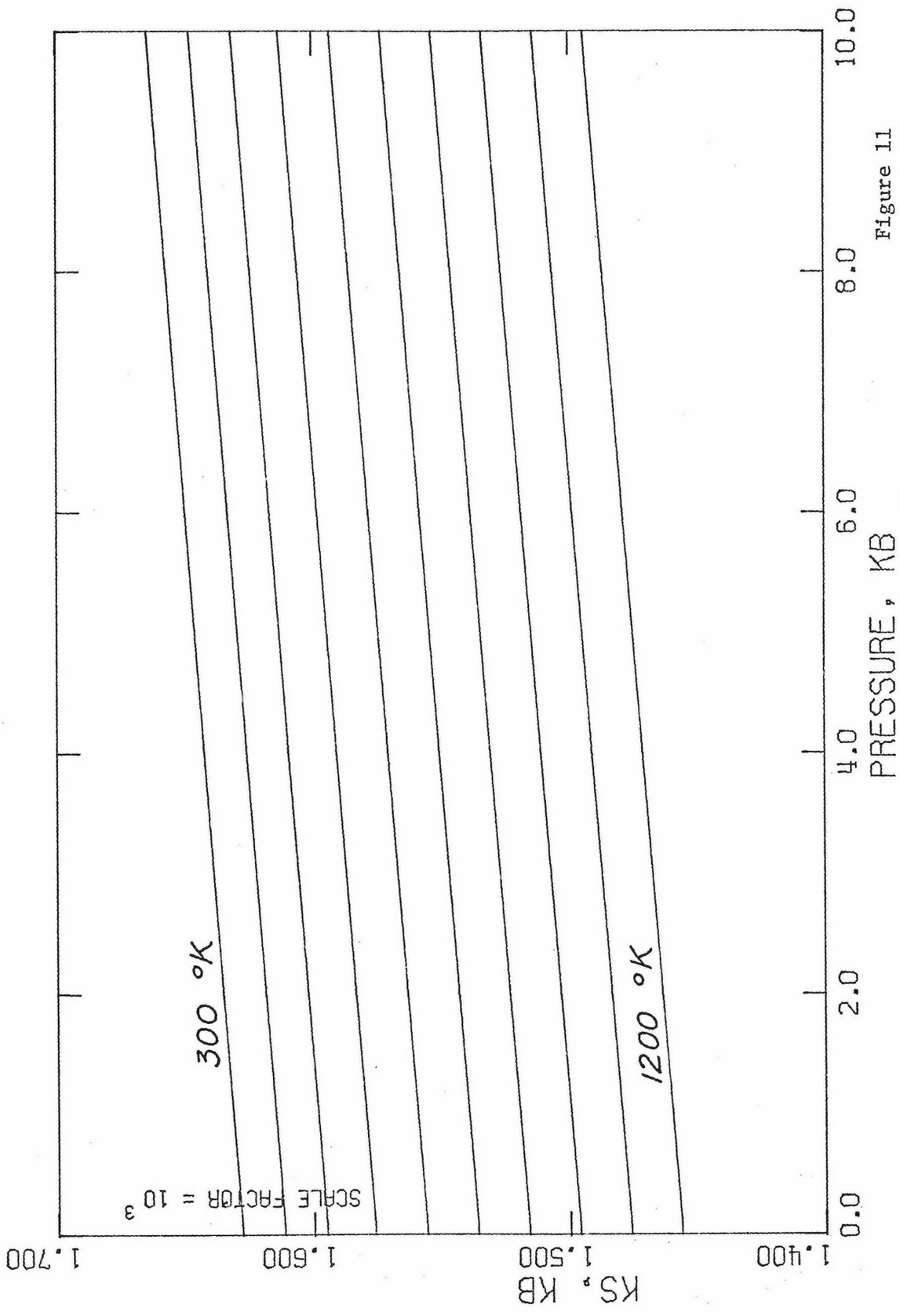
KS, KB
1.400
1.500
1.600
1.700
SCALE FACTOR = 10 3
300 °K
1200 °K
0.0
2.0
4.0
6.0
8.0
10.0
PRESSURE, KB

Figure 11

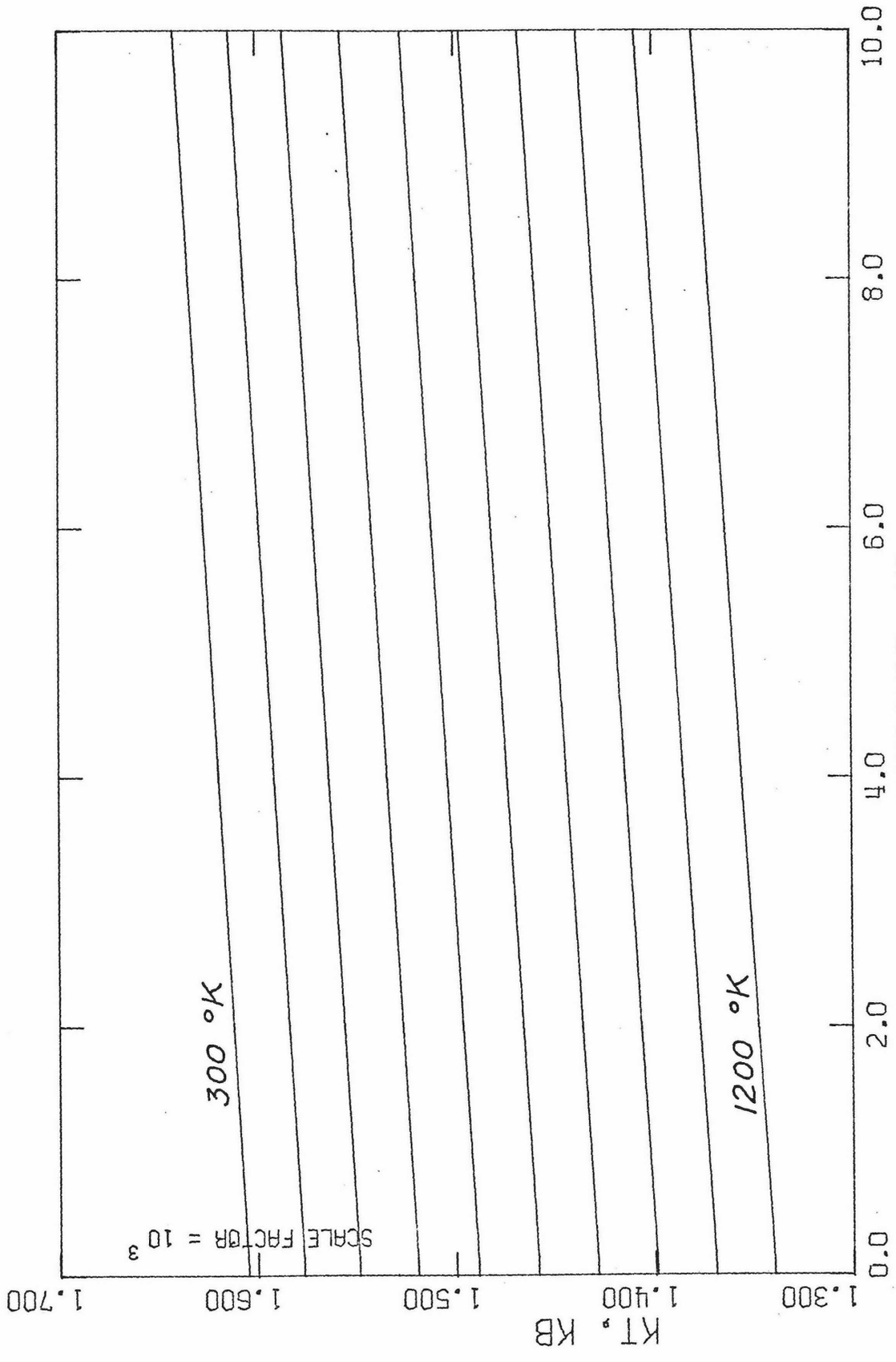
KT, KB
1.300
1.400
1.500
1.600
1.700
SCALE FACTOR = 10^3
300 °K
1200 °K
0.0
2.0
4.0
6.0
8.0
10.0
PRESSURE, KB

Figure 12

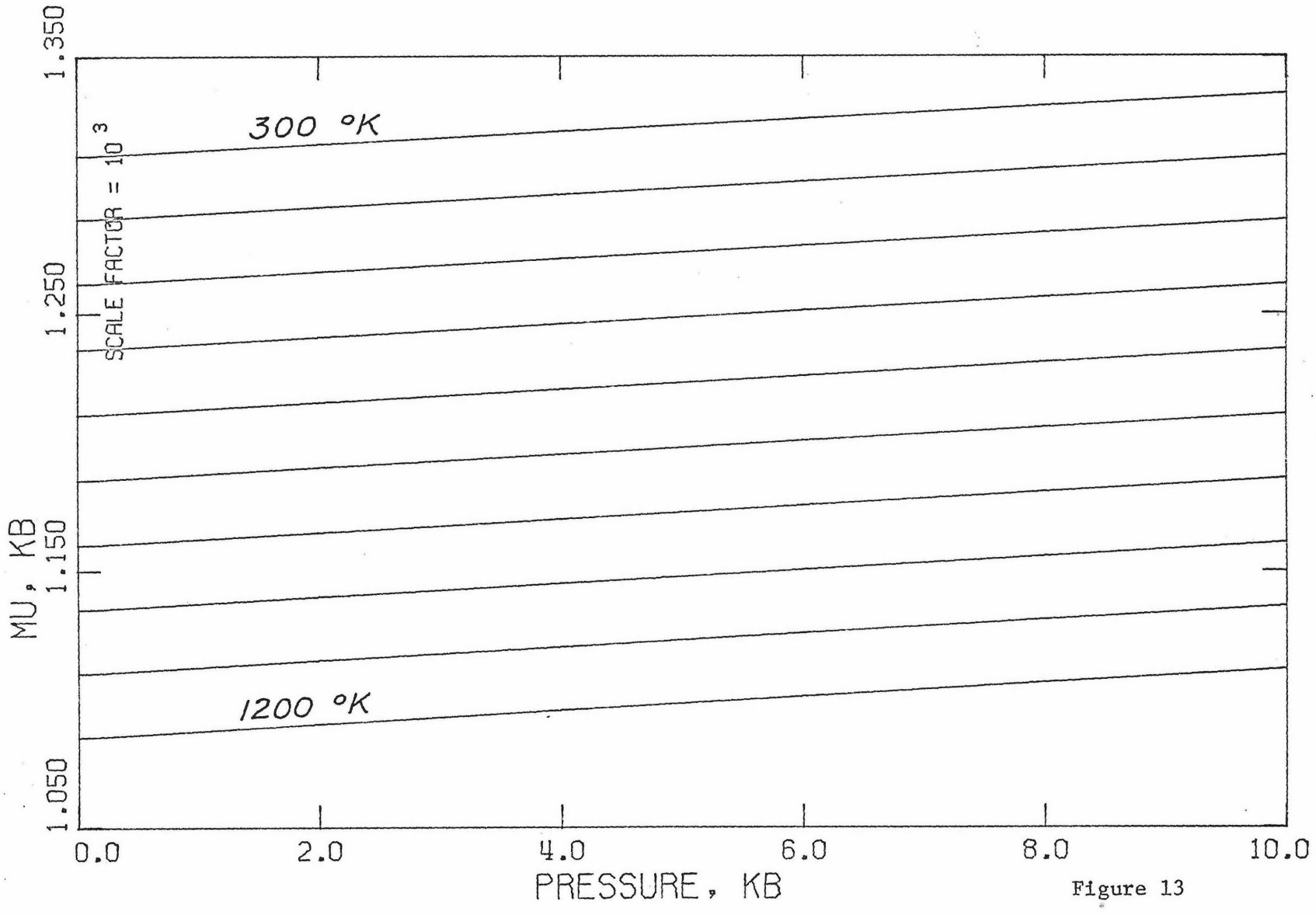
1.350
1.250
1.150
1.050
MU, KB
SCALE FACTOR = 10^3
300 °K
1200 °K
0.0
2.0
4.0
6.0
8.0
10.0
PRESSURE, KB

Figure 13

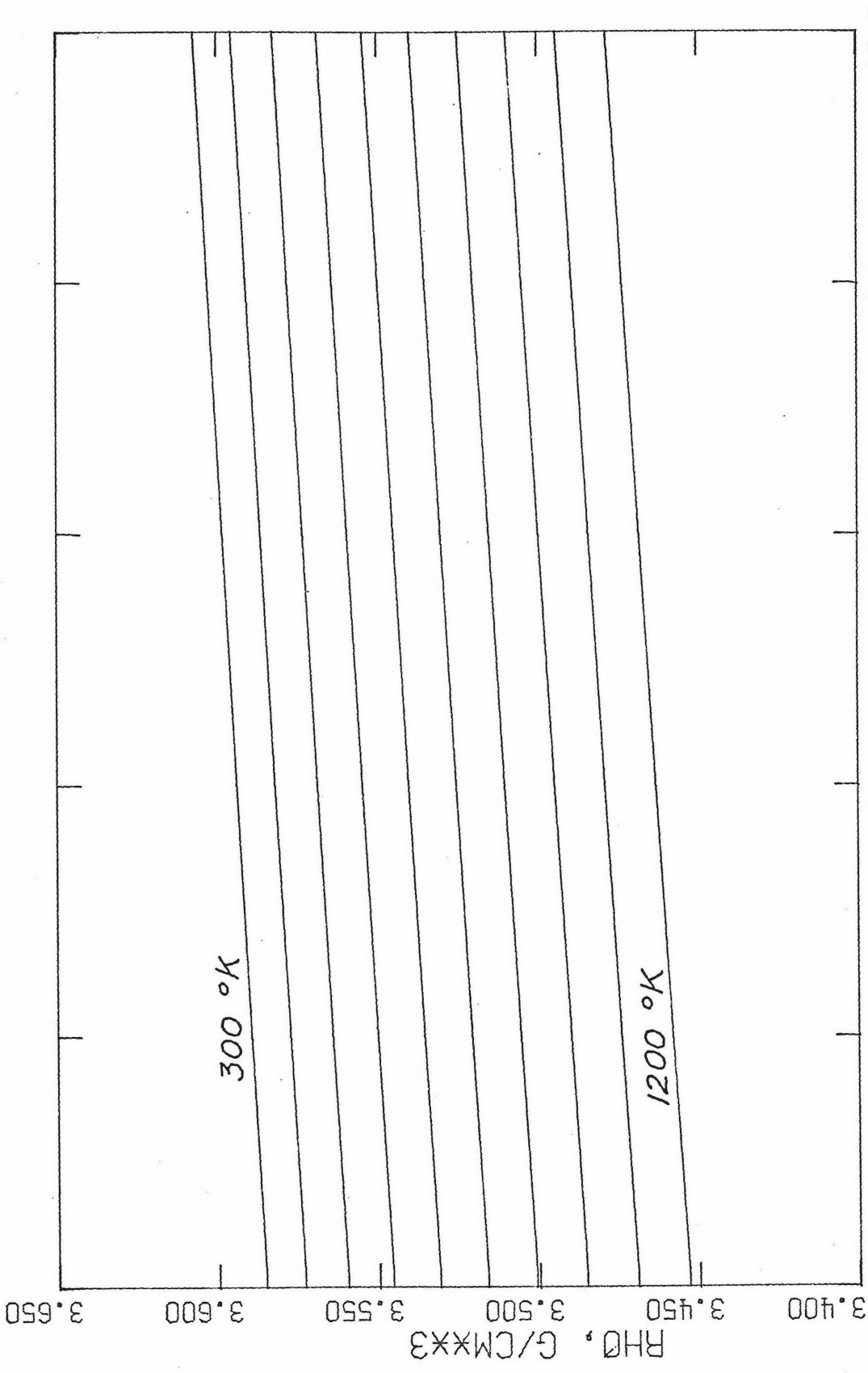
RHO, G/CM**3
3.400
3.450
3.500
3.550
3.600
3.650
PRESSURE, KB
0.0
2.0
4.0
6.0
8.0
10.0
300 °K
1200 °K

Figure 14

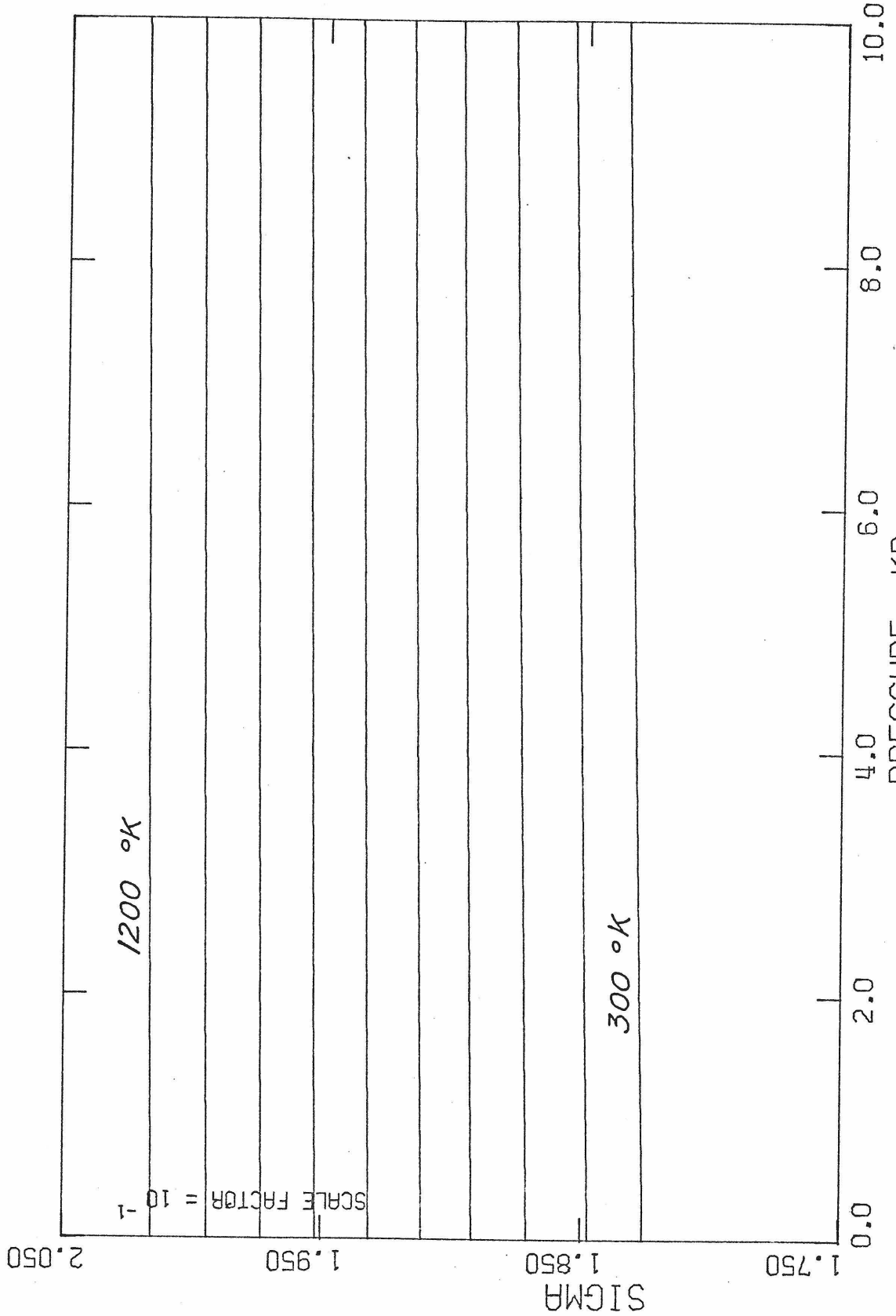
SIGMA
1.750
1.850
1.950
2.050
PRESSURE, KB
0.0
2.0
4.0
6.0
8.0
10.0
300 °K
1200 °K
SCALE FACTOR = 10 -1

Figure 15

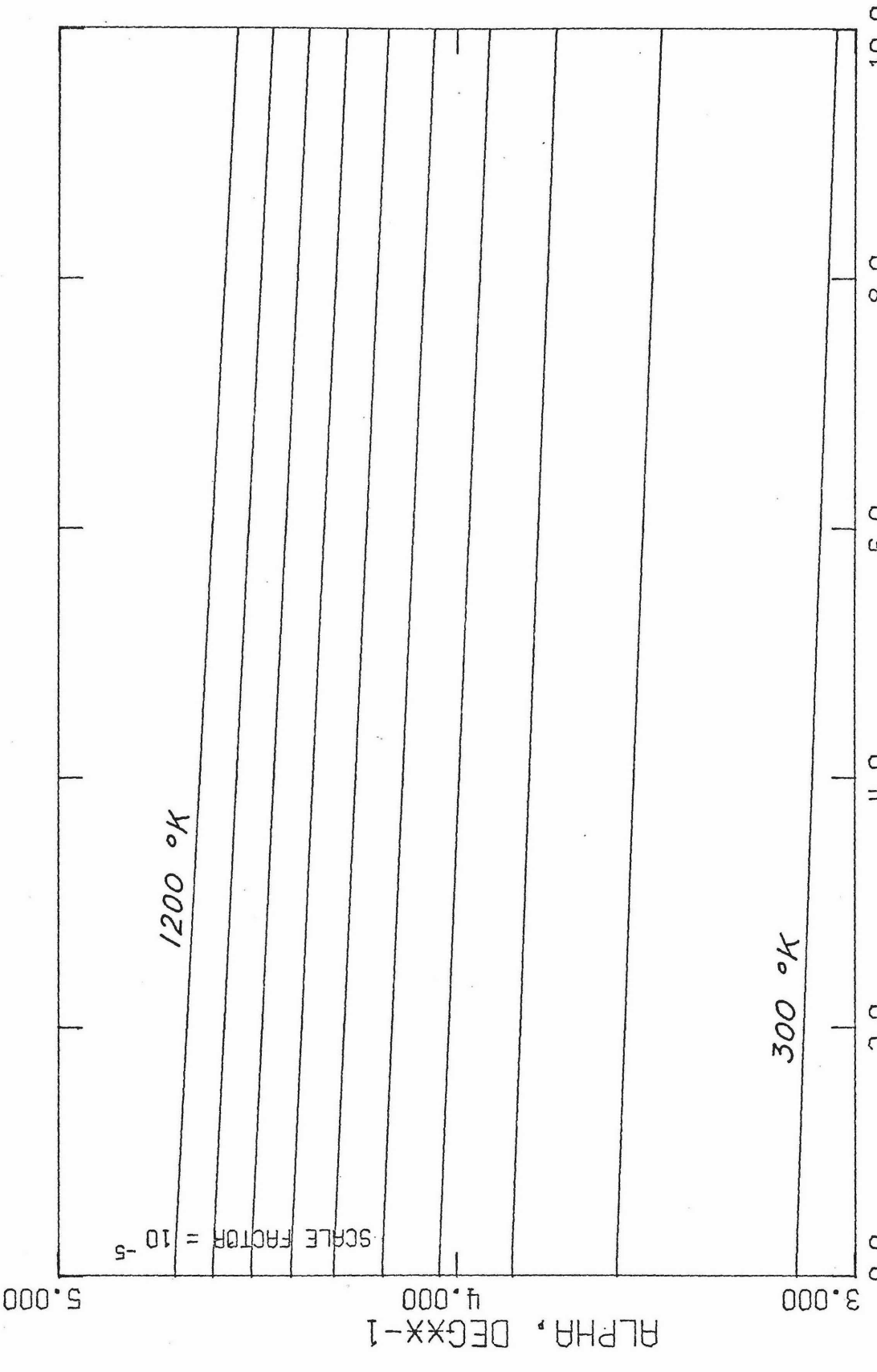
ALPHA, DEGXX-1
5.000
4.000
3.000
SCALE FACTOR = 10 -5
1200 °K
300 °K
0.0
2.0
4.0
6.0
8.0
10.0
PRESSURE, KB

Figure 16

Appendix A

COUPLING OF ULTRASONIC ENERGY THROUGH LAPPED SURFACES

Ultrasonic interferometric methods are generally recognized as the most precise, and potentially most accurate, means of determining elastic moduli. The great sensitivity available with this method has recommended its use in determining the pressure derivatives of elastic moduli, especially since small samples may be used, a requirement imposed by the small volumes available in high pressure vessels. These qualities make it desirable to use ultrasonic interferometry to measure the change of elastic moduli due to elevated temperature alone or due to both pressure and temperature. The principal difficulty which one encounters is the temperature limit imposed by the material used to bond the transducer to the specimen.

This problem has been avoided, for example, by Krause (1963) who used a very long sample, so that the end to which the transducer was fixed was not exposed to high temperatures. An alternate approach has been to attempt to devise bond materials capable of withstanding high temperatures. Fisher and Renken (1963) have used a water glass based bond, Slagle (1965) has successfully employed an epoxy, and also a sintered gold bond. The disadvantage of these is principally their failures due to the stresses induced at the transducer-bond-specimen interfaces at elevated temperatures.

The most satisfactory bond consists of no bonding material at all, which suggests lapping the surfaces against each other and wringing them together. If the specimens were metals, the transducers would have been lapped directly onto them. The pulse superposition method (McSkimin, 1961a) would have been used to measure the ultrasonic time delay in the specimens. The availability of lithium niobate transducers, operable to above 1000°C, allows subjecting the transducers themselves to the same operating conditions as the specimen. However, the specimens were inorganic oxides, and it was impractical to attempt to wring the transducer on the metalized conductive coating. This problem was resolved by using the method of phase comparison (McSkimin, 1961b) employing a short (about 5cm) vitreous silica buffer rod, with the transducer fixed to one end, and the specimen wrung on to the other. This assembly was placed into a small furnace designed to operate inside a 10 kbar pressure vessel.

Since the transducer end of the buffer rod would be subjected to moderate temperatures (ca. 200-300°C) a suitable bond was Araldite epoxy resin. This material, when heated gently, softens and can be worked to provide a very thin bond. It has excellent acoustic transmission properties and was successfully used at 9 gigacycles by Lewis (1966). Initially, the end of the buffer rod was plated with silver, but the resin attached the silver destroying the conductive coating. This has been avoided by using gold instead.

This wrung on bond has been successfully employed with the buffer to temperatures in excess of 800°K. Failures occurred with the quality of the plating. The surfaces which were lapped together adhered throughout the entire temperature cycle. To test this technique, measurements upon a specimen of polycrystalline magnesium oxide were performed. The results are shown in the figure for both the longitudinal and shear modes. The frequency data are normalized to the room temperature value, and are plotted as frequency ratio versus temperature. The slopes found here agree to within 1% of those reported for MgO by Schreiber and Anderson (1966).

Employing the wrung on bond will allow the application of ultrasonic interferometric measurements upon small specimens as a function of both pressure and temperature. These data are important in determining the parameters for a more complete description of the equation of state of solids.

REFERENCES

Fisher, E. S., and C. J. Renken, Coupling cements for ultrasonic-wave velocity measurements at high temperatures, J. Acoust. Soc. Am., 35, 1055, 1963.

Fisher, E. S., and C. J. Renken, Single-crystal elastic moduli and the hcp → bcc transformation in Ti, Zr, and Hf, Phys. Rev., 135, A482, 1964.

Krause, J. T., Differential path method for measuring ultrasonic velocities in glasses at high temperatures, J. Acoust. Soc. Am., 35, 1-4, 1963.

Lewis, M. F., Elastic constants of magnesium aluminate spinel, J. Acoust. Soc. Am., 40, 728 (L), 1966.

McSkimin, H. J., Notes and references for the measurement of elastic moduli by means of ultrasonic waves, J. Acoust. Soc. Am., 33, 606, 1961a.

McSkimin, H., J., Pulse superposition method for measuring ultrasonic wave velocities in solids, J. Acoust. Soc. Am., 33, 12-16, 1961b.

Schreiber, E., and O. L. Anderson, Temperature dependence of the velocity derivatives of periclase, J. Geophys. Res., 71, 3007-3012, 1966.

Slagle, O. D., The elastic constants of some alkali halides as a function of temperature and composition, Ph.D. Thesis, Pennsylvania State University, December, 1965.

FIGURE CAPTION

Longitudinal and shear frequency data versus temperature for polycrystalline MgO.

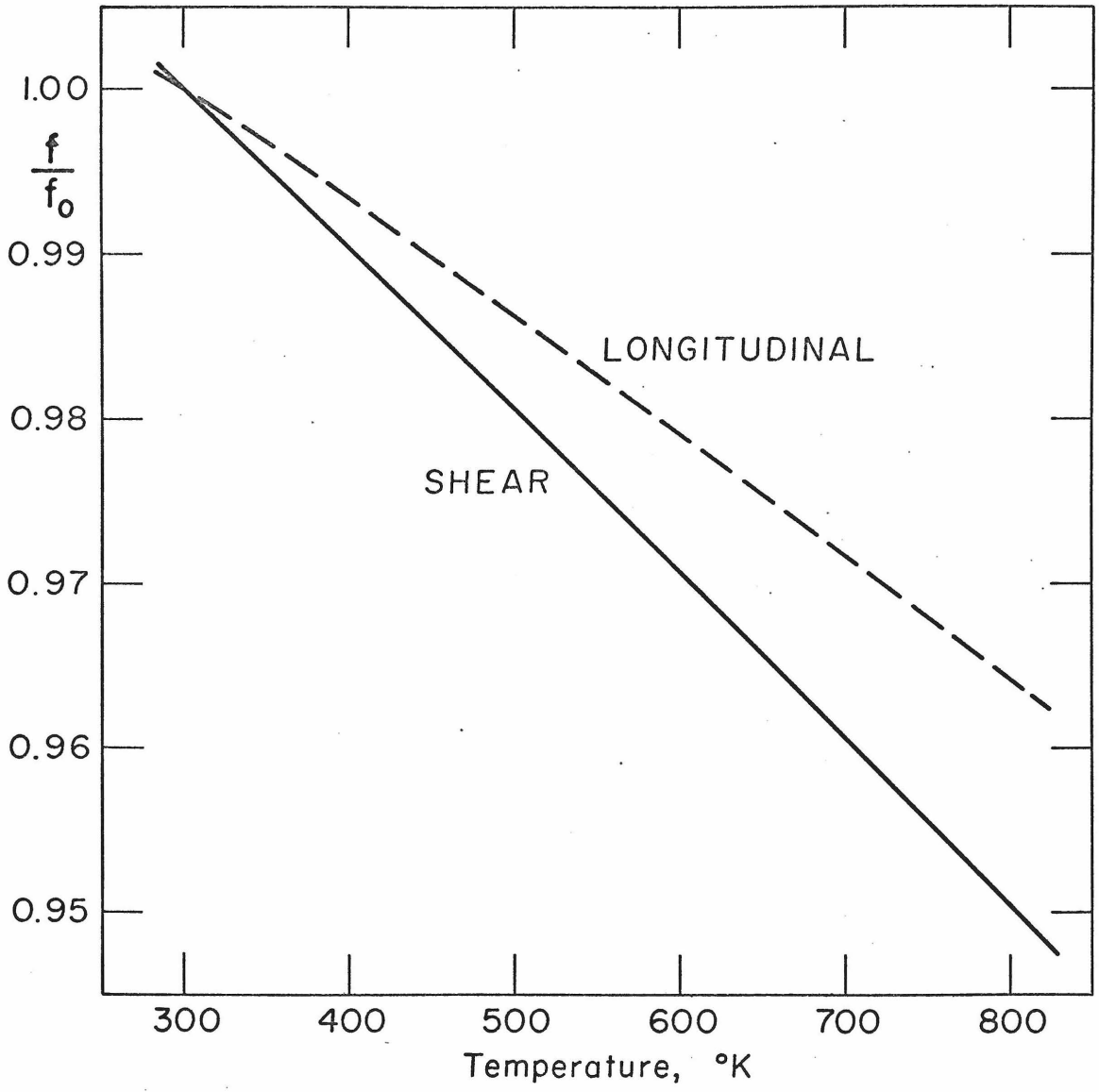
1.00
f/f0
0.99
0.98
0.97
0.96
0.95
LONGITUDINAL
SHEAR
300
400
500
600
700
800
Temperature, °K

Appendix B

COUPLING OF ULTRASONIC ENERGY THROUGH LAPPED SURFACES AT HIGH TEMPERATURE AND PRESSURE

Elastic constants and their variation with temperature and pressure are of great interest in solid earth geophysics. To date most measurements of the elastic constants of geophysically interesting materials have been made as a function of temperature at atmospheric pressure, or in the vicinity of room temperature as a function of pressure. Therefore, there is little information on the variation of the temperature derivatives of the elastic constants as a function of pressure or the temperature dependence of the pressure derivatives. Values for the temperature dependence of the pressure derivatives have been reported for quartz by Soga (1968), for periclase by Schreiber and Anderson (1966a), and for alumina by Schreiber and Anderson (1966b) at low temperatures. However, it is the higher derivatives determined at elevated temperatures which are of primary interest for geophysical interpretation and quation of state theory (Thomsen and Anderson, 1969).

It is the purpose of this Appendix to present the approach taken at this laboratory to measure these cross derivatives. Some data points taken at high temperature and pressure are also given.

In a previous Appendix the success of an ultrasonic interferometric technique employing a buffer-rod to obtain data on the elastic constants to 800°K at atmospheric pressure has been demonstrated. This technique has been successfully applied to velocity measurements under both temperature and pressure.

Figure 1 shows a cross section of the furnace assembly which was used inside the gas high-pressure apparatus. In the furnace the gas volume is kept to a minimum, and convection is eliminated wherever possible. The heating element is noninductive. Two layers of Kanthal A-1 wire are wound on pyrophyllite shells. The wire is in one piece: thus both electrical connections are made on one end. Two thermocuples are in contact with the sample. All parts of the furnace are constructed of pyrophyllite except for the end piece where the transducer is located. This piece is constructed of brass and serves as a heat sink to keep the transducer temperature low. Figures 14 through 21 show pictures of individual furnace parts and give working drawings. The coupling of ultrasonic energy between the buffer-rod and the sample is accomplished by hand lapping the contacting surfaces. The transducer end of the buffer-rod was coated with platinum paste (from Hanovia Liquid Gold Division of Engelhard Industries) and baked at 800°C. This procedure was repeated three times before the surface was polished and the quartz transducer bonded to it with Araldite epoxy resin.

Using the procedure described above, good signals at temperatures of 1073°K and pressure of 8 kb have been obtained. A representative signal is shown in Figure 2, which was taken at 800°K and 7 kb. When the sample is held at high temperatures for several days, some diffusion between the quartz buffer-rod and the MgO sample occurs. The resulting adhesion is so effective that the buffer-rod shows surface cracks once it is returned to room temperature. The onset of this cracking is observed by a rapid deterioration of the ultrasonic echoes as displayed on the oscilloscope. Figure 3 shows the normalized frequency versus temperature for atmospheric pressure and some representative points at 8 kb for a sample of polycrystalline MgO.

REFERENCES

Schreiber, E., and O. L. Anderson, Temperature dependence of the velocity derivatives of periclase, J. Geophys. Res., 71, 3007-3012, 1966a.

Schreiber, E., and O. L. Anderson, Pressure derivatives of the sound velocities of polycrystalline alumina, J. Am. Cer. Soc., 49, 184-190, 1966b.

Soga, N., The temperature and pressure derivatives of isotropic sound velocities of α-Quartz, J. Geophys. Res., 73, 827-829, 1968.

Thomsen, L., and O. L. Anderson, On the high temperature equation of state in solids, J. Geophys. Res. (in press).

FIGURE CAPTIONS

Figure 1. Furnace assembly used in high-pressure vessel.

Figure 2. Echo pattern showing both the RF signal (top trace) and the detected video signal (bottom trace). See text.

Figure 3. Normalized shear and compressional frequency versus temperature at atmospheric pressure, plus two points taken at 8 kb.

Figure 4. Furnace parts with housing and inserts. Outer furnace shell has coarse spacing in the center to compensate for slide losses and achieve a constant temperature at the sample location.

Figure 5. Furnace assembly complete with connectors in place. Single crystal and buffer-rod in foreground.

Figure 6. Completed assembly plugged onto high pressure feed-through.

Figures 7 through 21. Parts drawings for specimen furnace.

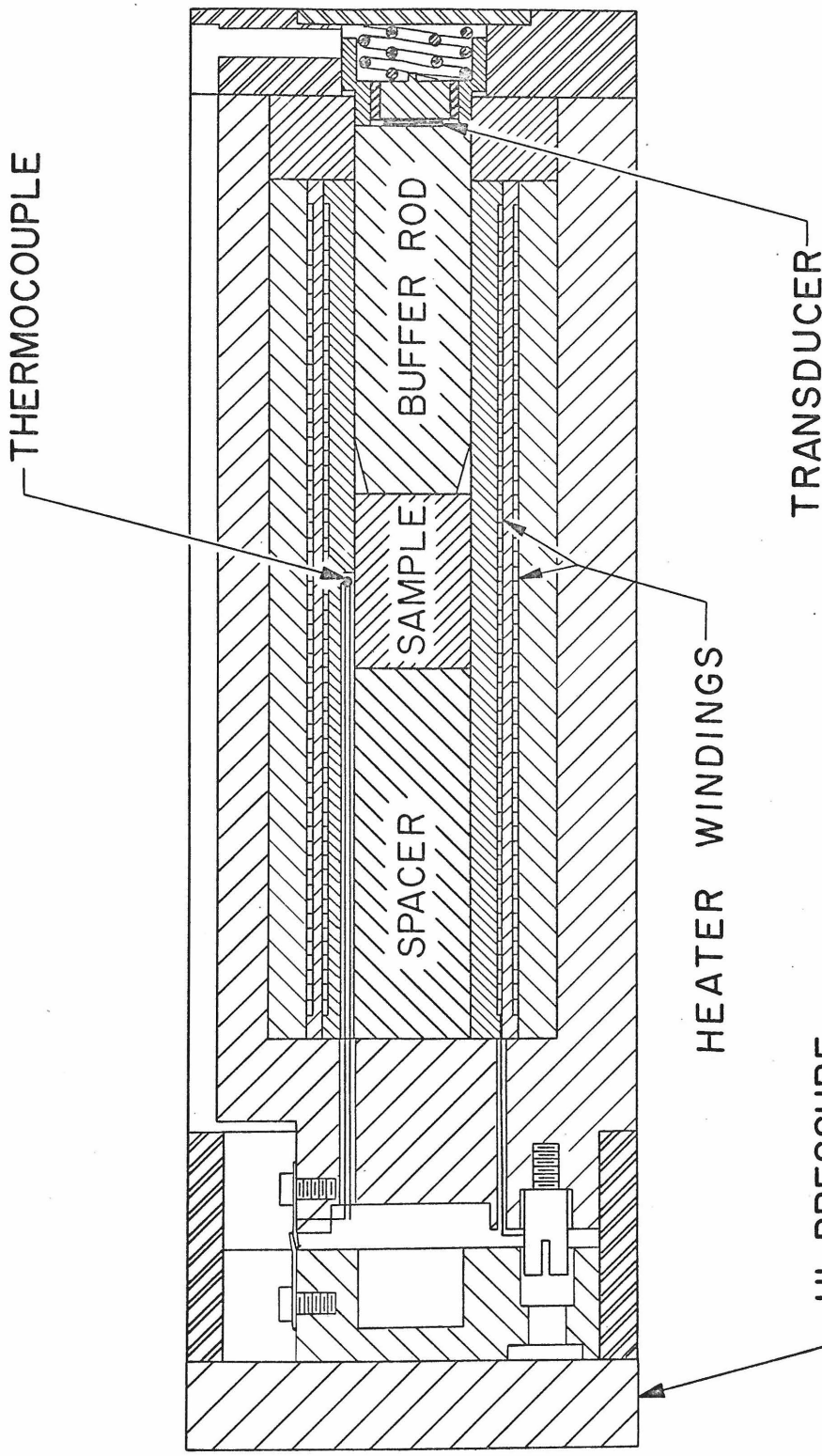
THERMOCOUPLE
BUFFER ROD
SAMPLE
SPACER
TRANSDUCER
HEATER WINDINGS
HI PRESSURE
FEED THRU

Figure 1

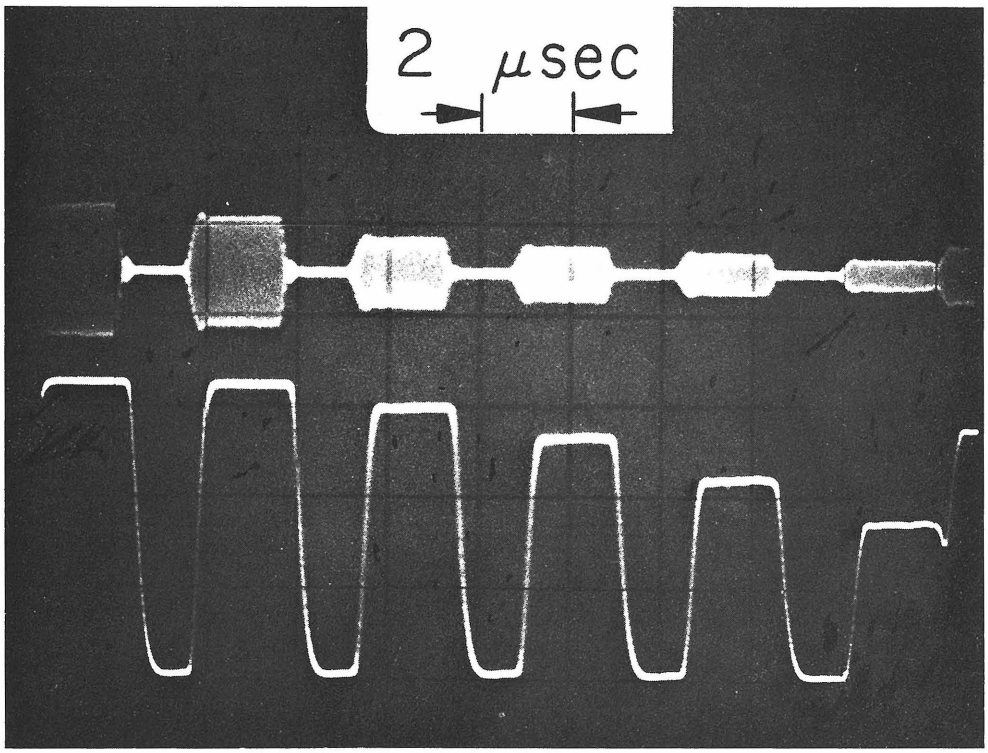

Figure 2

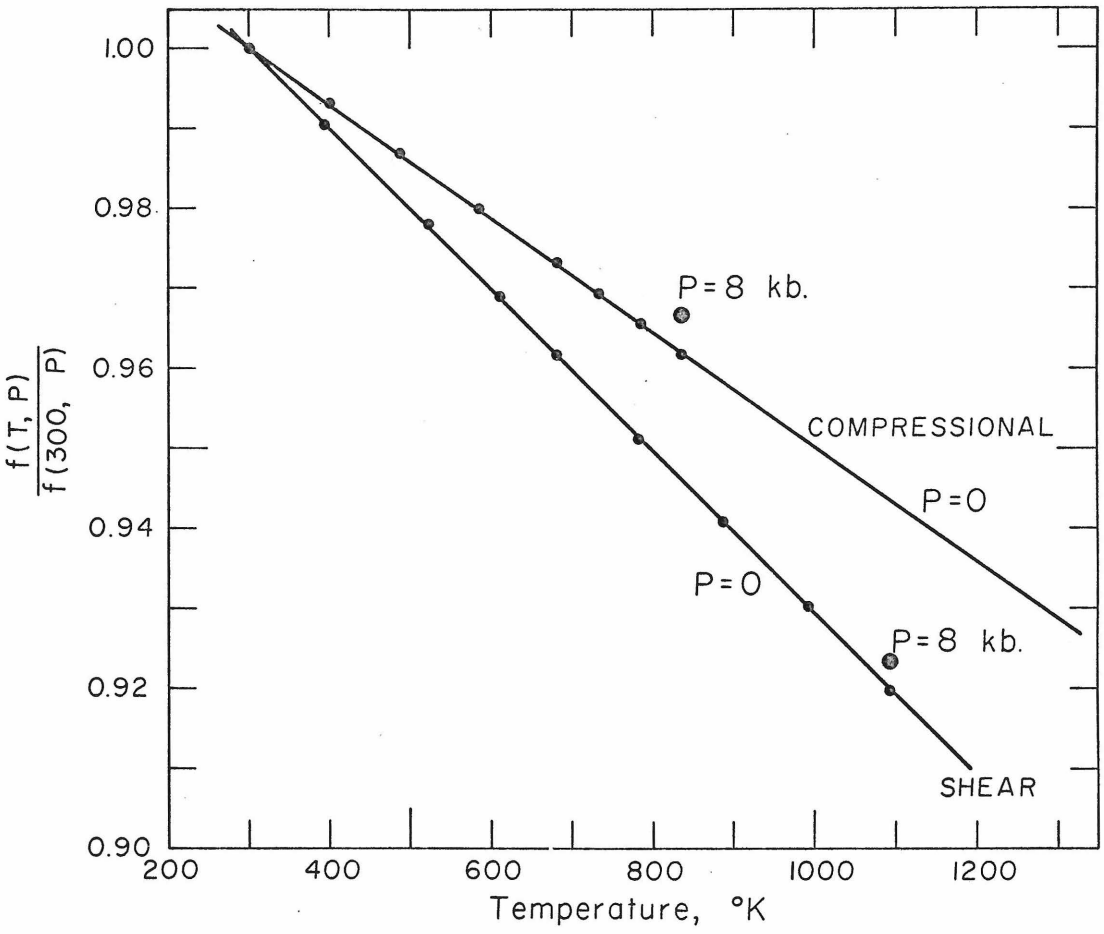
1.00
0.98
0.96
0.94
0.92
0.90
f(T, P) / f(300, P)
200
400
600
800
1000
1200
Temperature, °K
P = 8 kb.
COMPRESSIONAL
P = 0
P = 0
P = 8 kb.
SHEAR

Figure 3

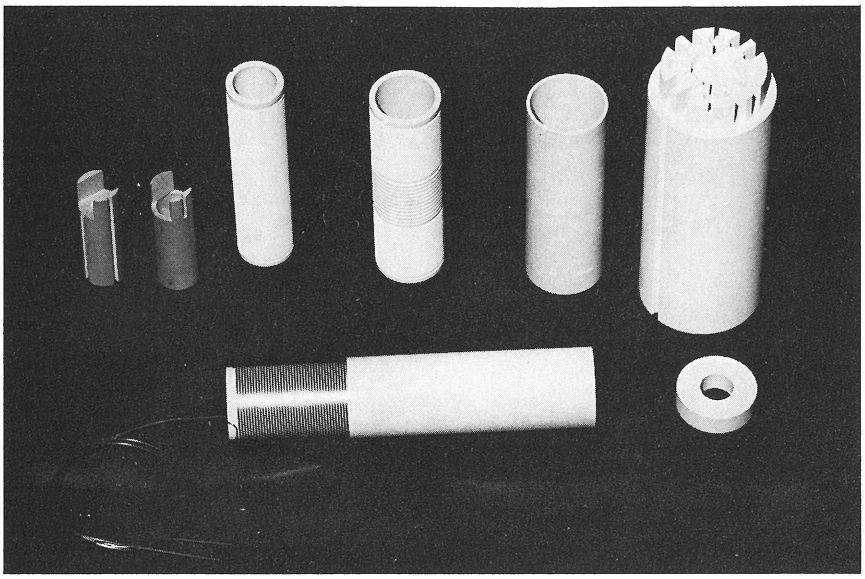

Figure 4

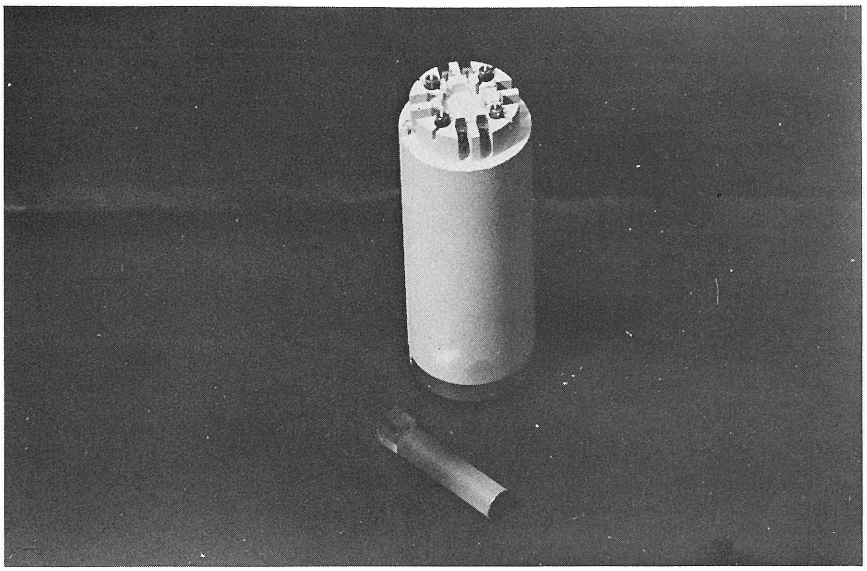

Figure 5

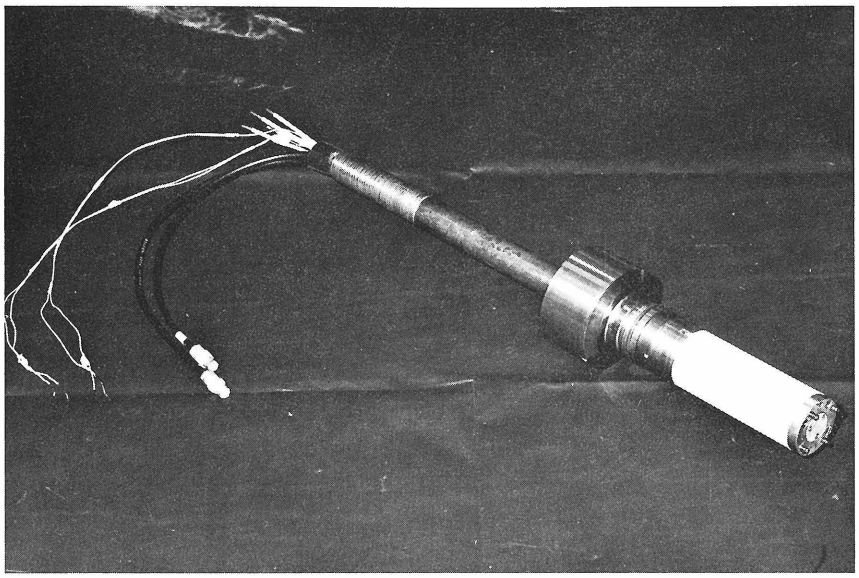

Figure 6

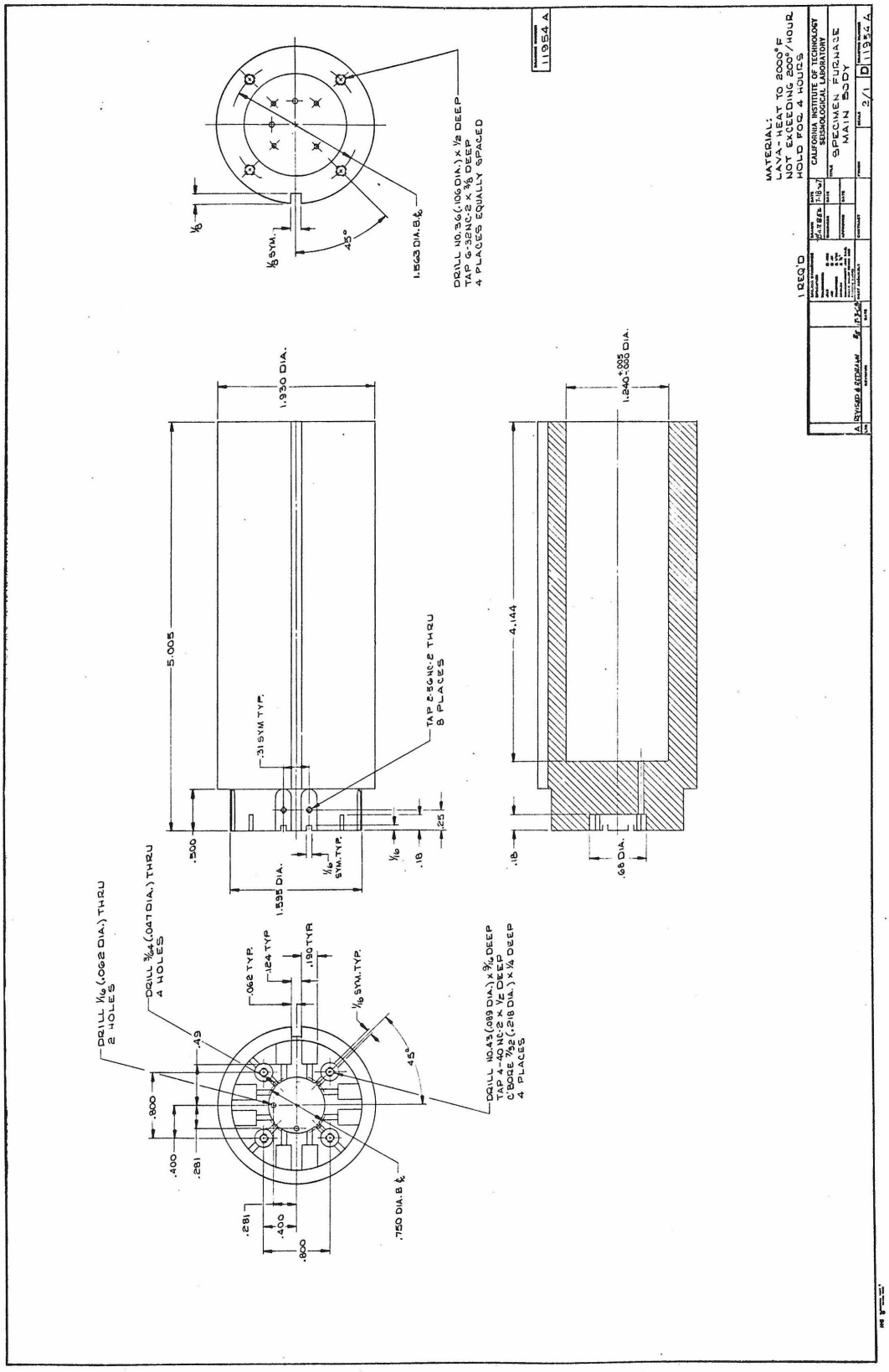
DRILL #0.336(.106 DIA.) x ½ DEEP
TAP G-32 NC-2 x ⅜ DEEP
4 PLACES EQUALLY SPACED
1.563 DIA. B.C.
45°
⅛ SYM.
⅛
11954 A
MATERIAL:
LAVA - HEAT TO 2000°F
NOT EXCEEDING 200°/HOUR
HOLD FOR 4 HOURS
1 REQ'D
CALIFORNIA INSTITUTE OF TECHNOLOGY
SEISMOLOGICAL LABORATORY
SPECIMEN FURNACE
MAIN BODY
2/1
D 11954
1.930 DIA.
5.005
.31 SYM. TYP.
TAP 8-56 NC-2 THRU
8 PLACES
.500
.18
.25
1.595 DIA.
4.144
1.240 +.005 -.000 DIA.
.68 DIA.
DRILL #16 (.062 DIA.) THRU
2 HOLES
DRILL 3/64 (.047 DIA.) THRU
4 HOLES
.49
.800
.400
.281
.068 TYP.
.124 TYP.
.190 TYP.
⅛ SYM. TYP.
45°
.750 DIA. B.C.
DRILL #0.43 (.089 DIA.) x 3/16 DEEP
TAP 4-40 NC-2 x ½ DEEP
C'BORE 7/32 (.218 DIA.) x ¼ DEEP
4 PLACES

Figure 7

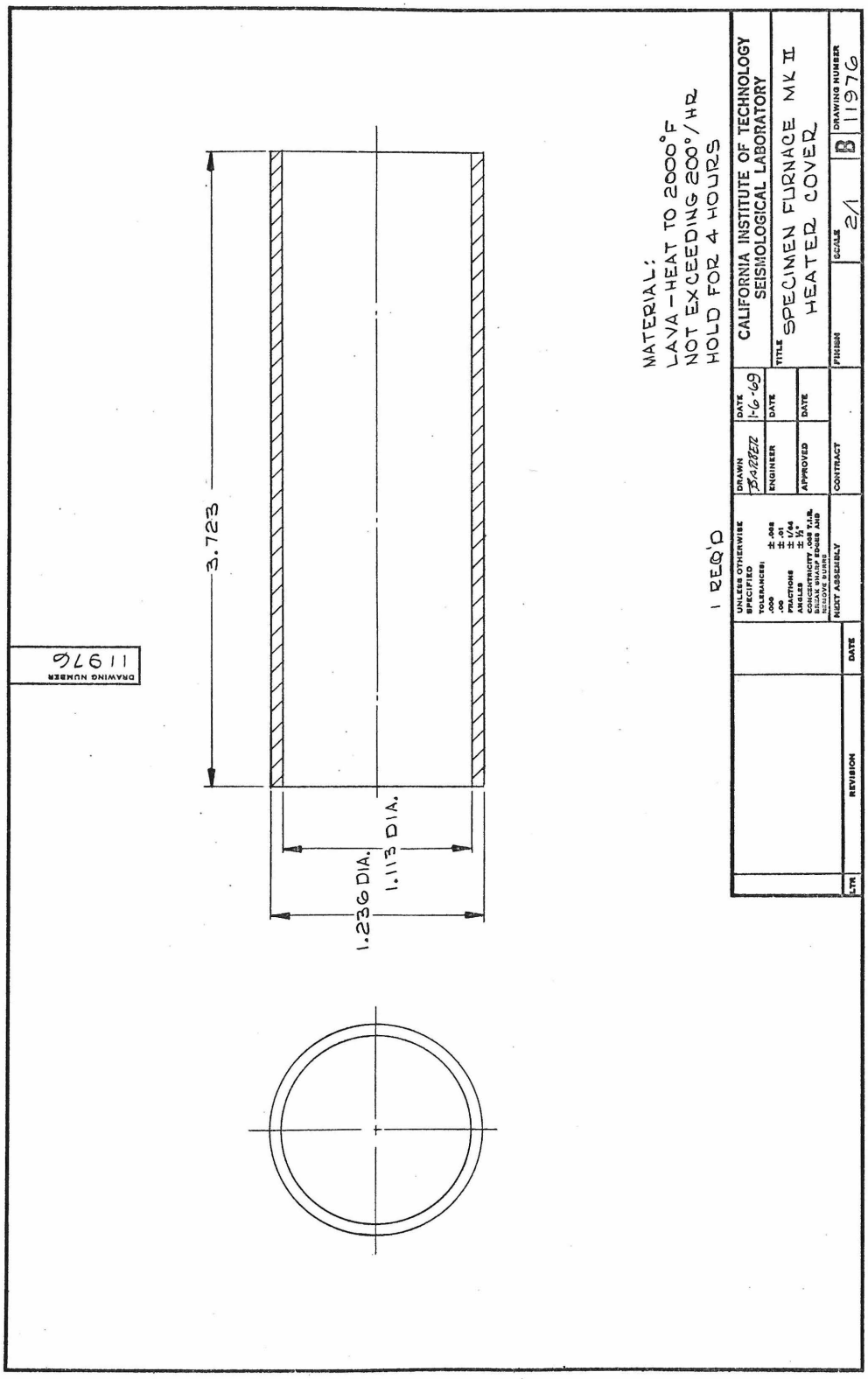
DRAWING NUMBER
11976
3.723
1.236 DIA.
1.113 DIA.
1 REQ'D
MATERIAL:
LAVA - HEAT TO 2000°F
NOT EXCEEDING 200°/HR
HOLD FOR 4 HOURS
UNLESS OTHERWISE SPECIFIED
TOLERANCES:
.000 ±.005
.00 ± .01
.0 ± 1/64
FRACTIONS ± 1/2°
ANGLES
CONCENTRICITY .005 T.I.R.
REMOVE BURRS
FIRST ASSEMBLY
DRAWN
ENGINEER
APPROVED
CONTRACT
DATE 1-6-69
CALIFORNIA INSTITUTE OF TECHNOLOGY
SEISMOLOGICAL LABORATORY
TITLE SPECIMEN FURNACE MK II
HEATER COVER
FINISH
SCALE 2/1
DRAWING NUMBER B 11976
LTR REVISION DATE

Figure 8

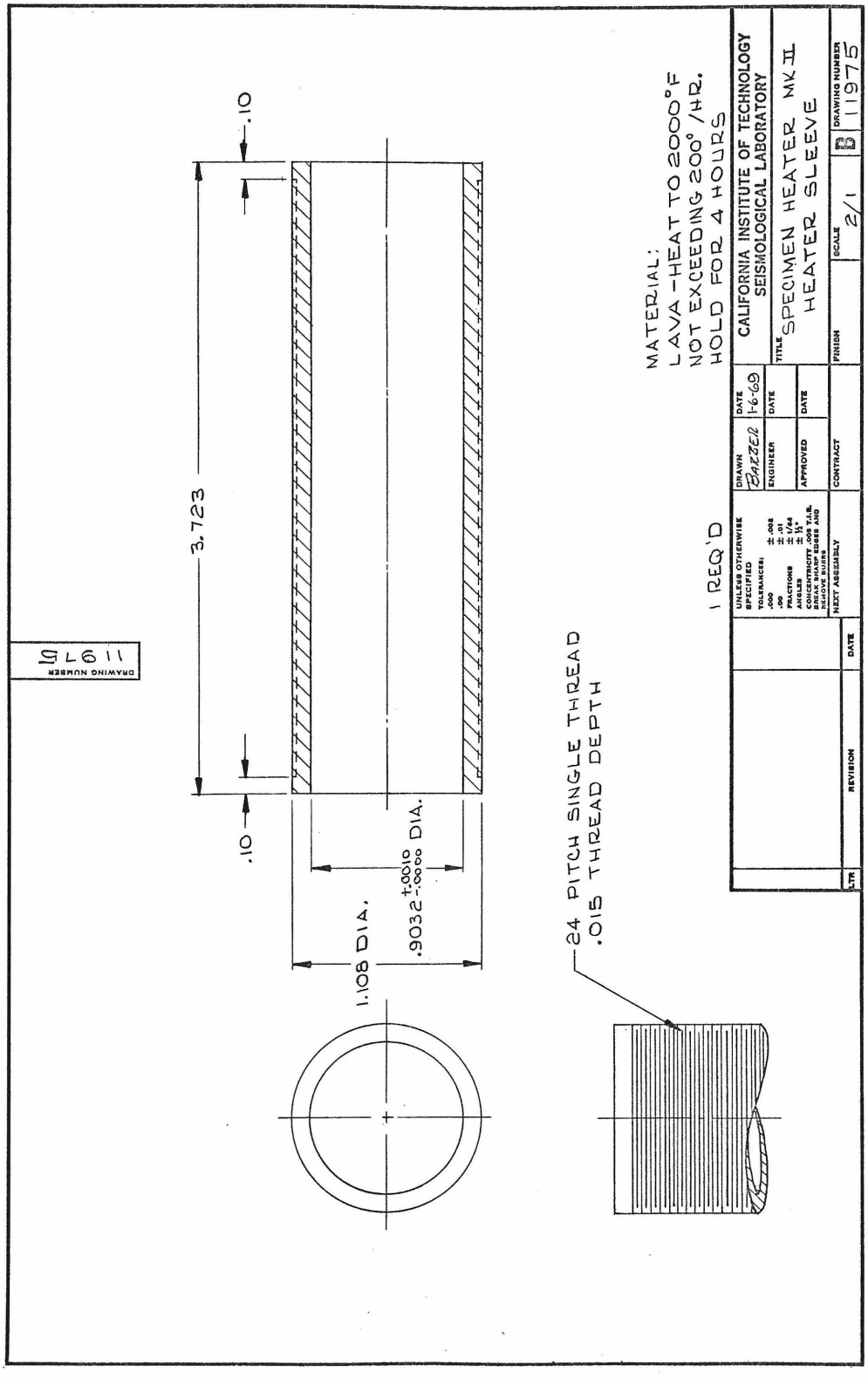
DRAWING NUMBER 11975
.10
3.723
.10
1.108 DIA.
.9032 +.0010 -.0000 DIA.
24 PITCH SINGLE THREAD
.015 THREAD DEPTH
1 REQ'D
MATERIAL:
LAVA - HEAT TO 2000°F
NOT EXCEEDING 200°/HR.
HOLD FOR 4 HOURS
UNLESS OTHERWISE SPECIFIED
TOLERANCES:
.000 ± .002
.00 ± .01
FRACTIONS ± 1/64
ANGLES ± 1/2°
CONCENTRICITY .005 T.I.R.
BREAK SHARP EDGES AND REMOVE BURRS
NEXT ASSEMBLY
DRAWN Baxter
DATE 1-6-69
ENGINEER
DATE
APPROVED
DATE
CONTRACT
FINISH
CALIFORNIA INSTITUTE OF TECHNOLOGY
SEISMOLOGICAL LABORATORY
TITLE SPECIMEN HEATER MK II
HEATER SLEEVE
SCALE 2/1
DRAWING NUMBER 11975
LTR
REVISION
DATE

Figure 9

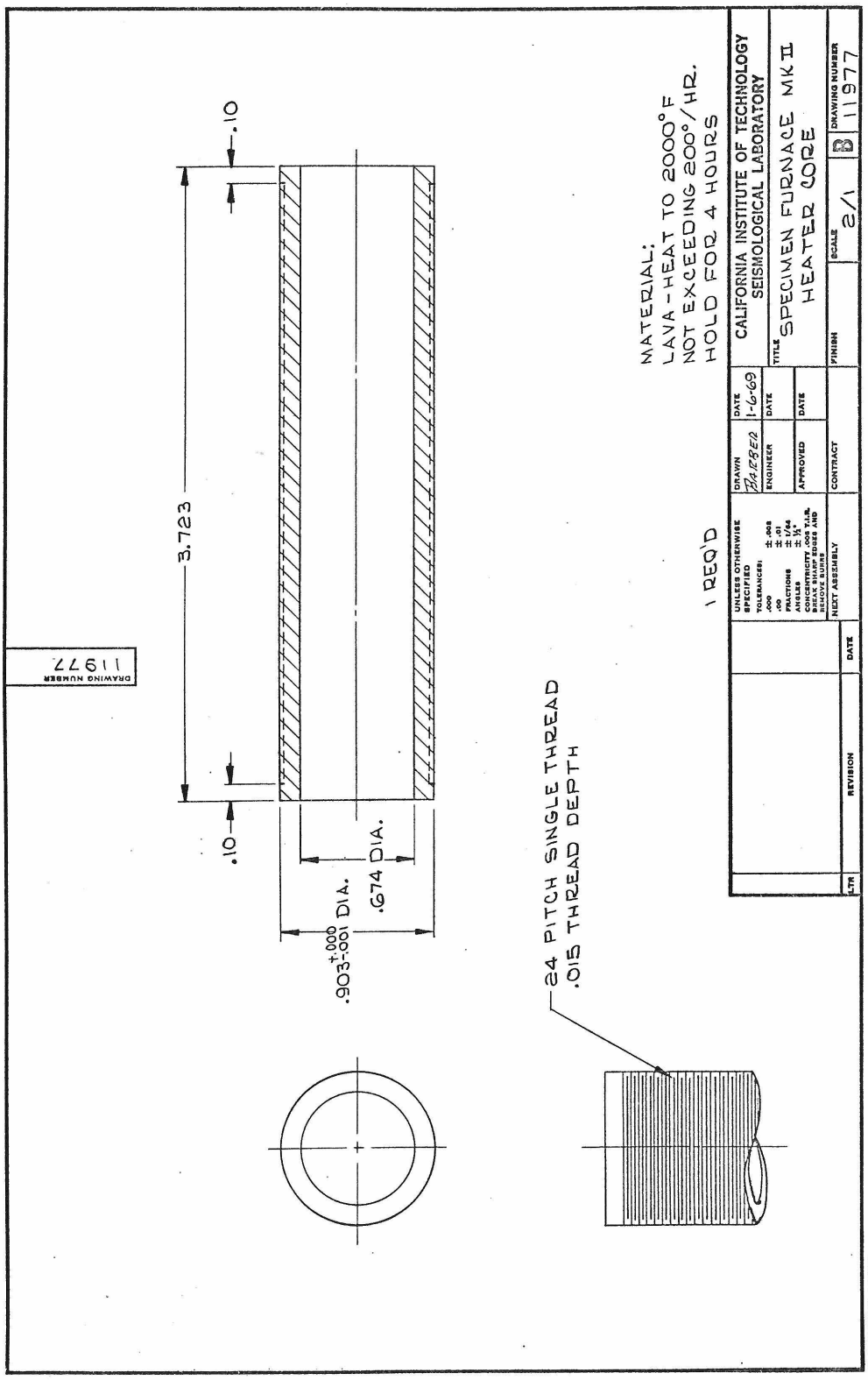
.10
3.723
.10
.903 +.000 -.001 DIA.
.674 DIA.
24 PITCH SINGLE THREAD
.015 THREAD DEPTH
1 REQ'D
MATERIAL:
LAVA-HEAT TO 2000°F
NOT EXCEEDING 200°/HR.
HOLD FOR 4 HOURS
DRAWING NUMBER
11977
CALIFORNIA INSTITUTE OF TECHNOLOGY
SEISMOLOGICAL LABORATORY
SPECIMEN FURNACE MK II
HEATER CORE
DRAWN
DATE 1-6-69
ENGINEER
APPROVED
CONTRACT
FINISH
SCALE 2/1
DRAWING NUMBER 11977
NEXT ASSEMBLY
REVISION
DATE
LTR

Figure 10

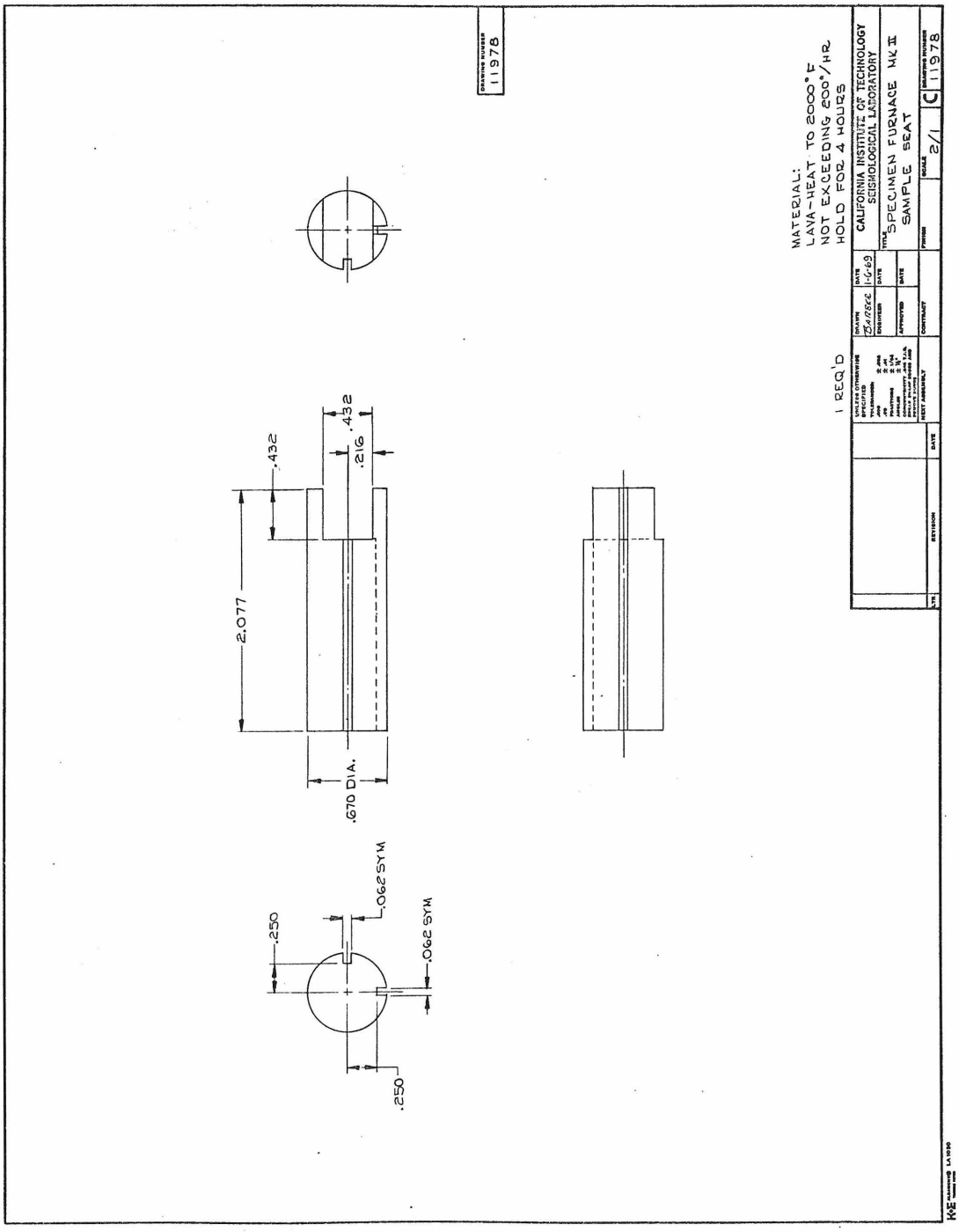
DRAWING NUMBER
11978
MATERIAL:
LAVA-HEAT TO 2000° F
NOT EXCEEDING 600°/HR
HOLD FOR 4 HOURS
1 REQ'D
CALIFORNIA INSTITUTE OF TECHNOLOGY
SEISMOLOGICAL LABORATORY
SPECIMEN FURNACE MK II
SAMPLE SEAT
SCALE 2/1
C
11978
.432
.216
.432
2.077
.670 DIA.
.062 SYM
.062 SYM
.250
.250

Figure 11

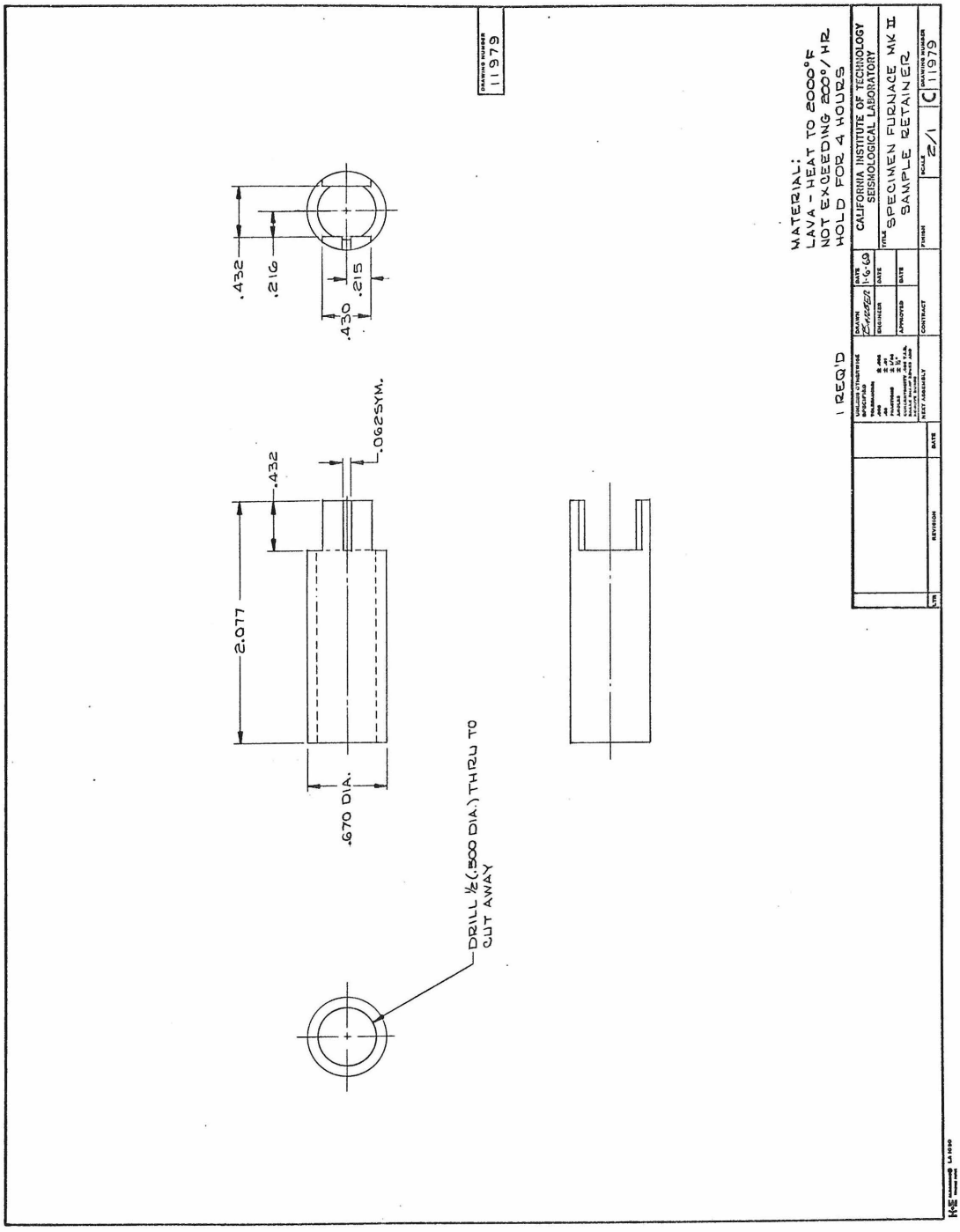
DRAWING NUMBER
11979
.432
.216
.430
.215
.062SYM.
.432
2.077
.670 DIA.
DRILL ½(.500 DIA.) THRU TO
CUT AWAY
1 REQ'D
MATERIAL:
LAVA - HEAT TO 2000°F
NOT EXCEEDING 200°/HR
HOLD FOR 4 HOURS
CALIFORNIA INSTITUTE OF TECHNOLOGY
SEISMOLOGICAL LABORATORY
SPECIMEN FURNACE MK II
SAMPLE RETAINER
SCALE 2/1
DRAWING NUMBER
C 11979

Figure 12

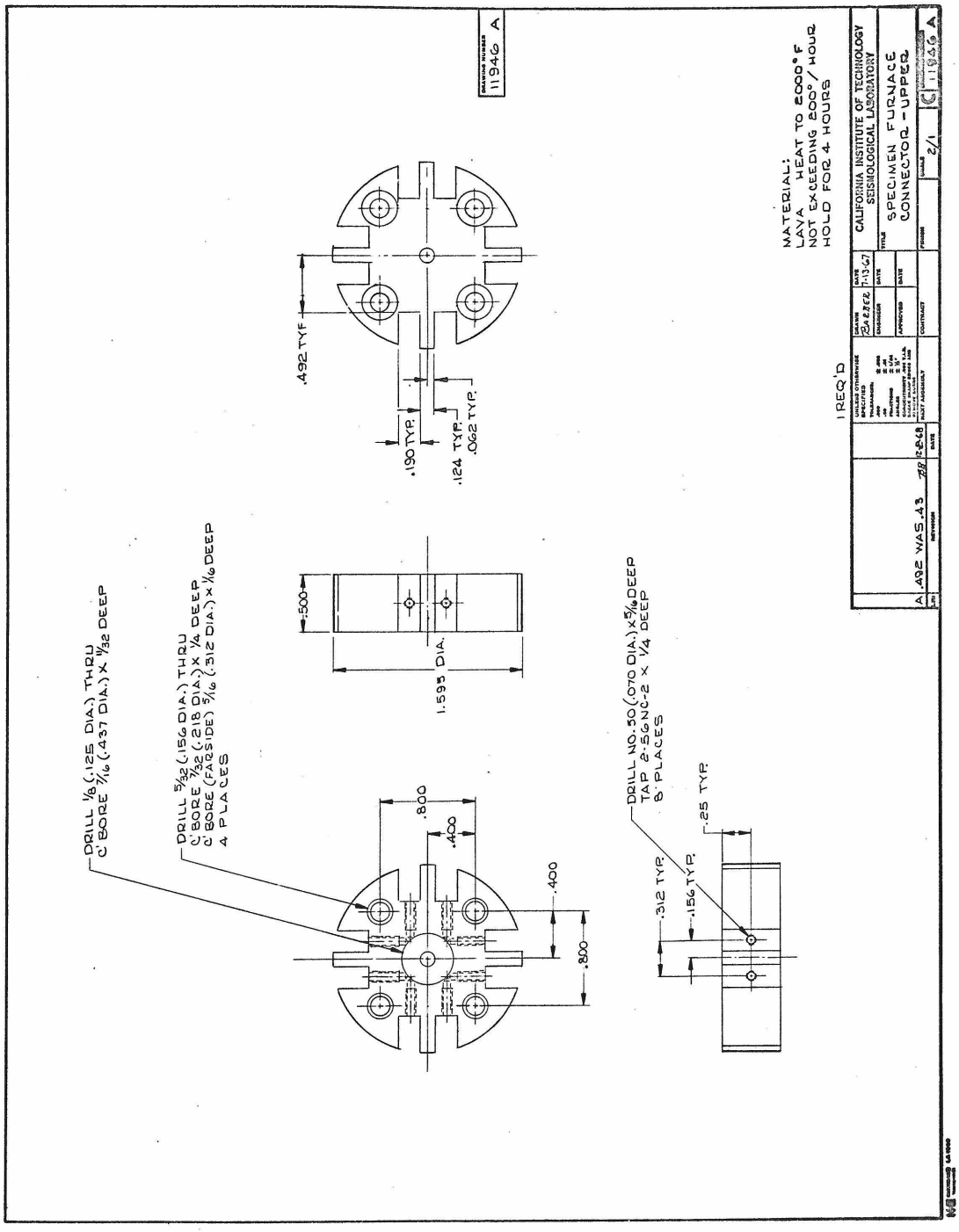
DRILL 1/8 (.125 DIA.) THRU
C'BORE 7/16 (.437 DIA.) X 1/32 DEEP
DRILL 5/32 (.156 DIA.) THRU
C'BORE 7/32 (.218 DIA.) X 1/4 DEEP
C'BORE (FAR SIDE) 5/16 (.312 DIA.) X 1/16 DEEP
4 PLACES
.800
.400
.400
.800
.500
1.595 DIA.
.492 TYP.
.190 TYP.
.124 TYP.
.062 TYP.
DRILL NO. 50 (.070 DIA.) X 5/16 DEEP
TAP 2-56 NC-2 X 1/4 DEEP
8 PLACES
.312 TYP.
.156 TYP.
.25 TYP.
MATERIAL:
LAVA HEAT TO 2000° F
NOT EXCEEDING 200°/HOUR
HOLD FOR 4 HOURS
1 REQ'D
DRAWING NUMBER
11946 A
A .492 WAS .43
CALIFORNIA INSTITUTE OF TECHNOLOGY
SEISMOLOGICAL LABORATORY
SPECIMEN FURNACE
CONNECTOR - UPPER
11946
SCALE 2/1
A

Figure 13

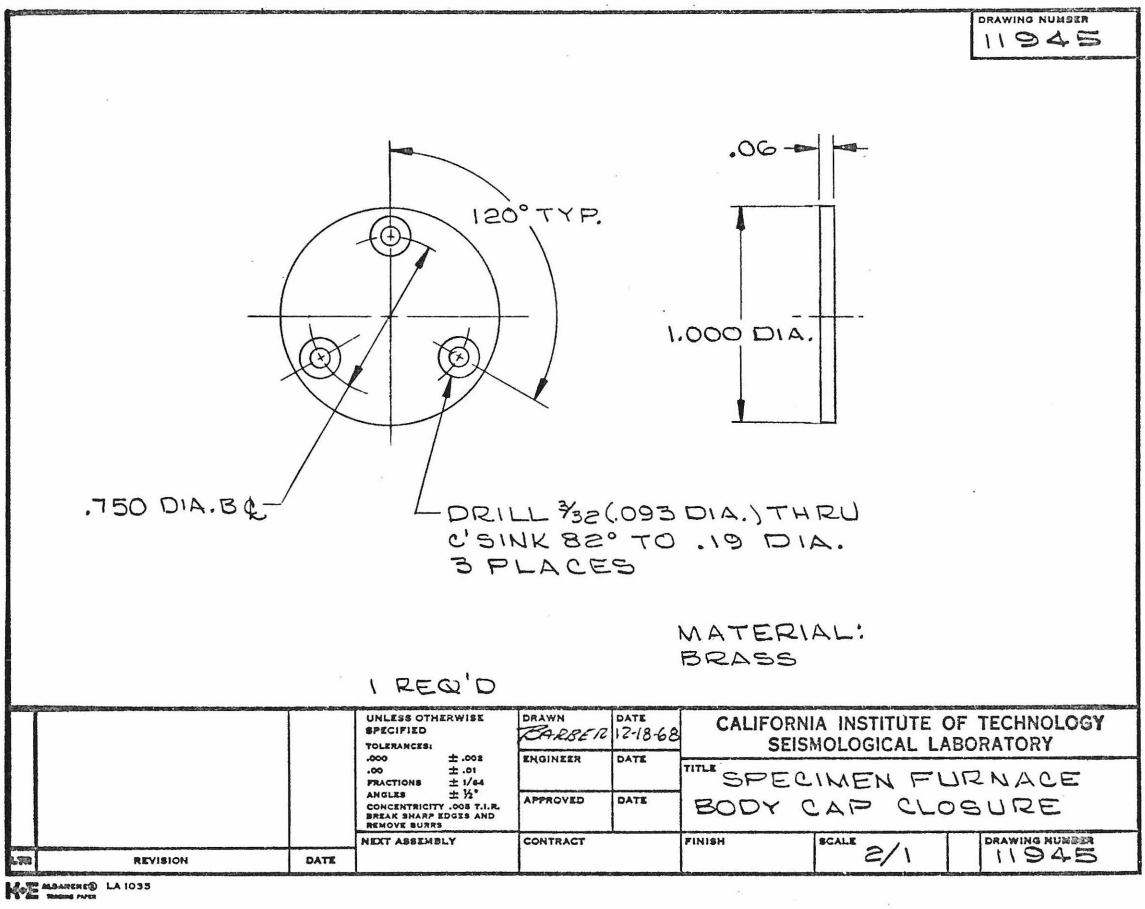
DRAWING NUMBER
11945
120° TYP.
.06
1.000 DIA.
.750 DIA. B ℄
DRILL 3/32 (.093 DIA.) THRU
C'SINK 82° TO .19 DIA.
3 PLACES
MATERIAL:
BRASS
1 REQ'D
UNLESS OTHERWISE SPECIFIED
TOLERANCES:
.000 ± .002
.00 ± .01
FRACTIONS ± 1/64
ANGLES ± ½°
CONCENTRICITY .005 T.I.R.
BREAK SHARP EDGES AND REMOVE BURRS
DRAWN
BARBER
DATE
12-18-68
ENGINEER
DATE
APPROVED
DATE
CALIFORNIA INSTITUTE OF TECHNOLOGY
SEISMOLOGICAL LABORATORY
TITLE
SPECIMEN FURNACE
BODY CAP CLOSURE
LTR
REVISION
DATE
NEXT ASSEMBLY
CONTRACT
FINISH
SCALE
2/1
DRAWING NUMBER
11945
K+E ALBARENE LA 1035

Figure 14

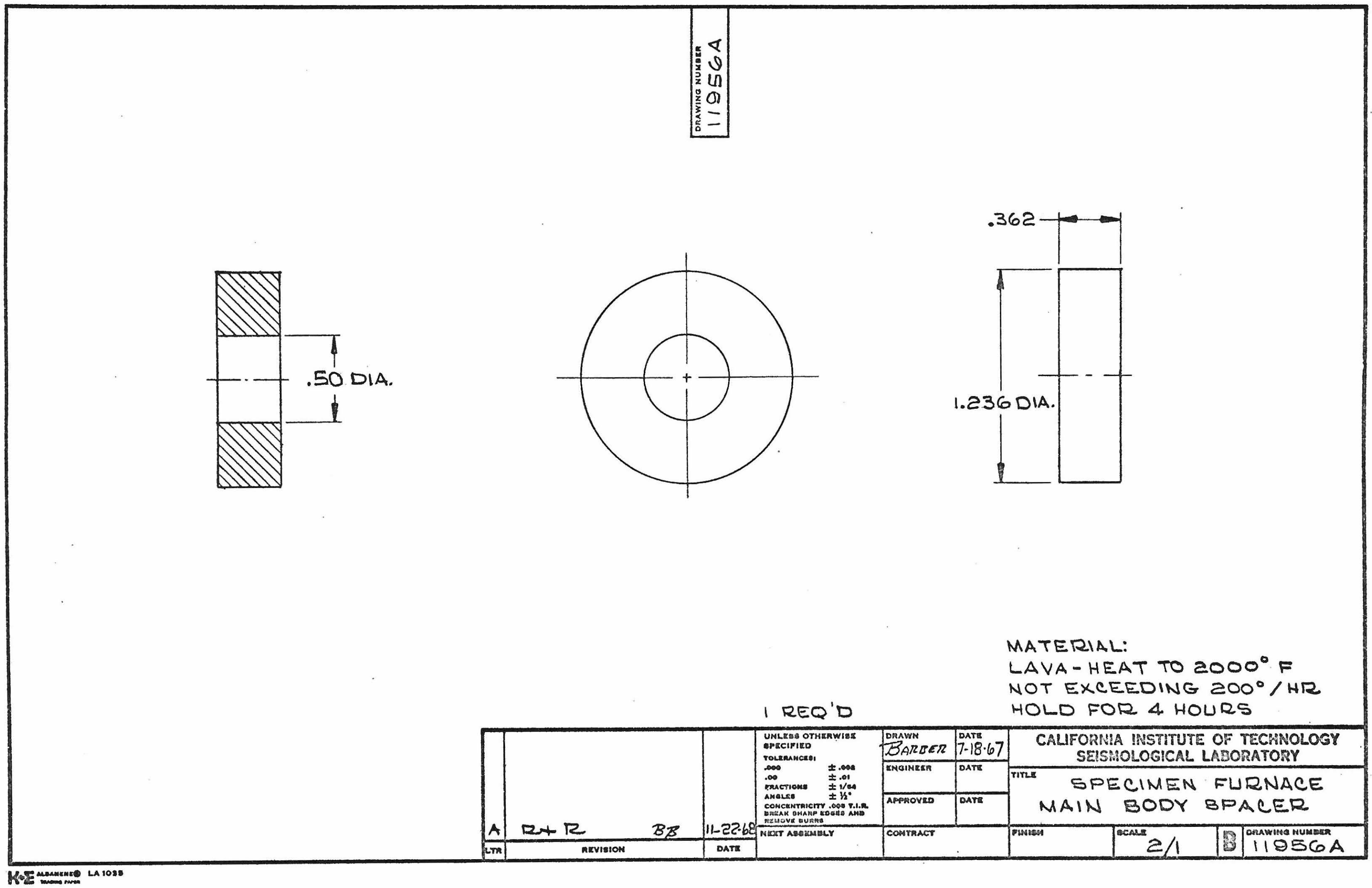
DRAWING NUMBER
11956A
.362
.50 DIA.
1.236 DIA.
MATERIAL:
LAVA - HEAT TO 2000° F
NOT EXCEEDING 200°/HR
HOLD FOR 4 HOURS
1 REQ'D
UNLESS OTHERWISE SPECIFIED
TOLERANCES:
.000 ± .005
.00 ± .01
FRACTIONS ± 1/64
ANGLES ± 1/2°
CONCENTRICITY .005 T.I.R.
BREAK SHARP EDGES AND REMOVE BURRS
DRAWN
BARBER
DATE
7-18-67
ENGINEER
APPROVED
CALIFORNIA INSTITUTE OF TECHNOLOGY
SEISMOLOGICAL LABORATORY
TITLE
SPECIMEN FURNACE
MAIN BODY SPACER
A
R+R
BB
11-22-68
LTR
REVISION
NEXT ASSEMBLY
CONTRACT
FINISH
SCALE
2/1
B
11956A

Figure 15

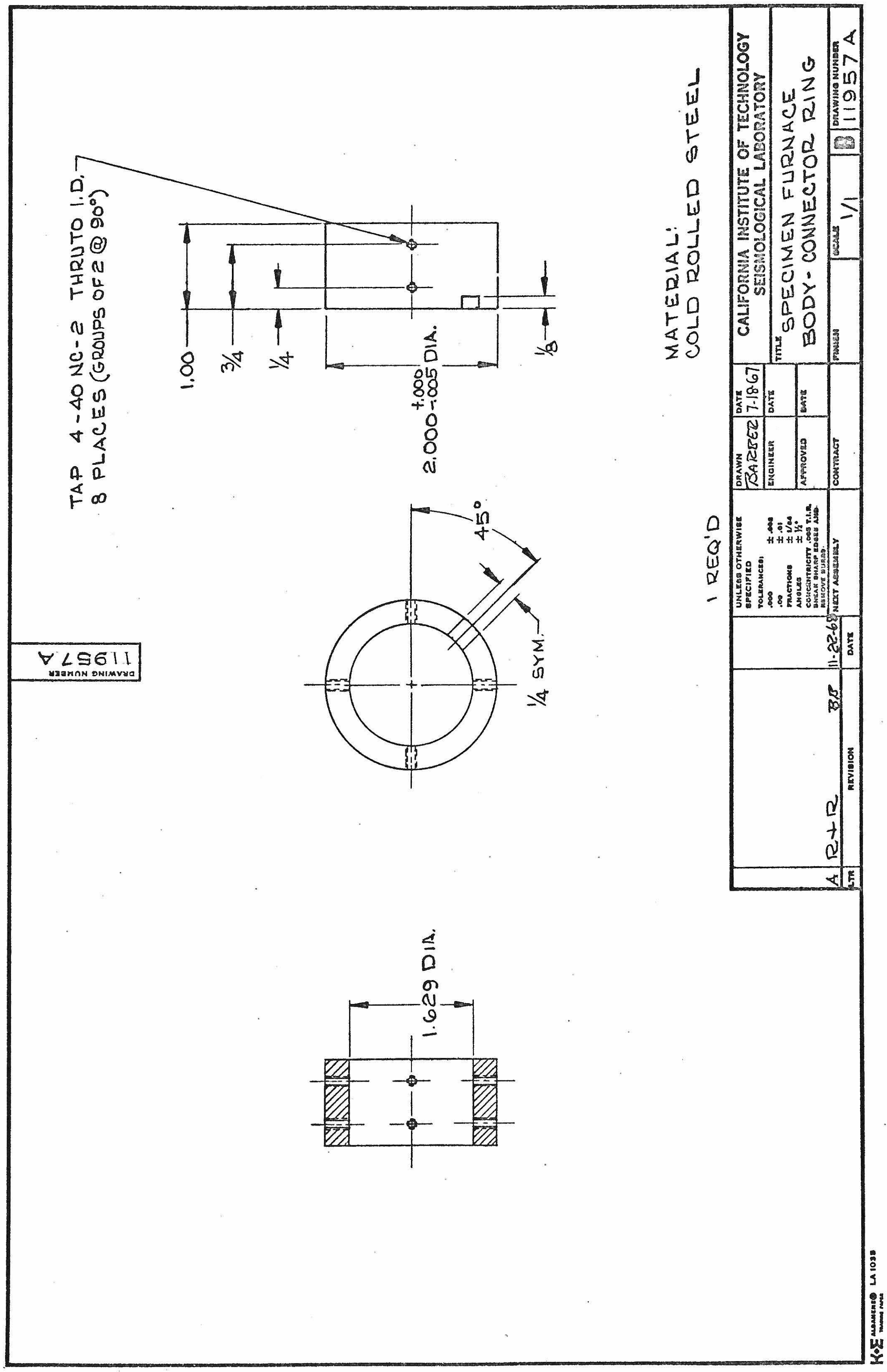
TAP 4-40 NC-2 THRU TO I.D.
8 PLACES (GROUPS OF 2 @ 90°)
1.00
3/4
1/4
1/8
+.000
2.000 -.005 DIA.
45°
1/4 SYM.
1.629 DIA.
MATERIAL:
COLD ROLLED STEEL
1 REQ'D
CALIFORNIA INSTITUTE OF TECHNOLOGY
SEISMOLOGICAL LABORATORY
SPECIMEN FURNACE
BODY-CONNECTOR RING
DRAWN BARBER
DATE 7-18-67
SCALE 1/1
B
DRAWING NUMBER 11957A
A R+R BB 11-22-68
11957A

Figure 16

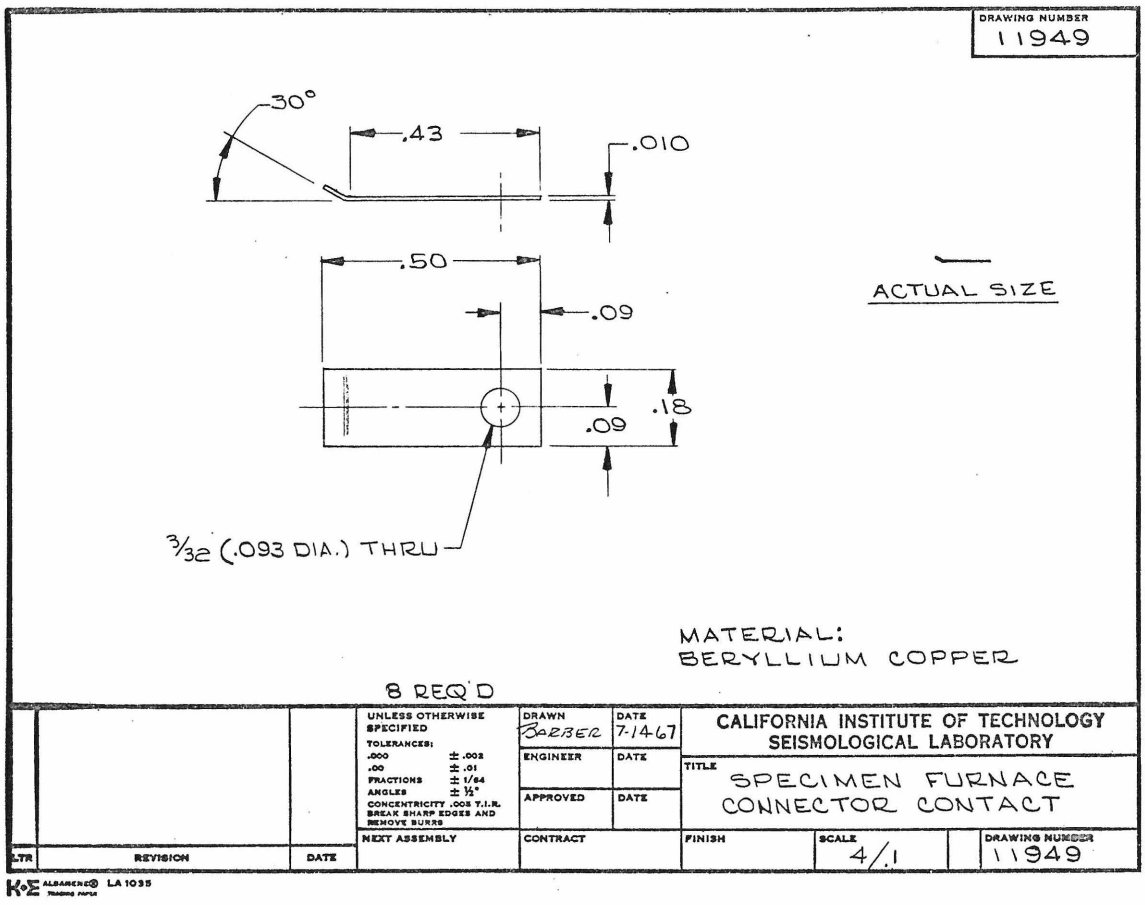
DRAWING NUMBER
11949
30°
.43
.010
.50
.09
.18
.09
3/32 (.093 DIA.) THRU
ACTUAL SIZE
MATERIAL:
BERYLLIUM COPPER
8 REQ'D
UNLESS OTHERWISE SPECIFIED
TOLERANCES:
.000 ± .002
.00 ± .01
FRACTIONS ± 1/64
ANGLES ± ½°
CONCENTRICITY .002 T.I.R.
BREAK SHARP EDGES AND REMOVE BURRS
DRAWN Barber
DATE 7-14-67
ENGINEER
DATE
APPROVED
DATE
CALIFORNIA INSTITUTE OF TECHNOLOGY
SEISMOLOGICAL LABORATORY
TITLE
SPECIMEN FURNACE
CONNECTOR CONTACT
LTR
REVISION
DATE
NEXT ASSEMBLY
CONTRACT
FINISH
SCALE 4/1
DRAWING NUMBER 11949
K•E ALBANENE LA 1035

Figure 17

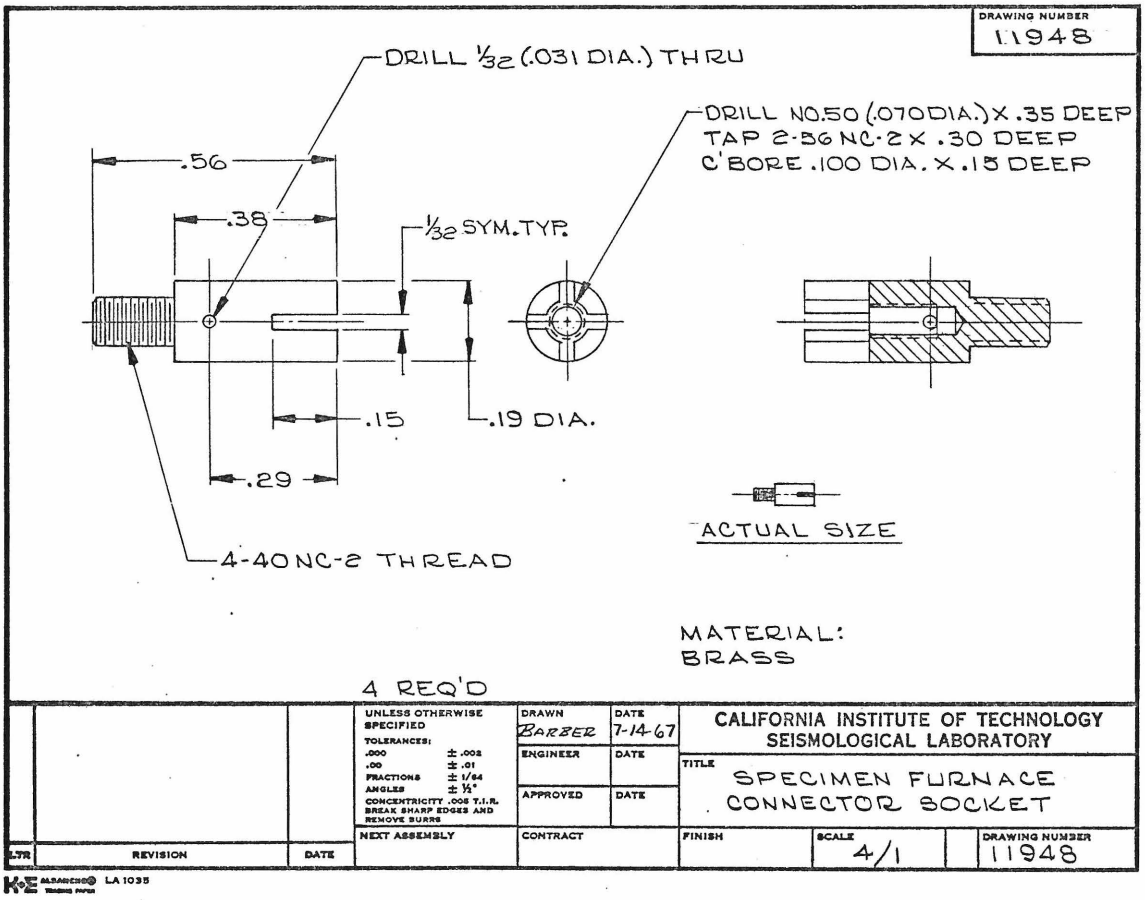
DRAWING NUMBER
11948
DRILL 1/32 (.031 DIA.) THRU
DRILL NO.50 (.070DIA.) X .35 DEEP
TAP 2-56 NC-2 X .30 DEEP
C'BORE .100 DIA. X .15 DEEP
.56
.38
1/32 SYM. TYP.
.15
.19 DIA.
.29
4-40 NC-2 THREAD
ACTUAL SIZE
MATERIAL:
BRASS
4 REQ'D
UNLESS OTHERWISE SPECIFIED
TOLERANCES:
.000 ± .002
.00 ± .01
FRACTIONS ± 1/64
ANGLES ± ½°
CONCENTRICITY .005 T.I.R.
BREAK SHARP EDGES AND REMOVE BURRS
DRAWN Barber
DATE 7-14-67
ENGINEER
DATE
APPROVED
DATE
CALIFORNIA INSTITUTE OF TECHNOLOGY
SEISMOLOGICAL LABORATORY
TITLE
SPECIMEN FURNACE
CONNECTOR SOCKET
NEXT ASSEMBLY
CONTRACT
FINISH
SCALE 4/1
DRAWING NUMBER 11948
LTR
REVISION
DATE
K+E ALBANY LA 1035

Figure 18

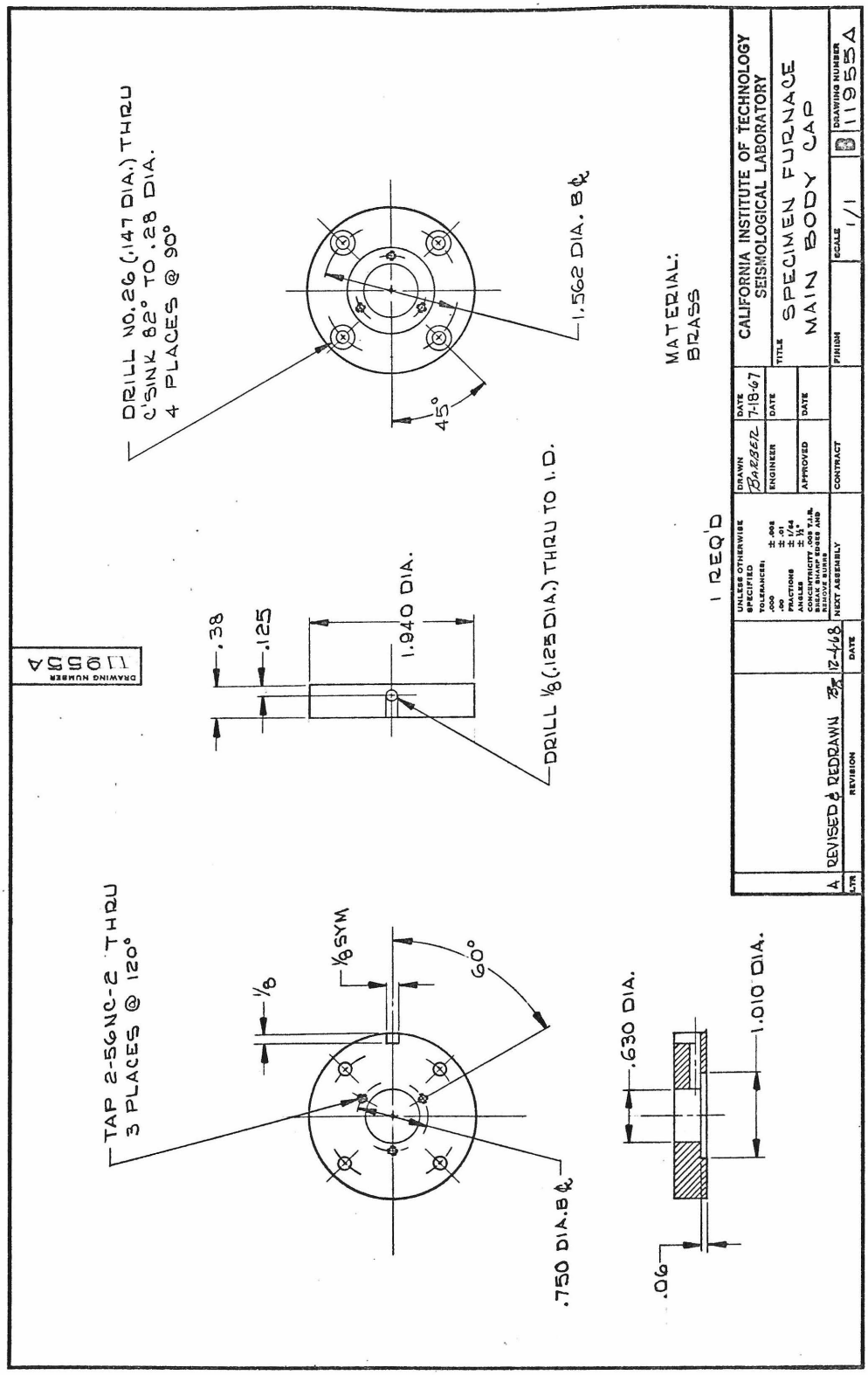
DRILL NO.26 (.147 DIA.) THRU
C'SINK 82° TO .28 DIA.
4 PLACES @ 90°
1.562 DIA. ℄
45°
.38
.125
1.940 DIA.
DRILL 1/8 (.125 DIA.) THRU TO I.D.
MATERIAL:
BRASS
1 REQ'D
TAP 2-56NC-2 THRU
3 PLACES @ 120°
1/8
1/8 SYM
60°
.750 DIA. ℄
.630 DIA.
1.010 DIA.
.06
DRAWING NUMBER
11955A
CALIFORNIA INSTITUTE OF TECHNOLOGY
SEISMOLOGICAL LABORATORY
SPECIMEN FURNACE
MAIN BODY CAP
DRAWN BARBER
DATE 7-18-67
ENGINEER
APPROVED
CONTRACT
FINISH
SCALE 1/1
DRAWING NUMBER 11955A
REVISED & REDRAWN
12-4-68
REVISION
DATE
NEXT ASSEMBLY

Figure 19

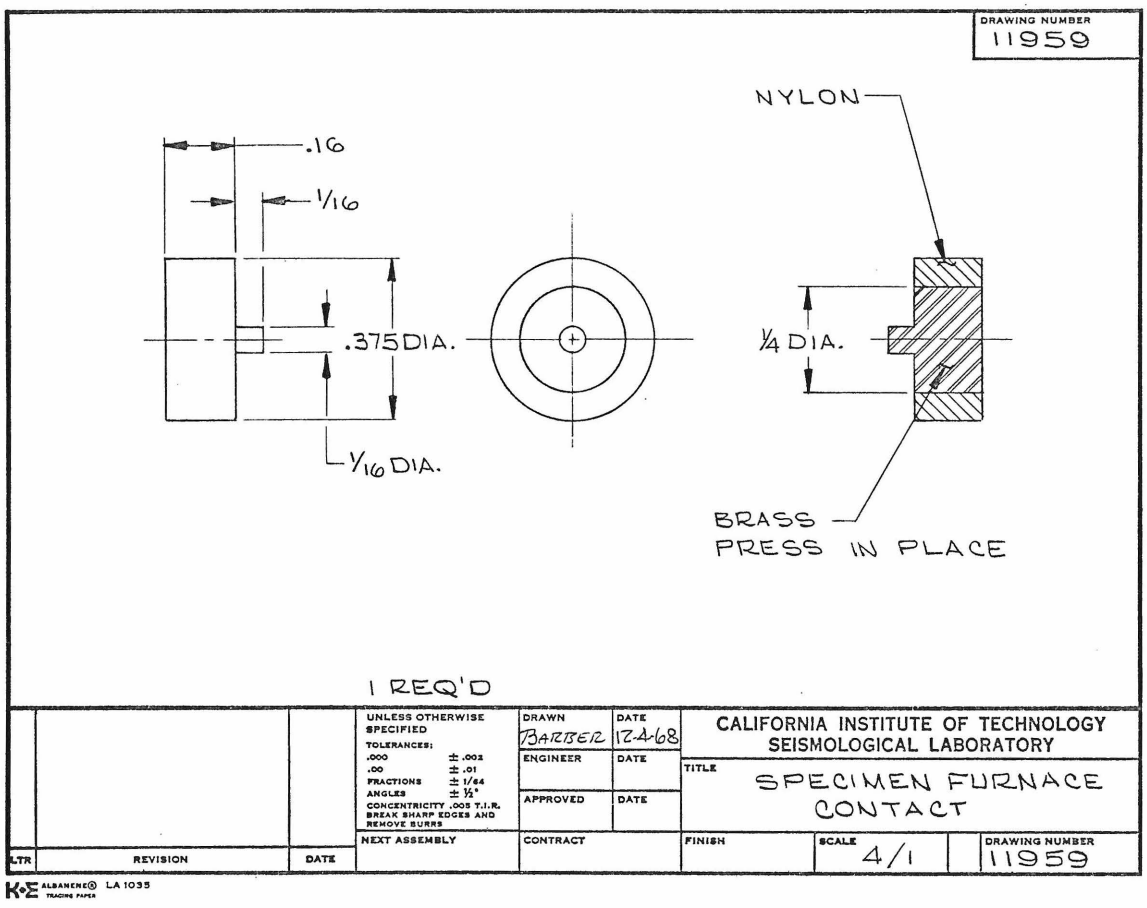
DRAWING NUMBER
11959
NYLON
.16
1/16
.375 DIA.
1/16 DIA.
1/4 DIA.
BRASS
PRESS IN PLACE
1 REQ'D
UNLESS OTHERWISE SPECIFIED
TOLERANCES:
.000 ± .002
.00 ± .01
FRACTIONS ± 1/64
ANGLES ± ½°
CONCENTRICITY .005 T.I.R.
BREAK SHARP EDGES AND REMOVE BURRS
DRAWN
BARBER
DATE
12-4-68
ENGINEER
DATE
APPROVED
DATE
CALIFORNIA INSTITUTE OF TECHNOLOGY
SEISMOLOGICAL LABORATORY
TITLE
SPECIMEN FURNACE CONTACT
NEXT ASSEMBLY
CONTRACT
FINISH
SCALE
4/1
DRAWING NUMBER
11959
LTR
REVISION
DATE
K•E ALBANENE® LA 1035 TRACING PAPER

Figure 20

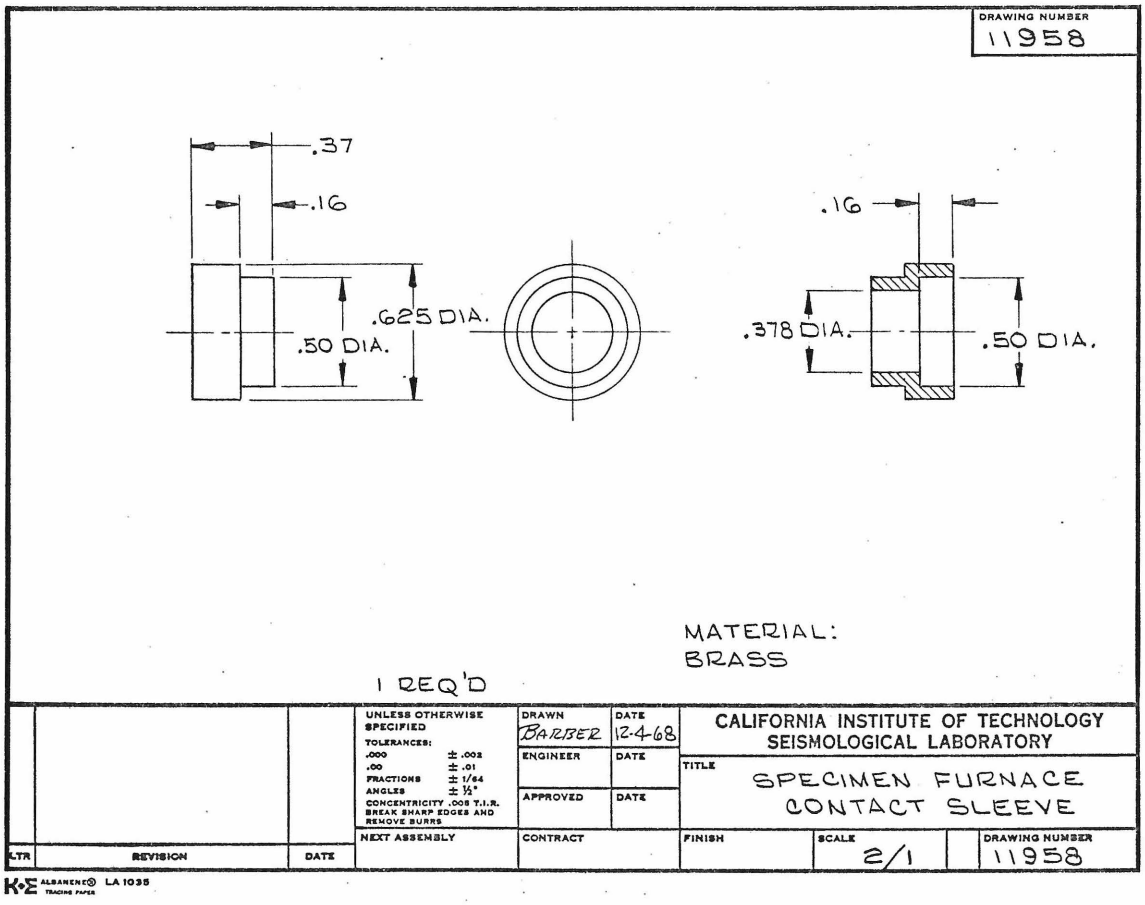
DRAWING NUMBER
11958
.37
.16
.625 DIA.
.50 DIA.
.16
.378 DIA.
.50 DIA.
MATERIAL:
BRASS
1 REQ'D
UNLESS OTHERWISE SPECIFIED
TOLERANCES:
.000 ± .002
.00 ± .01
FRACTIONS ± 1/64
ANGLES ± ½°
CONCENTRICITY .003 T.I.R.
BREAK SHARP EDGES AND REMOVE BURRS
DRAWN BARBER
DATE 12-4-68
ENGINEER
DATE
APPROVED
DATE
CALIFORNIA INSTITUTE OF TECHNOLOGY
SEISMOLOGICAL LABORATORY
TITLE
SPECIMEN FURNACE
CONTACT SLEEVE
LTR
REVISION
DATE
NEXT ASSEMBLY
CONTRACT
FINISH
SCALE 2/1
DRAWING NUMBER
11958
K•E ALBANENE® LA 1035

Figure 21

Appendix C

LEAK DETECTION IN HIGH PRESSURE GAS SYSTEMS

Most high pressure systems are plagued from time to time by small leaks. To find these leaks is often a cumbersome and frustrating process. Ultrasonic probes can be used in many cases to detect moderate leaks. Soap bubbles or similar techniques are messy and limited to easily accessible areas. Radioactive Krypton^{85} has successfully been used to detect leaks at a rate too small to be found by these other means.

The pressure system uses Argon as a pressure medium and is capable of generating 200,000 psi where the net volume filled by the compressed gas is approximately five cubic centimeters. One percent of Krypton is added to the Argon. The Krypton contains sufficient Kr^{85} so that its activity is 10 killicuries/liter (mc/l). Kr^{85} has a half life of 10.4 years and emits a soft gamma ray of 0.52 Mev and β particles with a maximum energy of 0.67 Mev. The β particles are efficiently shielded by the steel tubing in the pressure system but can be readily detected upon escape into the atmosphere with a β probe.

In a 5 cc volume, where the concentration of the added Krypton is 1%, with a 10 mc/l level of radioactivity, and at a pressure of 1 Kbar, a 1% volume loss in 10,000 seconds corresponds to approximately 20 counts/second. Much smaller leaks can be detected by increasing the proportion of Kr^{85} or by the use of higher pressures. The background count in the laboratory is less than one count per second. Therefore, our detection threshold under the conditions described is about a 1% leak per day (86400 sec).

The Krypton used on the tracer was obtained from the Union Carbide's Linde Division. The Radiation Detector was a Wm. Johnson and Associates, Inc., Model GSM-S with a GP-200 Probe. The cost of the gas for one pressure run with leak detection is less than one dollar.

Appendix D

CONSTRUCTION DETAILS OF HIGH PRESSURE INSTALLATION

The high pressure system is located at the Donnelley Seismological Laboratory of Caltech. It is subdivided into two basic parts; the control panel and the high pressure generating equipment. The control panel is located against an outside wall in a laboratory. The high pressure generating equipment is in a blast proof steel room in the garage area.

Figures 1, 2, and 3 show the physical arrangement of the high pressure equipment in the steel room. The floor space within this room is approximately 56 square feet (8' x 7'). There are three protective steel walls and one outside concrete wall; three feet thick. The steel walls are constructed of 3/8" cold rolled plate. They are hinged at the top and thus are hanging from a steel structure and can act as ballistic pendula. In case of a failure of the high pressure equipment part of the energy of flying parts is absorbed by the swinging walls, thus reducing the likelihood of puncturing them. The steel sheet against the laboratory wall is not free to swing, but is backed by a plaster board wall. Entry into the steel room is through a large door which (in the closed position) is an integral part of one of the hanging walls. An overhead one ton hoist is mounted on an H beam track which can swivel. Any piece of equipment within the room can be picked up and moved outside the

room for repair or onto the bed of a truck for shipment. The steel room and hoist structure are welded. This is important as a safety precaution, since the threads on bolts are easily sheared if they receive a direct hit, becoming undesirable projectiles. The sample vessel shown in Figure 1 is located approximately in the center of the room to insure easy accessibility. The location of the other high pressure components was arranged to keep high pressure tubing to a minimum and insure a coherent control panel within the laboratory. All long high pressure tubing is anchored at 8" intervals to avoid possible whiplashing in case of rupture. The structure which supports two check values CH1, CH2, four high pressure valves X2, X12, X17, X18, the manganin coil vessel and the intensifier I, as well as the associated high pressure tubing was constructed from Kindorf Channel, a channel erector system. The four high pressure valves are operated from the control panel with long extension handles. The liquid piston one to one converter, the intensifier and the high pressure vessel have a heavy steel sleeve around their main body to stop possible cracks and projectiles. The hydraulic pumps DP1 and DP2 are mounted securely to the floor. All tubing which is attached to these pumps is mounted such that it can follow the small vibrations of the pumps without coupling the vibrations to other equipment. The oil reservoir (Figure 2) is placed against a concrete wall at a level above the pumps and intensifiers. This provides for gravity

feeding the lines and reduces the problems assocated with priming the system after maintenance.

High pressure tubing is manufactured from a tough ductile stainless steel and has to be treated with some caution. Work hardening due to excessive bending or stretching while bending may embrittle the steel and cause it to fail under pressure. Conventional tube benders as they are used in the plumbing industry have a tendency to bend themselves instead of bending the tubing. A special rugged tube bender was therefore built which rolls the tube around a two inch radius.

The frame of the control panel in the laboratory is also constructed of Kindorf Channel. The panel (see Figures 4 and 5) is 3/16" aluminum which provides protection against possible break in pressure lines behind it. The highest pressure in the laboratory at any time is 60,000 psi and is confined to thin tubing and one gauge. No valves or pressure reservoirs above 30,000 psi are located outside the steel room. All gauges which read pressures above 3,000 psi have blowout backs. An intercom system connects the panel area with the steel room. It is not only used to communicate while placing a sample in the vessel (Figure 6) and simultaneously adjusting the electronic equipment, but also to listen to the performance of the pumps and the pistons during a pressure run. The experienced ear can detect many problems before they become severe.

While operating the high pressure system the steel room is locked and the area roped off. High pressure warning signs and two flashing red lights further indicate that the system is in operation.

FIGURE CAPTIONS

Figure 1. Pressure vessel located in protective steel room.

Figure 2. Hydraulic pumps and oil reservoirs located in protective steel room.

Figure 3. Top of pressure vessel, and one to one converter are shown in the left part of picture. Top right of picture shows location of high pressure valves X-17 and X-18. Center right shows location of thermally insulated box for Manganin coils. Thermal reference junction and electrical connections are located on top of pressure vessel.

Figure 4. Pressure system control panel.

Figure 5. Electronic equipment in foreground with pressure system control panel in background.

Figure 6. Furnace assembly being lowerd into high pressure vessel.

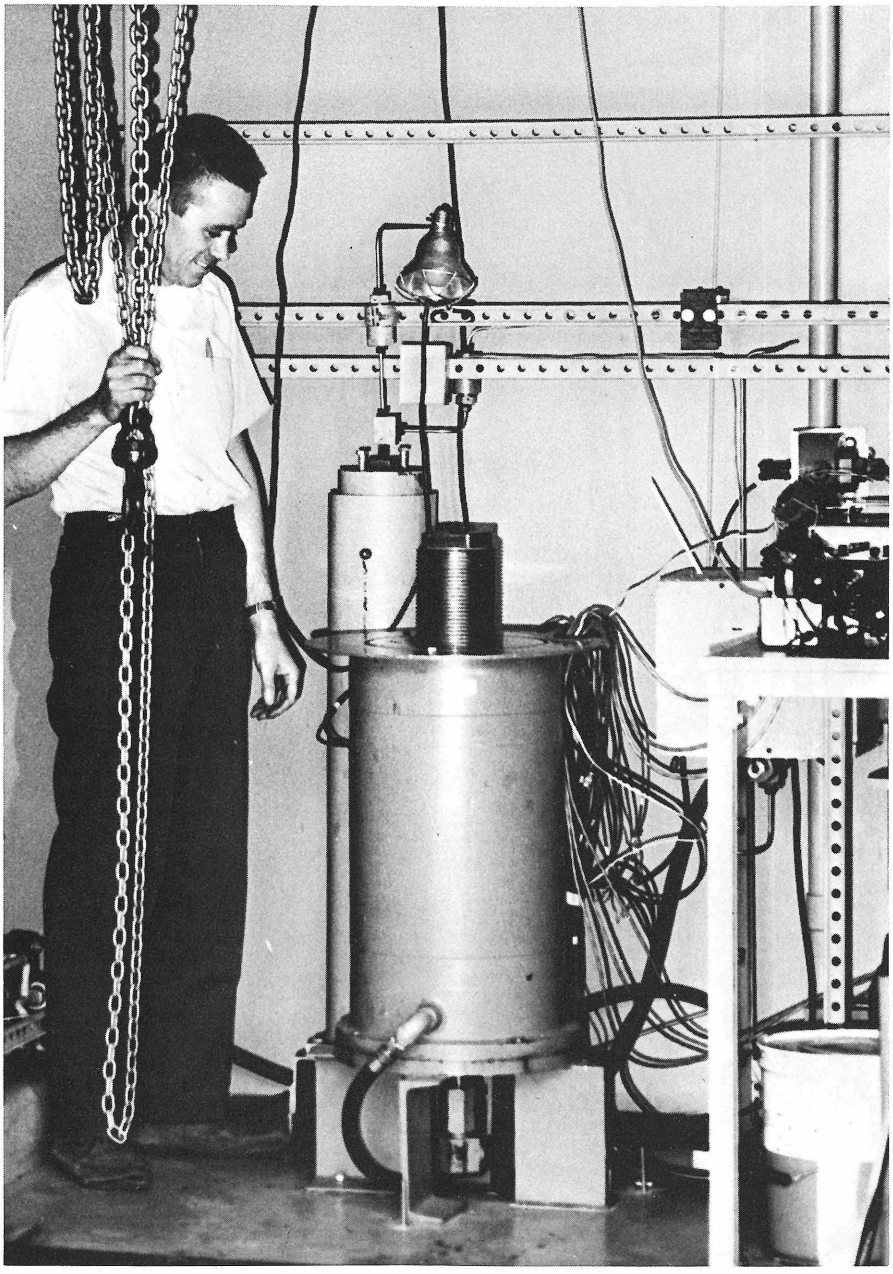

Figure 1

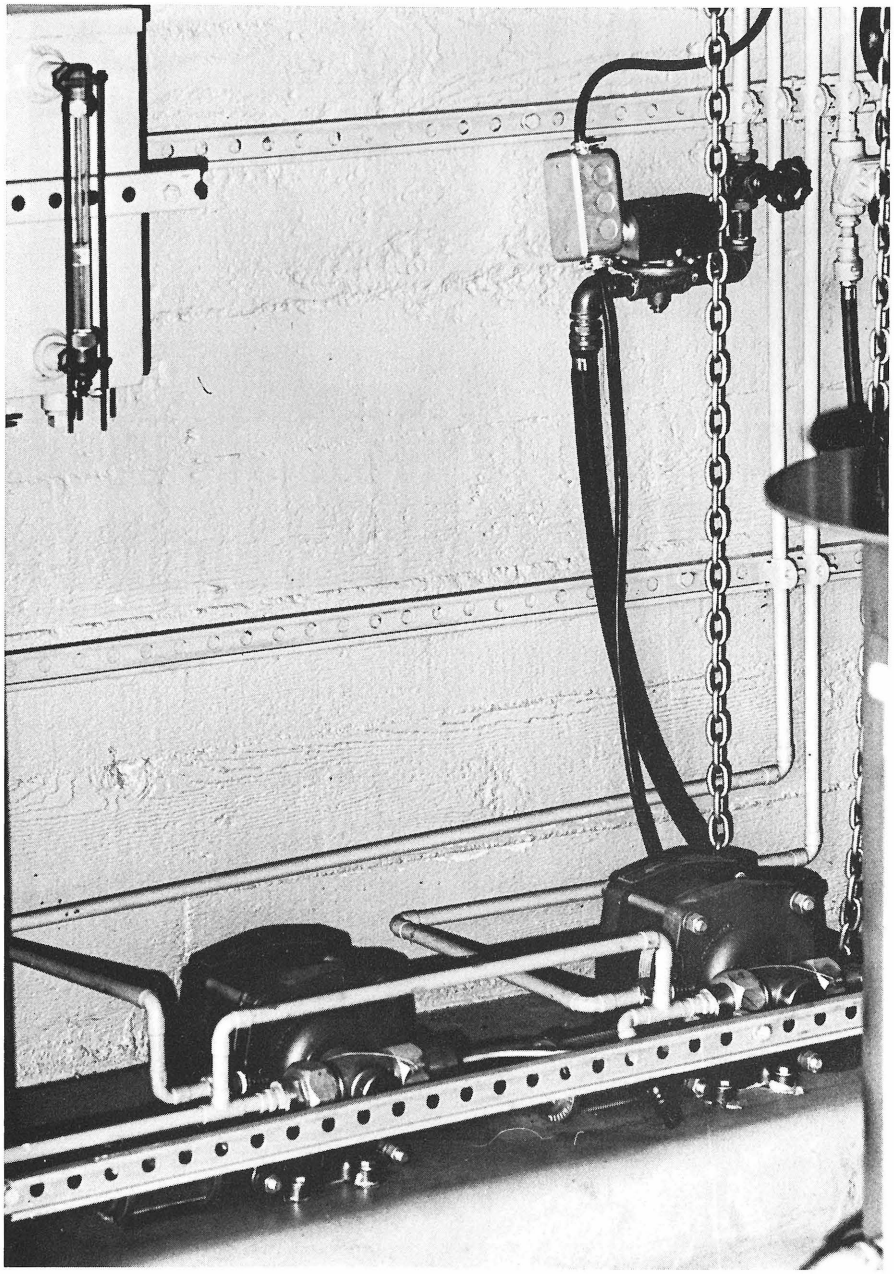

Figure 2

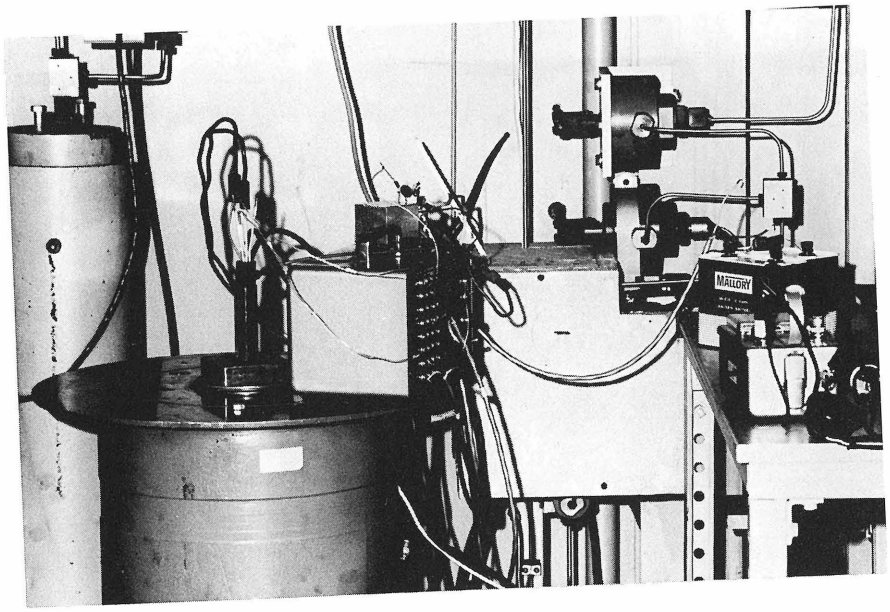

Figure 3

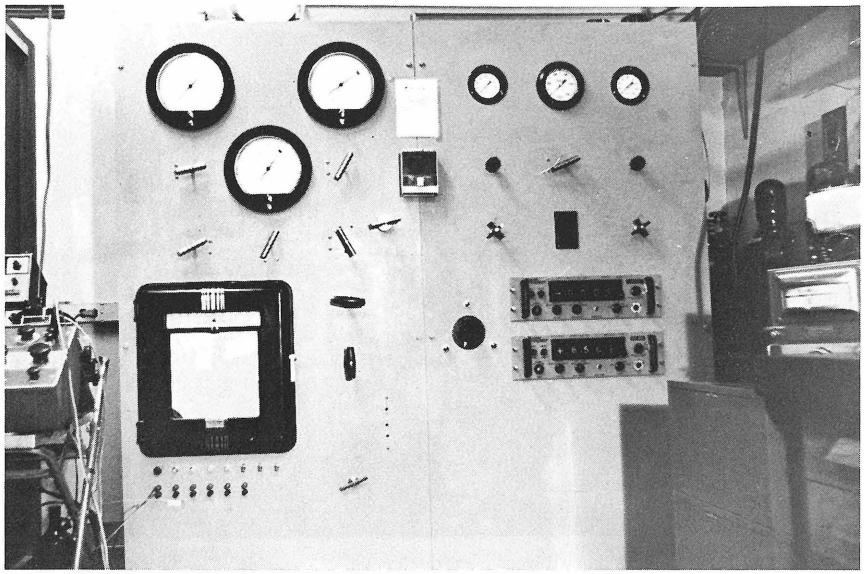

Figure 4

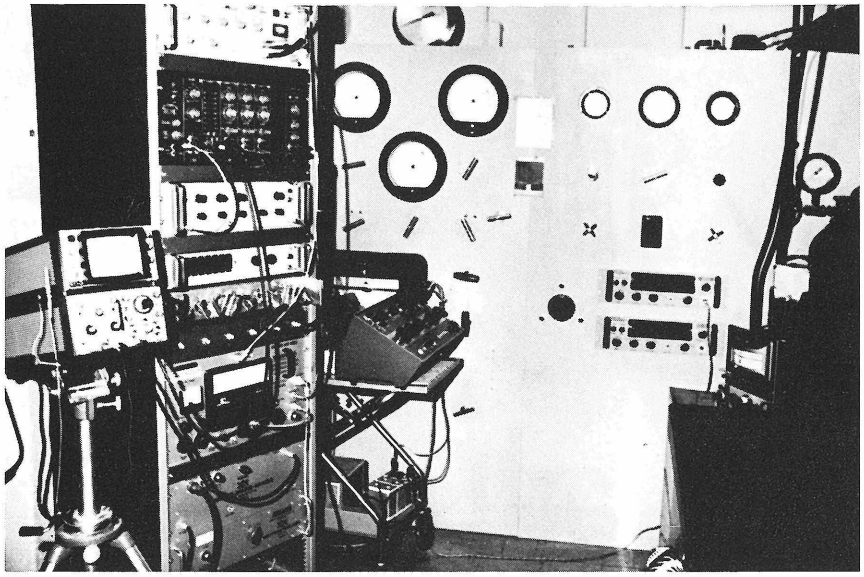

Figure 5

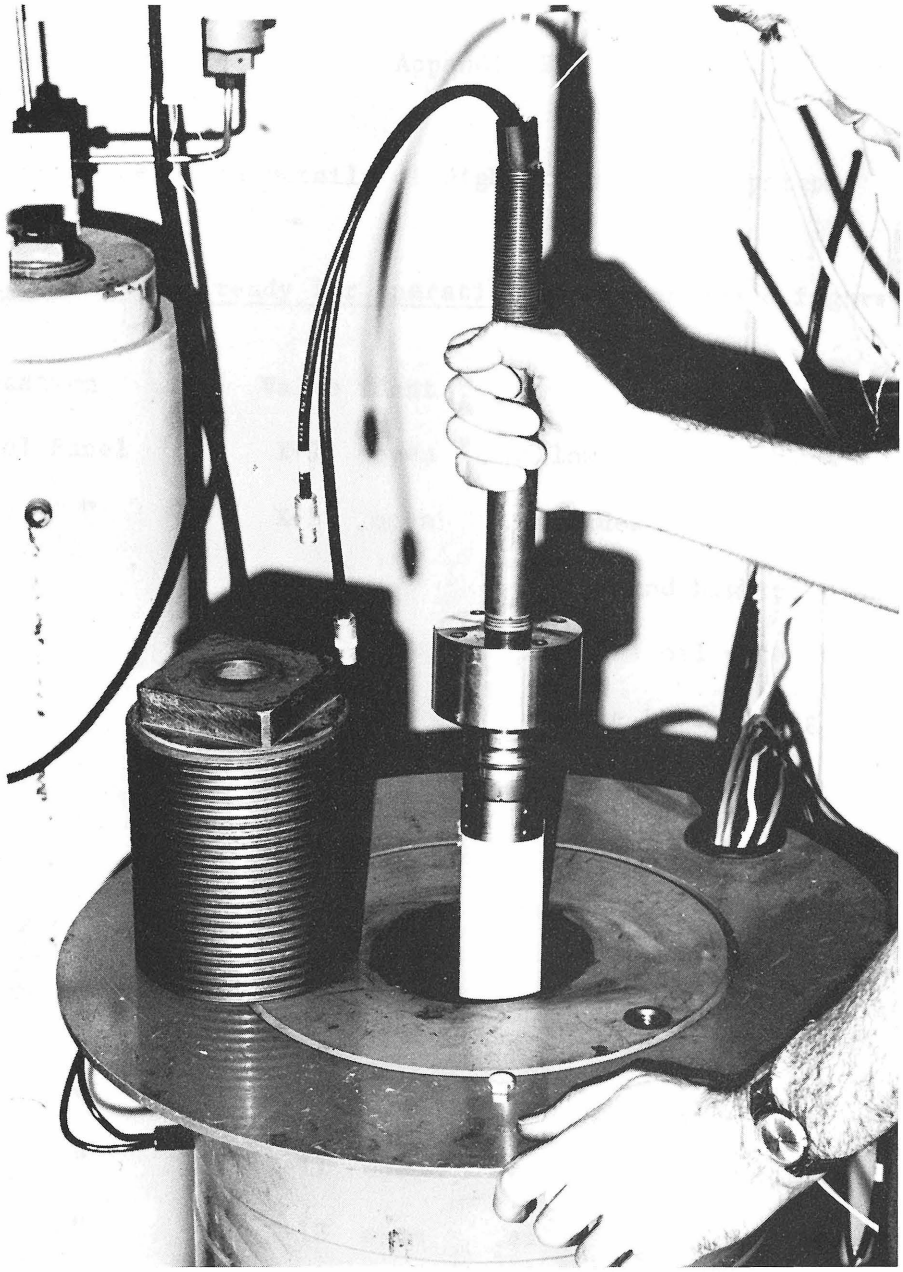

Figure 6

Appendix E

Operating Details of High Pressure Gas System

Initial condition ready for operation: (See attached figure)

Location	Valve ident.		Function
Control Panel	X-1	open	allows gas to charge LP and I
" "	X-2	open	provides additional path of gas to I and high pressure vessel.
" "	X-3	open	provides oil path to oil tank while LP is being primed
" "	X-4	open	provides oil path to oil tank while I is being primed
" "	X-5	open	used only in setting pressure
" "	X-6	open	regulators AP-1 and AP-2
" "	X-8	closed	prevent operation of DP1
" "	X-9	closed	" " " DP2
" "	X-11	open	to obtain accurate reading on G-2
" "	X-12	open	allows charging of high pressure vessel
by oil tank	X-13	open	supplies oil to DP1 and DP2
Air tank	X-14	open	supplies air pressure up to X-8 and X-9

Behind control panel	X-15	closed	provides Argon supply to laboratory in open position
" " "	X-16	closed	used for gas exhaust and vacuum connection in open position
Control panel	X-17	open	allows charging of system
	X-18	open	allow charging of system

Operation

1. Open X-16 connect vacuum pump (V.P.). Activate vacuum pump and run for several hours.

2. While the vacuum pump is running reset null on Manganin bridge if necessary.

3. Close X-16. Disconnect vacuum pump. Connect hose between Kr^{85} flow valve (F.V.) and adjust gas pressure to approximately 40 psi. Open X-16 and allow approximately 5 cc of Kr^{85} to pass into the pressure generating system by opening the flow valve for an appropriate time. Close X-16.

4. Close X-5. Turn AR-2 counterclockwise to stop. Pressure reading on G-6 should drop to zero. Open X-8 and advance AR-2 clockwise until DP1 is operating and G-4 shows 30,000 psi. Close X-8 and open X-5 slowly. The oil pressure on the liquid piston is now limited to 30,000 psi, which generates approximately 27,000 psi on the gas pressure side.

5. Use similar technique as in 3, to set maximum oil pressure on G-3 to 13,000 psi which corresponds to a maximum gas pressure of 200,000 psi.

6. Open Argon bottle and prime system to bottle pressure. G-7, G-1, G-8, and G-9 should all read bottle pressure.

7. Close X-1 and X-2. Open X-8 and let DP1 advance liquid piston until gas pressure stops increasing. If the LP has reached the end of a stroke before the gas pressure has reached 25,000 psi close X-18 and X-8. Open X-3 and X-1. The LP will now be primed again. Full return of the piston is indicated when G-4 shows no pressure upon the closing of X-3. When the piston has returned close X-1 and X-3 and open X-8. Repeat until G-2 and G-9 show at least 25,000 psi. X-8 may be left open to maintain a particular gas pressure in the presence of a small leak.

8. Close X-18 and X-4. The intensifier should be primed, ready for operation. Oepn X-9 slowly to advance intensifier piston. Compare gauges G-2 and G-9 with the readings from the Manganin bridge. Upon reaching a pressure of 30,000 psi close X-11 to protect G-2. Advance piston of intensifier further comparing G-9 and the manganin bridge up to 60,000 psi. At this pressure close X-17 and use manganin bridge only while reaching the desired pressure. Adjustment of AR-1 may be used to maintain constant pressure in the vessel in the presence of a small leak. If the piston reaches

the end of its stroke before the desired pressure is reached close X-12, open X-4 slowly only then open X-17, X-18, and X-11 in that order. The intensifier may now be recharged with the liquid piston level and the operation repeated.

9. When the experiment is finished, the pressure may simply be released by opening X-2, X-12, X-17 (in that order) making sure that the valve is open on the Argon bottle. Once this is done all other valves may be returned to the initial condition ready for operation.

FIGURE CAPTION

Schematic diagram of high pressure system.

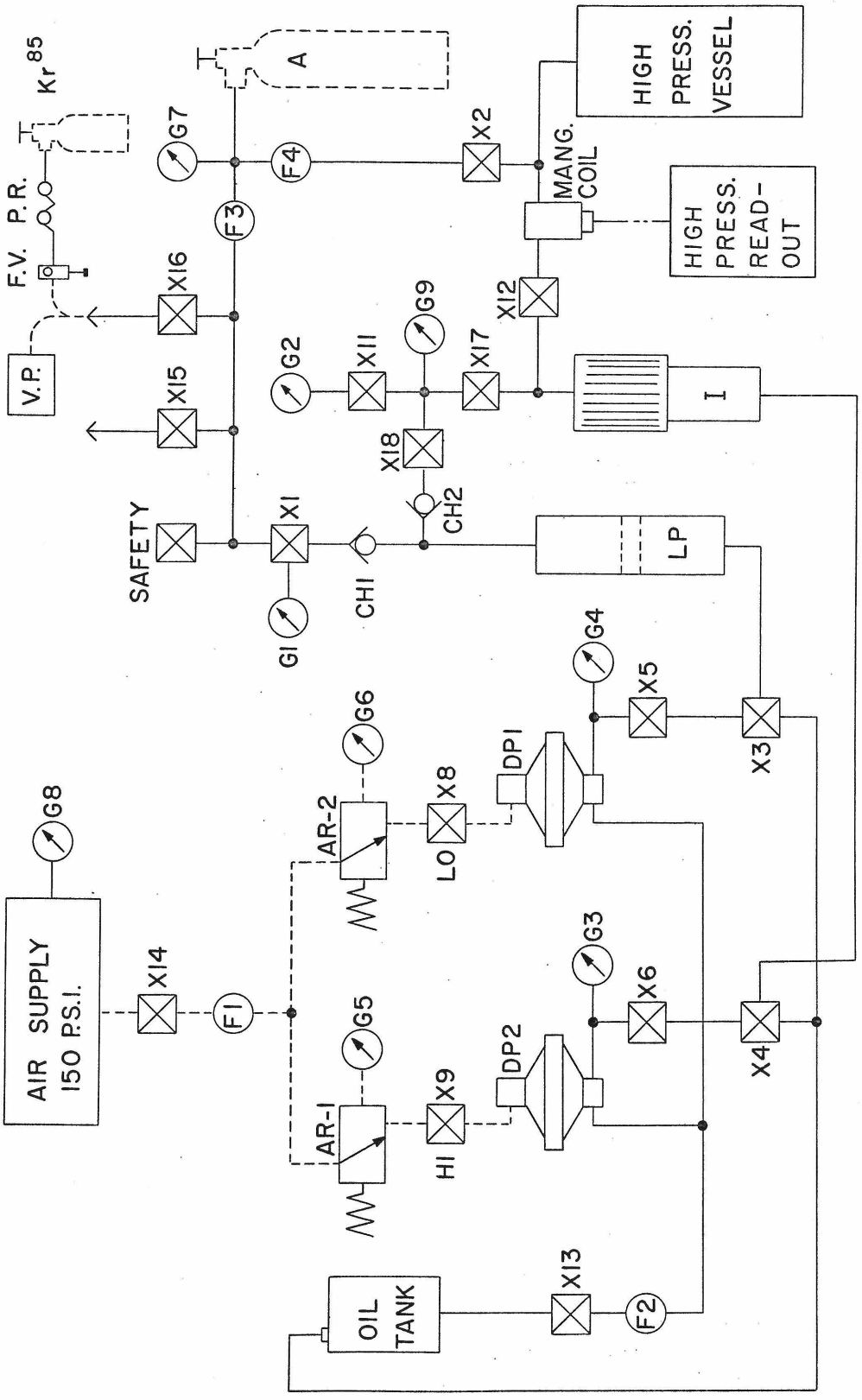
HIGH PRESS. VESSEL
A
Kr 85
G7
F4
X2
MANG. COIL
HIGH PRESS. READ-OUT
F.V.
P.R.
F3
X16
X12
G9
V.P.
G2
X11
X17
I
X15
X18
CH2
SAFETY
X1
LP
CH1
G1
G4
X5
X3
G6
DP1
G8
AIR SUPPLY 150 P.S.I.
AR-2
X8
LO
X14
F1
G3
X6
X4
G5
DP2
AR-1
X9
HI
X13
OIL TANK
F2

Appendix F

PRESSURE READOUT

The pressure gauges G-2 and G-9 are limited in range to 30,000 and 60,000 psi, respectively. Throughout their pressure range, and up to the system's capability, the pressure is determined with a manganin bridge.

Figure 1a shows the bridge circuit with the associated relays. Two manganin coils are mounted in a steel block. But only one coil is exposed to the pressure medium. The compensating coil, being at the same temperature as the active coil, reduces errors due to temperature fluctuations. Some temperature drift problems were, however, encountered. These were due to the use of electric high-pressure feedthroughs for the active coil, which introduces non-symmetrical thermal junctions. By inserting the steel block in a large aluminum heat sink within a closely controlled oven (40°C), this problem was eliminated. The other components of the bridge, with the exception of the 5 ohm nulling resistor, are mounted within a large heat sink in a separate oven. All solder connections were made with low thermal solder. The 5 ohm nulling resistor is a calibrated slide wire from a Leeds and Northrup potentiometer. The arrangement of the two ganged 2 ohm and the 100 ohm resistors assures symmetry and provides very sensitive balancing over a large range.

With a bridge supply voltage of 8.5 volts a balance can be achieved to a fraction of one microvolt.

The bridge power supply is shown in Figure 1b. It consists of a precision temperature compensated 15 volt supply, the output of which is divided, and further temperature stabilized with a zenor diode and a precision resistor. The latter two components are also located within the bridge oven. An impedance matching amplifier with unity gain, a high input impedance and low output impedance, assures a constant supply of voltage to the bridge under varying loads.

Under standard operating conditions, the pressure is determined with the calibrated 5 ohm nulling resistor. The resistance value which is required, is directly related to the pressure and is given in terms of slide wire calibration versus pressure in Figure 2.

The active manganin coil has been calibrated with a dead weight tester and has been found to have a pressure coefficient at 100,000 psi of 1.652×10^{-7} ohms per ohm per psi. Both coils have a nominal resistance of 120 ohms.

Calibration of the nulling resistor and check for possible hysteresis of the manganin coils is accomplished by switching a 100 ohm standard resistor into the bridge and determining the exact resistance of the coils. The potentials across the coils and the standard resistor are measured with a Leeds and Northrup K-5

potentiometer. The absolute accuracy of the pressure determinations is believed to be within .1%, reproducibility is better than .05%.

FIGURE CAPTIONS

Figure 1. Schematic of bridge circuit and associated power supply.

Figure 2. Pressure calibration curve for nulling potentiometer.

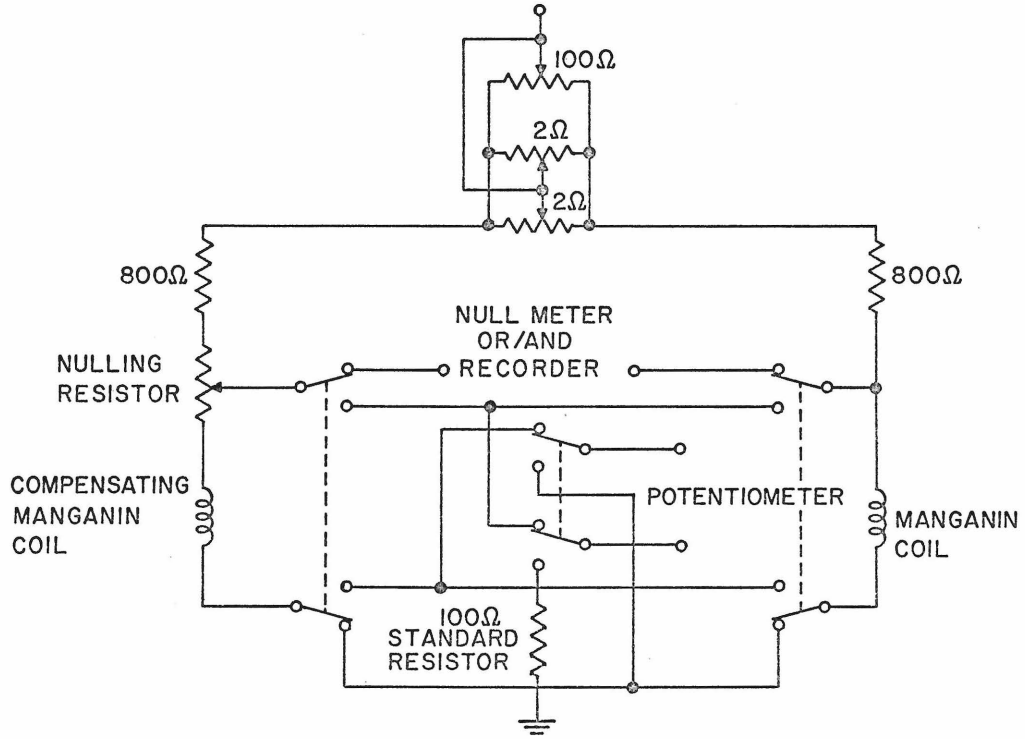

FIGURE IA

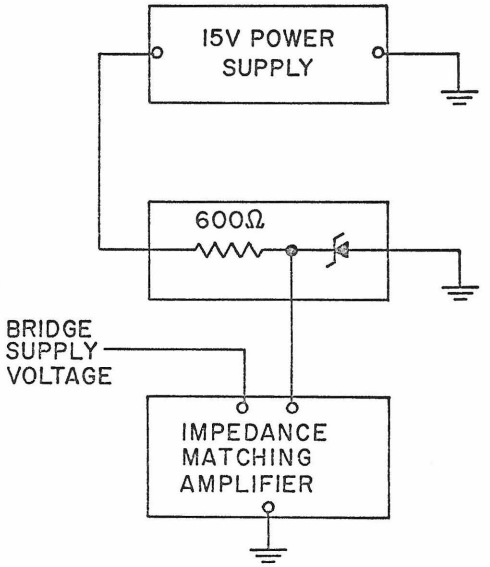

FIGURE IB

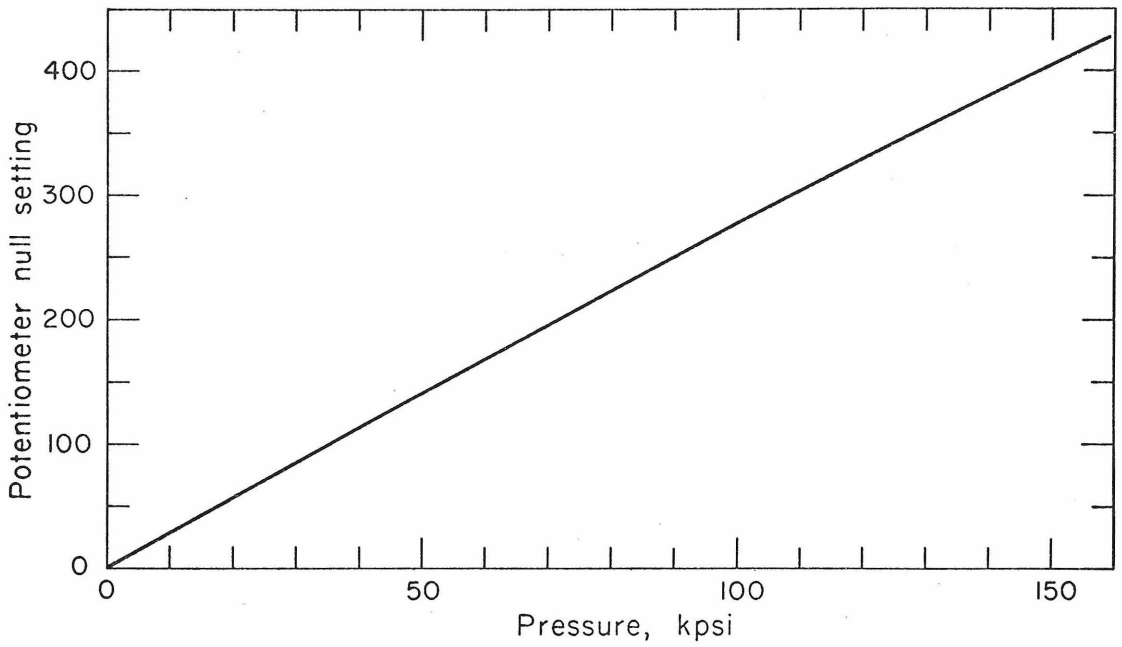
400
300
200
100
0
Potentiometer null setting
0
50
100
150
Pressure, kpsi

Figure 2